land

Special Issue Reprint

Ecology of the Landscape Capital and Urban Capital

Edited by
Teodoro Semeraro

mdpi.com/journal/land

MDPI

Ecology of the Landscape Capital and Urban Capital

Ecology of the Landscape Capital and Urban Capital

Guest Editor

Teodoro Semeraro

MDPI

Basel • Beijing • Wuhan • Barcelona • Belgrade • Novi Sad • Cluj • Manchester

Guest Editor
Teodoro Semeraro
Research Institute on
Terrestrial Ecosystems
(IRET-URT Lecce)
National Research Council of
Italy (CNR)
Lecce
Italy

Editorial Office
MDPI AG
Grosspeteranlage 5
4052 Basel, Switzerland

This is a reprint of the Special Issue, published open access by the journal *Land* (ISSN 2073-445X), freely accessible at: https://www.mdpi.com/journal/land/special_issues/ecology_capital.

For citation purposes, cite each article independently as indicated on the article page online and as indicated below:

Lastname, A.A.; Lastname, B.B. Article Title. *Journal Name* **Year**, *Volume Number*, Page Range.

ISBN 978-3-7258-5577-3 (Hbk)
ISBN 978-3-7258-5578-0 (PDF)
https://doi.org/10.3390/books978-3-7258-5578-0

Cover image courtesy of Aurelia Scarano

Contents

About the Editor

Teodoro Semeraro

I am a PhD researcher and ecologist specializing in environmental science and landscape and urban sustainability. As the Principal Investigator (PI) of the Strategic Environmental Assessment (SEA, Directive 2001/42/CE) for landscape and urban planning, I have managed complex processes that integrate technical evaluation, stakeholder engagement, and interdisciplinary collaboration. My responsibilities included designing and assessing plans, contracting consultants, and managing client relationships. Through these experiences, I have developed a transdisciplinary approach that bridges business investment needs, societal requirements, and ecological priorities. My expertise spans Geographic Information Systems (GISs), biodiversity assessment, ecosystem services evaluation, nature-based solutions, green Infrastructure analysis, and environmental assessments. These skills enable me to connect diverse disciplines and contribute to innovative and sustainable planning strategies.

Preface

Human-driven land use changes, such as urbanization and agriculture, are diminishing biodiversity and eroding ecological structures that sustain human life. Despite policy frameworks like Horizon 2020 and the European Biodiversity Strategy, there remains a gap between the implementation of green infrastructure and the effective integration of ecological, economic, and social processes. This Reprint is motivated by the urgent need to harmonize these dimensions, to enhance ecosystem services, and to address climate and sustainability challenges.

Teodoro Semeraro
Guest Editor

land

MDPI

Article

Assessment of Relationship between Climate Change, Drought, and Land Use and Land Cover Changes in a Semi-Mountainous Area of the Vietnamese Mekong Delta

Tran Van Ty [1,*], Kim Lavane [2], Phan Chi Nguyen [3], Nigel K. Downes [4], Nguyen Dinh Giang Nam [4], Huynh Vuong Thu Minh [4] and Pankaj Kumar [5,*]

1 Water Resource Engineering Faculty, College of Engineering, Can Tho University, Can Tho 900000, Vietnam
2 Department of Environment Engineering, CENRes, Can Tho University, Can Tho 900000, Vietnam
3 Department of Land Resources, CENRes, Can Tho University, Can Tho 900000, Vietnam
4 Department of Water Resources, CENRes, Can Tho University, Can Tho 900000, Vietnam
5 Institute for Global Environmental Strategies, Hayama 240-0115, Japan
* Correspondence: tvty@ctu.edu.vn (T.V.T.); kumar@iges.or.jp (P.K.)

Abstract: Agriculture in the Global South is innately susceptible to climatic variability and change. In many arid and semi-mountainous regions of the developing world, drought is regularly cited as a significant threat to agricultural systems. The objective of this study is to assess the impacts of climate change on drought and land use and land cover (LULC) change in a semi-mountainous region of the Vietnamese Mekong Delta. We assessed previous drought trends (1980–2020) and future drought in the context of climate change, in accordance with three selected scenarios from the Coupled Model Intercomparison Project Phase 6 global climate models which have recently been released by the Intergovernmental Panel on Climate Change (IPCC) (2021–2060) using the Standardized Precipitation Index (SPI). The change of land use for the period 2010–2020 was then assessed and the associated climatic variability explored. The results show that for the period 1980–2019, SPI 3 responds quickly to changes in precipitation, whereas SPI 9 showed a clear trend of precipitation over time. The first longest duration occurrence of drought for SPI 3, SPI 6, and SPI 9 patterns were respectively 15–16, 21, and 25 months at Chau Doc station, and respectively 11, 14–15, and 16–17 months at Tri Ton station. Future precipitation and both maximum/minimum temperatures are projected to increase in both the wet and dry seasons. In addition, for all-time series scales and climate change scenarios, the levels of drought were slight, followed by moderate. In the future, the humidity at Chau Doc station is expected to decrease, while the occurrence of drought events is expected to increase at Tri Ton station, particularly in SPI 6 patterns (110 drought events in 1980–2020, and up to 198 drought events in the future). Moreover, between 2010–2020, the agricultural land area was seen to decrease, replaced by non-agricultural land uses that were found to increase by 22.4%. Among the agricultural land area, forestry, rice crops, and upland rice were found to reduce by 7.5, 16.0, and 21.2%, respectively, while cash crops and perennial crops increased by 26.4% and 170.6%, respectively. Amongst other factors, it is concluded that the variability of climate has led to drought and thus impacted on the conversion of LULC in the study area. Due to low economic efficiency, changing climate conditions, and a lack of irrigated water, the area of rice crops, forestry, aquaculture, and upland rice decreased, replaced by land for orchards for fruit production and other cash crops.

Keywords: agriculture; drought; climate change; land-use and land-cover change (LULCC); An Giang province; Mekong delta

1. Introduction

Due to its natural sensitivity to weather fluctuations, agriculture is one of the sectors most at risk from the effects of climate change and variability [1,2]. Therefore, there is growing concern that both food security and agriculture-dependent livelihoods may be at risk [3]. In particular, drought occurrences pose a serious risk to the livelihood security of rural families [4,5]. Droughts occur virtually in all climatic zones and negatively impact natural habitats, ecosystems, society, and the economy. They are considered as the most common and harmful natural hazard [6–9]. Droughts severely influence the socioeconomic state of Thailand, Cambodia, Laos, and Vietnam on a regular basis and affect about 85% to 90% of the livelihoods of people residing in rural areas in the Lower Mekong Basin (LMB) region [10]. The LMB has experienced several extreme drought events in recent decades, including in the years 1992, 1999, 2003, 2015–2016, and 2019–2020 [10,11]. These led to substantial economic losses, primarily due to crop damages. The most extreme drought in 2016 caused USD 1.7 billion in damages in Thailand and caused water shortages in 18 out of 25 provinces, also affecting 2.5 million people in Cambodia. In Vietnam, the drought in 2016 is estimated to have cost USD 669 million, while the estimated recovery costs amounted to approximately USD 1.5 billion [10]. According to the results of Wang et al. [12], who used multiple indicators based on eleven Coupled Model Intercomparison Project Phase 6 (CMIP6) global climate models (GCMs) to assess global drought characteristics, future droughts will increase in most parts of the world. However, few studies have focused on the seasonal characteristics of drought in the LMB, in particular using the new CMIP6 outputs [7].

Precipitation shows strong spatial–temporal heterogeneity under global climate change, and assessing the variability of future precipitation is essential to understanding the impact of climate change on a range of natural and socioeconomic systems [13,14]. The latest outputs of CMIP6 models, based on a new set of possible alternative future scenarios, is more suitable for use thanks to improved spatial specificity and less uncertainty of precipitation compared with the CMIP5 projections [15]. The Sixth Assessment Report (AR6) of the Intergovernmental Panel on Climate Change (IPCC) highlights that the global surface temperature was 1.09 °C warmer during 2011–2020 than 1850–1900, with a higher increase across the land (1.59 °C) than over the oceans (0.88 °C). Precipitation is a key component of the hydrological cycle, combining atmospheric and land surface processes, and there is likely to be an increase in globally averaged precipitation across the land since 1950, with a higher rate after the 1980s [16–18]. However, at a regional scale, precipitation has been considerably found to increase (decrease) at high (low) latitudes in recent decades [19]. Changes in precipitation have impacted both water resources supply and management and progress towards the 2030 Sustainable Development Goals adopted by the United Nations (UN) in 2015 [20,21]. Therefore, understanding and exploring the relationship between climate change, future drought risk, and land use and land cover is important for the overall sustainability of the LMB because of its high human population density, susceptible infrastructure, and poor planning of land use and management practices [22,23].

Several authors have assessed climate change and its impacts in Southeast Asia (SEA) recently. Fei Ge et al. [24] used outputs from 15 climate models from the CMIP6 to evaluate projected changes in precipitation extremes for SEA by the end of the 21st century and suggested that CMIP6 multi-model ensemble medians showed better performance in characterizing precipitation extremes than individual models. Moreover, projected changes in precipitation extremes increased significantly over the Indochina Peninsula and the Maritime Continent. Supharatid et al. [25] projected changes in temperature and precipitation over mainland SEA using CMIP6 models to highlight the threats to Cambodia, Laos, Myanmar, Vietnam, and Thailand. They found that the effectiveness of anticipated climate change mitigation and adaptation strategies under SSP2-4.5 results in slowing down the warming trends and decreasing precipitation trends after 2050. All these findings imply that countries of SEA need to prepare appropriate adaptation measures in response to climate change. Recently research focused on the impact of future climate change on river discharge in Ho Chi Minh City (HCMC) [26]. They used a calibrated SWAT to simulate the discharge under seven GCMs derived from CMIP6 under three SSPs, with results suggesting that the climate of HCMC will be warmer and wetter by the end of the 21st century.

It has been clearly demonstrated that a knowledge gap exists, with a lack of studies considering the downscaled climate change impacts on drought and land use and land cover change at smaller scales, i.e., the provincial level required for adaptation planning. Short- and medium-term drought indicators like SPI 3 or SPI 6 were frequently used in studies on drought and its effects on agriculture in Vietnam and other nations [1,2,27–29]. In addition, a variety of drought indices are employed to evaluate the severity of a region's drought, but this requires more information [30–33]. The influence of SPI on LULC in the context of climate change is also found in many studies [33,34].

Short-term land use changes are often associated with human activities due to the development of society and change in land use according to market economy fluctuations in the absence of a long-term strategy [35,36]. In Vietnam, the two dominate land use functions are agricultural land and non-agricultural land [37].Usually there is a conversion of agricultural land for socioeconomic development purposes. Moreover, a change can occur within a land-use category (mainly within the agricultural land category). Such changes usually occur as a result of a land use type changing into a type of higher economic efficiency [38–40]. Often driving factors for land use change are low crop productivity due to erratic weather changes, irrigation water availability, soil suitability, and hydrometeorological and climate-related changes due to prolonged drought, saltwater intrusion, and sea level rise [41–43].

Therefore, the objective of this study is to assess the impacts of climate change on drought and land use and land cover changes (LULCC) in the upper section of the Vietnamese Mekong Delta (VMD). We first assess current and future drought in the context of climate change, according to three selected scenarios, using Standardized Precipitation Index (SPI). In addition, we explore change of land use for the period from 2010 to 2020 in An Giang province, taking the associated climatic variability into consideration.

2. Methodology

2.1. Study Area

An Giang is an upstream province of the Mekong River in Vietnam, with both plains and a semi-mountainous area concentrated in the districts of Tri Ton and Tinh Bien (Figure 1). An Giang has a natural area of 353,683 ha, equal to 1.03% of Vietnam's total land area, and is ranked fourth among the Mekong Delta provinces in terms of total agricultural area. In total, An Giang has 296,719 ha of land used for agriculture, according to the official land use data of 2019 (including 242,337 ha of land for rice cultivation, 11,648 ha of land for other annual crops, 25,343 ha of land for perennial crops, 11,643 ha of forestry land, 5530 ha of aquaculture land, and 219 ha of other agricultural land) [44,45]. The province has a population of approximately 1,907,401, with an ethnic population of 91,408 Khmer concentrated in the two mountainous districts of Tinh Bien and Tri Ton [46]. In 2020, the total planted area in the province was 707,100 ha (of which 637,200 ha are rice, 50,600 ha are crops, and 19,300 ha are fruit trees), with 1582 ha being planted forest [44]. The majority of An Giang's domestic and agricultural water needs are met by reservoirs in the semi-mountainous region [47]. As a result, changes in precipitation here have a significant effect on the local economy and livelihoods.

2.2. Drought Analysis

The Standardized Precipitation Index (SPI), developed by McKee et al. [27,48] is widely used worldwide [28,49–51]. In this study we used the SPI to calculate the impact of drought on agriculture and establish its frequency using various time steps, as well as for the two cropping seasons (summer–autumn and winter–spring). In order to assess the short- and medium-term drought levels, SPI 3, SPI 6, and SPI 9 tests were performed. Furthermore, the seasonal SPI was also calculated.

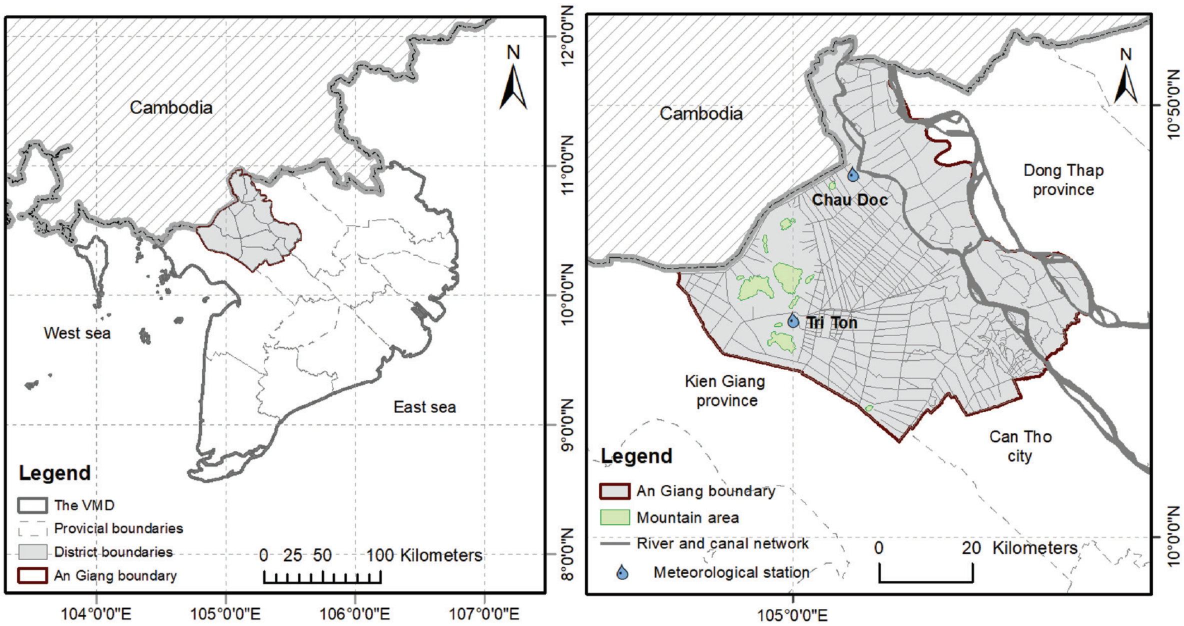

Figure 1. Location of An Giang province (**left**) and the utilized meteorological stations (**right**).

Assuming a precipitation series at a given timescale $X = x_1, x_2, x_3, \ldots, x_n$, $n = 1, 2, 3, \ldots, n$ represents the length of the series, and the distribution function $f(x, \theta)$ can best describe the distribution of the precipitation series X.

$$X \sim f(x,\theta) \tag{1}$$

where θ is the parameter sets of the function $f(x)$ that can be estimated based on the sample series X.

Then, the cumulative distribution function can be expressed as,

$$F(x) = \int_0^x f(x,\theta)dx \tag{2}$$

Equation (2) can be used to determine the cumulative probability of each observed precipitation event, xi. The *SPI* then undergoes an equiprobability transformation from the cumulative probability to the unit variance, zero mean, standard normal random variable Z.

$$SPI = \Phi^{-1}(F(X)) \tag{3}$$

where Φ^{-1} (•) is the inverse of a standard normal cumulative distribution function Φ (•) with zero mean and unit variance. Considering the fact that some kinds of distribution functions are not defined for $x = 0$, such as the Gamma function, an adapted statistic $H(x)$ can be expressed as Equation (4).

$$H(x) = q + (1-q)F(x) \tag{4}$$

where q is the probability of no precipitation, which can be computed by simply dividing the number of months (N) by the number of months (n) that have no precipitation (Vicente-Serrano, 2006) [52]. Equation (5) can then be used to describe the SPI computation process.

$$SPI = \Phi^{-1}(H(X)) \tag{5}$$

In this study, we used the SPI-based drought classification for Vietnam, in which SPI = −0.25 signifies the onset of drought conditions [53,54]. Drought begins when the

SPI first falls below the negative value of 0.25 or less and ends when the SPI returns to a positive value of 0.25 or higher (Table 1).

Table 1. The classification of drought and wet according to the SPI index.

Drought Levels	SPI Values	Drought Levels	SPI Values
Normal	0–0.24	Normal	(−0.24)–0
Very slightly wet	0.25–0.49	Very slight drought	(−49)–(−0.25)
Slightly wet	0.5–0.99	Slight drought	(−0.99)–(−0.5)
Moderately wet	1–1.44	Moderate drought	(−1.44)–(−1)
Severely wet	1.5–1.99	Severe drought	(−1.99)–(−1.5)
Extremely wet	>2	Extreme drought	<(−2)

2.3. Climate Change Scenarios

This study utilized the recent output from the CanESM5-CanOE ($2.81^0 \times 2.81^0$ grid) developed by the Canadian Centre for Climate Modeling and Analysis, Victoria, Canada. Data associated with this study is available from https://esgf-node.llnl.gov/search/cmip6/ (last accessed 10 September 2022). New outputs from CMIP6 have recently been released by the IPCC. While the CMIP5 projected the future climate based on greenhouse gas emissions represented by four representative concentration pathways (RCPs), namely RCP2.6, RCP4.5, RCP6.0, and RCP8.5 [55], the CMIP6 designed five scenarios called shared socioeconomic pathways (SSP), namely SSP1-2.6, SSP2-4.5, SSP4-6.0, and SSP5-8.5, to include socioeconomic factors such as the growth of population, economics, urbanization, and other factors [56]. The improvement of CMIP6 scenarios includes wider equilibrium climate sensitivity (ECS) with an increasing temperature range of 1.5–4.5 °C. The models in CMIP6 are expected to improve their capability and reduce uncertainty over the previous CMIP5 and CMIP3 [13,57].

In this study, the three scenarios, SSP1-RCP2.6 (SSP1-2.6), SSP2-RCP4.5 (SSP2-4.5), and SSP5-RCP8.5 (SSP5-8.5) were chosen for analysis [58,59]. Historical simulations (1850 to 2014) and projections (2015 to 2100) from CMIP6 GCMs were employed in this study, with the climatic variables consisting of daily maximum near-surface air temperature (tasmax, in K), daily minimum near-surface air temperature (tasmin, in K), and precipitation rate (pr, in mm/day). The study period was divided into three periods for equal comparison including historical (2000–2020), future (2021–2040), and (2041–2060). The mentioned climatic variables were downloaded by extracting the grid value that was the closest to the observation station grid point [7].

Since there is large uncertainty as to the extent to which climate change responses might alter emission scenarios, it should be noted that the selected scenarios (SSP1, SSP2, and SSP5) for this study are only two plausible descriptions of how future emissions might develop at low-average and high socioeconomic pathways. Precipitation output from this cannot be used due to biases between the simulated variables for the current (control) climate and observed values. The delta change approach was used to correct these biases by transferring the signals of climate change derived from a climate model simulation to the observed database, and this method is considered a better bias correction of precipitation on a monthly and seasonal basis [60,61]. In this study, the means were calculated on a monthly basis for each 20-year period of climate output. The 12 delta change factors for precipitation were used to perturb the observed database and calculated as follows:

$$\Delta P(j) = \frac{\overline{P}_{scen}(j)}{\overline{P}_{contr}(j)} \tag{6}$$

$$P_{\Delta}(i,j) = \Delta P(j) \times P_{obs}(i,j)\ (i = 1 \sim 31; j = 1 \sim 12) \tag{7}$$

where $\Delta P(j)$ is the delta factor; $\overline{P}_{contr}(j)$ and $\overline{P}_{scen}(j)$ are the precipitation in month j averaged for the 20-year control (2000–2020) and scenario (2021–2060) periods centered in 2040 simulated by the GCM; $P_{\Delta}(i, j)$ is the projected precipitation (bias-corrected precipitation) under the SSP1, SSP2, and SSP5 scenarios; $P_{obs}(I, j)$ is the observed precipitation representing current climate; suffixes i and j stand for the i^{th} day and the j^{th} month, respectively.

For temperature, absolute change is used for the delta change factors, as follows:

$$\Delta T(j) = \overline{T}_{scen}(j) - \overline{T}_{contr}(j) \tag{8}$$

$$T_{\Delta}(i, j) = T_{obs}(i, j) + \Delta T(j) \ (i = 1 \sim 31; j = 1 \sim 12) \tag{9}$$

where ΔT(j) is the delta change factor; $\overline{T}_{contr}(j)$ and $\overline{T}_{scen}(j)$ are the temperature in month j averaged for the 20-year control (2000–2020) and scenario (2021–2060) periods centered in 2040 simulated by the GCM; $T_{\Delta}(I, j)$ is projected temperature (bias-corrected temperature) under the SSP1, SSP2, and SSP5 scenarios.

The projected precipitation (bias-corrected precipitation) under the SSP1, SSP2, and SSP5 scenarios was then used to calculate the future SPI as presented in Equation (5).

2.4. Land Use and Land Cover Change

Data collected to assess the change in land use in the period from 2010 to 2020 in An Giang province included data, reports, and maps of land inventories from the Department of Natural Resources and Environment of An Giang province (DONRE). Then, we explored the change in land use through the synthesis, analysis, and construction of tables and charts to compare and evaluate the change in area of land use types by the descriptive statistics method. We also assessed the transition between land use types in the same period. At the same time, we explored the drivers of land use change. In addition, the map method has been used to normalize the data and overlap to determine the areas that have undergone change in the period from 2010 to 2020 using ArcGIS 10.6 software. The overlap diagram determining the land use change area for the period 2010 to 2020 with the GIS tool is depicted in Figure 2.

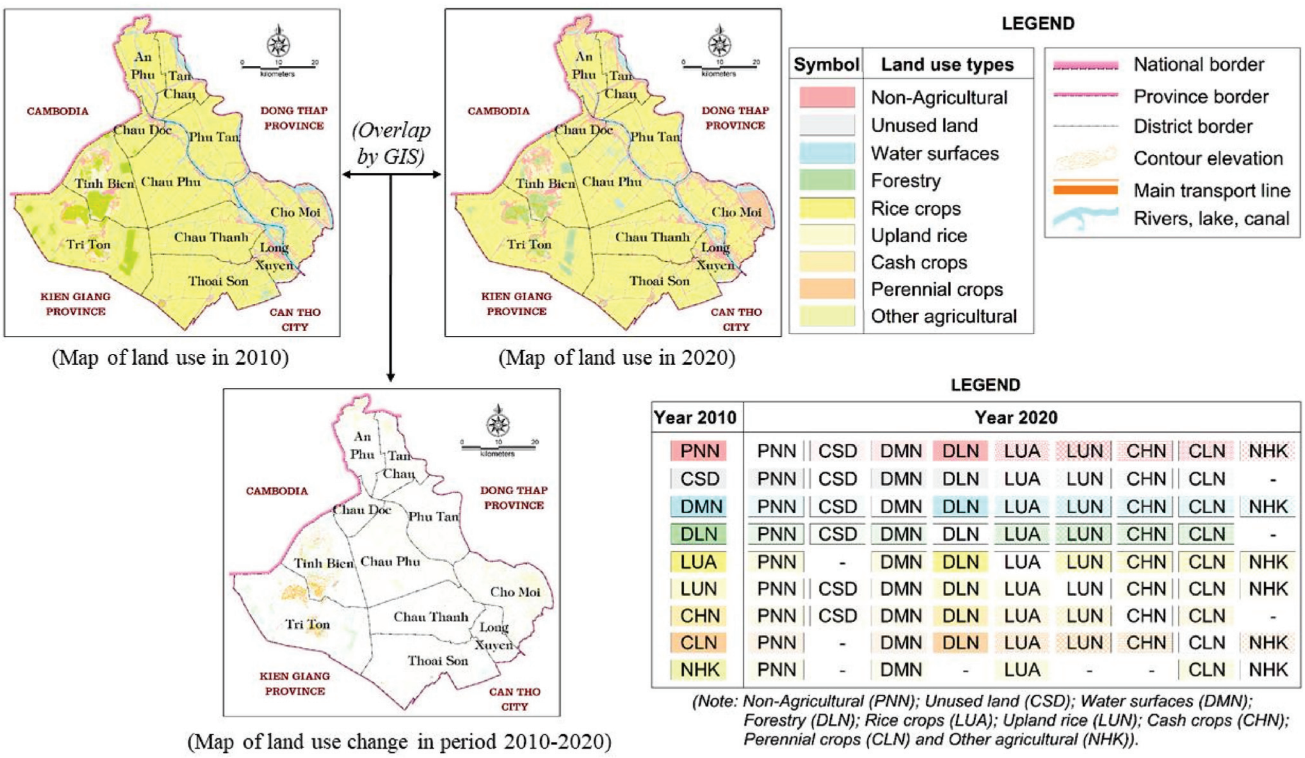

Figure 2. The overlap diagram for determining the land use change area for the period of 2010 to 2020.

3. Results and Discussion

3.1. Current Drought Assessment

Current drought based on the time series at 3, 6, and 9 monthly SPI for the Chau Doc and Tri Ton stations are shown in Figures 3 and 4, respectively. From Figure 3, it can be seen that the 3-month continuous drought (SPI 3) responds faster to changes in precipitation than the 6-month and 9-month continuous droughts, respectively. However, it is also indicated that the 6-month and 9-month continuous droughts show more clearly the seasonal variability of precipitation or events of drought or wetness over time. Comparing drought in Chau Doc and Tri Ton stations, it is clearly indicated that the drought SPI 3, SPI 6, and SPI 9 at Tri Ton station tend to gradually increase over time, with slightly less variation seen than those at Chau Doc station.

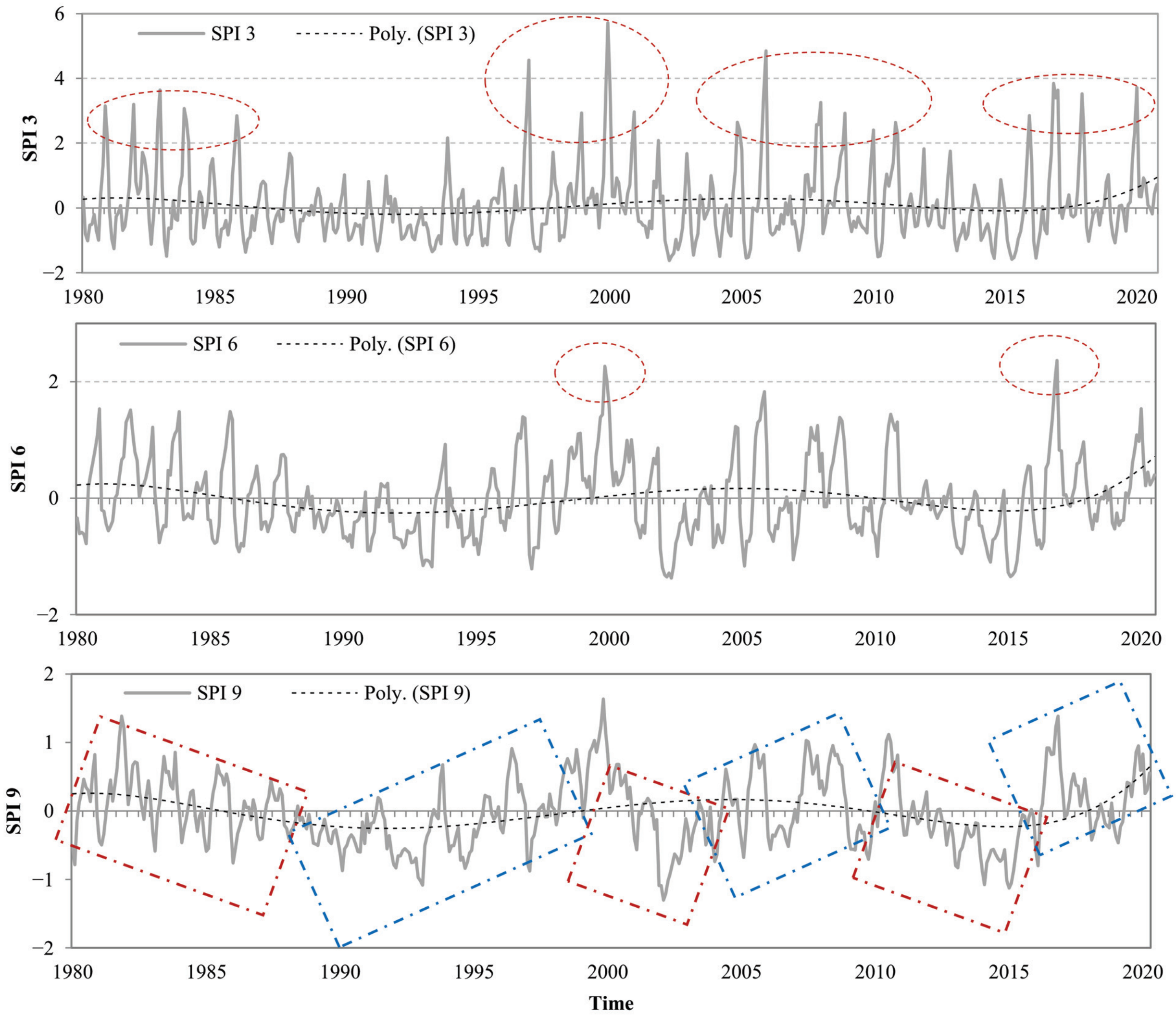

Figure 3. Drought time series at 3, 6, and 9 monthly SPI for the Chau Doc meteorological station. The best-fit lines using polynomial (Poly).

In addition, the frequency and duration of dry periods were determined using the SPI 3-, SPI 6-, and SPI 9-month drought time series from 1980 to 2019. Figures 3 and 4 also show that the variation in drought and wet periods over time is greater in Chau Doc than at Tri Ton Station. As SPI decreases over time, Tri Ton station shows more variation than Chau Doc station. This means that this area was drier between 1980 and 2019. The standard deviations for SPI 3-, SPI 6-, and SPI 9-month, respectively, were 0.74, 0.60, and 0.50 at Tri Ton Station, and 0.70, 0.46, and 0.47 at Chau Doc Station. Three consecutive months were found to appear more frequently at both stations than six and nine consecutive months.

However, the number of occurrences differed little between the 6-month and 9-month consecutive terms.

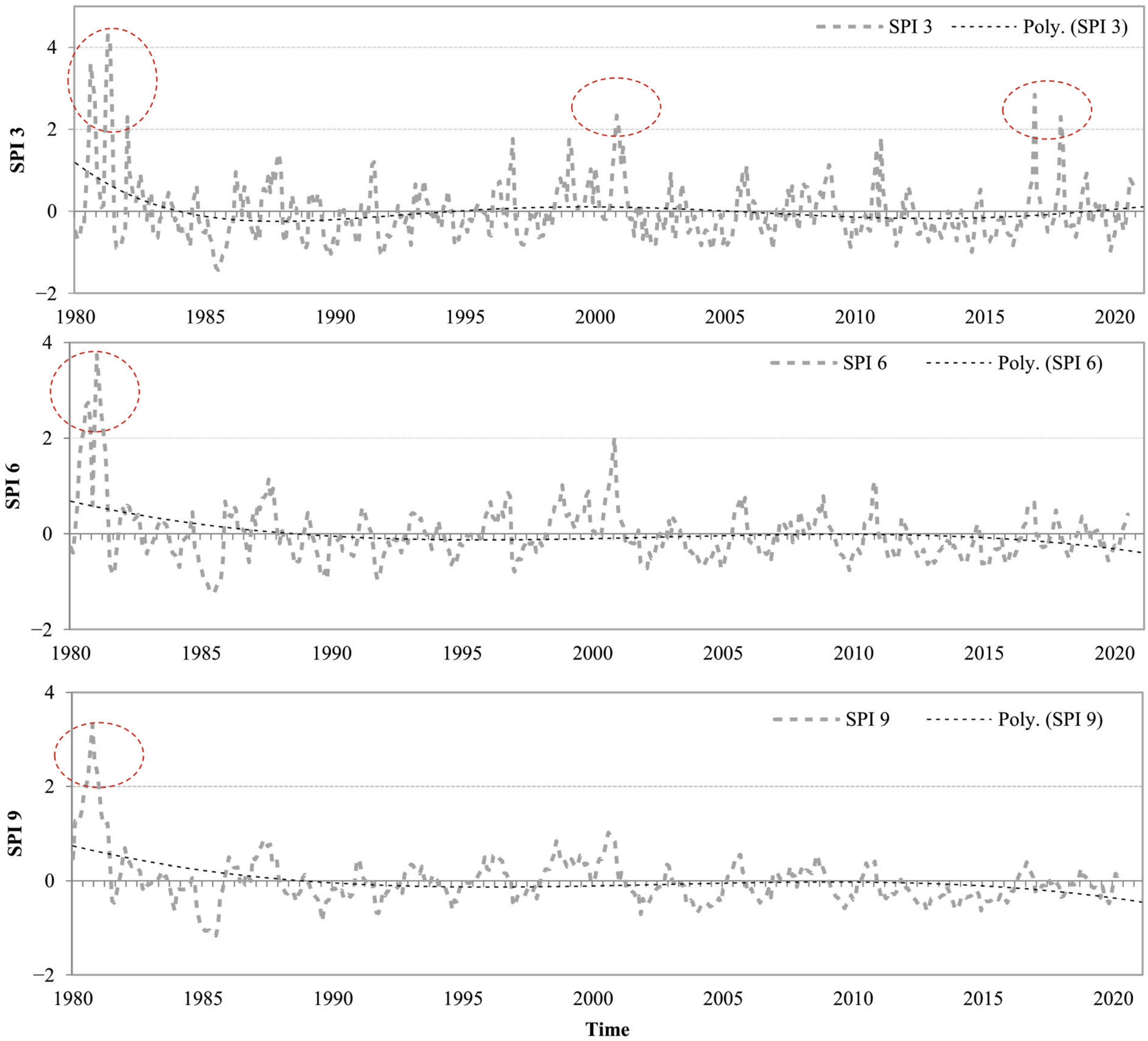

Figure 4. Drought time series at 3, 6, and 9 monthly SPI for the Tri Ton meteorological station. The best-fit lines using polynomial (Poly).

Details of SPI values for drought and wet durations for the 1980–2019 period at Chau Doc and Tri Ton stations are listed in Tables 2 and 3, respectively. From Tables 2 and 3, it can be seen that the longest durations of dry and wet periods were observed from 2013 to 2016 (25 months from October 2013 to June 2016) and 1998 to 2001 (33 months from March 1998 to July 2001), respectively, at Chau Doc station. The second and third droughts, on the other hand, lasted approximately as long as the first; specifically, the two occurrences of the second drought occurred for periods lasting between 21 and 23 months (February 1989 to July 1991 and September 1991 to January 1994). The first longest duration of drought for SPI 3, SPI 6, and SPI 9 patterns at Chau Doc station were 15–16, 21, and 25 months, respectively. At Tri Ton station, the first longest duration of drought for SPI 3, SPI 6, and SPI 9 patterns were 11, 14–15, and 16–17 months, respectively. At Chau Doc Station, the first longest duration of wet periods for SPI 3, SPI 6, and SPI 9 patterns were 10, 15, and 33 months, respectively, whilst at Tri Ton Station, the first longest duration of wet periods for SPI 3, SPI 6, and SPI 9 patterns were 10, 15, and 19 months, respectively. These results clearly indicate that the duration of drought and wet periods at Chau Doc is longer than those at Tri Ton.

Table 2. SPI values for periods of drought and wet durations in the timeframe of 1980–2019 at Chau Doc meteorological station.

	Chau Doc		
Characteristics	3-month	6-month	9-month
Number of SPI ≤ -0.25	129	91	72
The first longest duration/occurrence times of drought (month)	15–16/2	21/1	25/1
Time period, first longest duration	2012–2014, 2014–2015	1991–1993	2013–2016,
The second longest duration of drought (month)	11–12/2	19/2	21–23/2
Time period, second longest duration	1990–1991, 2001–2003	2012–2014, 2014–2016,	1989–1991, 1991–1993
The third longest duration of drought (month)	8–9/3	15/1	14–16/2
Time period, third longest duration	1989–1990, 1992–1993, 2009–2010	2002–2003	2002–2003, 2012–2014
Number of SPI ≥ 0.25	135	133	123
The longest duration of wet	10	15/1	33
Time period, first longest duration (month)	2016–2017,	1988–1989	1998–2001,
The second longest duration of wet (month)	9	13/1	12–13/2
Time period, second longest duration	2008–2009	2007–2009	2007–2009, 2010–2011
The third longest duration of wet (month)	8	12/2	10/2
Time period, third longest duration	1999–2000	1999–2000, 2010–2011	1981–1982, 2016–2017

Table 3. SPI values for drought and wet duration in the period of 1980–2019 at Tri Ton meteorological station.

	Tri Ton		
Characteristics	3-month	6-month	9-month
Number of SPI ≤ -0.25	116	73	34
The first longest duration/occurrence times of drought (month)	11/1	14–15/2	16–17/2
Time occurrence first longest duration	1985–1986,	2003–2005, 2012–2013,	2003–2005, 2012–2014,
The second longest duration of drought (month)	8–9/2	12–13/2	14–15/2
Time occurrence second longest duration	1991–1992, 2003–2004,	1984–1986, 2009–2010	2014–2016,
The third longest duration of drought (month)	7/3	8–9/3	11–12/3
Time occurrence third longest duration	1989–1990, 2012–2013, 2015–2016,	2001–2002, 2011–2012, 2014–2016	1984–1986, 2009–2010, 2013–2015
Number of SPI ≥ 0.25	122	109	96
The longest duration of wet	10/1	15/1	19/1
Time occurrence first longest duration (month)	1987–1988	1980–1981	1998–2000
The second longest duration of wet (month)	9/1	10/1	18/1
Time occurrence second long duration	1998–1999	1998–1999	1980–1982,
The third longest duration of wet (month)	7/2	9/3	12/1
Time occurrence third longest duration	1980–1981, 2000–2001	1981–1983, 1987–1988, 2000–2001	1986–1988

3.2. Future Drought Assessment

3.2.1. Climate Change

Delta changes in the monthly precipitation extracted directly from the grid cells of the CanESM5-CanOE emission scenarios SSP1-2.6, SSP2-4.5, and SSP5-8.5 closest to the stations in the study area were used to generate the monthly precipitation series, which was then used to calculate the corresponding SPIs. Details on the monthly delta change factors of precipitation (%), Tmax (°C), and Tmin (°C) of the scenario period (2021–2060) compared with the control period (2000–2020) under scenarios SSP1-2.6, SSP2-4.5, and SSP5-8.5 in the study area (at Chau Doc and Tri Ton stations), respectively, are shown in Figure 5a,b. The results of downscaled precipitation revealed that future precipitation in the study area would increase in both the wet and dry seasons under the three scenarios, with the highest increases seen in the wet season (period from mid-May to mid-November) in the month June, followed by September and July. Although it was found that there was an increase in precipitation in the dry season, with the highest percentage found in the month February and January, it should be noted that the "real" amount of increased precipitation volume is very modest.

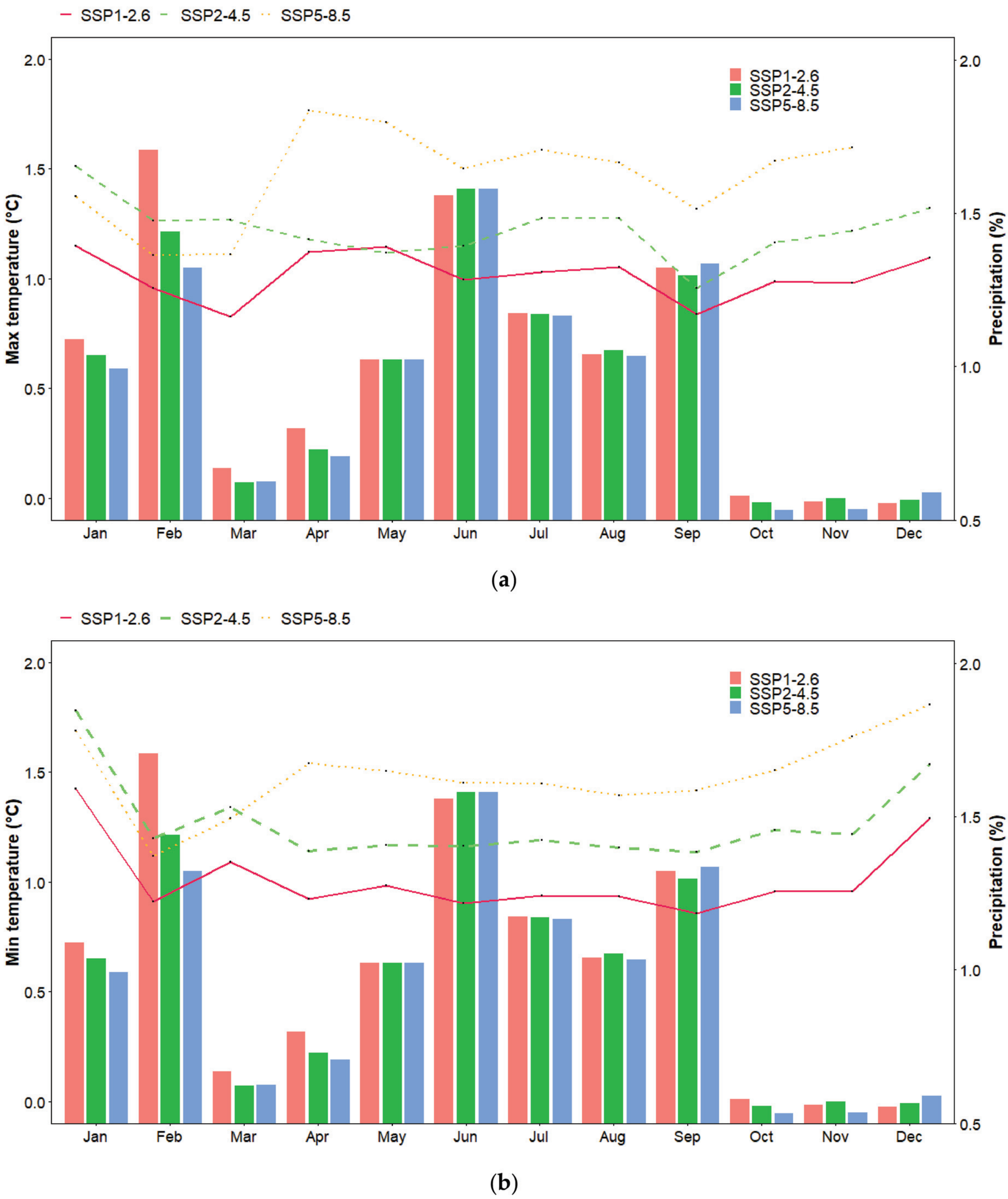

Figure 5. Delta change in precipitation (%) and (**a**) maximum temperature (°C) and (**b**) minimum temperature (°C) under climate change scenarios SSPI 2.6, SSP2 4.5, and SSP5 8.5 in the study area.

In addition, the maximum temperature was projected to increase both during the wet and dry seasons under all scenarios and at all stations. The dry season (mid-November to mid-May), showed the largest increase in maximum temperature. This increase in maximum temperature, consequently, would lead to an increase in potential evapo-transpiration

(ETo). Thus, this would impact the agricultural water resources and in turn lead to the conversion/change of crops or land use in the study area.

3.2.2. Future Drought Assessment (SPI 3, SPI 6, SPI 9 Patterns)

The different time series (SPI 3, SPI 6, SPI 9) for monthly drought patterns at Chau Doc and Tri Ton meteorological stations using various climate change scenarios are shown in Figures 6 and A1 with scenarios SSP1 2.6 (a), SSP2 4.5 (b), and SSP5 8.5 (c), respectively.

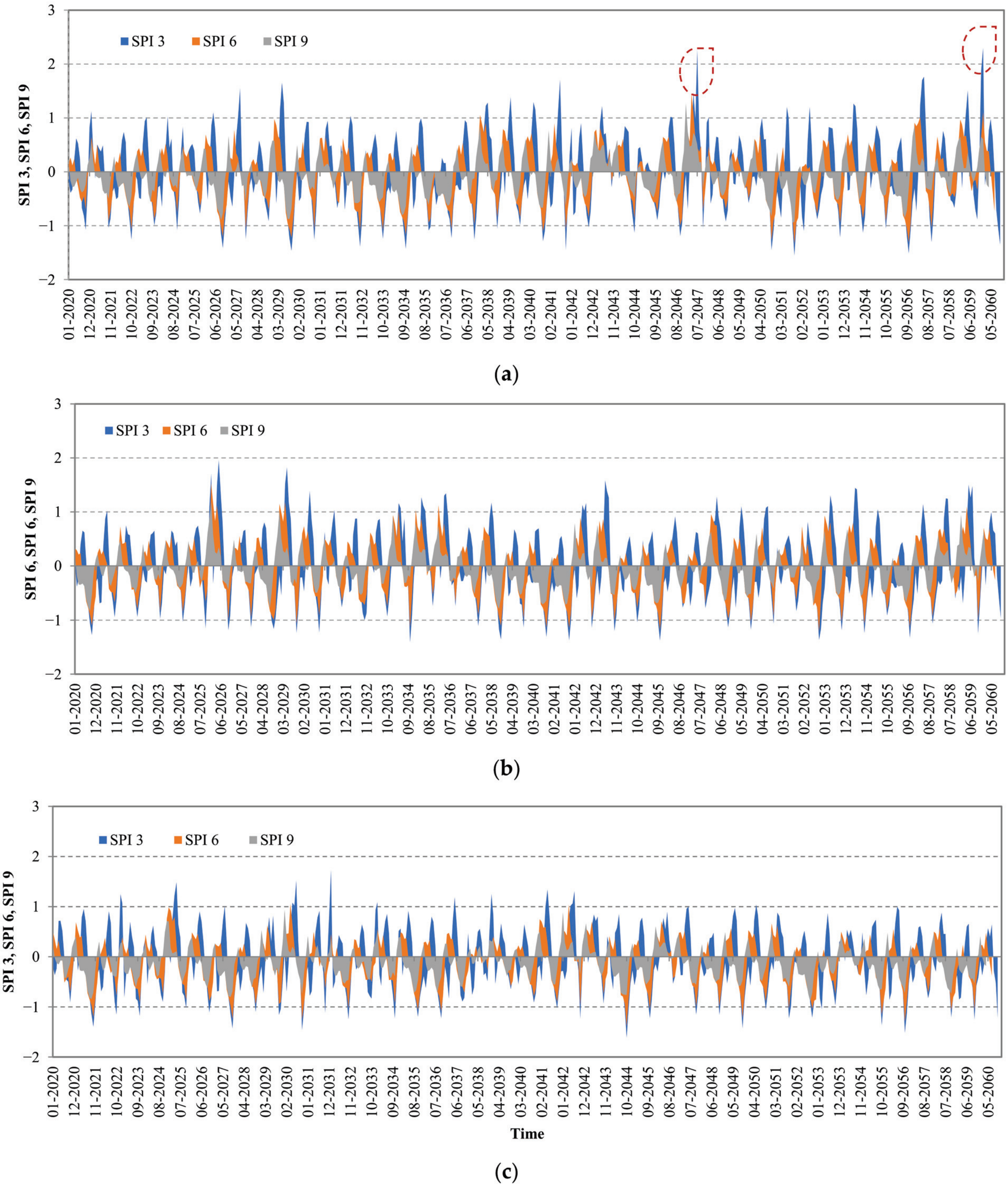

Figure 6. Different time series (SPI 3, SPI 6, SPI 9) for monthly drought patterns at Chau Doc meteorological station using various climate change scenarios, SSP1 2.6 (**a**), SSP2 4.5 (**b**), and SSP5 8.5 (**c**).

According to the precipitation data from the climate change scenarios for Chau Doc and Tri Ton stations, the level of precipitation tends to decrease, with only two extremely wet events occurring at Chau Doc station between 2020 and 2060. In comparison, Tri Ton station displayed significantly more events.

The results highlight that extreme wet or dry conditions are unlikely to occur in the VMD under the assessed climate change scenarios. There are multiple extremely wet seasons solely in the SSP1 2.6 scenario. However, in climate change scenarios, there is no discernible difference between SPI 3, SPI 6, and SPI 9. Additionally, the trend of SPI variation over time is ambiguous.

Table 4 and Figure A1 show the number of occurrences of drought and wet periods in the different patterns of SPI using climate change data at Chau Doc and Tri Ton stations, respectively. It can be seen that for Chau Doc meteorological station in the future, the duration of the drought shows little change, while the wet occurrence time has decreased for SPI 3, SPI 6, and SPI 9 under scenarios SSP1-2.6, SSP2-4.5, and SSP5-8.5. Meanwhile, at the Tri Ton station, the humidity level has changed little, while the occurrence of drought increases, particularly in SPI 6 patterns. SPI 6 shows 110 drought events from 1980 to 2020, but this is forecasted to increase to 198 drought events in the future.

Table 4. Number of occurrences of drought and wet period in the different patterns of SPI using climate change data at Chau Doc station.

Categories	SSP 1_2.6			SSP 2_4.5			SSP5_8.5		
	SPI 3	SPI 6	SPI 9	SPI 3	SPI 6	SPI 9	SPI 3	SPI 6	SPI 9
Extreme drought	0	0	0	0	0	0	0	0	0
Severe drought	2	0	0	2	0	0	2	0	0
Moderate drought	41	18	0	41	18	0	41	18	0
Slight drought	99	91	30	99	91	30	99	91	30
Very slight drought	0	0	0	0	0	0	0	0	0
Very slightly wet	29	68	91	29	68	91	29	68	91
Slightly wet	55	119	63	55	119	63	55	119	63
Moderately wet	64	24	6	64	24	6	64	24	6
Severe wet	25	2	1	25	2	1	25	2	1
Extreme wet	7	0	0	7	0	0	7	0	0

3.3. Land Use Land Cover Change from 2010 to 2020

Figure 7 presents the area of land use types in 2020 for An Giang province. It shows that agricultural land was the dominant land use, including specialized rice crops (triple rice and double rice), upland rice, cash crops, fruits, and other agricultural land, in which the area of specialized rice cultivation occupied 23.9×10^4 hectares (ha) and was distributed mainly in the districts along the Tien and Hau rivers such as An Phu, Cho Moi, Phu Tan, Chau Phu, Chau Thanh, and Thoai Son districts, as can be seen in Figure 8. In addition, the area of fruits accounted for 5.0% (1.76×10^4 ha) of the natural land area of the province; this type of farming has grown strongly in recent years because of its high economic efficiency compared to other agricultural land uses. Next, the area of cash crop land occupied 1.18×10^4 ha; this was one of the land use types that farmers preferentially select to replace inefficient rice crops. Other types of land use showed a smaller area and were distributed widely (Figure 7).

The area of land use types of An Giang province in the period from 2010 to 2020 showed a gradual increase in the area of non-agricultural land (by 22.4%), as can be seen in Figure 9. The reason was the conversion of agricultural land to non-agricultural land that aimed to meet the needs of socioeconomic development of the province, especially to meet the needs for the development of infrastructure systems and residential areas due to population growth. Moreover, forest and rice crop land showed a decreasing trend. In contrast, the area of land for cash crops and fruits increased (by 24.4 and 170.6%, respectively). The above transformation trend was due to the fact that the production efficiency of rice and forest land was not high, due to the influence of acid soil, unusual weather due to climate change, and fluctuating market prices. As such, farmers have tended to switch to other crops which have higher economic efficiency such as fruits and cash crops.

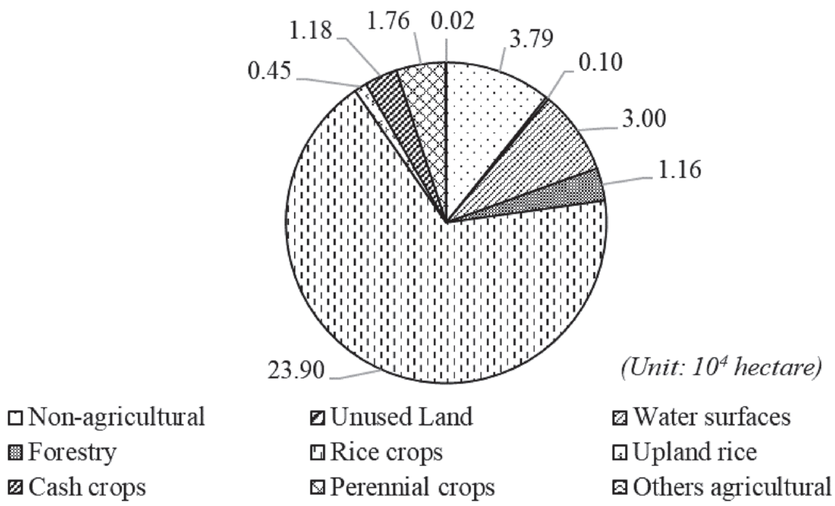

Figure 7. Percentage area of land use types in An Giang province in the year 2020.

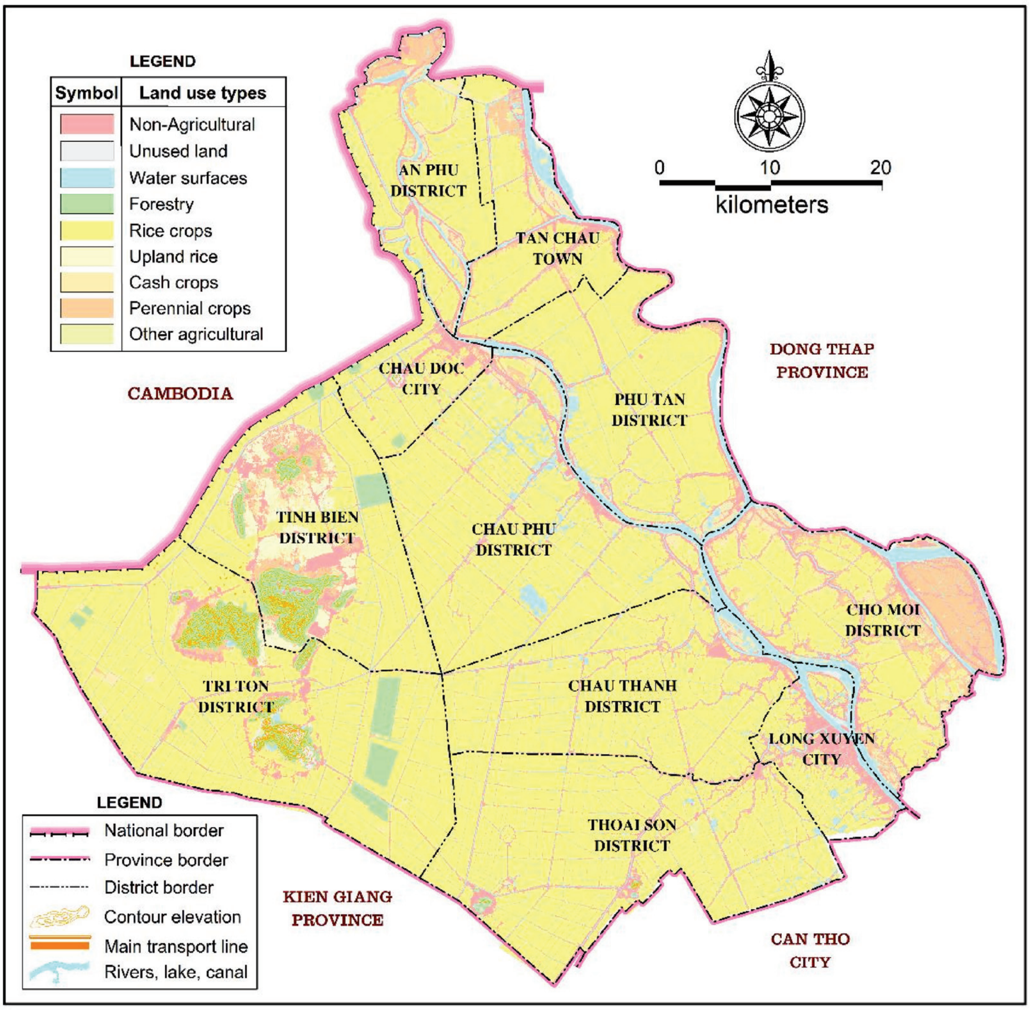

Figure 8. Land use map for An Giang province in the year 2020.

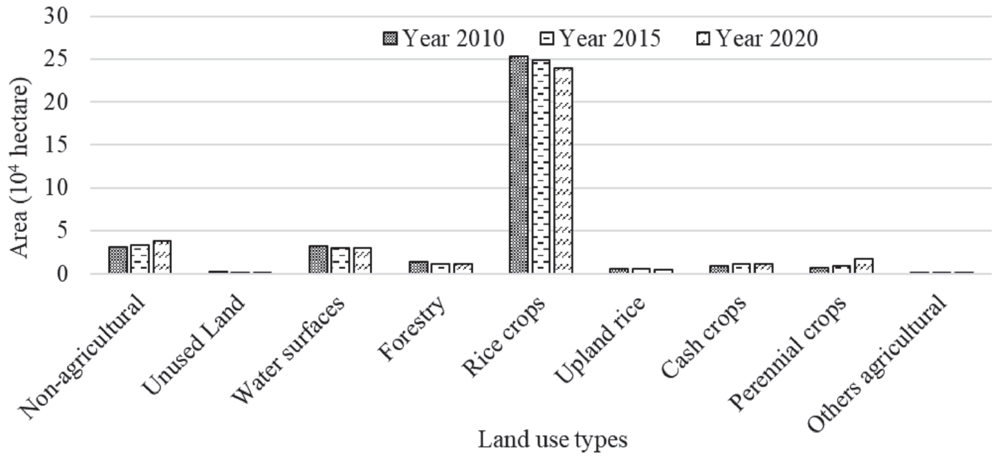

Figure 9. Changes in the area of land use types in the period of 2010–2020 in An Giang province.

Table 5 shows the area of rotation of different types of land use in the period of 2010–2020. As can be seen in Table 5, the transformation of land use types in An Giang province in the period from 2010–2020 shows widespread change.

Table 5. Land use change matrix for the period of 2010–2020 in An Giang province.

Year 2010 Year 2020	Non-Agricultural	Unused Land	Water Surfaces	Forestry	Rice Crops	Upland Rice	Cash Crops	Perennial Crops	Others Agricul-tural	Area 2010 (ha)
Non-Agricultural	26,118.8	8.6	1531.7	137.8	1464.8	94.5	432.4	1240.0	7.8	31,036.4
Unused Land	112.3	689.6	20.2	453.5	546.4	16.9	12.2	98.9	-	1949.9
Water Surfaces	3504.7	180.2	21,184.9	97.8	5570.2	61.1	736.6	849.5	15.1	32,200.1
Forestry	408.4	83.5	95.6	10,436.6	1726.1	117.7	322.8	684.6	-	13,875.2
Rice crops	5253.0	0.8	5941.0	160.2	22,5931.6	1495.6	5376.9	8621.3	51.9	252,832.3
Upland rice	397.9	10.4	66.2	77.1	1807.8	2469.0	524.6	296.7	7.4	5657.2
Cash crops	720.6	28.2	759.6	36.2	1510.8	54.6	3932.9	2278.0	-	9320.9
Perennial crops	1463.4	0.9	189.8	249.2	471.7	148.8	442.2	3530.0	10.7	6506.7
Others agricultural	9.7	1.4	2.1	0.5	47.4	-	-	5.2	84.7	151.0
Year 2020 (ha)	37,988.8	1003.5	29,791.1	11,649.0	239,076.5	4458.0	11,780.6	17,604.3	177.7	353,529.6

Figure 10 presents the map of land use changes for the period of 2010–2020 of An Giang province. From Figure 10, it is indicated that the area of other land types, such as surface water (aquaculture), has been converted to other types of land use, such as rice crops, cash crops, and fruits (as can be also seen in Table 5). This may be due to the reduced economic efficiency of aquaculture in recent years, following the sharp drop in the selling price of products. The area cultivated for rice crops also shows strong a conversion to upland rice and cash crops due to drought, which leads to a shortage of water for irrigation in the dry season. In addition, the area of land use for fruits converted from other types of land use, mainly rice and cash crops that have not brought high economic benefits. In general, the trend of changing land use types in An Giang province in the period of 2010–2020 was consistent with the province's socioeconomic development trend. However, the transformation was fragmented, not centralized, and difficult to manage and monitor for the local authorities.

The change of land use in the period from 2010 to 2020 was assessed, and when taking the associated climatic variability into consideration, it is shown that both maximum and minimum temperature were found to increase in both the wet and dry seasons under the three mentioned scenarios (especially in the dry season (mid-November to mid-May)); the increases in maximum temperature are found to be highest. The increase in the current drought frequency, as discussed previously, was found to be associated with LULCC. It is clearly indicated for the period of 2010–2020 that the area of agricultural land in An Giang province decreased and was replaced by non-agricultural land. This is due not only to its low economic efficiency, but also to changing climate conditions (especially max/min temperature) leading to a lack of irrigated water. Consequently, the area of rice crops, forestry, aquaculture, and upland rice was found to decrease within the agricultural land group (Table 5 and Figure 10).

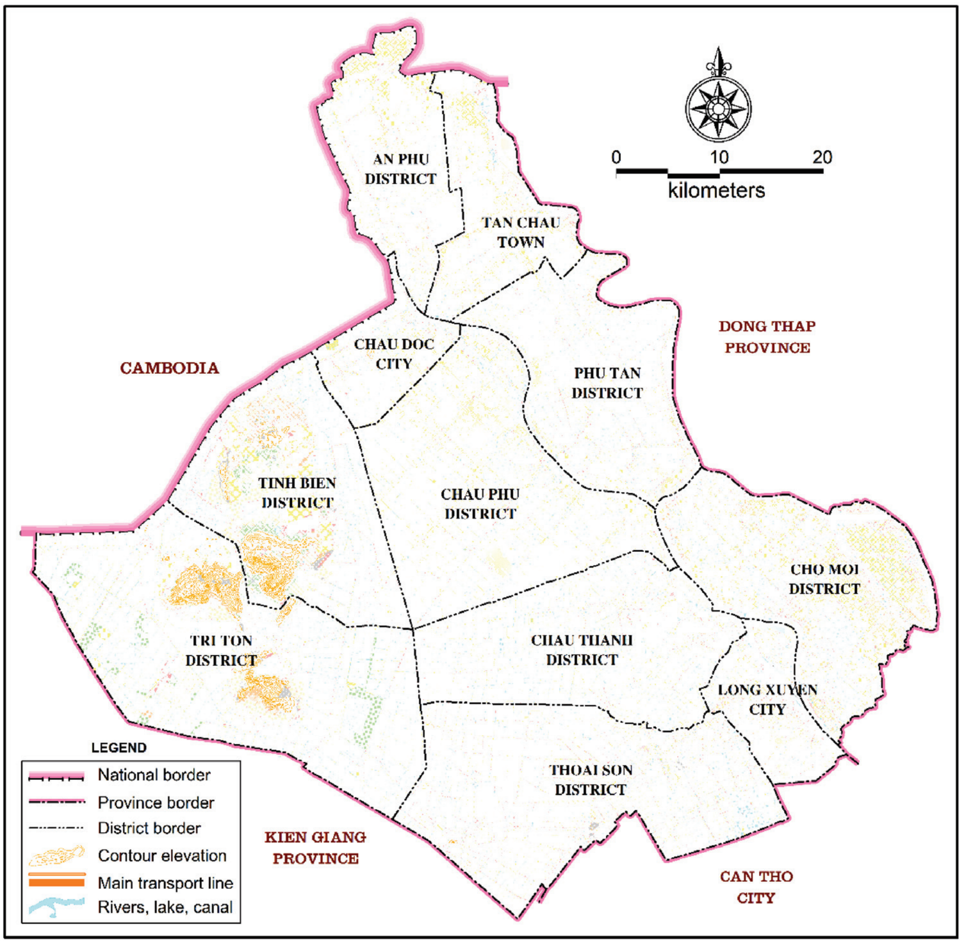

LEGEND

Year 2010	Year 2020								
PNN	PNN	CSD	DMN	DLN	LUA	LUN	CHN	CLN	NHK
CSD	PNN	CSD	DMN	DLN	LUA	LUN	CHN	CLN	-
DMN	PNN	CSD	DMN	DLN	LUA	LUN	CHN	CLN	NHK
DLN	PNN	CSD	DMN	DLN	LUA	LUN	CHN	CLN	-
LUA	PNN	-	DMN	DLN	LUA	LUN	CHN	CLN	NHK
LUN	PNN	CSD	DMN	DLN	LUA	LUN	CHN	CLN	NHK
CHN	PNN	CSD	DMN	DLN	LUA	LUN	CHN	CLN	-
CLN	PNN	-	DMN	DLN	LUA	LUN	CHN	CLN	NHK
NHK	PNN	-	DMN	-	LUA	-	-	CLN	NHK

(Note: Non-Agricultural (PNN); Unused land (CSD); Water surfaces (DMN); Forestry (DLN); Rice crops (LUA); Upland rice (LUN); Cash crops (CHN); Perennial crops (CLN) and Other agricultural (NHK)).

Figure 10. Map of land use changes for the period 2010—2020 in An Giang province.

4. Conclusions

For the period of 1980–2020, SPI 3 responded quickly to changes in precipitation, whereas SPI 9 showed a clear trend of precipitation over time. Moreover, for all-time series scales and climate change scenarios, the levels of drought in the study area were typically slight, followed by moderate. In the future, the wet period events at Chau Doc station are expected to decrease, while the occurrence of drought events is expected to increase at Tri Ton station in the semi-mountainous area.

Future precipitation and both maximum and minimum temperature are projected to increase both during the wet and dry seasons under scenarios SSP1-2.6, SSP2-4.5, and SSP5-8.5 at both Chau Doc and Tri Ton, of which, in the dry season (mid-November to mid-May next year), the increases in maximum and/or minimum temperature are found to be highest. This consequently would lead to an increase in potential evapo-transpiration (ETo) and impact on the water resources available for agriculture, and thus may ultimately lead to the conversion or change in crops or land use within the study area.

It is noted that in the period of 2010–2020, the area of agricultural land in An Giang province decreased and was replaced by non-agricultural land uses. Due to low economic efficiency, changing climatic conditions, and a lack water for irrigation, the area of rice crops, forestry, aquaculture, and upland rice tended to decrease within the agricultural land group, replaced by land for growing fruits and cash crops.

As only one RCM (CanESM5-CanOE) was considered in this study, future studies should investigate the outputs from other GCMs available from CMIP6 for the associated uncertainty analysis. In addition, the ensemble output from reliable GCMs based on their skill scores should be taken into consideration in the future.

Author Contributions: Conceptualization, H.V.T.M., P.K. and T.V.T.; methodology, P.K., H.V.T.M., P.C.N., K.L., N.K.D., N.D.G.N. and T.V.T.; formal analysis, H.V.T.M., P.C.N., K.L. and P.K.; writing—original draft preparation, K.L., N.D.G.N., H.V.T.M., P.C.N. and T.V.T.; writing—review and editing, T.V.T., K.L., N.K.D. and P.K. All authors have read and agreed to the published version of the manuscript.

Funding: This research received no external funding.

Institutional Review Board Statement: Not applicable.

Informed Consent Statement: Not applicable.

Data Availability Statement: Not applicable.

Conflicts of Interest: The authors declare no conflict of interest.

Appendix A

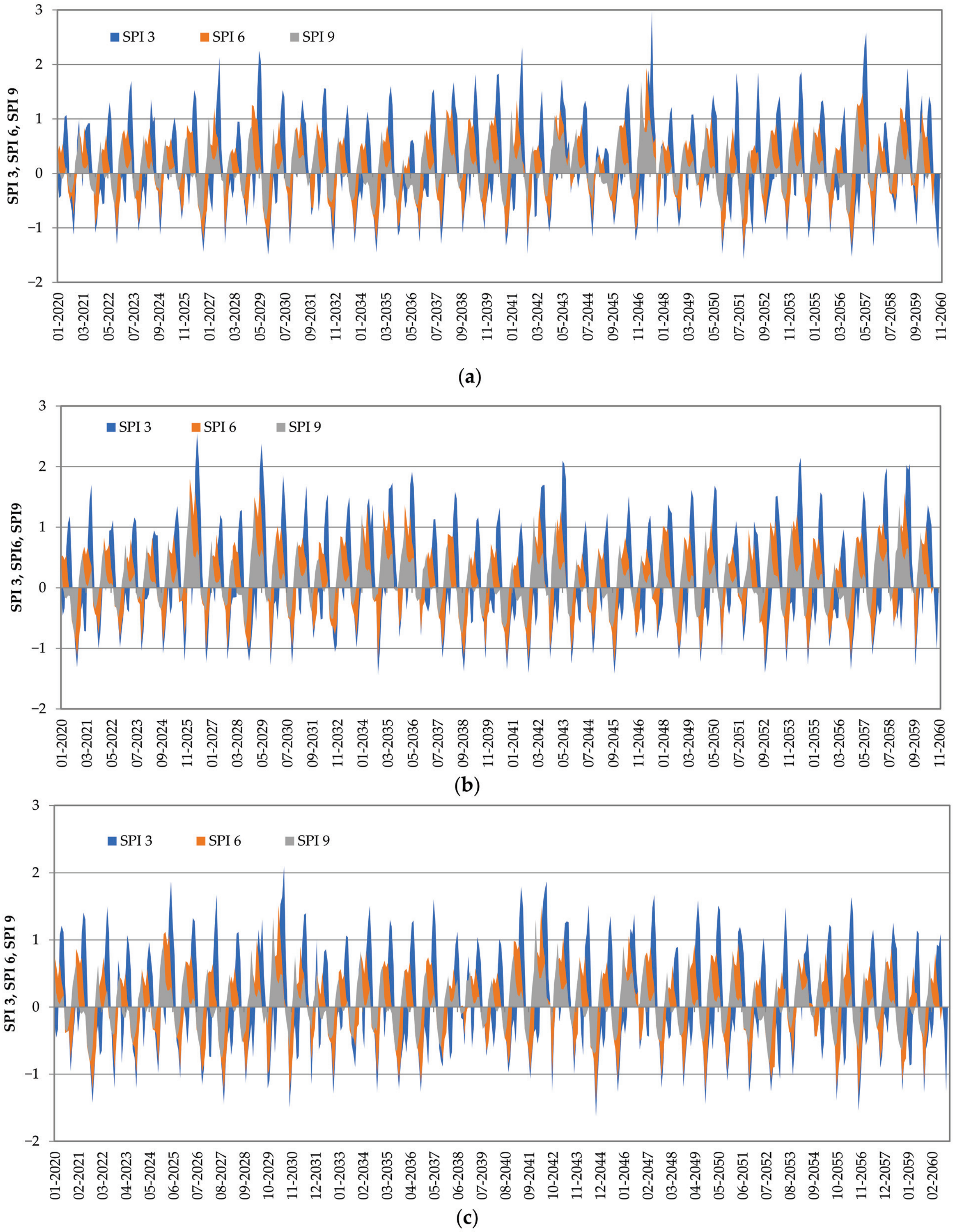

Figure A1. Different time series (SPI 3, SPI 6, SPI 9) for monthly drought patterns at Tri Ton meteorological station using various climate change scenarios, SSPI 2.6 (**a**), SSP2 4.5 (**b**), and SSP5 8.5 (**c**).

Appendix B

Table A1. Number of occurrences of drought and humidity in the different patterns of SPI using climate change data at Tri Ton station.

Categories	SSP 1_2.6			SSP 2_4.5			SSP5_8.5		
	SPI 3	SPI 6	SPI 9	SPI 3	SPI 6	SPI 9	SPI 3	SPI 6	SPI 9
Extreme drought	0	0	0	0	0	0	0	0	0
Severe drought	2	0	0	0	0	0	2	0	0
Moderate drought	41	18	0	36	20	0	36	19	0
Slight drought	99	91	30	94	87	23	108	83	34
Very slight drought	0	0	0	0	0	0	0	0	0
Very slightly wet	29	68	91	17	56	85	30	84	75
Slightly wet	55	119	63	64	126	72	73	106	46
Moderately wet	64	24	6	58	30	9	61	6	2
Severely wet	25	2	1	30	5	1	15	2	0
Extremely wet	7	0	0	9	0	0	1	0	0

References

1. Keshavarz, M.; Maleksaeidi, H.; Karami, E. Livelihood Vulnerability to Drought: A Case of Rural Iran. *Int. J. Disaster Risk Reduct.* **2017**, *21*, 223–230. [CrossRef]
2. Thao, N.T.T.; Khoi, D.N.; Xuan, T.T.; Tychon, B. Assessment of Livelihood Vulnerability to Drought: A Case Study in Dak Nong Province, Vietnam. *Int. J. Disaster Risk Sci.* **2019**, *10*, 604–615. [CrossRef]
3. Reed, M.S.; Podesta, G.; Fazey, I.; Geeson, N.; Hessel, R.; Hubacek, K.; Letson, D.; Nainggolan, D.; Prell, C.; Rickenbach, M. Combining Analytical Frameworks to Assess Livelihood Vulnerability to Climate Change and Analyse Adaptation Options. *Ecol. Econ.* **2013**, *94*, 66–77. [CrossRef]
4. Angassa, A.; Oba, G. Herder Perceptions on Impacts of Range Enclosures, Crop Farming, Fire Ban and Bush Encroachment on the Rangelands of Borana, Southern Ethiopia. *Hum. Ecol.* **2008**, *36*, 201–215. [CrossRef]
5. Keshavarz, M.; Karami, E. Farmers' Decision-Making Process under Drought. *J. Arid Environ.* **2014**, *108*, 43–56. [CrossRef]
6. Tfwala, C.; Mengistu, A.; Seyama, E.; Mosia, M.; van Rensburg, L.; Mvubu, B.; Mbingo, M.; Dlamini, P. Nationwide Temporal Variability of Droughts in the Kingdom of Eswatini: 1981–2018. *Heliyon* **2020**, *6*, e05707. [CrossRef] [PubMed]
7. Dong, Z.; Liu, H.; Hu, H.; Khan, M.Y.A.; Wen, J.; Chen, L.; Tian, F. Future Projection of Seasonal Drought Characteristics Using CMIP6 in the Lancang-Mekong River Basin. *J. Hydrol.* **2022**, *610*, 127815. [CrossRef]
8. Barbosa, P.; Masante, D.; Arias Muñoz, C.; Cammalleri, C.; De Jager, A.; Magni, D.; Mazzeschi, M.; McCormick, N.; Naumann, G.; Spinoni, J. *JRC Technical Report, Droughts in Europe and Worldwide 2019–2020*; Publications Office of the European Union: Luxembourg, 2021.
9. Vicente-Serrano, S.M.; Quiring, S.M.; Pena-Gallardo, M.; Yuan, S.; Dominguez-Castro, F. A Review of Environmental Droughts: Increased Risk under Global Warming? *Earth-Sci. Rev.* **2020**, *201*, 102953. [CrossRef]
10. Basin, M.R. *Mekong River Commission Drought Management Strategy for the Lower Mekong Basin 2020–2025*; Mekong River Commission Secretariat: Quai Fa Ngum, Vietnam, 2019.
11. Te, N. Drought Management in the Lower Mekong Basin. In Proceedings of the 3rd South Asia Water Forum, Kuala Lumpur, Malaysia, 22–26 October 2007; pp. 13–15.
12. Wang, T.; Tu, X.; Singh, V.P.; Chen, X.; Lin, K. Global Data Assessment and Analysis of Drought Characteristics Based on CMIP6. *J. Hydrol.* **2021**, *596*, 126091. [CrossRef]
13. Chen, F.; Gao, Y.; Wang, Y.; Li, X. A Downscaling-Merging Method for High-Resolution Daily Precipitation Estimation. *J. Hydrol.* **2020**, *581*, 124414. [CrossRef]
14. Zhao, N.; Jiao, Y.; Zhang, L. Projections of Precipitation Change from CMIP6 Based on a New Downscaling Method in the Poyang Lake Basin, China. *J. Hydrol. Reg. Stud.* **2022**, *42*, 101138. [CrossRef]
15. Rivera, J.A.; Arnould, G. Evaluation of the Ability of CMIP6 Models to Simulate Precipitation over Southwestern South America: Climatic Features and Long-Term Trends (1901–2014). *Atmos. Res.* **2020**, *241*, 104953. [CrossRef]
16. Andersson, E.; Bauer, P.; Beljaars, A.; Chevallier, F.; Hólm, E.; Janisková, M.; Kållberg, P.; Kelly, G.; Lopez, P.; Mcnally, A. Assimilation and Modeling of the Atmospheric Hydrological Cycle in the ECMWF Forecasting System. *Bull. Am. Meteorol. Soc.* **2005**, *86*, 387–402. [CrossRef]
17. Masson-Delmotte, V.; Zhai, P.; Pirani, A.; Connors, S.L.; Péan, C.; Berger, S.; Caud, N.; Chen, Y.; Goldfarb, L.; Gomis, M. The IPCC finalized the first part of the Sixth Assessment Report, Climate Change 2021. In Proceedings of the Physical Science Basis, the Working Group I contribution to the Sixth Assessment Report on 6 August 2021 during the 14th Session of Working Group I and 54th Session of the IPCC, Cambridge, UK and New York, NY, USA, 26 July–6 August 2021; Volume 16, p. 2.

18. Pascale, S.; Lucarini, V.; Feng, X.; Porporato, A. Analysis of Rainfall Seasonality from Observations and Climate Models. *Clim. Dyn.* **2015**, *44*, 3281–3301. [CrossRef]
19. Deininger, M.; McDermott, F.; Cruz, F.W.; Bernal, J.P.; Mudelsee, M.; Vonhof, H.; Millo, C.; Spötl, C.; Treble, P.C.; Pickering, R. Inter-Hemispheric Synchroneity of Holocene Precipitation Anomalies Controlled by Earth's Latitudinal Insolation Gradients. *Nat. Commun.* **2020**, *11*, 1–9. [CrossRef]
20. United Nations. Transforming Our World: The 2030 Agenda for Sustainable Development. Available online: https://wedocs.unep.org/20.500.11822/9814 (accessed on 9 June 2022).
21. Pokhrel, Y.; Felfelani, F.; Satoh, Y.; Boulange, J.; Burek, P.; Gädeke, A.; Gerten, D.; Gosling, S.N.; Grillakis, M.; Gudmundsson, L. Global Terrestrial Water Storage and Drought Severity under Climate Change. *Nat. Clim. Change* **2021**, *11*, 226–233. [CrossRef]
22. Irannezhad, M.; Minaei, M.; Ahmadian, S.; Chen, D. Impacts of Changes in Climate and Land Cover-Land Use on Flood Characteristics in Gorganrood Watershed (Northeastern Iran) during Recent Decades. *Geogr. Ann. Ser. Phys. Geogr.* **2018**, *100*, 340–350. [CrossRef]
23. Irannezhad, M.; Liu, J. Evaluation of Six Gauge-Based Gridded Climate Products for Analyzing Long-Term Historical Precipitation Patterns across the Lancang-Mekong River Basin. *Geogr. Sustain.* **2022**, *3*, 85–103. [CrossRef]
24. Ge, F.; Zhu, S.; Luo, H.; Zhi, X.; Wang, H. Future Changes in Precipitation Extremes over Southeast Asia: Insights from CMIP6 Multi-Model Ensemble. *Environ. Res. Lett.* **2021**, *16*, 024013. [CrossRef]
25. Supharatid, S.; Nafung, J.; Aribarg, T. Projected Changes in Temperature and Precipitation over Mainland Southeast Asia by CMIP6 Models. *J. Water Clim. Change* **2022**, *13*, 337–356. [CrossRef]
26. Khoi, D.N.; Sam, T.T.; Chi, N.T.T.; Linh, D.Q.; Nhi, P.T.T. Impact of Future Climate Change on River Discharge and Groundwater Recharge: A Case Study of Ho Chi Minh City, Vietnam. *J. Water Clim. Change* **2022**, *13*, 1313–1325. [CrossRef]
27. McKee, T.B.; Doesken, N.J.; Kleist, J. *Drought Monitoring with Multiple Time Scales*; Applied Climatology, American Meteorological Society: Dallas, TX, USA, 1995; pp. 233–236.
28. Hong, N.V.; Tho, P.T.; Giai, N.S. The Ability to Use SPI Index in Assessing the Effects of Dry and Wet Conditions on Rice Yield in the Can Tho—Hau Giang Region. *J. Sci. Clim. Change* **2018**, *5*, 36–42.
29. Caloiero, T.; Sirangelo, B.; Coscarelli, R.; Ferrari, E. Occurrence Probabilities of Wet and Dry Periods in Southern Italy through the SPI Evaluated on Synthetic Monthly Precipitation Series. *Water* **2018**, *10*, 336. [CrossRef]
30. Danandeh Mehr, A.; Sorman, A.U.; Kahya, E.; Hesami Afshar, M. Climate Change Impacts on Meteorological Drought Using SPI and SPEI: Case Study of Ankara, Turkey. *Hydrol. Sci. J.* **2020**, *65*, 254–268. [CrossRef]
31. Abbasi, A.; Khalili, K.; Behmanesh, J.; Shirzad, A. Drought Monitoring and Prediction Using SPEI Index and Gene Expression Programming Model in the West of Urmia Lake. *Theor. Appl. Climatol.* **2019**, *138*, 553–567. [CrossRef]
32. Yahaya, T.I.; Muhammed, M. Assessing Rainfall Variability Impacts Using Agricultural Index (ARI) on Cassava Growth in Ilorin Area of Kwara State, Nigenia. *Int. J. Environ. Policy Issues. Geo-Stud. Forum* **2013**, *6*, 158–170.
33. Won, J.; Choi, J.; Lee, O.; Kim, S. Copula-Based Joint Drought Index Using SPI and EDDI and Its Application to Climate Change. *Sci. Total Environ.* **2020**, *744*, 140701. [CrossRef]
34. Sierra-Soler, A.; Adamowski, J.; Malard, J.; Qi, Z.; Saadat, H.; Pingale, S. Assessing Agricultural Drought at a Regional Scale Using LULC Classification, SPI, and Vegetation Indices: Case Study in a Rainfed Agro-Ecosystem in Central Mexico. *Geomat. Nat. Hazards Risk* **2016**, *7*, 1460–1488. [CrossRef]
35. McNicoll, G. Regions at Risk: Comparisons of Threatened Environments. *Popul. Dev. Rev.* **1996**, *22*, 380–381. [CrossRef]
36. Veldkamp, A.; Lambin, E.F. Predicting Land-Use Change. *Agric. Ecosyst. Environ.* **2001**, *85*, 1–6. [CrossRef]
37. TT Duong, M.; Samsura, D.; van der Krabben, E. Land Conversion for Tourism Development under Vietnam's Ambiguous Property Rights over Land. *Land* **2020**, *9*, 204. [CrossRef]
38. Appelt, J.L.; Garcia Rojas, D.C.; Verburg, P.H.; van Vliet, J. Socioeconomic Outcomes of Agricultural Land Use Change in Southeast Asia. *Ambio* **2022**, *51*, 1094–1109. [CrossRef] [PubMed]
39. Andrianto, A.; Komarudin, H.; Pacheco, P. Expansion of Oil Palm Plantations in Indonesia's Frontier: Problems of Externalities and the Future of Local and Indigenous Communities. *Land* **2019**, *8*, 56. [CrossRef]
40. Lognonné, P.; Banerdt, W.B.; Pike, W.; Giardini, D.; Christensen, U.; Garcia, R.F.; Kawamura, T.; Kedar, S.; Knapmeyer-Endrun, B.; Margerin, L. Constraints on the Shallow Elastic and Anelastic Structure of Mars from InSight Seismic Data. *Nat. Geosci.* **2020**, *13*, 213–220. [CrossRef]
41. Benevenuto, R.F.; Agapito-Tenfen, S.Z.; Vilperte, V.; Wikmark, O.-G.; van Rensburg, P.J.; Nodari, R.O. Molecular Responses of Genetically Modified Maize to Abiotic Stresses as Determined through Proteomic and Metabolomic Analyses. *PLoS ONE* **2017**, *12*, e0173069. [CrossRef]
42. Rosenzweig, C.; Elliott, J.; Deryng, D.; Ruane, A.C.; Müller, C.; Arneth, A.; Boote, K.J.; Folberth, C.; Glotter, M.; Khabarov, N. Assessing Agricultural Risks of Climate Change in the 21st Century in a Global Gridded Crop Model Intercomparison. *Proc. Natl. Acad. Sci. USA* **2014**, *111*, 3268–3273. [CrossRef]
43. Ashraf, M.A.; Akbar, A.; Askari, S.H.; Iqbal, M.; Rasheed, R.; Hussain, I. Recent Advances in Abiotic Stress Tolerance of Plants through Chemical Priming: An Overview. *Adv. Seed Priming* **2018**, 51–79.
44. Department of Agriculture and Rural Development An Giang. *Report on the Results of Agricultural Production in 2020 on the Agricultural Production Development Plan in 2021*; Department of Agriculture and Rural Development An Giang: Long Xuyen, An Giang, Vietnam, 2021; p. 35.

45. General Statistical Office of Vietnam (GSO). *Statistical Yearbook of An Giang 2020*; An Giang Statistical Office: Long Xuyen, An Giang, Vietnam, 2020.
46. General Statistics Office Of Vietnam (GSO). *Statistical Year Book of Vietnam 2019*; General Statistics Office Of Vietnam: Ha Noi, Vietnam, 2019.
47. Minh, H.V.T.; van Ty, T.; Avtar, R.; Kumar, P.; Le, K.N.; Ngan, N.V.C.; Khanh, L.H.; Nguyen, N.C.; Downes, N.K. Implications of Climate Change and Drought on Water Requirements in a Semi-Mountainous Region of the Vietnamese Mekong Delta. *Environ. Monit. Assess.* **2022**, *194*, 766. [CrossRef]
48. McKee, T.B.; Doesken, N.J.; Kleist, J. The Relationship of Drought Frequency and Duration to Time Scales. In Proceedings of the 8th Conference on Applied Climatology, Boston, MA, USA, 17–22 January 1993; Volume 17, pp. 179–183.
49. Agnew, C. Using the SPI to Identify Drought. *Natl. Drought Mitig. Cent. Univ. Neb. Linc.* **2000**, *1*, 6–12.
50. Soleimani, H.; Ahmadi, H.; Zehtabian, G. Comparison of Temporal and Spatial Trend of SPI, DI and CZI as Important Drought Indices to Map Using IDW Method in Taleghan Watershed. *Ann. Biol. Res.* **2013**, *4*, 46–55.
51. Ty, T.V.; Hoai, D.T.T.H.; Minh, H.V.T. Mapping Meteorological Drought in the Mekong Delta under Climate Change. *Can. Tho. Univ. J. Sci.* **2015**, *2025*, 226–233.
52. Vicente-Serrano, S.M. Differences in Spatial Patterns of Drought on Different Time Scales: An Analysis of the Iberian Peninsula. *Water Resour. Manag.* **2006**, *20*, 37–60. [CrossRef]
53. Thang, N.V.; Khiem, M.V. The Assessment and Estimate Dry Condition by SPI Indicator for the VMD Bu Using the SPI Index. *Vietnam J. Hydrometeorol.* **2017**, *6*, 1–9.
54. Minh, H.V.T.; Lavane, K.; Ty, T.V.; Downes, N.K.; Hong, T.T.K.; Kumar, P. Evaluation of the Impact of Drought and Saline Water Intrusion on Rice Yields in the Mekong Delta, Vietnam. *Water* **2022**, *14*, 3499. [CrossRef]
55. IPCC. *Climate Change 2014: Synthesis Report. Contribution of Working Groups I, II and III to the Fifth Assessment Report of the Intergovernmental Panel on Climate Change*; Intergovernmental Panel on Climate Change: Geneva, Switzerland, 2014; p. 151.
56. Eyring, V.; Bony, S.; Meehl, G.A.; Senior, C.A.; Stevens, B.; Stouffer, R.J.; Taylor, K.E. Overview of the Coupled Model Intercomparison Project Phase 6 (CMIP6) Experimental Design and Organization. *Geosci. Model Dev.* **2016**, *9*, 1937–1958. [CrossRef]
57. Try, S.; Tanaka, S.; Tanaka, K.; Sayama, T.; Khujanazarov, T.; Oeurng, C. Comparison of CMIP5 and CMIP6 GCM Performance for Flood Projections in the Mekong River Basin. *J. Hydrol. Reg. Stud.* **2022**, *40*, 101035. [CrossRef]
58. Riahi, K.; Krey, V.; Rao, S.; Chirkov, V.; Fischer, G.; Kolp, P.; Kindermann, G.; Nakicenovic, N.; Rafai, P. RCP-8.5: Exploring the Consequence of High Emission Trajectories. *Clim. Change* **2011**, *10*, 1007.
59. Thomson, A.M.; Calvin, K.V.; Smith, S.J.; Kyle, G.P.; Volke, A.; Patel, P.; Delgado-Arias, S.; Bond-Lamberty, B.; Wise, M.A.; Clarke, L.E. RCP4. 5: A Pathway for Stabilization of Radiative Forcing by 2100. *Clim. Change* **2011**, *109*, 77–94. [CrossRef]
60. Hay, L.E.; Wilby, R.L.; Leavesley, G.H. A Comparison of Delta Change and Downscaled GCM Scenarios for Three Mountainous Basins in the United States 1. *JAWRA J. Am. Water Resour. Assoc.* **2000**, *36*, 387–397. [CrossRef]
61. Ines, A.V.; Hansen, J.W. Bias Correction of Daily GCM Rainfall for Crop Simulation Studies. *Agric. For. Meteorol.* **2006**, *138*, 44–53. [CrossRef]

land

Article

Identification of Facade Elements of Traditional Areas in Seoul, South Korea

Donghwa Shon [1], Giyoung Byun [2] and Soyoung Choi [3,*]

[1] Department of Architecture, Chungbuk National University, Cheongju 28644, Republic of Korea
[2] Department of Civil and Environmental Engineering, Korea Advanced Institute of Science and Technology, Daejeon 34141, Republic of Korea
[3] Institute of Construction and Environmental Engineering, Seoul National University, Seoul 08826, Republic of Korea
* Correspondence: y5087@snu.ac.kr; Tel.: +82-2-880-8869

Abstract: The Bukchon area in Seoul boasts a high density of Hanok, the traditional Korean architecture representing the region. Because the Hanok facade plays a vital role in the streetscape formation, we must record it in terms of social, cultural, historical, artistic, and scenic values. However, recording the facade of an existing Hanok building through drawing or image information is time consuming and labor intensive, and therefore costly. Further, its digital conversion is inherently difficult. This study proposes the use of deep learning to identify the form elements that comprise the Hanok facade. Three-dimensional modeling was performed on 405 well-preserved Hanok facades in the region, and 2808 items of image data were created under similar conditions and at differing angles. Labeling was performed on the shape elements of the Hanok facade, and a methodology was established to identify the facade elements using MASK R-CNN. The type of roof, windows, the lower part of the outer wall, and the design were identified with high accuracy.

Keywords: deep learning; mask R-CNN; Hanok; facade; form element

1. Introduction

A street is the smallest unit of city through which humans can navigate the city and the combination of streets defines its physical form and image [1,2]. Additionally, it is the smallest unit of public space that contains daily human life and continues to create the region's characteristics. To restore localities and improve the image and competitiveness of the city as a whole, it is crucial to understand street-level spaces [3]. We must maintain and restore local characteristics by overcoming the limitations of area management methods such as zoning, and by implementing unique rules (codes) in the street that reflect regional characteristics [4,5]. In Korea, the "District unit plans" and "Special street zones" systems stipulate detailed building standards at the street level [6,7].

The street space comprises various physical elements, such as architecture, roads, landscaping, and humans, and buildings are the essential elements. A building is a socio-cultural product, an artificial structure created by human beings through social agreement, following local rules [8]. For this reason, buildings significantly contribute to forming regional characteristics by influencing the streetscape. The exterior of a building exposed to the street space comprises elements such as the number of floors, outline of the building, color, windows and doors, structure, and finishing materials, and the combination of these elements determines the character of the street. Understanding the morphological rules of the building exterior makes it easy to establish a street unit policy based on locality or to make an architectural design.

To understand the morphological rules of the exterior of buildings in the region, we must examine the available records. Building exterior records of traditional buildings in densely populated areas are useful because planning information for such areas is no longer available. Studies are being conducted to record historical, artistic, and scenic values of traditional areas that are losing their local characteristics because of development. For instance, facade drawings are prepared through actual measurements or recorded as photographic information of existing buildings. Additionally, there are attempts to create three-dimensional records by obtaining 3D shape information using a sensor. These records are provided with high-quality information through web services [9–13]. However, it is difficult to understand the locality well through the rules concerning building exteriors alone. Therefore, in addition to recording drawings, images, and shape information, detailed form elements that form the exterior of a building should be classified and recorded. Further, features occurring in a region can be presented as a form-based code (FBC) [14].

Building exterior information is crucial in digital twin advancement and the implementation of building information modeling (BIM) information conversion in addition to value records for exploring the locality. Adding data properties to image or shape information can be extended and linked with the BIM model. Form elements can be identified from image information and built into digital data through a pre-designed BIM library. However, classifying the exterior information of each building located in the street space is time consuming and expensive. Modern buildings can utilize digital drawing information; however, for traditional buildings without drawings, exterior information must be newly recorded. A deep learning-based image processing method, which has been actively and extensively researched, is expected to effectively identify the form elements constituting the exterior of a building.

This study utilizes a deep learning model to identify the form elements that constitute the facade of a traditional South Korean building, the Hanok. Before applying the model to modern buildings with a diverse morphological range, we first applied it to traditional buildings with complex forms, but simple combination principles. The deep learning model utilized detectron2's Mask R-CNN. The target site was a building (Hanok) constructed recently in a traditional area (Bukchon) in Jongno-gu, Seoul, Korea (Figure 1). After selecting well-preserved Hanok cases, these were modeled with BIM (Revit) similarly to the actual ones, and 2808 images rendered under the same conditions were extracted. After labeling the form elements constituting the Hanok facade, the form elements were identified through Mask R-CNN (Figures 1 and 2).

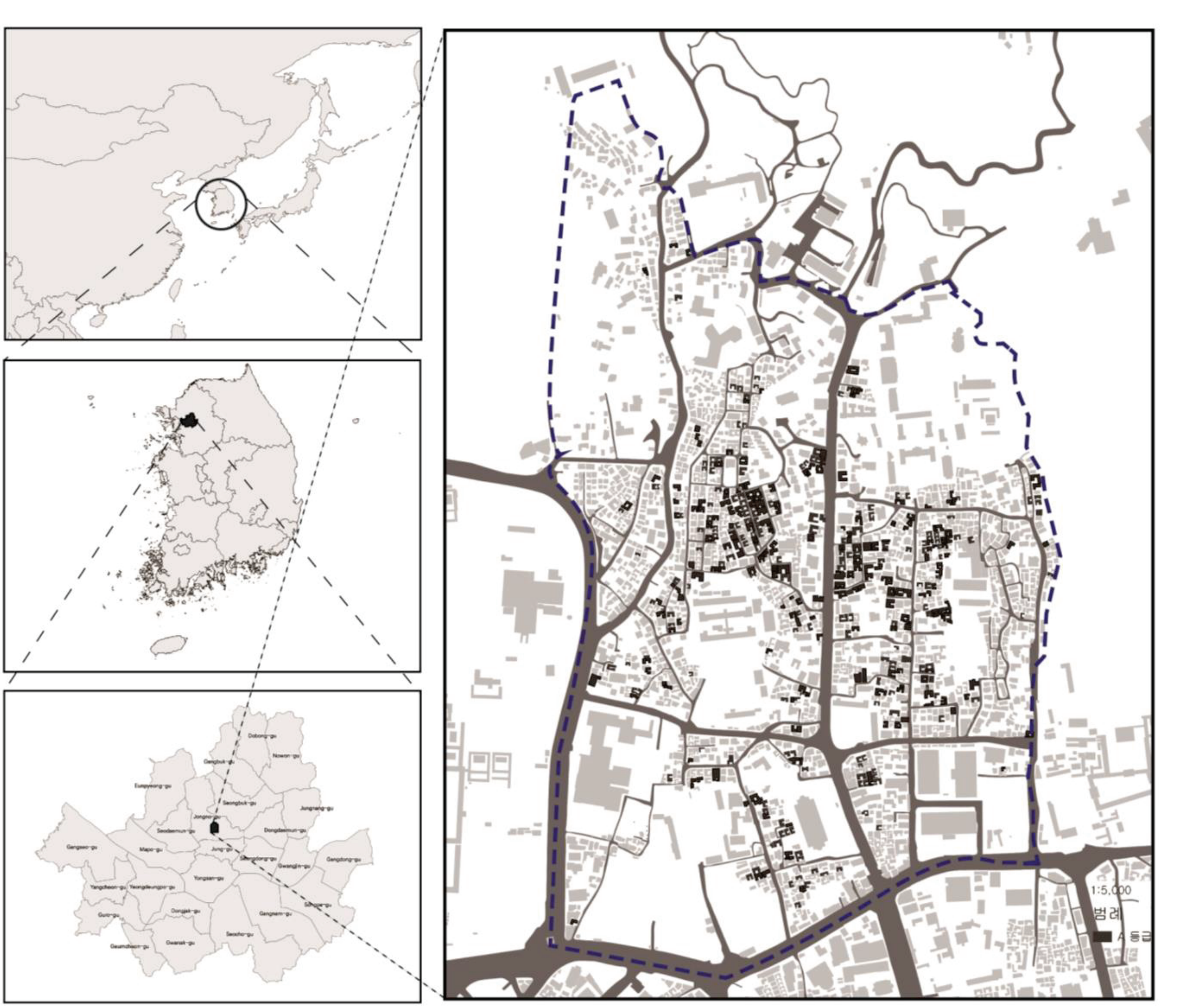

Figure 1. Location and target Hanok in the Bukchon area in Seoul, Korea.

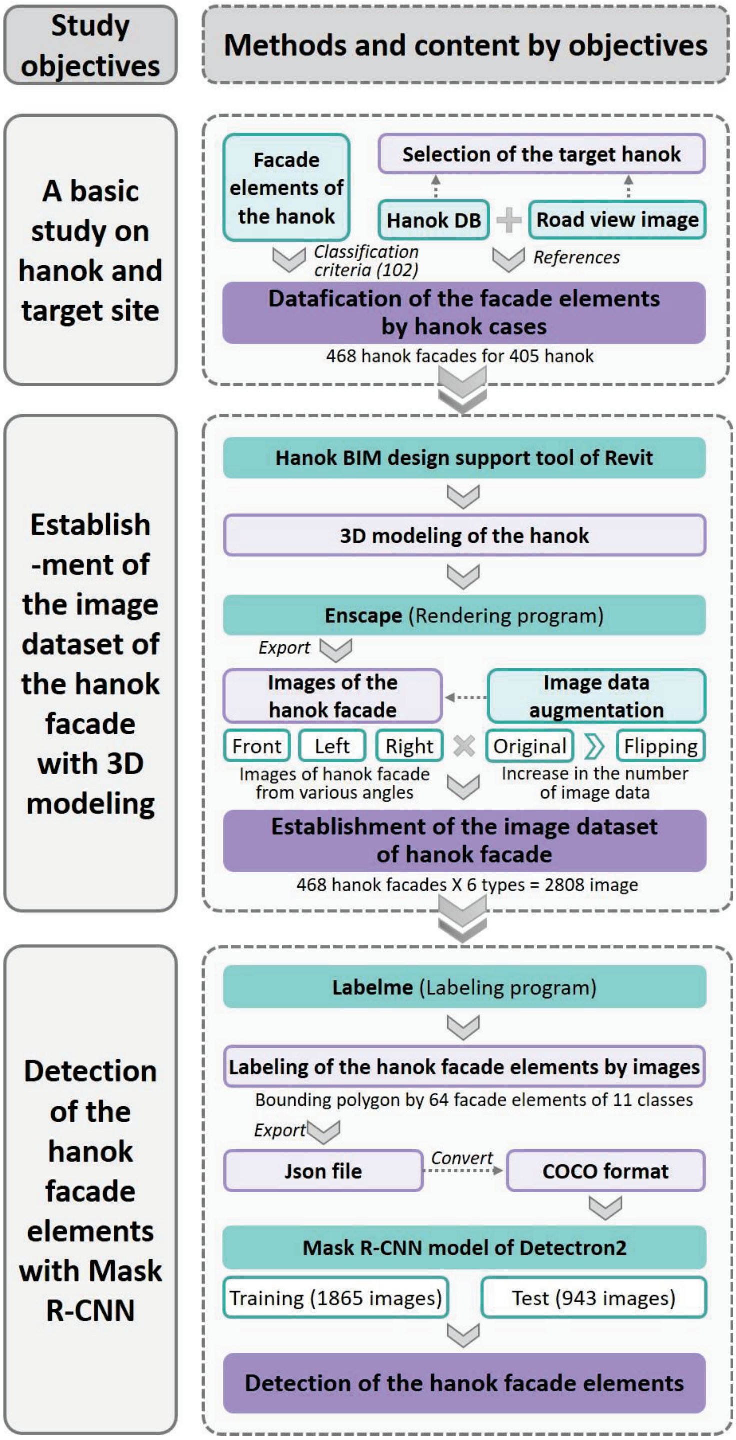

Figure 2. Flowchart of research.

2. Literature Review

2.1. Street and Place

A street is the smallest unit of public space where daily life occurs [1]. Visitors experience the city first from the street, and the city is formed and defined by a combination of these streets [1,2]. A street is a space that can be easily encountered in daily life and where locality is well revealed [15]. Although numerous researchers have mentioned the importance of street spaces, they are often underestimated compared to urban planning or architectural design within a lot.

Urban planning in several countries, including the United States [16], Canada [17], France [18], Japan [19], and South Korea [20], determines architectural behavior through zoning. Zoning is an urban management tool that suppresses the quantitative expansion of the city by controlling the building behavior in an area after classifying the developmental scope and use of the area [21]. Lots can be classified into residential, commercial, and industrial types, and the density, height, size, green area, and parking can be regulated. Single-use zoning allows a village to form a community of local residents, but it is difficult to access for visitors [1]. In contrast, downtown areas are easy for visitors to access but have a disadvantage in that it is difficult to form a community [1]. To compensate for each disadvantage, multiuse zones in which different uses are mixed have emerged. With the mixing of residential and commercial areas, there are examples of a balance between attracting visitors and improving the community of local residents [1]. Although this was developed to subdivide the use area, because it was a top-down plan that prioritized efficient management, it was laborious to consider the characteristics of the area or community. Regional characteristics can be approached with the concept of place, and it is difficult to include the sociocultural values, residents' activities, and physical characteristics of the region in detail. Accordingly, street unit plans are based on regions or places that appeared under New Urbanism [22]. New Urbanists attempted to manage the quality level of the public area with a street unit plan and proposed a detailed regulation plan for the shape of the building [22]. Local officials proposed the shape-based code to maintain regional characteristics by establishing rules for controlling the shape of buildings [4,5].

In a street space, places are formed through the physical environment, human social activities, meanings, and experiences [23]. The physical environment of the street is composed of various elements, such as buildings, walking paths, landscaping, and roads, and contains the social activities and meanings of the region. In particular, the essential element that composes the street space is buildings, and they are crucial in shaping the atmosphere of the street space while representing the regional characteristics. Because a building is an artificial structure created by human beings through social agreement, it contains local rules, such as the number of floors, building outline, color, windows, structure, and finishing materials [8]. Because a building is a social and cultural product of human beings, it is apparent that understanding the shape of a building comprehends all aspects of a local place. However, by understanding the physical rules, we can understand the sociocultural meaning and activities of the region. Furthermore, we can use regional characteristics by presenting a specific form known as FBC.

2.2. Traditional Architecture in the Modern Period of Seoul: Urban Hanok in Bukchon

In Seoul, traditional buildings are concentrated in the Bukchon area (Figure 3). Located next to the Gyeongbokgung Palace and Changdeokgung Palace in the center of Seoul, it was the residence of influential people during the Joseon Dynasty. Recently, it is being used as a residential area while preserving traditional buildings [24]. However, in the early 1900s, as the population exploded in Seoul, the housing crisis escalated, and the land in the Bukchon residential area was divided to build Hanok [24]. As it was built by dividing a lot, the walls and the building were matched, and an urban Hanok with a narrow yard was constructed [24]. This type of Hanok was continuously built until the 1960s, but began to be demolished because of rapid development [24]. However, in 2000, a social movement for preserving traditional sites emerged. Through government funding and repair support policies, the number of Hanoks increased and the region established itself as a representative traditional building concentration area in Seoul [24].

Figure 3. Streetscape and urban Hanok in the Bukchon area.

The Bukchon area is formed along the valley that flows north to south. Naturally formed streets, those created through land readjustment in the early 1900s, and roads expanded until the 1980s reached the current road system [24]. The street width in these areas varies from a narrow street of approximately 2 m to a wide road where cars can pass, but most are narrow. In addition, when dividing a large lot, the street is connected to the dwellings in each lot, and the buildings and streets arranged along the south side show regularity [25].

Hanoks in the Bukchon area are built on a dense background by dividing a large lot and on the street boundary to form a unique streetscape. Therefore, urban Hanoks in the Bukchon area are morphologically different from those in the suburbs. Furthermore, since urban Hanok were built in modern times, materials such as glass, tiles, and bricks were also used and supplied in a relatively standardized form [25]. Hanok legally refers to a building with a wooden main structure with columns, beams, and a Korean-style roof, and reflects the traditional Korean architectural style [26]. The Hanok exposed from the street can be identified by such legally defined features and the stylobate, outer walls, openings, gates, and walls, and the facade is composed according to the combination of these elements. In some cases, Hanoks in the Bukchon area have traditional elements that are well preserved, and in others, were improved in the modern era.

2.3. Image Processing for Building Facade

Object detection in computer vision (CV) was used to detect features through a rather cumbersome process. However, with the advent of deep learning technology, the level of technology from object detection to classification has expanded, and the accuracy of object detection using learning data has increased. A deep learning model for image processing has been developed based on convolutional neural networks (CNNs) [27]. Since the development of the R-CNN model [28], an early object detection model, in 2013, various deep learning models have emerged. Faster R-CNN [29], you only look once (YOLO) [30,31], and Detectron are representative models that have improved accuracy, speed, and platform versatility. Recognition technology using elemental features has been steadily developed in the field of deep learning. Using a neural network, a classifier that categorizes possible distortions in images into four categories and quantifies the level of image distortion to obtain a special and more accurate estimate of image quality [32,33] was trained.

Mask R-CNN is effective for object identification with complex shapes [34]. It is more accurate than the rectangular area object identification model because the object segments it. The model selects candidates for areas where objects in the image are likely to be and undergoes a two-step process of extracting latent features of classification, bounding box regression, and segmentation. It has achieved high accuracy for complex shapes, but it is computationally taxing.

Research on identifying exterior building information using deep learning technology has been conducted to identify components or detect construction or structural combinations. These studies have primarily focused on extracting building outlines, facade features, and exterior wall materials. Before the deep learning technology was applied, the building outline, brightness, and feature points were extracted based on CV. A minimum spanning tree (MST) algorithm was proposed to analyze image pixels to identify windows or doors on the elevation of a building with a probability of 70% [35]. A study to detect the entrance or windows of a building by extracting and synthesizing the characteristics of lines, colors, and textures has also been conducted [36]. Another study was conducted to identify the shape of the roof using aerial photographs. Hipped, flat, and gable roofs were classified based on the pattern of the pixel structure of the shape image [37]. As the resolution of aerial photographs has increased over time, it has become possible to precisely obtain the shape of buildings and texture and location information of materials [38,39]. With the application of deep learning technology, the preprocessing process is simplified, and higher identification is possible. However, it is still often used in parallel with CV. The outline and protrusion features of the building exterior were extracted using image-processing techniques, and the building was recognized using a deep learning model [40]. The features of the building were extracted from the image, and the location and direction of the building were estimated using a 2D map [40]. R-CNN was used to classify East Asian buildings, and the YOLO model was used to identify the simple exterior shapes of traditional buildings [41]. In this study, YOLO was used to identify complex structural forms and elements with large morphological differences [41]. Images were extracted from the 3D map, and information on the exterior shape of the downtown buildings was extracted using a faster R-CNN [42]. A window identification methodology of more than 90% was proposed using open 3D maps [42]. Additionally, a method for identifying windows using Mask R-CNN in building facade images was presented [43].

3. Building an Image Dataset of Hanok Facade Using 3D Modeling

Existing architectural facade deep learning research was conducted using building photos captured by researchers, photos in architectural books, and road view images for analysis. However, external environmental conditions and factors other than architectural elements are unpredictable. That is, depending on the weather, light, and shade, the illumination inside the building may differ. Furthermore, it may be difficult to secure a complete building image owing to obstacles in the road, such as trees, cars, and benches. In addition, since the building is three-dimensional, the facade may appear different depending on the angle, but it may be difficult to reflect the complete appearance if it is analyzed using only one facade image per building. In this respect, this study constructs an image dataset via rendering the complete exterior facade unaffected by the external environment at various angles by 3D modeling the Hanok building using "Revit BIM".

3.1. Selection of Target Site

After selecting the target site, standardized Hanok 3D modeling was implemented for the actual Hanok. The target site was located in the Bukchon area of Seoul, which is South Korea's representative Hanok concentration area. This area is a place where small and medium-sized urban Hanoks were collectively built as the urban structure was modernized in the 1930s. Because the Hanoks in Bukchon were built in large quantities, various materials such as wood form the standard. Furthermore, the exterior of the area has been well preserved through the Bukchon Renovation Project. Therefore, the area was selected as the modeling target site as the exterior was standardized and well preserved while maintaining the characteristics of a traditional Hanok.

The Bukchon area includes Gahoe-dong, Samcheong-dong, Palpan-dong, Hwa-dong, Sogyeok-dong, Songhyeon-dong, Sagan-dong, Anguk-dong, Jae-dong, Gye-dong, and Wo nseo-dong. In 2016, the National Hanok Center conducted a complete enumeration survey focusing on these areas and classified existing Hanoks into A, B, and C grades. Grade A refers to a Hanok with both upper and lower structures and two or more of the materials of the wall/window/roof are in good condition [44]. This study implements standardized Hanok modeling for grade A Hanoks. This grade is suitable for modeling because these Hanoks are well preserved and are of considerable cultural value. Bukchon has 598 grade A Hanoks. This study excluded commercial and religious facilities and two-story Hanoks. Furthermore, 63 Hanoks distinguished by separate facades because they were adjacent to two or more roads were classified into individual cases. Finally, a standardized facade image of an urban Hanok was implemented by modeling 405 Hanok cases and producing 468 Hanok facade images.

3.2. 3D Modeling of Hanoks Using Revit BIM

3.2.1. Classification of the Components of Building Exterior and Form Elements of Hanok

When modeling Hanoks, we must first identify the components of the building exterior and form elements of each case. After establishing a form elements classification system based on Shon's (2018) [3] raw dataset, which was digitized by conducting a complete enumeration survey on the facade elements of existing Bukchon Hanoks, the facade elements of 405 Hanok cases were digitized by referring to the road view image. Shon (2018) largely classified the form elements of the urban landscape into 26 form elements based on the building plan/facade/street elements and 133 detailed form elements [3] (Figures 3–10). The plan elements of Hanoks are not apparent on the facade, but they affect the outline and shape of the buildings depending on the classification, main house type, layout type, orientation of the road, and plan. Furthermore, the facade is composed of visual and direct form elements. These elements also include the main gate type, main gate location, difference between ground level and road, distance between road and building line, slope, window type, wall configuration, exterior wall lower part, outer wall middle part, outer wall decoration, roof type, rafter color, eave type, stylobate type, and eave length. Finally, street elements include road materials, road width, fence wall type, and fence wall form.

Figure 4. Main house types (A) Reprinted/adapted with permission from Ref. [3]. 2018, Donghwa Shon: These are classified according to the plan of the main house and the shape of facade is different for each type.

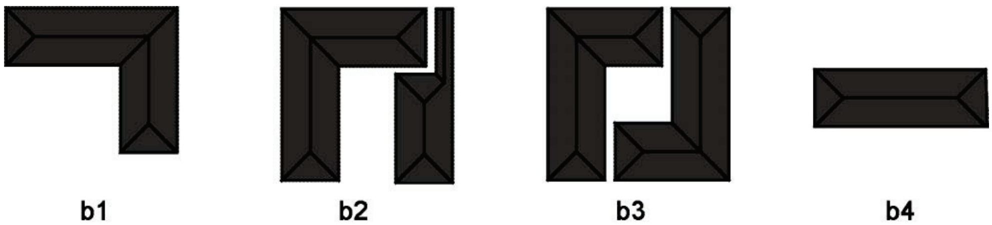

Figure 5. Layout types (B) Reprinted/adapted with permission from Ref. [3]. 2018, Donghwa Shon: Depending on the layout of the main house and gate building, the plan and facade of the Hanok differ. For example, even if it is the same ㅁ-shaped layout, when only main house is ㅁ-shaped (a3 + b3) and when the ㄱ-shaped main house and ㄱ-shaped gate building are combined (a1 + b3), the facade is different due to the continuity of the roof and the wall. For this reason, classes A and B are distinguished.

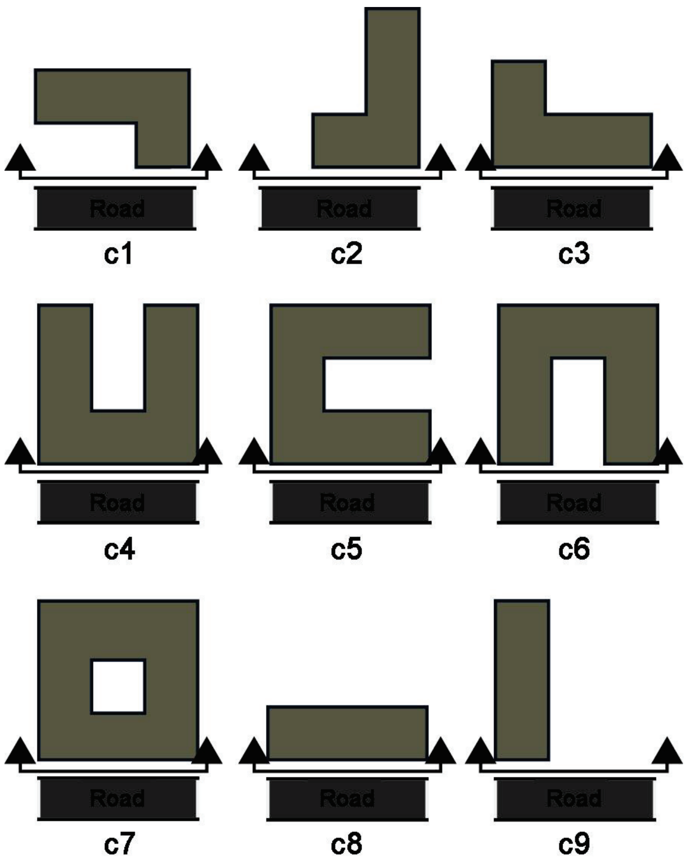

Figure 6. Orientation of the road (C) Reprinted/adapted with permission from Ref. [3]. 2018, Donghwa Shon: Even in the same Hanok, the facade varies depending on the direction facing the road.

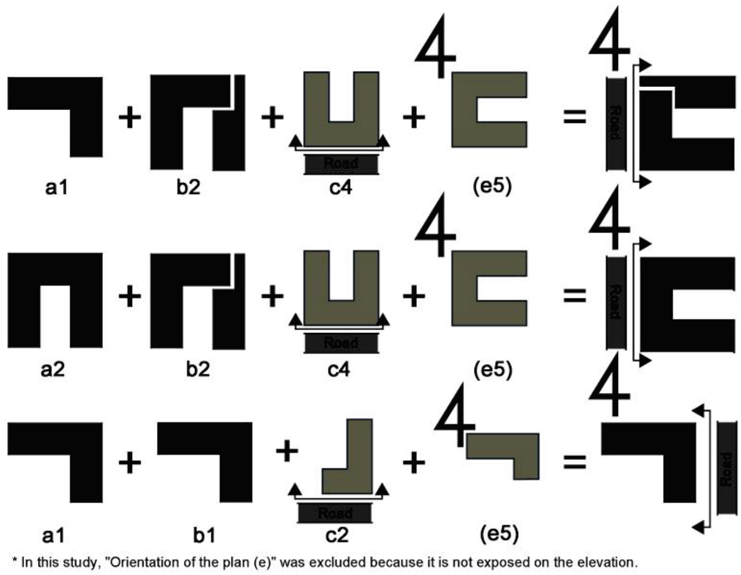

Figure 7. Plan form facing the road (A + B + C) Reprinted/adapted with permission from Ref. [3]. 2018, Donghwa Shon: The facade appears in various ways according to the combination of the type and layout of the main house and gate building, and the orientation of the road. These images are exemplary images that various facades can appear depending on the combination of elements for each class A, B, and C.

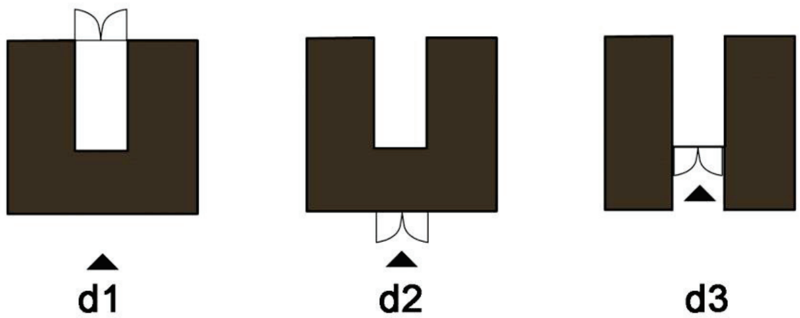

Figure 8. Location of the main gate in the plan (D) Reprinted/adapted with permission from Ref. [3]. 2018, Donghwa Shon: When the main gate is on a different elevation, the facade consists of outer walls and windows without a gate (d1). And when there is a gate, the gate is located on the same line as the wall (d2) or on the setback from the wall line (d3).

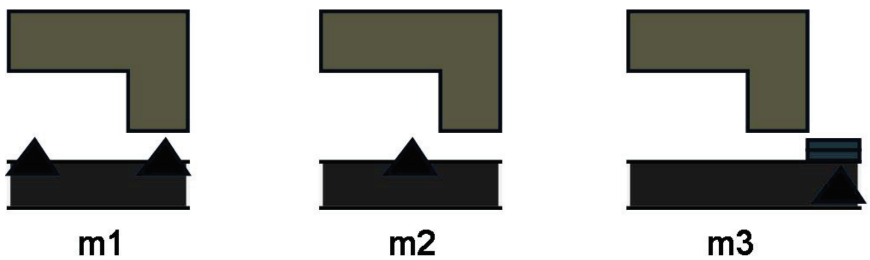

Figure 9. Location of the main gate in the facade (M) Reprinted/adapted with permission from Ref. [3]. 2018, Donghwa Shon: It is distinguished whether the main gate is located on the side, in the center, or outside of the building.

Table 1. Components of building exterior and form elements of Hanok.

Components of Building Exterior (7)	Facade Form Elements (21)	Detailed Form Elements (102)
Placement	Main house types (A) *	ㄱ-shaped plan (a1), ㄷ-shaped plan (a2), ㅁ-shaped plan (a3), ㅡ-shaped plan (a4)
	Layout types (B) *	ㄱ-shaped layout (ㄱ-shaped main house, b1), ㄷ-shaped layout (ㄱ-shaped and ㅡ-shaped gate building, b2), ㅁ-shaped layout (ㄱ-shaped main house and ㄱ-shaped gate building, b3), ㅡ-shaped layout (ㅡ-shaped main house, b4)
	Orientation of the road (C) *	Under the ㄱ-shaped plan (c1), right of the ㄱ-shaped plan (c2), top of the ㄱ-shaped plan (c3), left of the ㄷ-shaped plan (c4), under the ㄷ-shaped plan (c5), right of the ㄷ-shaped plan (c6), side of the ㅁ-shaped plan (c7), long side of ㅡ-shaped plan (c8), short side of ㅡ-shaped plan (c9)
Roof	Roof types (W)	Hipped roof (w1), hipped-and-gabled roof (w2), gabled roof (w3), gabled roof and hipped-and-gabled roof (w4), hipped-and-gabled roof and hipped roof (w5), gabled roof and hipped roof (w6)
	Rafter color (X)	Color (x1), colorlessness (x2)
	Eave types (Y)	Single eave (y1), double eave (y2)
Main gate	Main gate types (L)	Pyeong daemun gate (flat gate, l1), ilgak daemun gate (two-pillar gate, l2), iron gate (l3), no gate in facade (l5)
	Location of the main gate on the plan (D) *	No gate in facade (d1), same as the wall line (d2), set back from the wall line (d3)
	Location of the main gate in facade (M) *	End of the building (m1), center of the building (m2), outside the building (m3)
Outer wall	Facade width (F) *	~6 m (f1), 7~9 m (f2), 10~12 m (f3), 13~15 m (f4), 16~18 m (f5), 19~21 m (f6), 22~24 m (f7)
	Wall configuration (S) *	Flat wall (s1), pillar wall (s2)
	Lower part of the wall (T)	Sagoseog (18–20 cm cubic granite, t1), natural stone (t2), layers with roof tile (t3), plastered wall (t4), gray brick (t5), red brick (t6), cement (t7), tile (t8), glass (t9)
	Middle part of the wall (U)	Sagoseog (18–20 cm cubic granite, u1), natural stone (u2), layers with roof tile (u3), plastered wall (u4), gray brick (u5), red brick (u6), cement (u7), tile (u8), glass (u9)
	Exterior wall decoration (V)	Grid rounding (v1), floral pattern (v2), design pattern (v3), not applicable (v6)
	Window types (R)	Grid (r1), jeongja (r3), ahja (r4), bitsal (r5), wanja (r6), general window (r7), yongja (r8), no window (r9)
Stylobate	Stylobate types (K)	Natural stone stylobate (k1), rectangular stone stylobate (k2), cement stylobate (k3), brick stylobate (k4)
Fence wall	Fence types (I)	Sagoseog and brick and roof tile (i1), natural stone and roof tile (i2), sagoseog and layers with roof tile and roof tile (i3), sagoseog and roof tile (i4), layers with roof tile and plastered wall and roof tile (i5), sagoseog and floral pattern and roof tile (i6), brick/tile and roof tile (i7), cement and roof tile (i8), no fence (i9)
	Fence forms (J)	Entire fence at a different level than the road (j1), partial fence at a different level than the road (j2), entire fence at the same level as the road (j3), partial fence at the same level as the road (j4)

Table 1. *Cont.*

Components of Building Exterior (7)	Facade Form Elements (21)	Detailed Form Elements (102)
Site	Level difference between ground and road (N) *	−1~0 m (n1), 0~0.5 m (n2), 0.5~1 m (n3), 1~2 m (n4), 2~3 m (n5)
	Level difference of ground (Q) *	Difference between ground level and road (q1), no difference between ground level and road (q2)
	Slope of ground (P)	Slope (p1), no slope (p2)

* Only the Hanok form elements presented by Shon (2018), corresponding to the facade of the target site in the current study, are organized and classified [3]. All of these classes and elements were used for the 3D modeling of a Hanok. However, classes marked with ( ) * were excluded from the Mask R-CNN analysis because of recognition problems in Chapter 4, and the other classes and elements were utilized in the analysis.

Among the existing 26 form elements presented in Shon (2018), four elements (i.e., the orientation of the plan, road width, road material, and distance between the road and building line) were excluded because they are not visible on the facade [3]. Furthermore, the length of the eaves was excluded from the classification factor because it was difficult to implement short eaves of at most 600 mm with a design automation program, and the eaves were unified as 1200 mm. Finally, the 21 form elements appearing on the facade were classified into 102 detailed form elements as presented in Table 1, and 3D modeling was conducted for each Hanok. To improve the recognition and performance of Mask R-CNN analysis, standardized modeling was conducted for each detailed form element. Specifically, each member or mapping source and facade form element was unified and modeled for each detailed element. For a facade width of 10 m, it will be modeled as 12 m, and each element within a facade width will be modeled to the largest dimension. The wall design pattern uses one unified pattern rather than a pattern image for each actual Hanok.

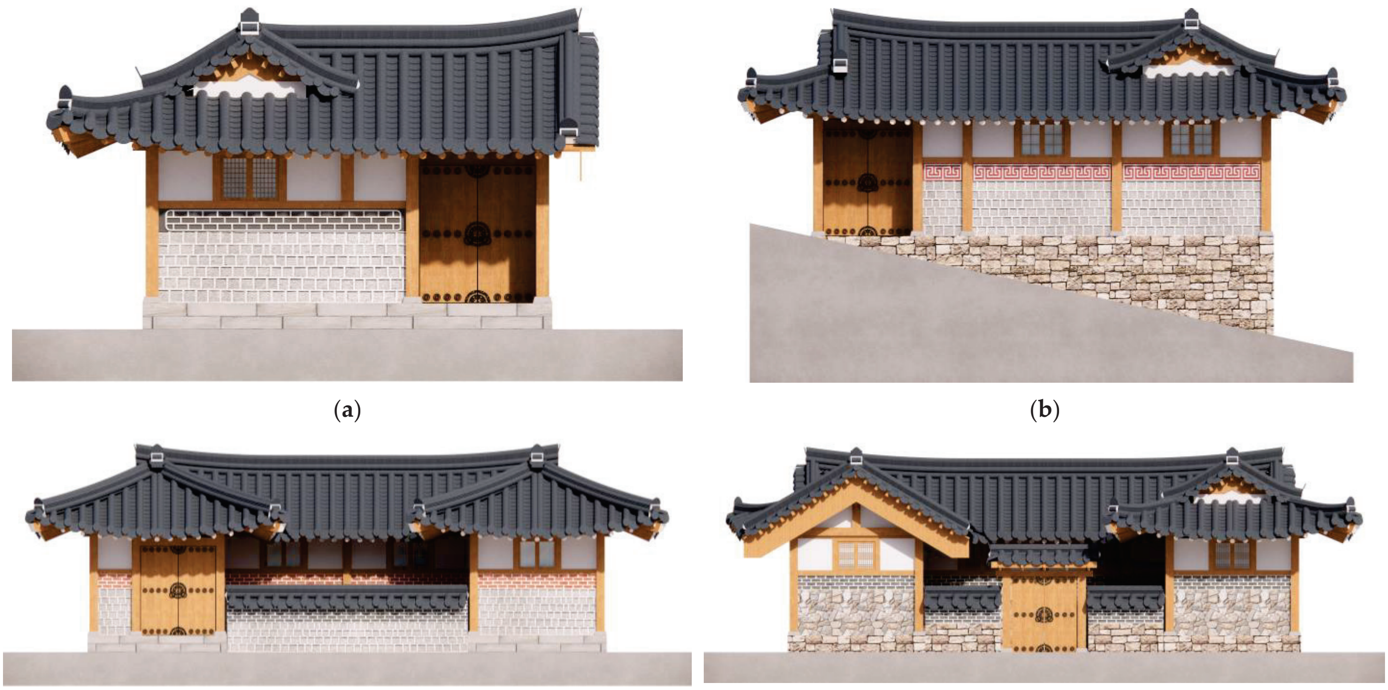

(**a**) (**b**)

(**c**) (**d**)

Figure 10. *Cont.*

(**e**)

(**f**)

(**g**)

(**h**)

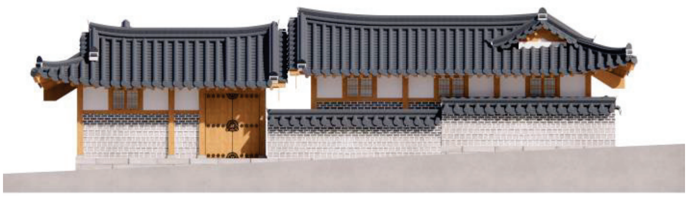

(**i**)

(**j**)

Figure 10. Facade image of Hanok by the combination of form elements. Reprinted/adapted with permission from Ref. [3]. 2018, Donghwa Shon: The facade of a Hanok is composed of a combination of various elements. These figures are exemplary images showing the facade of each Hanok by the combination of elements simplified with the alphabets in Table 1. (**a**) a2 + b2 + c5 + w3 + x2 + y1 + l1 + d3 + m1 + f1 + s1 + t1 + u5 + v1 + r3 + k2 + i9 + j5 + n2 + q2 + p2; (**b**) a2 + b2 + c5 + w2 + x1 + y1 + l1 + d3 + m1 + f2 + s2 + t1 + u6 + v2 + r8 + k1 + i9 + j5 + n4 + q2 + p1; (**c**) a2 + b2 + c6 + w1 + x1 + y1 + l1 + d2 + m2 + f3 + s2 + t1 + u6 + v6 + r7 + k2 + i1 + j3 + n2 + q2 + p2; (**d**) a2 + b2 + c5 + w4 + x1 + y1 + l2 + d1 + m2 + f2 + s1 + t2 + u5 + v6 + r1 + k1 + i9 + j5 + n2 + q2 + p2; (**e**) a2 + b2 + c5 + w2 + x1 + y2 + l1 + d3 + m2 + f2 + s2 + t8 + u8 + v3 + r7 + k2 + i9 + j5 + n2 + q2 + p2; (**f**) a1 + b1 + c1 + w3 + x2 + y1 + l2 + d2 + m2 + f2 + s2 + t4 + u4 + v4 + r1 + k2 + i5 + j3 + n5 + q2 + p1; (**g**) a2 + b2 + c4 + w4 + x1 + y1 + l1 + d3 + m2 + f2 + s2 + t1 + u5 + v6 + r1 + k1 + i1 + j4 + n3 + q2 + p1; (**h**) a3 + b3 + c7 + w6 + x1 + y1 + l1 + d2 + m2 + f3 + s2 + t2 + u3 + v6 + r1 + k1 + i2 + j4 + n2 + q2 + p2; (**i**) a2 + b2 + c4 + w4 + x2 + y1 + l1 + d2 + m1 + f3 + s2 + t1 + u5 + v6 + r1 + k2 + i1 + j2 + n2 + q1 + p1; (**j**) a3 + b3 + c7 + w2 + x1 + y2 + l2 + d2 + m2 + f3 + s2 + t4 + u4 + v6 + r6 + k1 + i1 + j1 + n2 + q2 + p1.

3.2.2. 3D Modeling of Hanok Using an Automatic Design Program

The "Hanok BIM design support tool", which is a Hanok automatic design program of Revit, was used to perform standardized 3D modeling [45] (Figure 11). The software uses "Kan" as the basic module unit of the plan, which is a program that designs and models Hanoks in the order of body structure, roof structure, and roof tiling. Specifically, a space, such as a pillar and a wall, is first partitioned using a "Kan" module to plan the body structure. A roof structure to be installed at the top of this body structure is planned.

Subsequently, a member that converts and combines each "family" into a member body and conjunctive parts with an actual shape is completed, and rafters and roof tiles are automatically placed in the final modeling form.

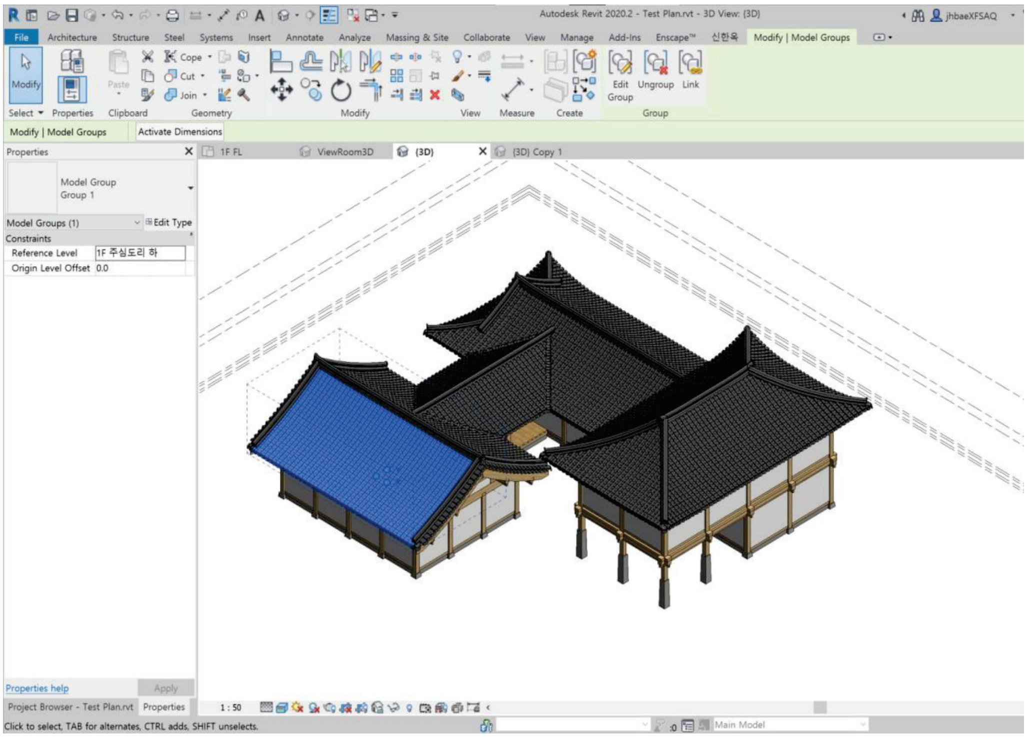

Figure 11. 3D modeling of Hanok using an automatic design program [45].

The aforementioned tool automatically models a Hanok by optimizing and connecting various members created as a "family" according to the size or type/form of the member planned by the designer. However, members may be unexpectedly connected, and some areas may not be created. Therefore, among the ones modeled using the program, the designer must arbitrarily modify and supplement the parts that are modeled differently from the actual ones. After 3D modeling of the Hanok case of the target site based on the form elements classified in Section 3.2.1, the profile, parameters, or dimensions of the member were modified in the review stage for parts where the facade form did not match the existing Hanok case.

3.3. Building an Image Dataset of Hanok Facade

A total of 468 Hanok facade images for 405 Hanok cases were extracted from Mask R-CNN analysis using the executing program "Enscape". First, an appropriate mapping image for each member was applied using a material library and a mapping source, and the material bump and reflection values were appropriately set. Furthermore, the background and atmosphere such as illumination (i.e., sunlight and shadow), cloudiness, saturation, and color temperature were appropriately set to reveal the facade images of the Hanok. The setting values were applied equally to all of the facade images to improve the accuracy of the Mask R-CNN analysis. Furthermore, because the facade of the actual building is clear from various angles as well as the front when walking, the facade image was extracted by rendering the front and the side slightly rotated to the left and right. Essentially, facade images in three different directions were extracted for one facade case. To prevent the distortion of the facade image according to the camera viewpoint, the rendering projection mode was set to orthographic instead of perspective. The rendering image was output with the same size and resolution (1920 X 1080) for all Hanok facades for Mask R-CNN analysis. In addition, to improve the performance of the CNN analysis and prevent overfitting, numerous image datasets were required and, in this respect, the image data augmentation (DA) methods were also performed. DA performs geometric and photometric transformations of an image, and geometric methods include flipping, cropping, translation, and rotation [46,47]. The number of images was augmented using a horizontal flipping method that can retain the complete facade image of a Hanok. The modeled Hanok uses standardized members of the Hanok BIM design support tool, and each of these members is symmetrical, so the appearance of the general Hanok can be maintained even if it is horizontally flipped. Finally, 2808 image datasets were constructed by extracting six types of facade images, including those in three different directions and each horizontal flipped image, for one Hanok facade case (Figure 12).

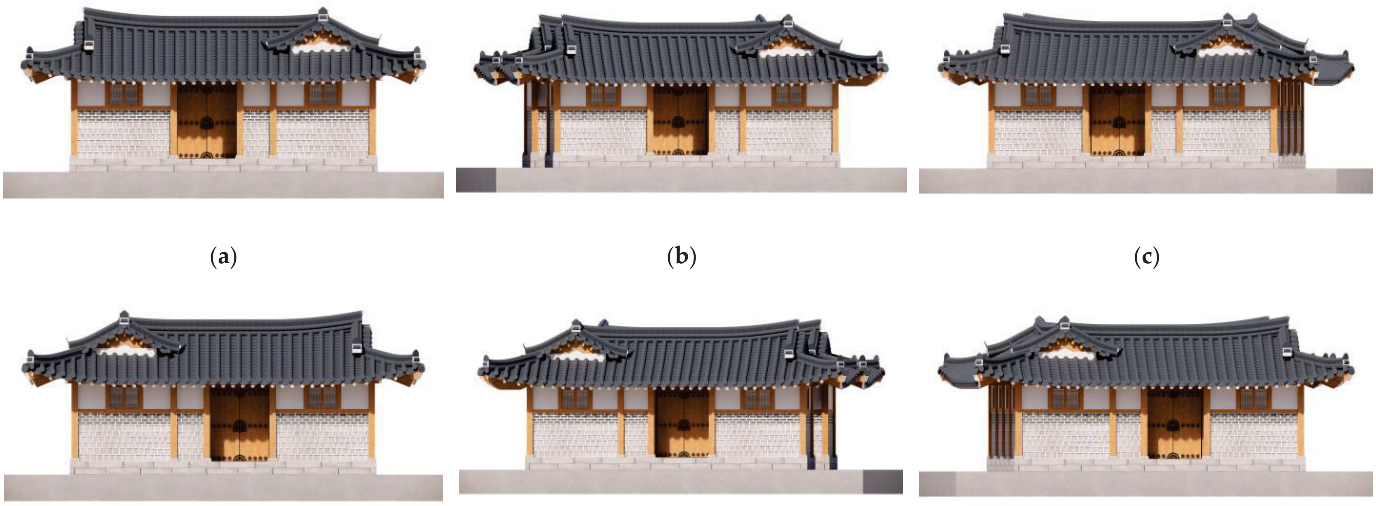

(**a**) (**b**) (**c**)

(**d**) (**e**) (**f**)

Figure 12. Data augmentation of facade images. (**a**) Front image, (**b**) left side image, (**c**) right side image, (**d**) flipped front image, (**e**) flipped left image, (**f**) flipped right image.

4. Experiment and Results

Based on the image dataset constructed in Section 3, we briefly describe the experimental performance plan to classify and identify the elements of a Hanok building using deep learning technology and verify the performance. First, the experimental process and results used to verify the performance of the model are explained. Thereafter, the process of extracting Hanok building element information using image processing techniques from the extracted images and the experimental results are schematically described.

4.1. Mask R-CNN for Hanok Exterior Element Detection

Before the development of deep learning technology, researchers used machine learning approaches such as support vector machine (SVM) and histogram of oriented gradient (HOG) for object detection and image classification. For object detection, the selective search algorithm, which is a mathematical algorithm technique for image data, was used [48]. As the convolution neural network (CNN) model of deep learning began outperforming SVM in image classification, an object detection model was created in which only the image classification part of the model was transformed into a CNN, known as R-CNN. The main methods for object detection and segmentation in images are faster R-CNN [29] and YOLO [30,31].

We used the Mask R-CNN model to classify the Hanok exterior elements. Instance segmentation was used to extract significant elements for detection. This was conducted because we can detect objects and classify specific elements such as patterns of exterior elements. It distinguishes and recognizes different entities even if they have the same class and combines object detection and semantic segmentation. In Mask R-CNN, a mask is applied to classify each class as an instance within the region of interest (ROI). Subsequently, for the classification calculated through the classification layer, color is applied to the pixels determined to have an instance to proceed with instance segmentation. Mask R-CNN is a structure in which a mask branch that predicts the segmentation task for each ROI is added to the existing faster R-CNN. It comprises three branches: classification, bounding box regression, and segmentation mask, and performs three tasks simultaneously. The mask branch is a small-sized fully connected network (FCN) that predicts a segmentation mask that determines whether an object is present for each of the K-classes per pixel in a pixel-to-pixel manner. Furthermore, the ROI pooling of the existing faster R-CNN was replaced with the ROI align layer to preserve the object's spatial location, that is, location information [34]. Mask R-CNN of the Detectron2 platform provided by Facebook Artificial Intelligence Research was used for learning [49]. The structure of Mask R-CNN is explained in Figure 13.

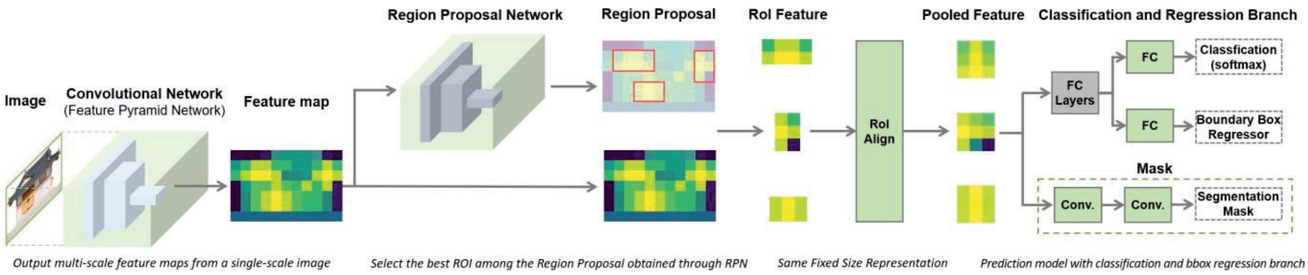

Figure 13. Structure of Mask R-CNN.

4.2. Labeling for Segmentation

We performed labeling of exterior elements to apply the Mask R-CNN model focused on detecting Hanok exterior elements. Because Hanok images and elements are not included in the COCO dataset, we trained the new custom model. For training, we first labeled the elements. To perform the labeling, we first set the labels of the elements of the image dataset. A total of 9 out of 21 classes were excluded owing to a problem in recognizing the results of the pilot test. Elements A and B could not be segmented by checking the image of the plane alone. This would have been possible if a rendering image had been taken. It is difficult to verify C with a flat image; therefore, it is expected that the result will be obtained if a rendered image with a 3D background is trained in 3D in the future. In addition, because of the nature of segmentation for the purpose of classification, it is difficult to classify elements consisting of numerical values such as length and width, namely D, M, F, N, and Q, through training because the specific location is unknown. The Labelme program was used to label elements in the flat image of Hanok, and 64 elements were labeled. Each element is labeled and saved as a JavaScript object notation (JSON) file. In general, when a deep learning model is trained to detect or classify an object, coordinate values for a box or shape corresponding to an object area in an image are displayed. In the detection model, a rectangle box is used, but in segmentation, we must categorize the target even if it is the same target; hence, we need to extract polygonal cross section values. An example where the bounding range of a polygon shape marks the object area of the image is illustrated in Figure 14.

We trained a deep learning segmentation model by setting bounding boxes for Hanok elements in the extracted image information. Boundary polygon settings were manually set for all images in the training and test datasets. Additionally, boundary polygons were extracted using Labelme open-source software [50]. Labelme supports object scoping and metadata extraction for model training. When training a deep learning model, images are required, and it is important to include metadata or annotations containing object information in the images. Metadata includes information such as boundary polygon coordinates, label name, image path, and size, and is stored in JSON format.

Figure 14. Example of labeling using Labelme.

To utilize the Mask R-CNN model of Detectron2, the COCO format file is required. The format was changed using a code that changes the JSON file to COCO format. The changed format is then used for training. The visualization result of the Hanok elements that were labeled is presented in Figure 15. Each element shows a unique ID value and color. Bounding polygons were set to classify elements from Hanok images.

Figure 15. Visualization of labeled examples.

An example of a JSON file obtained with Labelme before using it for training is presented in Table 2. The result of labeled elements of the Hanok image was extracted. The label ID is different because each image has different elements. The "label" value is the output id of the element that we labeled from Labelme. Thereafter, we changed to the COCO format for training.

Table 2. JSON format metadata structure of labeled image.

Key Values		Description	Item Values (Example)	Data Format
version		JSON Format Version	"4.6.0"	STRING
flags		Null	{ . . . }	STRING
shapes		Shape Format	[. . .]	LIST
L	label	Image Class	"a1"	STRING
L	points	Bounding box coordinate	{...}	DICTIONARY
L	group_id	Null	Null	STRING
L	Shape_type	Type of Shape	"polygon"	STRING
L	flags	Null	null	STRING
... (continued)				

Unlike the JSON file, the COCO format consists of id, image_id, category_id, segmentation, area, bbox, and iscrowd, and each of the 64 labels in the last category is expressed as a value from 0 to 63 (Table 3). Table 3 is an example of a COCO Format JSON file used for training. In the given example, Hanok elements' information was extracted from the image. In this format, we should focus on "category_id". The "category_id" key value includes category number of elements. The "category_id" serves to enable segmentation of objects in the training process.

Table 3. COCO Format metadata for training.

Key Values		Description	Item Values (Example)	Data Format
annotations		Annotations	[...]	LIST
L	id	Order of Images	{...}	INT
L	image_id	Order of Images	"0"	INT
L	category_id	Id of Labels	"13"	INT
L	segmentation	Segmentation Coordinate	[. . .]	DICTIONARY
L	area	Area of Pixel	"115,672.0"	INT
L	bbox	Bounding box coordinate	[. . .]	LIST
L	iscrowd	Single or Multi Object	"0 or 1"	INT
... (continued)				

4.3. Results of Segmentation

In this section, we describe the results of classifying the exterior elements of a Hanok building using a deep learning model. To classify the elements in the Hanok model image, the Mask R-CNN model was used in the Detectron2 environment. Because 2808 images were acquired, approximately 1900 (70%) were used for training, and approximately 900 (30%) were used for testing. For learning hyperparameters, the learning rate was set to 0.0005 and the maximum number of iterations was set to 5000. Additionally, we used the early stopping feature of training to stop when loss reduction no longer occurred on subsequent iterations, thus reducing the training time. The process repeated approximately 1200 times before stopping. The loss graph of the model is presented in Figure 16. The total loss value of the model is 0.015694.

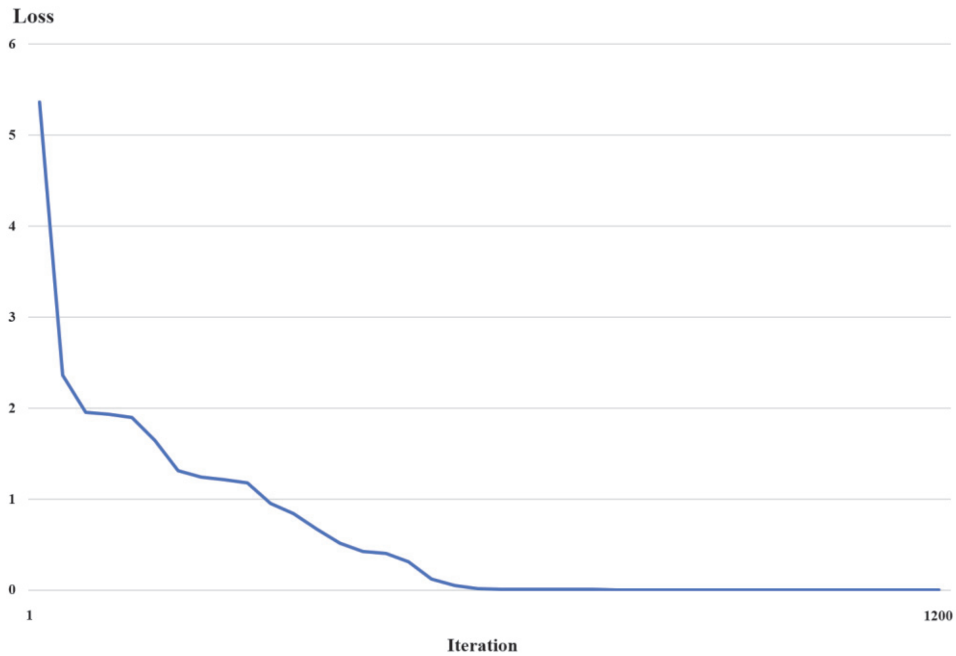

Figure 16. Losses by iteration.

Accuracy in instance segmentation is calculated as average precision (AP). Before determining AP, one needs to understand the intersection over union (IoU). IoU is used as an object detection evaluation index and indicates that the overlap of the correct answer area overlaps with the predicted area. The higher the IoU value, the better the object detection. AP means mAP in the threshold range of the corresponding IoU. The numbers next to it, such as AP50 and AP75, are AP (averaged over IoU thresholds) thresholds. AP50 is the average of IoU exceeding 0.5. AP75 is the average of IoUs exceeding 0.75. The results of AP are reported in Table 4 below.

$$\text{IoU}(\text{Intersection of Union}) = \frac{Overapping\ Region}{Combined\ Region}$$

Table 4. AP value of the experiment.

mAP	mAP_{50}	mAP_{75}
62.6	**78.75**	**69.41**

We performed segmentation by labeling 64 elements. The outer wall, stylobate, and gate of the Hanok were mainly accurately detected and segmented. The segmentation results are illustrated in Figure 17 below. Of the 21 classes, 12 labeled classes (I, J, K, P, R, T, U, V, L, W, X, and Y) were well segmented. Therefore, among the horizontal elements, the facade elements except for the width of the road and other elements that can affect the shape and contour of the building were well distinguished. This demonstrates that elements outside the Hanok can be distinguished by shape and color. This method can be used for the pre-processing of more detailed classification methods in future studies.

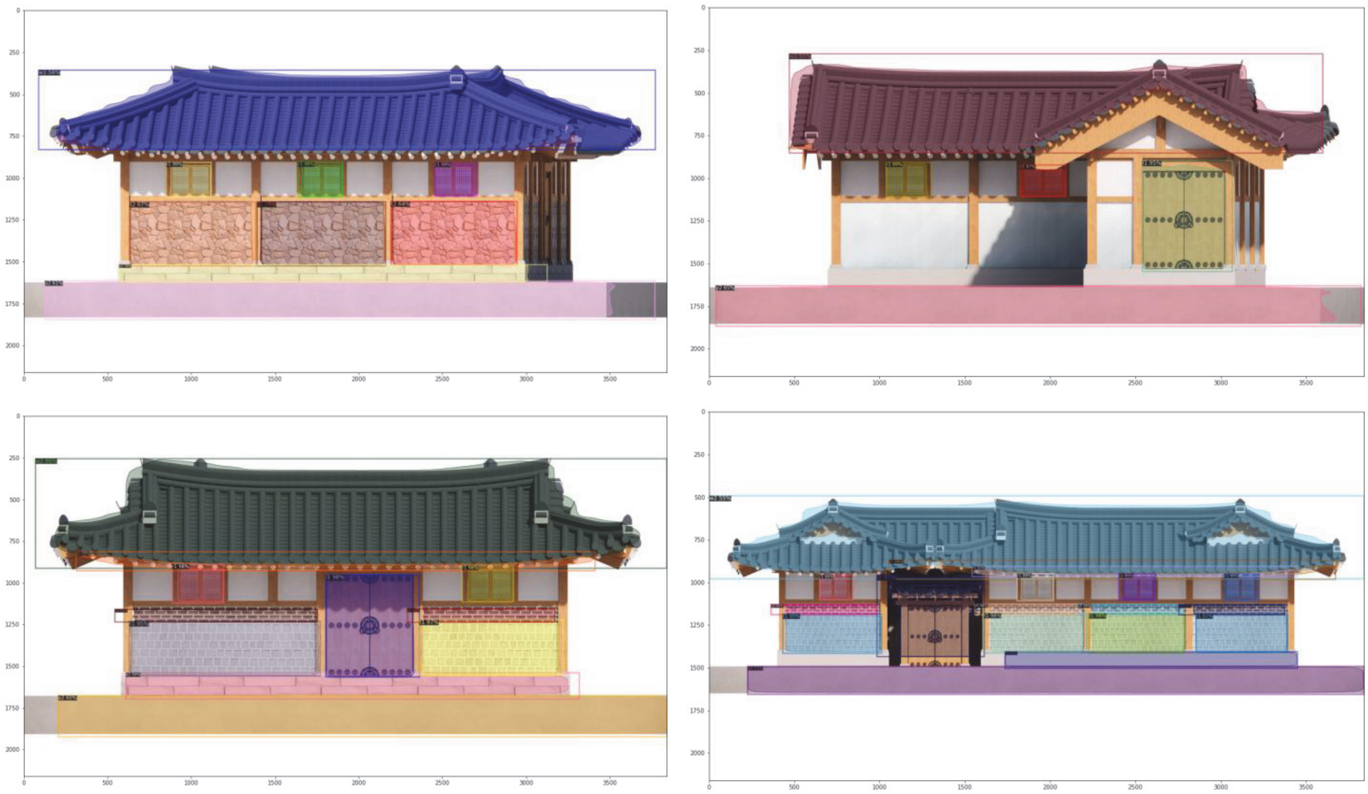

Figure 17. Segmentation results of Hanok image.

5. Conclusions

This study classified and detected the external elements of Hanok buildings using deep learning and image processing technology to recognize and classify the information of Hanok elements. We used the Mask R-CNN model of Detectron2 to detect and segment elements outside of the Hanok. In general, the segmentation was satisfactorily conducted, and the type of roof, windows, the lower part of the outer wall, and the design were segmented with high accuracy. The contribution of this research is twofold. First, a model for learning images, such as the exterior of a Hanok, was developed using Hanok images that had not been previously attempted. Extensive architectural research has attempted to segment Hanok images.

Second, this study obtained satisfactory classification accuracy using the latest image segmentation model and proposed a method for recognizing and extracting information regarding elements outside of a Hanok. The proposed method can be adopted in future studies to automatically acquire basic Hanok information. It can also be used for pre-processing to recognize more detailed information regarding the elements outside the Hanok. This research can be a good pilot study to discriminate external factors by training images of various Hanok types and materials.

However, there were several limitations. Although the roof type was well understood, it was difficult to detect and segment the facade layout because it was difficult to train considering the elements such as the main house type, layout type, and road layout direction. Furthermore, although the type of gate was well identified, it was difficult to determine its location. These were difficult to determine because the specific coordinate values of the component class were not properly given. In future studies, it is expected that the current limitations can be supplemented by the measurement and training of aerial view images and specific position values. Moreover, in this paper, the train and test steps are conducted using 3D modeling data suitable for the purpose of the experiment. In future studies, experiments can be conducted using actual Hanok images in the verification stage such as performance evaluation.

Author Contributions: Conceptualization and methodology, D.S. and G.B.; software, formal analysis, and data curation, S.C.; writing—original draft preparation, D.S.; writing—review and editing, G.B.; visualization and supervision, S.C.; funding acquisition, D.S. All authors have read and agreed to the published version of the manuscript.

Funding: This work was supported by the National Research Foundation of Korea (NRF) grant funded by the Korean government (MSIT) (NRF-2021R1F1A1061804).

Acknowledgments: The authors wish to express their gratitude to the anonymous reviewers for the comments and suggestions provided, which have been very helpful in improving the paper.

Conflicts of Interest: The authors declare no conflict of interest.

References

1. Jacobs, J. *Death and Life of Great American Cities*; Random House: New York, NY, USA, 1961.
2. Lynch, K. *The Image of the City*; The MIT Press: Cambridge, MA, USA, 1960.
3. Shon, D. Analysis of Traditional Urban Landscape Composition Using Data Mining. Ph.D. Thesis, Seoul National University, Seoul, Republic of Korea, 2018.
4. Kropf, K. *The Handbook of Urban Morphology*; John Wiley & Sons: Hoboken, NJ, USA, 2018.
5. Hall, A.C. Dealing with incremental change: An application of urban morphology to design control. *J. Urban Des.* **1997**, *2*, 221–239. [CrossRef]
6. Korean Law Information Center. Building Act. Available online: https://www.law.go.kr/ (accessed on 2 December 2022).
7. Korean Law Information Center. ENFORCEMENT DECREE OF THE NATIONAL LAND PLANNING AND UTILIZATION ACT. Available online: https://www.law.go.kr/ (accessed on 2 December 2021).
8. Markus, T.A. *Buildings and Power, Freedom and Control in the Origin of Modern Building Types*; Routledge: England, UK, 1993.
9. Vworld Map. Available online: https://vworld.kr/v4po_main.do (accessed on 15 November 2021).
10. Seoul City 3D Map. S-MAP. Available online: https://smap.seoul.go.kr/ (accessed on 15 November 2022).
11. Google Earth, 3D Map. Available online: https://earth.google.com/web/ (accessed on 15 November 2022).
12. Daum Kakao Map. Available online: http://map.daum.net (accessed on 15 November 2022).
13. Naver Map. Available online: http://map.naver.com (accessed on 25 November 2022).
14. Form Based Code Institute.2022. Available online: https://formbasedcodes.org/definition/ (accessed on 15 November 2022).
15. Halprin, L. *The Landscape as Matrix. Ekistics, Vol 32*; Oct.; Oxford University Press: New York, NY, USA, 1971.
16. Planning in the 20th Century. 2022. Available online: https://urbanla.weebly.com/history-of-planning.html (accessed on 20 December 2022).
17. Zoning in Canada. 2022. Available online: https://www.thecanadianencyclopedia.ca/en/article/zoning (accessed on 20 December 2022).
18. Town Planning Code in France. 2022. Available online: https://www.legifrance.gouv.fr/codes/id/LEGITEXT000006074075/ (accessed on 20 December 2022).
19. Law of Urban Planning in Japan. 2022. Available online: https://elaws.e-gov.go.jp/document?lawid=343AC0000000100 (accessed on 20 December 2022).
20. Law of Zoning in South Korea. 2022. Available online: https://www.law.go.kr/LSW/eng/engLsSc.do?menuId=2&section=lawNm&query=%EA%B5%AD%ED%86%A0%EA%B3%84%ED%9A%8D&x=36&y=20#liBgcolor0 (accessed on 20 December 2022).
21. Elliott, D. *A Better Way to Zone: Ten Principles to Create More Livable Cities*; Island Press: Washington, DC, USA, 2008.
22. Congress for the New Urbanism. *Charter of the New Urbanism*; McGraw-Hill Professional: New York, NY, USA, 1999.
23. Relph, E. *Place and Placelessness*; Pion Limited: London, UK, 1976.
24. Jeong, S.; Song, I.; Moon, H. *Report of Bukchon Master Plan*; Seoul City Press: Seoul, Republic of Korea, 2001.
25. Song, I. Study on the Types of Urban Traditional Housing in Seoul from 1930 to 1960. Ph.D. Thesis, Seoul National University, Seoul, Republic of Korea, 1990.
26. The Korean Law Information Center. Act on Value Enhancement of Hanok and Other Architectural Assets. 2021. Available online: https://www.law.go.kr/ (accessed on 14 June 2021).
27. Lecun, Y.; Boser, B.; Denker, J.S.; Henderson, D.; Howard, R.E.; Hubbard, W.; Jackel, L.D. Backpropagation applied to handwritten zip code recognition. *Neural Comput.* **1989**, *1*, 541–551. [CrossRef]
28. Girshick, R.; Donahue, J.; Darrell, T.; Malik, J. Rich Feature Hierarchies for Accurate Object Detection and, Semantic Segmentation. In Proceedings of the IEEE Conference on Computer, Vision, and Pattern Recognition (CVPR), Columbus, OH, USA, 24–27 June 2014; pp. 580–587.
29. Ren, S.; He, K.; Girshick, R.; Sun, J. Faster R-CNN: Towards real-time object detection with region, proposal networks. *IEEE Trans. Pattern Anal. Mach. Intell.* **2015**, *39*, 91–99. [CrossRef] [PubMed]
30. Redmon, J.; Divvala, S.; Girshick, R.; Farhadi, A. You Only Look Once: Unified, Real-time Object Detection. In Proceedings of the 29th IEEE Conference on Computer Vision and Pattern, Recognition, Las Vegas, NV, USA, 27–30 June 2016; pp. 779–788.
31. Tian, Y.; Yang, G.; Wang, Z.; Wang, L.; Liang, Z. Apple detection during different growth stages in orchards using the improved YOLO-V3 model. *Comput. Electron. Agric.* **2019**, *157*, 417–426. [CrossRef]

32. Yan, C.; Teng, T.; Liu, Y.; Zhang, Y.; Wang, H.; Ji, X. Precise no-reference image quality evaluation based on distortion identification. *ACM Trans. Multimed. Comput. Commun. Appl. (TOMM)* **2021**, *17*, 1–21. [CrossRef]
33. Yan, C.; Meng, L.; Li, L.; Zhang, J.; Wang, Z.; Yin, J.; Zheng, B. Age-invariant face recognition by multi-feature fusionand decomposition with self-attention. *ACM Trans. Multimed. Comput. Commun. Appl. (TOMM)* **2022**, *18*, 1–18. [CrossRef]
34. He, K.; Gkioxari, G.; Dollar, P.; Girshick, R. Mask R-CNN. In Proceedings of the IEEE International Conference on Computer Vision (ICCV), Venice, Italy, 22–29 October 2017; pp. 2980–2988.
35. Koo, W.; Yokoda, T.; Takizawa, A.; Kato, N. Image Recognition Method on Architectural Components from Architectural Photographs Glass: Openings Recognition Based on Bayes Classification. *Archit. Inst. Jpn.* **2006**, *121*, 123–128.
36. Talebi, M.; Vafaei, A.; Monadjemi, A. Vision -based entrance detection in outdoor scenes. *Multimed. Tools Appl.* **2018**, *77*, 26221. [CrossRef]
37. Koo, W.; Takizawa, A.; Kato, N. A Study on discriminating roof types from aerial image. *Archit. Inst. Jpn.* **2007**, *72*, 99–105. [CrossRef]
38. Karsli, F.; Dihkan, M.; Acar, H.; Ozturk, A. Automatic building extraction from very high-resolution image and LiDAR data with SVM algorithm. *Arab. J. Geosci.* **2016**, *9*, 635. [CrossRef]
39. Cai, W.; Wen, X.; Tu, Q.; Guo, X. Research on image processing of intelligent building environment based on recognition technology. *J. Vis. Commun. Image Represent.* **2019**, *61*, 141–148. [CrossRef]
40. Armagan, A.; Hirzer, M.; Roth, P.M.; Lepetit, V. Accurate Camera Registration in Urban Environments Using High-Level Feature Matching. In Proceedings of the British Machine Vision Conference (BMVC), London, UK, 2 September 2017.
41. Ji, S.-Y.; Jun, H.-J. Deep learning model for form recognition and structural member classification of east asian traditional buildings. *Sustainability* **2020**, *12*, 5292. [CrossRef]
42. Shon, D.; Noh, B.; Byun, N. Identification and extracting method of exterior building information on 3D map. *Buildings* **2022**, *12*, 452. [CrossRef]
43. Sun, Y.; Malihi, S.; Li, H.; Maboudi, M. Deepwindows: Windows instance segmentation through an improved mask R-CNN using spatial attention and relation modules. *ISPRS Int. J. Geo-Inf.* **2022**, *11*, 162. [CrossRef]
44. Architecture & Urban Research Institute. *Hanok Statistics White Paper*; Auri Press: Sejong, Republic of Korea, 2017.
45. AUTODESK, BIM Hanok Tool. 2022. Available online: https://www.autodesk.com/autodesk-university/ko/class/saeloun-seolgye-bangbeobloneul-tonghae-hanogeul-swibgo-ppaleuge-seolgyehal-su-issneun-BIM#video (accessed on 28 November 2022).
46. Taylor, L.; Nitschke, G. Improving deep learning with generic data augmentation. In Proceedings of the 2018 IEEE Symposium Series on Computational Intelligence (SSCI), Bengaluru, India, 15 May 2018; pp. 1542–1547.
47. Shorten, C.; Khoshgoftaar, T.M. A survey on image data augmentation for deep learning. *J. Big Data* **2019**, *6*, 60. [CrossRef]
48. Van de Sande, K.E.; Uijlings, J.R.; Gevers, T.; Smeulders, A.W. Segmentation as selective search for object recognition. In Proceedings of the 2011 International Conference on Computer Vision, Washington, DC, USA, 6–13 November 2011; pp. 1879–1886.
49. Detectron2. 2019. Available online: https://github.com/facebookresearch/detectron2 (accessed on 15 November 2022).
50. Labelme. 2022. Available online: https://github.com/wkentaro/labelme (accessed on 15 November 2022).

land

MDPI

Article

Pull and Push Drivers of Giant-Wave Spectators in Nazaré, Portugal: A Cultural Ecosystem Services Assessment Based on Geo-Tagged Photos

António Azevedo

School of Economics and Management, University of Minho, 4710-057 Braga, Portugal; antonioa@eeg.uminho.pt

Abstract: This paper maps the cultural ecosystem services (CES) of a well-known giant-wave hotspot located in Nazaré, Portugal. The paper adopts a qualitative approach combining an auto-ethnographic direct observation of a journey and the content analysis of photos and videos posted on the YouTube and Facebook pages of tourists and operators. A total of 44 geotagged photos from a sample of 6914 photos retrieved from Flickr allowed the classification and spatial distribution of several CES: (1) recreational—surf activities; (2) aesthetic—photography; (3) spiritual—dark tourism and risk recreation; (4) intangible heritage—maritime knowledge; (5) scientific—wave height forecast; (6) sense of place; and (7) social relations. The paper also proposes a theoretical framework that highlights the pull drivers (risk recreation, storm chasing, or spectacular death voyeurism) and the push drivers (e.g., marketing campaigns and wave forecasts alerts) that explain the behaviors of the big-wave spectators/chasers during the experience journey. Public decision-makers, destination marketing organizations, tourism operators, and business entrepreneurs must acknowledge the relevance of journey mapping in order to identify the moments of stress and the touchpoints associated with peak/positive experiences generated by these CES. This study confirms some push and pull factors assessed by previous studies.

Keywords: cultural ecosystem services; coastal tourism; risk recreation; spectacular death voyeurism; storm chasing; geotagged photos; Praia do Norte (Nazaré, Portugal)

1. Introduction

The coastal town of Nazaré in Portugal became the "mecca" of giant waves (see Figure 1) when, on 1 November 2011, Garret McNamara rode a giant wave [1]. The process of adaptation and training started two years before (2009), when the Nazaré Municipal authorities challenged the surfer to test the uniqueness of their waves. The international recognition of the waves was achieved through several world Guinness records and World Surf League (WSL) awards. The whole story is portrayed in the HBO documentary "One hundred-foot wave" [2].

The awareness of Nazaré as a surf tourism destination exponentially increased with the publication of photographs of surfers riding the waves and beating Guinness records [3]. Since then, the international media has been highlighting the shift in the strategic positioning of this small fisherman's town, from a (summer) beach destination to a (winter) giant-wave surfing/chasing destination [4].

Table 1 shows the evolution of the number of hotel guests from 2010 (before the buzz marketing around Nazaré) and 2019 (the year before the COVID-19 pandemic). It increased 295% in this nine-year period, from 44,931 to 132,466 tourists per year. The highest increase occurred among USA tourists. This positive effect on tourism for Nazaré is a direct consequence of Garret McNamara's accomplishment in November of 2011 [1]. Nevertheless, according to Statistics Portugal, Nazaré's population has decreased from

14,383 inhabitants in 2009 to 14,180 in 2018. However, during the big wave periods, the town's population increases ten-fold, to almost 100,000 people [2].

Figure 1. Nazaré, Portugal (location map): surfer riding a big wave, the rescue team of water bikes and the spectators/big-wave chasers. Source: Facebook page of "Praia do Norte" [5].

Table 1. Comparative evolution of the number of hotel guests, according to their home countries: in 2010 (before Garret McNamara's first famous giant wave ride) and 2019 (the last available data without the effect of the COVID-19 pandemic).

	Portugal (2010)	Portugal (2019)	Oeste (2010)	Oeste (2019)	Nazaré (2010)	Nazaré (2019)	Variation 2010–2019(%)
Total	13,537,040	25,249,904	286,305	650,917	44,931	132,466	295%
Portugal	6,705,460	9,941,747	199,516	361,351	27,389	58,115	212%
UE27/UE28	12,112,682	10,602,067	266,678	194,081	39,934	48,466	121%
Germany	728,784	1,602,066	7469	25,853	1031	6630	643%
Spain	1,375,842	2,069,645	21,066	52,749	4667	11,797	253%
France	574,828	1,641,912	12,156	40,404	2951	13,271	450%
Italy	365,368		6549		1159		
The Netherlands	351,635		2905		351		
UK	1,111,197	2,042,867	5322	12,227	991	1156	117%
Africa		195,954		1258		237	
USA/America	266,248	2,648,454	3647	55,038	741	12,469	1683%
Asia		993,201		20,887		7899	
Oceania		173,699		3309		1000	

Source: Statistics Portugal.

The Nazaré Canyon is an undersea canyon just off the coast of Nazaré, Portugal, in the Eastern Atlantic Ocean. It has a maximum depth of at least 5000 m (16,000 ft) and is about 230 km long [3]. The Hydrographic Institute explains big waves as immense swells emerging from the west and northwest directions entering the coastal region. The wave's refraction is based on the differences between the canyon's depth and the continental shelf. This causes a change in the direction through the canyon, which leads to an increase in speed. According to the steep vertical variation of the canyon, the depth reduction causes a shoaling effect, which means that the wave length is reduced while an increase in the wave height occurs [4,5].

This paper maps and evaluates the cultural ecosystem services (CES) of this giant-wave hotspot. *Cultural Ecosystem Services* (CES) are defined as "the non-material and intangible benefits arising from multi-dimensional human-nature relationships, such as cultural heritage, place identity, spiritual enrichment, cognitive development and learning" [6].

The phenomenon of giant waves in Nazaré has received the attention of several researchers [1,2,7,8].

Nevertheless, there is a gap in the literature because the assessment and spatial mapping of the cultural ecosystem services provided by this nature attraction were not investigated in previous studies. Moreover, the extant literature did not analyze the relationship between these CES and the push and pull drivers of several groups of individuals/stakeholders who play different roles and perform different activities in this coastal hotspot. Furthermore, few papers have examined the motivations and behaviors of water sport spectators.

Therefore, this paper provides an innovative contribution to the field and investigates the following research questions:

RQ1. What kind of cultural ecosystem services (CES) are provided by the Nazaré undersea canyon? In particular, this paper will focus on the recreational, aesthetical, and spiritual CES that are imbedded in the surf tourism experience journey.

RQ2. What are the influences of external factors on the spatial distribution of cultural services?

RQ3. What are the push/pull motivations and drivers of the giant-wave chasers/spectators?

Furthermore, research into the customer experience/customer journey has received attention from several authors [9–12], as well as the tourism and hospitality industry [13–16]. Lemon and Verhoef (p. 71) defined *customer experience* as a "multidimensional construct focusing on a customer's cognitive, emotional, behavioral, sensorial and social responses to a firm's offerings during the customer's entire purchase journey" [17]. Moreover, Bolton et al. conceptualized customer experiences within a three-dimensional space, bringing together the digital, physical, and social realms [18]. Therefore, a fourth research question emerged:

RQ4. How is the giant-wave tourist's experience journey? This paper provides a new tool for destination managers and tourism operators by proposing a holistic theoretical framework that describes the influences of the push and pull drivers at different stages of the tourist's journey.

The paper adopted a qualitative approach by combining photos taken during auto-ethnographic direct observation and the content analysis of the description of geotagged photos with videos from social media platforms, such as YouTube, Facebook, and Flickr.

2. Literature Review

This section presents the state-of-art of the previous studies regarding the classification and mapping of coastal cultural ecosystem services. This study assesses the pull and push factors of CES that benefit several categories of individuals: (1) big-wave surfers; (2) risk recreationists (non-big-wave surfers); (3) big-wave spectators/storm chasers; (4) local residents; (5) the firms of big-wave surf clusters that provide support services and products of this sport (e.g., hospitality and accommodation, safety, rescue crews, protection clothing, and equipment); (6) cultural heritage tourists. Because the giant-wave season is in the winter, this paper did not consider sun and beach tourists.

2.1. Mapping Cultural Ecosystem Services (CES)

Several attempts were made to map marine and coastal ecosystem services (ES) [19–21]. The literature provides solid theoretical and scientific support for the use of Flickr geotagged photos in order to assess and valuate recreational and aesthetic CES [22–29].

Moreover, an increasing number of studies are examining the distribution and congruence of ecosystem services, often with the goal of identifying areas that will provide multiple ecosystem service hotspots. There is paucity of data on most ecosystem services and, therefore, proxies are frequently used to map their distribution [30–36].

The classification taxonomy of marine and coastal CES, developed by the Common International Classification of Ecosystem services (CICES) v5.1 [37], comprises the following eleven categories: (1) recreation and leisure; (2) aesthetic; (3) cultural heritage and identity; (4) spiritual, sacred and/or religious; (5) educational; (6) inspiration for culture, art and design; (7) sense of place; (8) social relations; (9) scientific; (10) existence; and (11) intellectual and representative interactions (group). Garcia Rodrigues et al. made an exhaustive list of all the terms and labels that were found in the literature concerning the coastal CES for each category [38].

2.2. Motivations and Segmentation of the Demand for Coastal and Marine Destinations

This paper examines other specific motivators and segmentation criteria that explain the demand of the coastal CES. Carvache-Franco et al. (2019, 2020) identified six motivational factors for choosing coastal destinations: authentic coastal experience, heritage and nature, learning, novelty and social interaction, physical activities, and sun and beach [39,40]. These authors showed the existence of two segments of visitors: (1) "Beach lovers" formed by tourists who have high motivations in such aspects related to the sun and the beach; (2) "multiple coastal motives", i.e., grouped tourists who have high values in all the motivational dimensions. Moreover, Nagy et al. made a segment analysis of water sport tourism and the cluster analysis yielded four clusters based on sports and tourism motivations, namely: sports-oriented, leisure-ignoring, leisure-oriented, and social-oriented groups [41].

2.3. Recreation and Leisure

2.3.1. Risk Recreation (Big-Wave Surfers and Active Risk Recreationists)

According to Fluker (p. 7), *surf tourism* can be defined as [42]: "the act of people traveling to either domestic locations for a period of time not exceeding six months, or international locations for a period of time not exceeding twelve months, who stay at least one night, and where the active participation in the sport of surfing, where the surfer relies on the power of the wave for forward momentum, is the primary motivation for destination selection" [43].

Nazaré is a destination for giant-wave surfers, who may be classified into the category of active (extreme) risk recreation tourists. Boudreau et al. defined adventure recreation as "self-initiated nature-based physical activities that generate heightened bodily sensations (e.g., vestibular sensations arising from quick acceleration in varying dimensions of space) and require skill development to manage unique perceived and objective risks (p. 2)" [44].

At the 'extreme' end of the nature sport spectrum (e.g., activities such as B.A.S.E. (buildings, antennae, space, earth) jumping, big=wave surfing, waterfall kayaking, rope-free climbing), the most likely outcome of a mismanaged error or accident is death. Thus, many psychologists view this behavior as irrational and deviant, resulting from ignorance or the inability to self-regulate [45]. This extreme sport is not only performed by men; in Nazaré, it is common to see female surfers, such as Maya Gabeira (Brasil), Joana Andrade (Portugal), and Justine Dupont (France) [46].

According to systematic literature reviews by Boudreau et al. [44] and Gstaettner et al. [47], there are several explanations for participation in adventure recreation (e.g., opportunities for mastery, overcoming fear, socializing, identity construction, connecting with nature) [48–50]. Giddy and Webb compiled nine push factors that are determinants of the conditions and significance of the environment, which in turn are positively correlated with the satisfaction in adventure tourism: thrill, risk, physical challenge/skills development, enjoying nature/nature appreciation, overcoming nature, environmental education, novelty, escapism, and socialization [51].

Risk recreation activities also foster hedonic, eudaemonic, and therapeutic aspects of subjective well-being (SWB) by supporting the satisfaction of basic psychological needs for autonomy, competence, relatedness, and beneficence [44,52,53], or the search for freedom [54].

Giddy and Webb claimed that a recent probing of risk/thrill-seeking notions surrounding motivations and experiences has led to the identification of a wider range of psychological states, such as 'rush,' 'edgework,' or 'flow' [49,51,55,56]. Boudreau et al. proposed that experiencing a flow state (i.e., an effortless and enjoyable state of feeling deeply in control and fully immersed in an activity) may provide a strong motivation for continued participation in adventure recreation [44,57–59]. This theory is similar to the adventure experience paradigm (AEP) of Martin and Priest [60], which predicts peak adventure as a consequence of a balance in perceived risk and competence [61]. Flow—since its conception—has been studied in adventure recreation contexts and it is a particularly important motive for big-wave surfers [62–65].

Moreover, Clough et al. and Buckley claimed that some self-achievement experiences involve potential physical risks; they may awake the euphoria related to heroic overcoming of challenges and the encounter with natural primitiveness [66,67].

The "absorption" factor established by Magyaródi et al. includes the other dimensions of the original concept (items about engagement, the quality of the experience, change of time perception, or forgetting about the environment) [68].

2.3.2. Sensation Seeking, Gaze, and Spectacular Death Voyeurism (Passive Big-Wave Spectators)

This paper extends the understanding of risk recreation motivation to those who enjoy watching others performing risk recreation activities (see Table 2). For example, commercial adventure tourists, although drawn to an activity for the sake of risk, fear, and excitement, simultaneously felt safe and protected within commercial operating settings [69] and admitted that 'it's more like watching an exciting but consequence-free film of [an adventure activity] than being in one' (p. 18) [70].

Table 2. Giant-wave surf tourism segments: characteristics, push and pull drivers, and cultural ecosystem services.

	(Active) Giant-Wave Surfers	Surf Tourists (Non-Big-Wave Surfers)	Risk Recreationists	(Passive) Giant-Wave Chasers/Spectators
Major characteristics	(Professional) surfers and their rescue teams who are specialized in giant-wave riding	Active participation in surf sport activities in non-big-wave swell	Tourists who participate in risk activities, such as riding giant waves in boats or water bikes with driver	Spectators who enjoy watching surfers and/or giant waves
Push factors (internal motivators)	Extreme risk recreation thrill, risk, flow, physical challenge, skills development, overcoming nature and fear, euphoria, seeking for adrenalin, imminent death risk	Sense of belonging to the surf lifestyle/community, connection with nature, socialization, identity construction	Risk/adventure recreation hedonic, eudaemonic and therapeutic aspects of subjective well-being (SWB) 'peak', 'transcendent', or 'cathartic' experiences	Connection with nature, sensation seeking, gaze, spectacular death voyeurism, thanatopsis, storm chasing, and awe-inspiring experiences
Pull factors (external motivators)	Organized events and advertising campaigns	Organized events and advertising campaigns Films and documentaries Nazaré ambassadors (e.g., Garret MacNamara)	Tourism operators who provide risk recreation experiences	Giant-wave forecasting/alerts Advertising campaigns Films and documentaries
Cultural Ecosystem Services	Recreational Sense of place Social Relations Scientific	Recreational Social Relations Sense of place Educational	Recreational	Recreational, aesthetic, spiritual, sacred and/or religious Social relations Sense of place

Source: Author's elaboration.

The act of watching in tourism is associated with the concept of "tourist gaze" introduced by the sociologist Urry, who argued that the centrality of the visual in contemporary culture is mirrored in tourism, and that our desires to visit places and the ways we learn to visually appreciate those places are not merely individual and autonomous but are socially organized [71]. Moreover, the act of watching is also in the definition of *sport tourism* of Gibson (p. 10): "leisure-based travel that takes individuals temporarily outside of their home communities to play, watch physical activities or venerate attractions associated with these activities" [72].

There are few studies that investigate sporting events from the perspective of spectators [73]. Horbel et al. found that the context of value creation is positively associated with the "service ecosystem of a sport event" [74]. Sporting events offer immersive "servicescapes" [75], experiencescapes, or sensoryscapes [76], which can enhance the value of the experience [77,78].

For example, Wang et al. [79] studied the phenomenon of tidal bore-watching activities in China, which is a phenomenon caused by the leading edge of the incoming tide forming a wave of water that travels up a river or narrow bay against the prevailing current [80]. Regarding tide-watching, visitors tend to believe that it involves relatively low risk, because most people watch tidal bores by standing along the riverbank. Such perceptions, however, ignore the strong power and unpredictability of a tidal bore, which may open up the possibility of tourists being hurt or whirled away by "tsunami-like" tides.

The motivation to watch surfers riding giant waves can be explained by the seeking for adrenalin and thrill sensations triggered by the imminent death risk of this extreme sport spectacle [81,82]. Zuckerman defined *sensation seeking* construct as: "a personality trait defined by the seeking of varied, novel, complex and intense sensations and experiences, and the willingness to take physical, social, legal and financial risks for the sake of such experience" (p. 27) [83].

2.4. Spiritual, Sacred, and/or Religious: Storm-Chasing and Awe-Inspiring Experiences

The proneness to watch the dangerous performances of big-wave riders can be associated with lighter dark tourism theories and motivators, such as [84]:

(a) The concept of "thanatopsis," defined by Stone [85] as "the reflection and contemplation of death and dying" usually present in dark tourism also related with the notion of "death drive" [86,87].
(b) The psychoanalytical notion of "voyeurism" of the spectacular death and death desire [88–91].
(c) The notion of "mortality salience", defined by Gordillo et al. as the "awareness of the inevitability of one's own death . . . " (p. 286) [92–94].
(d) The terror management theory, which states that human beings are uniquely aware of their own mortality leading, in turn, to fear or terror of death. Consequently, various strategies are used within everyday life to manage such terror [85,86,95].

The giant-wave phenomenon is usually associated with winter storms and hurricanes in the Atlantic Ocean. Therefore, there is an overlap between risk recreation and storm-chasing tourism. Part of the motives that attract people to Nazaré is the unique combination of nature elements that is enhanced by the storms season in the winter. Several studies aimed to understand the interest in severe weather that spur people to embark on storm-chasing tourism [96,97]. Boulais focused on the ways severe weather was depicted in participants' discourse and on storm-chasing companies' websites [98]. Data revealed six non-mutually exclusive depictions of severe weather: passion, a spectacular sight, a dangerous encounter, a rewarding challenge, a treat, and a reminder of humanity's powerlessness.

Giant waves can trigger stimuli for extraordinary, 'pure', 'peak', 'transcendent', or 'cathartic' episodes/experiences, because awe emotions can be generated when individuals confront natural wonders, inspired by the sacred or mystic aura of the place [99–101].

Pearce et al. defined *awe* as an intense (and usually positive) emotion often experienced by individuals visiting nature-based tourism destinations; it has the potential to nurture strong connections between individuals and their environment [101]. Bonner and Friedman [102] provided a conceptual clarification of the complexity and multifaceted nature of the concept of awe proposed by Schneider [103]. They identified ten themes that helped to explain the concept of awe: profoundness, connectedness, numinous, vastness, existential awareness, openness and acceptance, ineffable wonder, presence, heightened perception, and fear.

2.5. Sense of Place and Social Relations: Socioeconomic Implications for the Local Community (Local Residents and Firms/Investors of the Surf Cluster)

The giant-wave phenomenon also leverages CES related with the sense of place and the identity building of Nazaré residents, who have social interactions/relations with visitors, in particular giant-wave chasers and surf tourists. Surfing, as a lifestyle, has been grounded in surf culture, which is recognized as a potential attraction factor for certain surf destinations. The perceptions of the surf culture contribute to a better overall destination image and a higher loyalty towards the destination [104].

In order to understand the transformation of Nazaré from the anthropological and sociological perspectives, Ferreira made an ethnographic film [6] of the daily life activities and imaginary activities after the big-wave "boom" [105]. This documentary captures the emotions, the sense of place, and the identity traces of Nazaré local people and how their pride and self-esteem have increased since the town started to attract international tourists.

On the other hand, Cunha-e-Sá et al. estimated the economic impact of a three-year media campaign involving private and public institutions to promote big waves and tourism, launched by Nazaré Qualifica and the municipality of Nazaré [8]. After this marketing media campaign, the site became a more popular tourist destination by providing the required "informational media infrastructure" campaign that allowed for the worldwide recognition of the value of big waves.

Cunha-e-Sá et al. estimated that the number of domestic visitors (42,161) and international visitors (35,500) whose average expenditures per visitor and trip were, respectively, EUR 72 and 92. According to an optimistic scenario, the economic impact for the four-year period (2010–2014) was about EUR 10 million. Overall, the total reported expenditures related to big waves were EUR 283,847 during 2010–2013, of which, EUR 26,948 were public expenditures; that is, investments of the local municipality [8].

Nevertheless, Wieser [2] and Bradsahw [7] also addressed some negative consequences of the tourism boom in Nazaré, especially in terms of the social impacts in residents' quality of life and the potential negative environmental implications. Bradshaw rose the question: "When the weather systems give the green light for big waves, surf enthusiasts flood the town head to the cliff tops in the hope of witnessing goliath waves, but at what cost are these new visitors on Nazaré's social carrying capacity?" [7]. Crowding and exceeding carrying capacity are factors that threaten the sustainability of surf tourism destinations [106].

2.6. Other Types of Cultural Ecosystem Services: Aesthetic, Cultural Heritage, Inspiration for Culture, Art and Design, Scientific, and Educational (Cultural Heritage Tourists)

Furthermore, there are other CES that benefit the cultural heritage tourists and the local community. According to Iliev [107], there is a strong motivation on the side of the tourists to engage in the pleasure of aesthetics that allow simulation and encourage emotion. Nazaré also inspires projects related to culture and art, such as the Nazaré Criativa project, which promotes local cultural heritage, particularly, living traditions and unique places, going far beyond what is offered in terms of experiences and activities in Nazaré [108]. All activities revolve around stories, traditions, presentations, places, and people of Nazaré.

Regarding the scientific and educational CES, Carapuço et al. claimed that selecting the adequate communication trigger effectively boosts scientific knowledge transfer and raises the predisposition conditions for the audience to be receptive of non-trivial ocean-related scientific topics [109]. "The Nazaré Wave: a trigger for learning" was revealed to be a highly successful initiative and similar strategies may be adopted in other projects aimed at increasing coastal and ocean literacy. The cluster of the surf, which comprises several products (surf boards, wetsuits, and big-wave gear items) and services (schools of surf, water bikes rescue teams, etc.), has been increasing as a direct consequence of this scientific development.

3. Methodology

This paper assesses and maps the deep motivations/pull drivers of giant-wave spectators. Therefore, this study adopts an interpretivist/ constructivist paradigm by combining different qualitative methods, such as an auto-ethnographic direct observation and the content analysis of videos and geotagged photos retrieved from social media platforms, such as YouTube, Facebook, and Flickr. Flickr is a major image-sharing website, with more than 60 million monthly active users (in 2022) who upload 1 million photos worldwide daily, according to Yahoo reports. Using Flickr's API method, called *flickr.photos.search*, the author was able to extract 6914 public photos taken in a 5 km radio around Nazaré's lighthouse building, located at a latitude of 39.60698 and longitude of −9.08402. These photos were taken by 165 photographers who traveled from 30 different countries. The majority came from Portugal (19.3%), followed by Spain (15.1%), the USA (11.4%), France (9%), and Italy (9%).

The method extracted the following relevant information: photo ID, owner ID, taken date of photo, title, tags, latitude, longitude, accuracy, number of views, text description, and URL. Here is the link of the API method used. In order to access the metadata of the photos, the reader must ask Flickr a researcher API Key code and replace the string "[researcher API key]" in the formula:

https://www.flickr.com/services/rest/?method=flickr.photos.search&api_key=[researcherAPIkey]&user_id=&content_type=1&lat=39.60698&lon=-9.08402&radius=5&radius_units=km&extras=description%2C+date_taken%2C+owner_name%2C+tags%2C+views%2C+url_o&format=rest (accessed on 31 October 2022)

The use of visual anthropology, (including visual auto-ethnography and photo elicitation) as research methods is well supported in the literature [110–115]. Visual research methods usually collect: (1) 'found' images (pre-existing photographs and film); (2) researcher created images; and (3) respondent-created or user-generated images.

4. Discussion of Results

Section 4.1 presents the author's auto-ethnographic journey that allowed the assessment of the push and pull factors of giant-wave spectators/storm chasers linked to recreational, aesthetic, and spiritual CES. The content analysis of the Flickr photos presented in Section 4.2 complements the assessment of the CES that benefit the residents, the firms of the surf clusters, and the cultural heritage tourists.

4.1. Auto-Ethnographic Study: Mapping Journey of "Giant Waves" Chaser Tourists

On 25 February of 2022, the author traveled to Nazaré to watch the "giant waves" phenomenon. The journey started several weeks before, with the daily monitoring of several websites [7] that forecast the significant wave heights. There are also webcams [8] that allow tourists to confirm the quality of the swell before traveling to Praia do Norte.

Mach et al. described this journey using the term 'surgical strike' that has been co-opted into the surfing vernacular to differentiate a particular surf trip, which can be domestic or international, where a surfer targets a specific surf-break based on detailed forecasting data and a deep understanding of the variable factors that lead to the best possible conditions at that surf-break [116]. Real Watersports describes them this way: "'Surgical strikes' are when you travel specifically for perfect weather conditions (swell/wind or both) rather than on a calendar like most humans do... Recreational enthusiasts should partake in at least one surgical strike in their lifetime—and probably many more . . . If you only have two weeks off a year and you miss the epic score during your break, then you have to wait another year to roll those 2/52 odds again. Strike out too many years in a row and it starts to really eat at you" [117].

Then, on 21 February, four days before, the forecast for the wave height according to several sources was about 10 m (which can increase three-fold due to the canyon effect), reaching the maximum rating of 10 points (See Figure 2). Because most hotels in Nazaré only allow free cancelation of the booking until three/four days before the date of arrival, tourists have to make the decision to travel based on the odds that the forecast is correct.

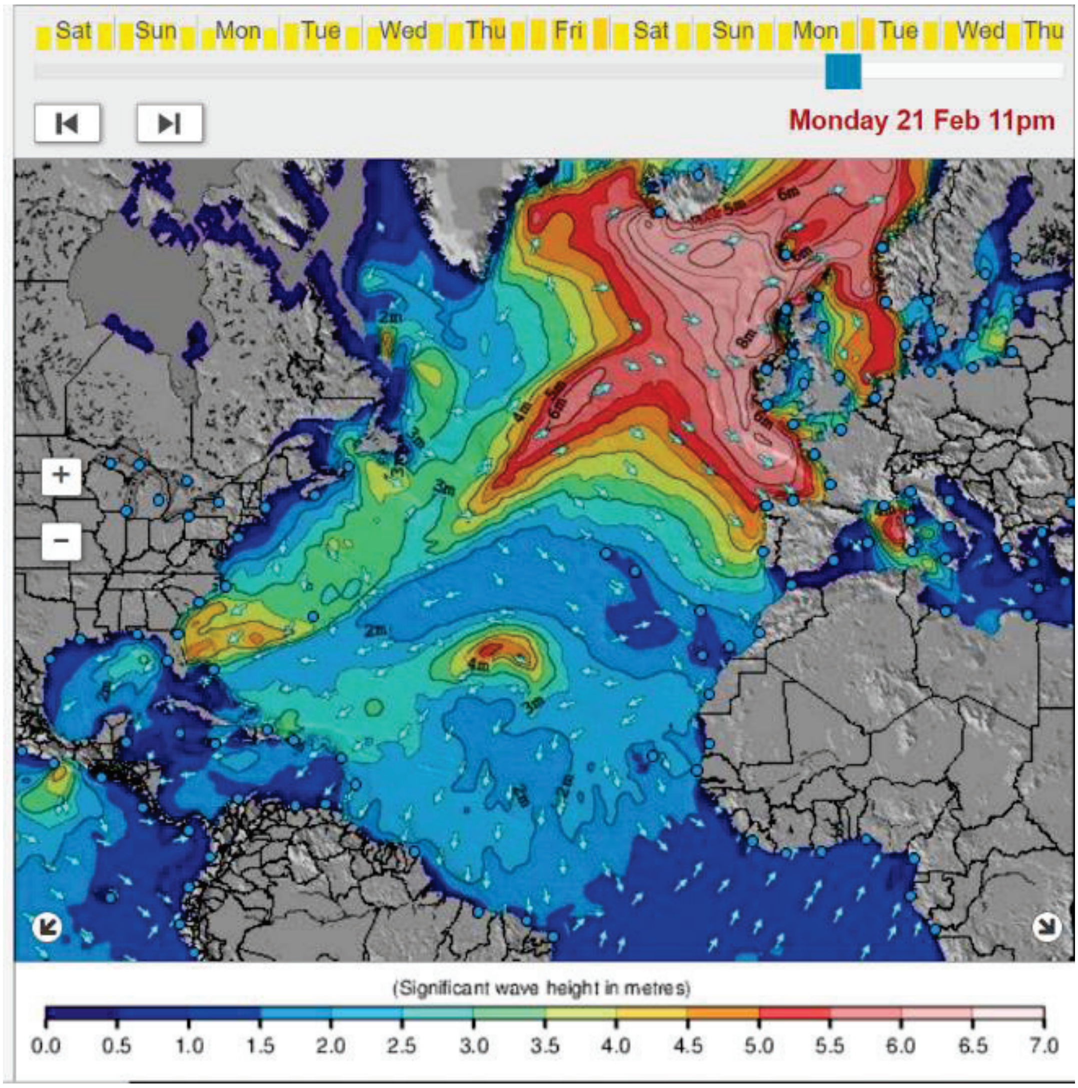

Figure 2. Print screen of the wave height forecast published on the website pt-surf-forecast.com.

Early in the morning on 25 February, hundreds of "giant-waves" pilgrims walked to the surroundings of the Praia do Norte beach in order to obtain the best spot to watch the waves. Figure 3 presents four photos taken by the author during the ethnographic trip, showing the crowd that patiently waited for the "biggest" one, hoping that a surfer in the water rode it, and earned applause, similar to an acrobat in the circus. A successful (sometimes epic) riding excites the crowd and triggers peak emotions, as portrayed in some videos shared on social media [9].

For example, the Facebook page of Praia do Norte [10] published several photos of that day, which complemented the analysis of the journey. Those photos and videos shared by the spectators to YouTube that day (see Table 3) are examples of the electronic word-of-mouth during the advocacy/post-experience stage. During the journey, it was possible to confirm the influence of some push factors (waves forecasting; social media alerts) that ignited the pull factors that emerged in the literature review, such as willingness to connect with nature, sensation seeking, awe, or spectacular death voyeurism (see Table 2).

Figure 3. Authors' photos taken on the ethnographic trip showing the spectators of giant waves.

Table 3. Examples of the videos posted on YouTube less than 24 h after (accessed on 26 February 2022).

	24 h after Views	24 h after Comments
https://www.youtube.com/watch?v=HFvtuZe_yG0	2470	0
https://www.youtube.com/watch?v=fHxG5cGrwtc	1281	0
https://www.youtube.com/watch?v=i8VfVs9D2lY	20863	24
https://www.youtube.com/watch?v=PRls6pTIpKI	2388	4
https://www.youtube.com/watch?v=TLFZ0QSMM6M	1244	6
https://www.youtube.com/watch?v=0nGbRrVw8sA	19	

4.2. Content Analysis of Photos Extracted from the Flickr Platform (User-Generated Content)

Then the author selected 44 photos from a sample of 6914 photos retrieved with Flickr's API method, called *flickr.photos.search*. The selection of the photos was based on the content analysis of the photo, on the significant content of the title, tags, and text descriptions (see Table 4). The major criterion included every new portrayed cultural ecosystem service, thus aiming for maximum diversification of the CES inventory. The classification of CES was based on the classification taxonomy of marine and coastal CES provided by the Common International Classification of Ecosystem services (CICES) v5.1, as detailed in Section 2.1 in the literature review [37].

Table 4. Cultural Ecosystem Services (CES1 and CES2) depicted in the selection of photos retrieved by the Flickr API method flickr.photos.search (all accessed on 31st October 2022).

Legend	Photo ID	Date Taken	Views	url_o	Description	CES 1	CES 2
A1	30644542680	2016-09-15 19:29:20	67	https://live.staticflickr.com/5490/30644542680_e7c0420bb6_o.jpg	Beach at sunset	Aesthetical	Photography
A2	30559157036	2016-10-12 13:08:03	1571	https://live.staticflickr.com/5767/30559157036_05891a1a45_o.jpg	Windows architecture	Aesthetical	Immaterial heritage
A3	49309306977	2018-06-09 21:23:43	556	https://live.staticflickr.com/65535/49309306977_e8220593fe_o.jpg	Fisherman at the beach	Aesthetical	Social relations
H1	23442799314	2015-09-29 12:03:32	52	https://live.staticflickr.com/5749/23442799314_33cd5fb436_o.jpg	Museum	Heritage	
H2	35499908875	2016-05-08 18:03:47	1444	https://live.staticflickr.com/4254/35499908875_11e5de01a1_o.jpg	Traditional fishing boats	Heritage	Sense of Place
H3	27324003121	2016-05-10 20:27:11	2634	https://live.staticflickr.com/7418/27324003121_4867c51b2b_o.jpg	Old traditional boats	Heritage	Photography
H4	31096429260	2016-06-17 14:28:32	1459	https://live.staticflickr.com/5556/31096429260_aee2133724_o.jpg	Lighthouse	Heritage	
H5	30464527935	2016-10-10 16:29:50	800	https://live.staticflickr.com/5333/30464527935_7d079741ec_o.jpg	Nazaré, Portugal	Heritage	Religious
H6	35867788775	2017-06-15 13:52:01	609	https://live.staticflickr.com/65535/35867788775_2c24644592_o.jpg	Old Chapel	Heritage	Religious
H7	40443397174	2018-03-28 09:11:32	27,568	https://live.staticflickr.com/789/40443397174_b217c32347_o.jpg	Old traditional boats	Heritage	Photography
H8	45275272174	2018-11-16 15:08:21	69	https://live.staticflickr.com/4825/45275272174_f66ffdb179_o.jpg	Nazaré	Heritage	
H9	51853849021	2021-07-08 14:41:21	120	https://live.staticflickr.com/65535/51853849021_d1cde46804_o.jpg	The XIX century elevator	Heritage	Industrial tourism
H10	51385715125	2021-07-08 19:12:48	232	https://live.staticflickr.com/65535/51385715125_1f7dd7d9fa_o.jpg	Fort of Sao Miguel Arcanjo and Lighthouse	Heritage	Sense of Place
H11	51708646208	2021-11-23 17:57:57	188	https://live.staticflickr.com/65535/51708646208_70179d3964_o.jpg	Praia do Norte and Forte de Sao Miguel Arcanjo	Heritage	Photography
H12	51711091674	2021-11-26 14:02:00	40	https://live.staticflickr.com/65535/51711091674_3bd7abdc3e_o.jpg	Traditional Gastronomy (Octopus, Squid and Cod)	Heritage	
H13	52065438755	2022-05-10 17:42:17	371	https://live.staticflickr.com/65535/52065438755_c255ec11c2_o.jpg	Traditional women costume	Heritage	Social relations
H14	52065438755	2022-05-10 17:42:17	371	https://live.staticflickr.com/65535/52065438755_c255ec11c2_o.jpg	Local woman with traditional costume	Heritage	Social relations

Table 4. *Cont.*

Legend	Photo ID	Date Taken	Views	url_o	Description	CES 1	CES 2
I1	51517746386	2016-05-10 21:44:40	1907	https://live.staticflickr.com/65535/51517746386_893630dfa4_o.jpg	Traditional folklore dancers	Inspiration for art	Immaterial heritage
I2	51545291535	2016-05-10 21:45:45	3406	https://live.staticflickr.com/65535/51545291535_165ab27249_o.jpg	Folklore, traditional dancer	Inspiration for art	Immaterial heritage
I3	33172810631	2016-05-10 22:09:45	2580	https://live.staticflickr.com/686/33172810631_070d5bf8bc_o.jpg	Folklore, traditional dances	Inspiration for art	Immaterial heritage
I4	51354506906	2021-07-08 19:01:27	270	https://live.staticflickr.com/65535/51354506906_57fc33932a_o.jpg	The Dear Statue (Religious Tales and Legends)	Inspiration for art	Immaterial heritage
IR	31821785883	2015-09-26 15:57:17	316	https://live.staticflickr.com/562/31821785883_ac60b142d9_o.jpg	Dry fish	Intellectual Interactions	Immaterial heritage
K1	52303308475	2019-11-05 18:07:13	7588	https://live.staticflickr.com/65535/52303308475_6aeebfcdf1_o.jpg	Rescue water bikes	Local knowledge	Intellectual Interactions
K2	51970578966	2022-03-30 01:10:37	9537	https://live.staticflickr.com/65535/51970578966_1440ef6c84_o.jpg	Rescue water bikes	Local knowledge	Intellectual Interactions
R1	33104397152	2017-02-21 10:16:50	2093	https://live.staticflickr.com/593/33104397152_ccb4fe5c4c_o.jpg	Surf	Recreational	
R2	32396344154	2017-02-23 11:47:54	1231	https://live.staticflickr.com/3699/32396344154_a8aab87912_o.jpg	Surf Museum	Recreational	Intellectual Interactions
R3	34932097764	2017-06-12 13:25:52	1263	https://live.staticflickr.com/4023/34932097764_18fde34226_o.jpg	Nazaré Beach	Recreational	
R4	49598254706	2018-02-10 11:30:29	82	https://live.staticflickr.com/65535/49598254706_8577f26e55_o.jpg	Giant-wave watching	Recreational	Sense of Place
R5	51852851952	2021-07-08 15:42:18	154	https://live.staticflickr.com/65535/51852851952_686aac1472_o.jpg	Beach	Recreational	
R6	51916354356	2021-10-22 17:08:46	146	https://live.staticflickr.com/65535/51916354356_455accacfb_o.jpg	Surf Museum	Recreational	Intellectual Interactions
R7	52234045249	2022-07-22 17:49:43	1595	https://live.staticflickr.com/65535/52234045249_f50abfd0b8_o.jpg	Nautical/Water Sports	Recreational	
Sc1	51722296037	2021-07-28 16:59:49	167	https://live.staticflickr.com/65535/51722296037_b2281a64df_o.jpg	Local flora at the dunes	Scientific	Educational
Sc2	52228935753	2022-07-18 11:28:31	9	https://live.staticflickr.com/65535/52228935753_6f328a25d3_o.jpg	Local flora	Scientific	Educational
P1	18825114028	2015-05-19 21:38:12	373	https://live.staticflickr.com/288/18825114028_c751c0947e_o.jpg	Nazaré´s houses	Sense of Place	
Sr1	24259959260	2012-11-01 17:00:39	114	https://live.staticflickr.com/1469/24259959260_e6ac23bcdc_o.jpg	Local saleswoman	Social relations	Sense of Place
Sr2	23885164329	2015-09-29 13:53:30	237	https://live.staticflickr.com/1699/23885164329_96738aab3a_o.jpg	Square in Sitio	Social relations	Sense of Place
Sr3	22503253129	2015-11-07 15:31:16	11	https://live.staticflickr.com/633/22503253129_571316c7a1_o.jpg	Local drink (“Ginja”)	Social relations	Heritage

Table 4. *Cont.*

Legend	Photo ID	Date Taken	Views	url_o	Description	CES 1	CES 2
Sr4	31749444817	2016-05-08 18:05:00	2353	https://live.staticflickr.com/4864/31749444817_7f440568d2_o.jpg	Local women	Social relations	
Sr5	28174732962	2016-05-08 18:05:20	9220	https://live.staticflickr.com/7006/28174732962_f9841522ac_o.jpg	Drying fish on the beach	Social relations	Intellectual Interactions
Sr6	30539707936	2016-10-12 12:14:27	811	https://live.staticflickr.com/5543/30539707936_fa6c790d44_o.jpg	Fish Market	Social relations	
Sr7	49203125521	2019-12-05 18:02:48	1150	https://live.staticflickr.com/65535/49203125521_fb62d6ea16_o.jpg	Fishing Boat	Social relations	Sense of Place
Sr8	52229410705	2022-07-18 11:50:40	9	https://live.staticflickr.com/65535/52229410705_da1640f416_o.jpg	Fishing Boat	Social relations	
Sr9	52450403706	2022-07-23 18:11:21	4	https://live.staticflickr.com/65535/52450403706_9c1b141d35_o.jpg	Selling dry fish	Social relations	
Sp	52067734430	2022-02-14 05:28:32	215	https://live.staticflickr.com/65535/52067734430_8f0da3689c_o.jpg	Religious Tales and Legends	Spiritual	Immaterial heritage

Using the classification proposed by Garcia Rodrigues et al. [38], the two most explicit cultural ecosystem services depicted in the photos (CES 1 and CES 2) were reported.

The majority of photos show recreational and leisure activities related with water and nautical sports, in particular, scenes of surfers riding giants waves in Praia do Norte, under the surveillance of the rescue teams. The second category of photos portray the Nazaré beach located on the south side of the cliffs during the summer holidays.

Furthermore, this content analysis identified the other types of CES: (1) aesthetical (e.g., landscape photography); (2) man-made immovable heritage (e.g., the museum, the Fort of Sao Miguel Arcanjo/lighthouse, the elevator of the XIX century or the religious buildings); (3) movable heritage (e.g., traditional fishing boats); (4) immaterial heritage (e.g., the local fish gastronomy or the women traditional costumes); (5) the inspiration for art and design (e.g., folklore and traditional dances); (6) local knowledge as a form of intellectual and representative interaction (e.g., drying fish techniques—see Figure 4, rescue water bikes driving tactics to ride the giant waves); (7) social relations depicted in the fishing activities, in the fish market, and other street shops.

Figure 4. Author's photos taken on the ethnographic trip showing some examples of cultural ecosystem services of heritage and inspiration for art.

Nazaré is a land of legends and tales, which are rich sources of CES related to the immaterial heritage and the inspiration for culture, art, and design. The origin of the name "Nazaré" itself is explained by a statue of the Virgin brought from Nazareth (in present-day Israel) in the 4th century, which was previously lost but was found centuries later. Another famous story says that the Virgin appeared to a local nobleman in 1182 who was hunting deer. He was about to fall off the edge of a cliff on his horse and was miraculously stopped just in time. This legend was the inspiration for the "Dear" Statue [11] (made by Agostinho Pires and Adália Alberto), which combined the legendary origins of Nazaré with giant-wave surfer characteristics. It stands tall on the road to the lighthouse and it has been captured in many tourists' photos (see Figure 4).

In terms of scientific/educational cultural ecosystem services, besides the study of the biology of the flora and fauna of the region (under and out of the sea), giant-wave tourism has leveraged the scientific study related to the forecasts and measurements of the wave heights. The Hydrographic Institute of the Portuguese Navy [12] developed several projects that increased scientific knowledge about the Nazaré's Canyon and the giant-wave formation.

4.3. Analysis of Spatial Distribution of CES Based on Geotagged Photos

In order to analyze the spatial distribution of the photos, Figure 5 presents a Google Earth map that was built with a kml file on the latitude and longitude coordinates uploaded by photographers. The first column of Table 4 corresponds with the legend code in Figure 5, thus allowing the identification of the dominant CES portrayed in the photo. Figure 6 are amplifications of the partial zones signaled in Figure 5: zone A, around the lighthouse fortress; zone B, in the town center.

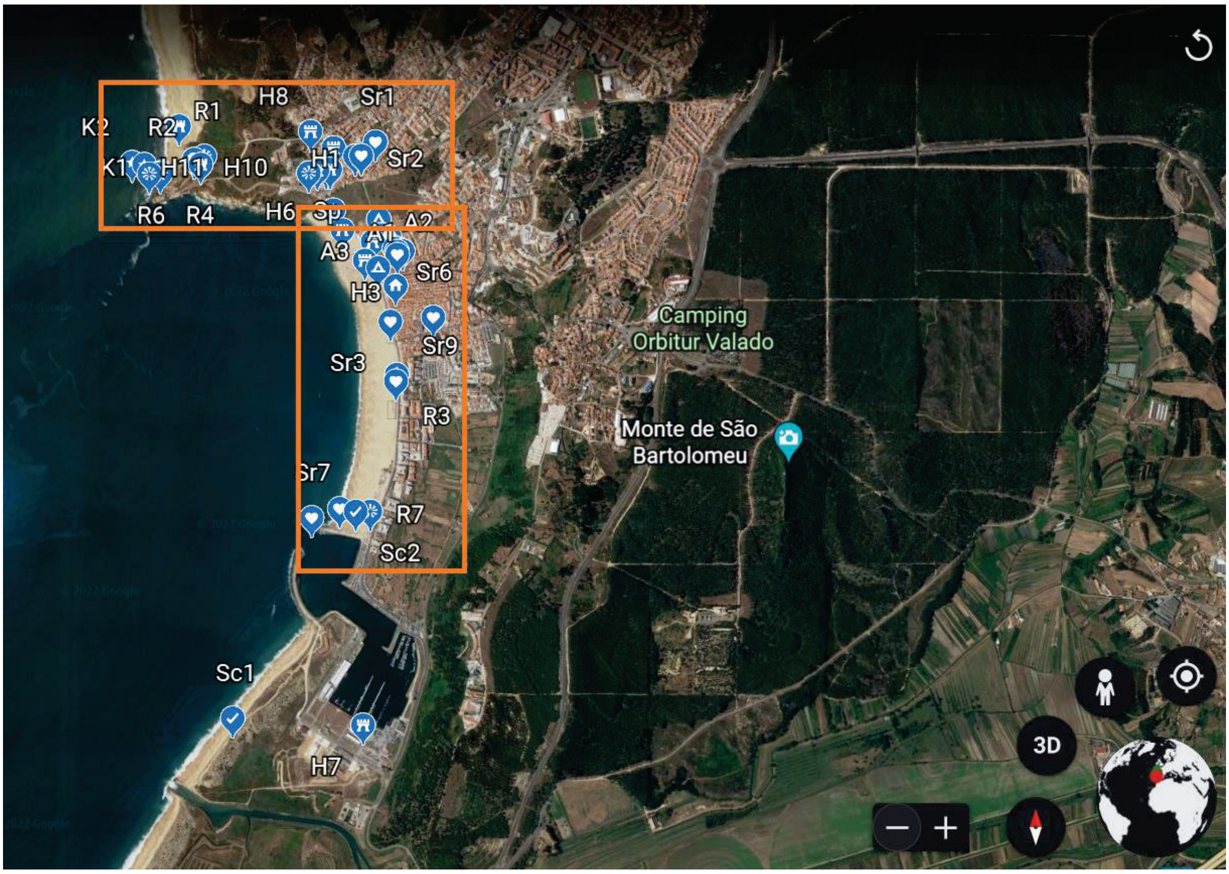

Figure 5. Google Earth map of the spatial distribution of the photos.

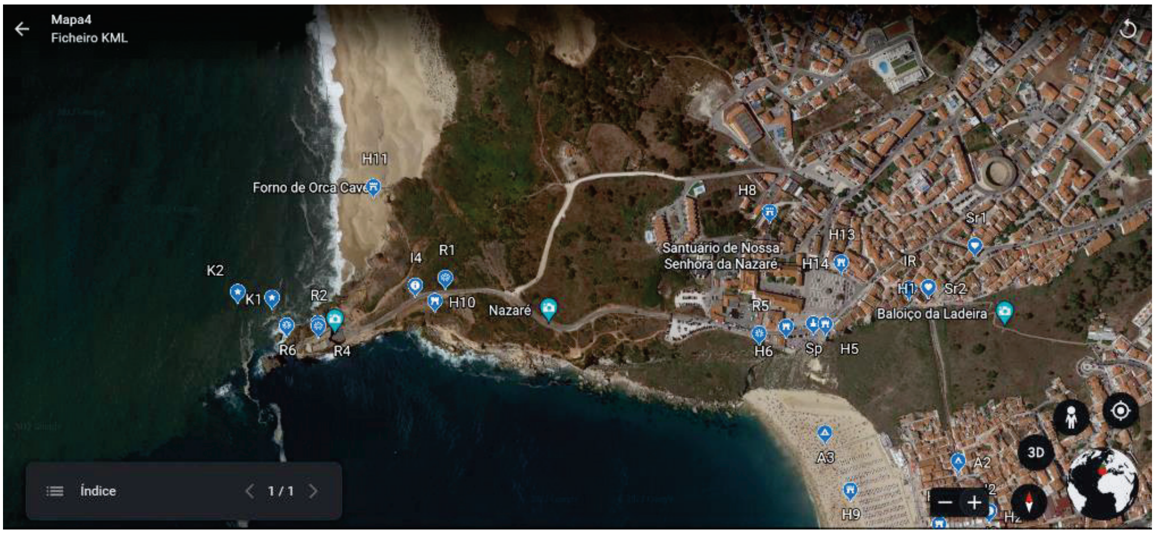

(a)

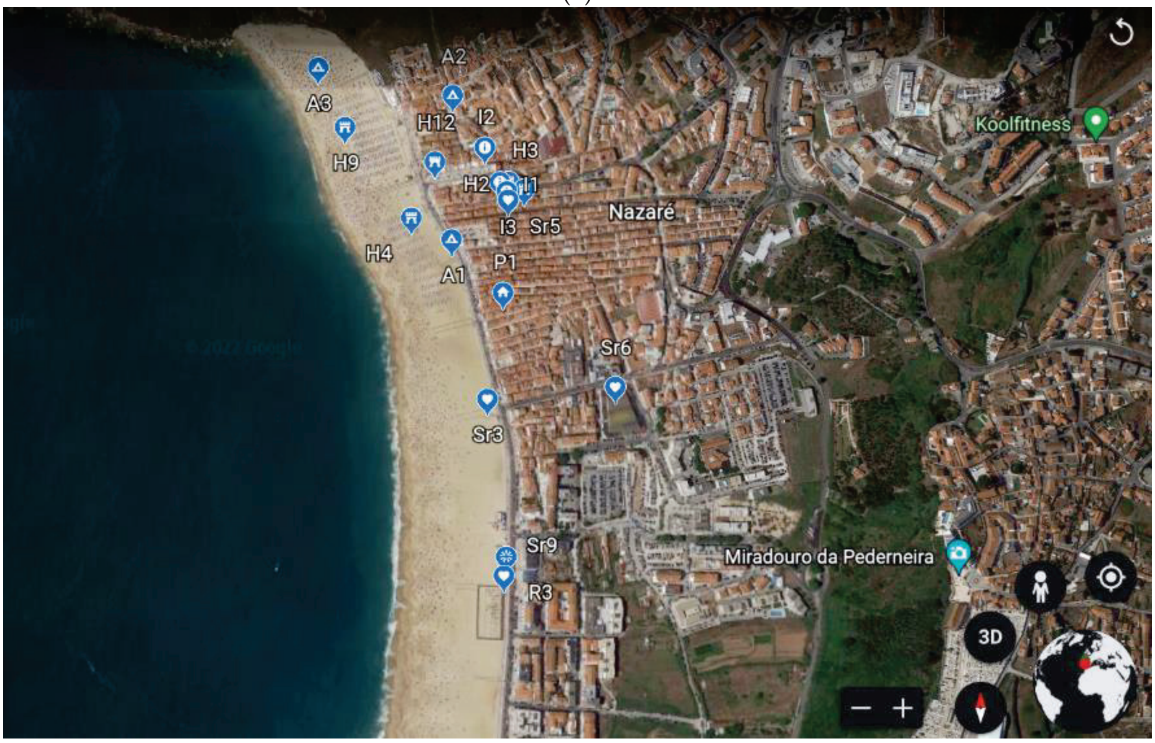

(b)

Figure 6. (**a**) Amplification of Google Earth map Zone A (around the Fortress); (**b**) amplification of Google Earth map Zone B (Nazaré town center).

The spatial distribution is influenced by the geographic and orographic characteristics of the territory, as the photos that depict recreational (R), and local knowledge (K) ecosystem services were taken in the best spot to watch the giant-wave—the cliffs around the lighthouse fortress, where the undersee canyon is located (see Figure 6). In the urban areas, such as Nazaré's town center, the photos portray mostly CES related with heritage (H), aesthetical (A), and social relations (Sr). Therefore, the spatial distributions of CES are also influenced by the concentration of inhabitants as suggested by previous studies [36].

Another example of scientific CES, i.e., a direct consequence of the giant-wave boom, involves the innovation and development of a lot of products related with the safety of the surfers in Nazaré. Andrew Cotton describes a list of 14 items of his surf gear that includes, for example, an impact/float vest for paddling and tow surfing big waves. It has loads of foam on the chest but none on the stomach, which makes it really nice to paddle in; it also has foam side panels and back panels and two side zips with overhead entry, which makes it harder for it to be ripped off in violent wipeouts.

5. Conclusions: Theoretical and Managerial Implications

5.1. Theoretical Framework of a Giant-Wave Chaser's Experience Journey

Based on previous sections of the literature review, this paper proposes a theoretical framework (see Figure 7) describing the push and pull factors that influence the tourist's experience journey of the giant-wave spectator/chaser. Considering the chronological order from the left to the right, this study found that during the awareness stage the giant-wave tourist is exposed to several push factors, such as the Nazaré Municipality advertising campaigns, McNamara stories, or film documentaries. During the consideration and planning stages, the alerts of wave forecasts ignite the pull motivators, impelling the organization of the trip.

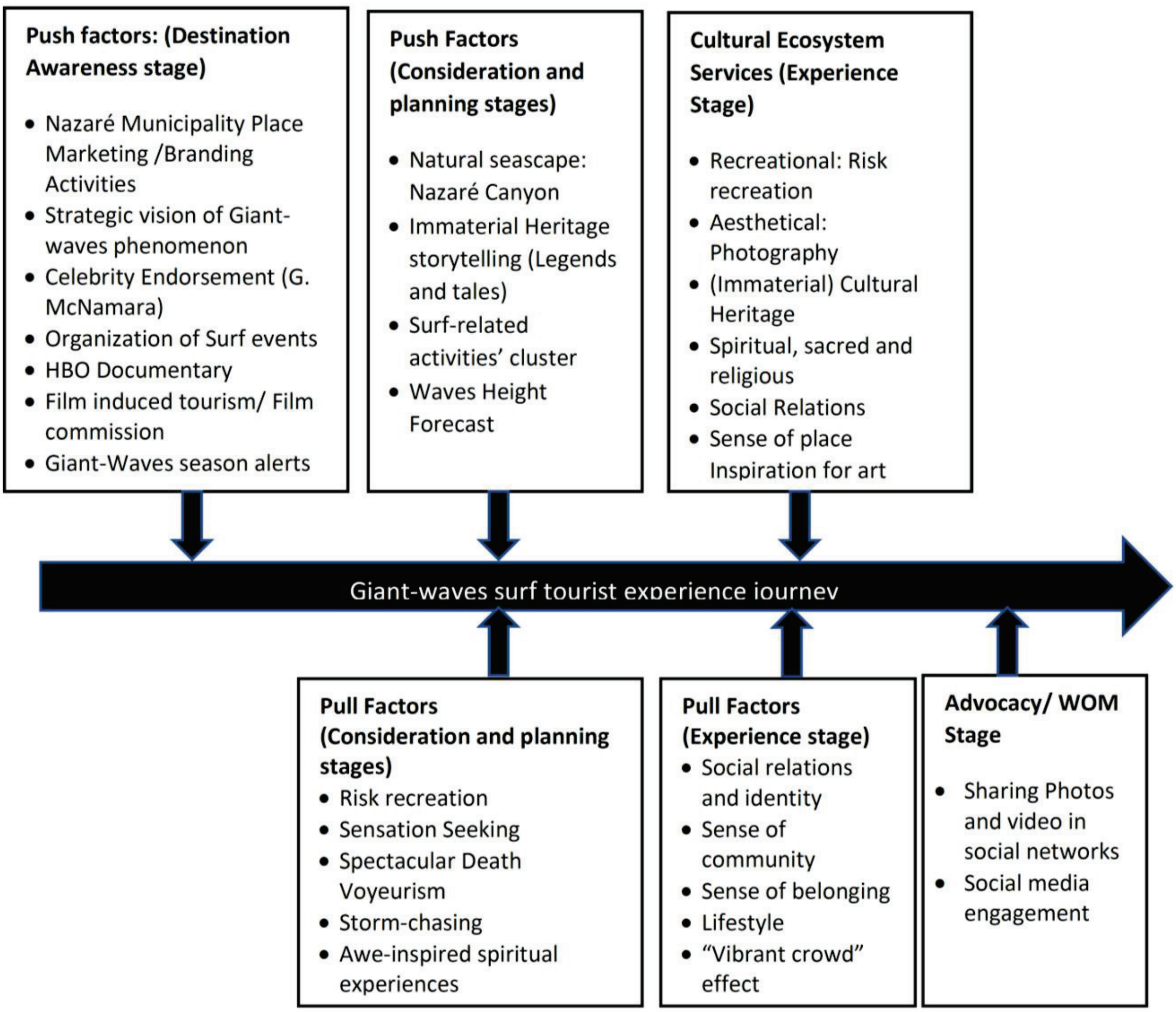

Figure 7. Theoretical framework of a tourist's experience journey of the giant-wave spectator/chaser.

During the experience stage, the giant-wave tourist captures the benefits of all the CES provided by the landscape and this nature attraction, which in turn are moderated by the individual pull factors, such as the propensity to socialize or the sense of belonging to this "tribe" of giant-wave chasers. At the end of the journey, the tourist shares his/her "peak" moments and emotions on social media, thus promoting the electronic word-of-mouth among family, friends, and peers.

5.2. Managerial Implications

The phenomenon of giant waves in Nazaré leveraged the increase of tourism and the local economy and inspired the strategic shift in the positioning of Portugal's destination branding. More recently, the website Visitportugal has launched an advertising campaign, i.e., "Portuguese waves", promoting the country as a (winter) surf destination [13] and aiming to reduce the tourism seasonality [118,119].

This paper provides useful information for regional public decision-makers, destination marketing organizations, tourism operators, and business entrepreneurs. The geotagged social media photos allowed the researcher to assess the most relevant maritime/coastal cultural ecosystem services in Nazaré, Portugal. Tourism operators and business entrepreneurs can use this mapping tool to support their business location decisions.

For example, risk recreationists (non-big-wave surfers) is a new market niche that is starting to be explored by new businesses (e.g., boat cruises that allow tourists to have closer views of big waves [14]).

From a theoretical perspective, this study did not confirm some of the pull factors suggested by previous studies. The comments from the user-generated photos and videos did not provide explicit evidence that giant-wave chasers are conscious of the motivations related to risk recreation and imminent/spectacular death voyeurism. Further research should adopt other methodologies, such as depth interviews in order to capture those unconscious drivers and deeper motivations.

Public decision-makers, destination marketing organizations, tourism operators, and business entrepreneurs must acknowledge the relevance of journey mapping in order to identify the moments of stress and the touchpoints associated with peak/positive experiences generated by these CES. These hotpots also provide the information about tourists' most frequent journeys, which can feed the design of innovative coastal tourism experiences. Multi-thematic coastal tourism routes or trails may contribute to attract new visitors, to enrich their journeys, to increase the staying time and satisfaction and, ultimately, promote electronic word-of-mouth. Further research may estimate the demand and assess the economic impact of surf tourism for the region.

There a lot of events (such as the Tudor Nazaré Tow Surfing Challenge) that attract more tourists every year. Nevertheless, according to Wieser [2], Bradshaw [7], or Muller [120], crowding and exceeding the carrying capacity may threaten the social and environmental sustainability of surf tourism in Nazaré and in other surf spots in Western Europe.

Funding: This research was funded by the Multiannual Funding of the Landscape, Heritage, and Territory Laboratory (Lab2PT), reference UID/04509/2020, financed by national funds (PIDDAC) through the FCT/MCTES (*Fundação para Ciência e Tecnologia*, Portugal).

Data Availability Statement: Data is available on request.

Conflicts of Interest: The authors declare no conflict of interest.

Notes

1 https://www.theguardian.com/sport/2011/nov/13/garrett-mcnamara-surfing-record-wave, accessed on 31 October 2022.

2 Official trailer of HBO documentary: https://youtu.be/znCNT-9k_Ws, accessed on 31 October 2022.

3 (e.g., the front cover of the newspaper "The Times" of 30th January of 2013).

4 https://www.nytimes.com/2018/11/11/world/europe/nazare-portugal-surfing-big-waves.html; https://www.theguardian.com/travel/2022/nov/04/nazare-portugal-watching-surfers-ride-monster-waves, accessed on 31 October 2022.

5 Source: https://www.facebook.com/praiadonortenazare/posts/10160210246034993, accessed on 31 October 2022.

6 https://vimeo.com/575472527/3476555f3a, accessed on 31 October 2022.

7 https://www.surf-forecast.com/weather_maps/North-Atlantic?over=none&type=htsgw; https://pt.surf-forecast.com/; https://www.ipma.pt/pt/maritima/hs/, accessed on 31 October 2022.

8 https://beachcam.meo.pt/en/livecams/praia-do-norte-canhao-nazare/, accessed on 31 October 2022.

9 https://www.facebook.com/reel/1333419030760250, accessed on 31 October 2022.

10 https://www.facebook.com/praiadonortenazare/posts/10160210246034993, accessed on 31 October 2022.

11 https://www.atlasobscura.com/places/veado, accessed on 31 October 2022.

12 https://www.hidrografico.pt/index/en, accessed on 31 October 2022.

13 https://ie.linkedin.com/posts/visitportugal_portuguese-waves-activity-6990634210155741184-KYGF?trk=public_profile_like_view, accessed on 31 October 2022.

14 https://www.facebook.com/nazarewaterfun, accessed on 31 October 2022.

References

1. Teixeira, D.D. Quebras Estruturais na Procura Turística: O Caso das Ondas Gigantes da Nazaré. Master's Thesis, Faculty of Economics of University of Porto, Porto, Portugal, 2019.
2. Wieser, N.K. Causes and Development Impacts of the Tourism Boom Exemplified by Nazaré. Ph.D. Dissertation, Karl-Franzens-Universität Graz, Graz, Austria, 2019.
3. Cunha, P.P.; Gouveia, M.P. *The Nazaré Coast, the Submarine Canyon and the Giant Waves: A Synthesis*; Working Paper; University of Coimbra: Coimbra, Portugal, 2015.
4. Do Carmo, J.S.A. Dominant processes that amplify the swell towards the coast: The Nazaré Canyon and the giant waves. *Res. Soc. Dev.* **2022**, *11*, e578111133804. [CrossRef]
5. Hydrographic Institute. Ondas na Nazaré, Como se Forma. Available online: https://www.hidrografico.pt/info/3 (accessed on 9 November 2022).
6. Langemeyer, J.; Calcagni, F.; Baró, F. Mapping the intangible: Using geolocated social media data to examine landscape aesthetics. *Land Use Policy* **2018**, *77*, 542–552. [CrossRef]
7. Bradshaw, L. Surfing the Innovation Waves: Surf Tourism in Portugal. In *Tourism Innovation in Spain and Portugal*; Leitão, J., Ratten, V., Braga, V., Eds.; Springer: Cham, Switzerland, 2021; pp. 149–166.
8. Cunha-e-Sá, M.A.; Freitas, R.; Nunes, L.C.; Otrachshenko, V. On nature's shoulders: Riding the big waves in Nazaré. *Tour. Econ.* **2018**, *24*, 369–385. [CrossRef]
9. Becker, L.; Jaakkola, E. Customer experience: Fundamental premises and implications for research. *J. Acad. Mark. Sci.* **2020**, *48*, 630–648. [CrossRef]
10. Bueno, E.V.; Weber, T.; Bomfim, E.; Kato, H. Measuring customer experience in service: A systematic review. *Serv. Ind. J.* **2019**, *39*, 779–798. [CrossRef]
11. Følstad, A.; Kvale, K. Customer journeys: A systematic literature review. *J. Serv. Theory Pract.* **2018**, *28*, 196–227. [CrossRef]
12. Jain, R.; Aagja, J.; Bagdare, S. Customer experience—A review and research agenda. *J. Serv. Theory Pract.* **2017**, *27*, 642–662. [CrossRef]
13. Chang, S. Experience economy in hospitality and tourism: Gain and loss values for service and experience. *Tour. Manag.* **2018**, *64*, 55–63. [CrossRef]
14. Hu, L.; Olivieri, M. Social media management in the traveller's customer journey: An analysis of the hospitality sector. *Curr. Issues Tour.* **2021**, *24*, 1768–1779. [CrossRef]
15. Taheri, B.; Prayag, G.; Muskat, B. Introduction to the special issue: Consumer experience management and customer journeys in tourism, hospitality and events. *Tour. Manag. Perspect.* **2021**, *40*, 100877. [CrossRef]
16. Zhang, T. Co-creating tourism experiences through a traveler's journey: A perspective article. *Tour. Rev.* **2019**, *75*, 56–60. [CrossRef]
17. Lemon, K.N.; Verhoef, P.C. Understanding customer experience throughout the customer journey. *J. Mark.* **2016**, *80*, 69–96. [CrossRef]
18. Bolton, R.; McColl-Kennedy, J.; Cheung, L.; Gallan, A.; Orsingher, C.; Witell, L.; Zaki, M. Customer experience challenges: Bringing together digital, physical and social realms. *J. Serv. Manag.* **2018**, *29*, 776–808. [CrossRef]
19. Caro, C.; Cunha, P.P.; Marques, J.C.; Teixeira, Z. Identifying ecosystem services research hotspots to illustrate the importance of site-specific research: An Atlantic coastal region case study. *Environ. Sustain. Indic.* **2020**, *6*, 100031. [CrossRef]
20. Culhane, F.E.; Robinson, L.A.; Lillebø, A.I. Approaches for estimating the supply of ecosystem services: Concepts for ecosystem-based management in coastal and marine environments. In *Ecosystem-Based Management, Ecosystem Services and Aquatic Biodiversity: Theory, Tools and Applications*; Springer: Cham, Switzerland, 2020; pp. 105–126.
21. Da Silva, C.V.; Ortigão, M.; Willaert, T.; Rosa, R.; Nunes, L.C.; Cunha-e-Sá, M.A. Participatory Geographic Information Systems (PGIS): Alternative approaches to identify potential conflicts and positional accuracy in marine and coastal ecosystem services. *Mar. Policy* **2021**, *131*, 104650. [CrossRef]
22. Azevedo, A.; Duenas, M.P.M.; Costas, G.B. Innovation on Research Methods: Geotagged Photos as a Proxy Tool to Map Heritage and Cultural Ecosystem Services Hotspots. In *Tourism Innovation in Spain and Portugal*; Leitão, J., Ratten, V., Braga, V., Eds.; Springer: Cham, Switzerland, 2021; pp. 63–88.

23. Clemente, P.; Calvache, M.; Antunes, P.; Santos, R.; Cerdeira, J.O.; Martins, M.J. Combining social media photographs and species distribution models to map cultural ecosystem services: The case of a Natural Park in Portugal. *Ecol. Indic.* **2019**, *96*, 59–68. [CrossRef]
24. Cunha, J.; Elliott, M.; Ramos, S. Linking modelling and empirical data to assess recreation services provided by coastal habitats: The case of NW Portugal. *Ocean Coast. Manag.* **2018**, *162*, 60–70. [CrossRef]
25. Ghermandi, A.; Camacho-Valdez, V.; Trejo-Espinosa, H. Social media-based analysis of cultural ecosystem services and heritage tourism in a coastal region of Mexico. *Tour. Manag.* **2020**, *77*, 104002. [CrossRef]
26. Gosal, A.S.; Geijzendorffer, I.R.; Václavík, T.; Poulin, B.; Ziv, G. Using social media, machine learning and natural language processing to map multiple recreational beneficiaries. *Ecosyst. Serv.* **2019**, *38*, 100958. [CrossRef]
27. Oteros-Rozas, E.; Martín-López, B.; Fagerholm, N.; Bieling, C.; Plieninger, T. Using social media photos to explore the relation between cultural ecosystem services and landscape features across five European sites. *Ecol. Indic.* **2018**, *94*, 74–86. [CrossRef]
28. Richards, D.R.; Friess, D.A. A rapid indicator of cultural ecosystem service usage at a fine spatial scale: Content analysis of social media photographs. *Ecol. Indic.* **2015**, *53*, 187–195. [CrossRef]
29. Richards, D.R.; Tunçer, B. Using image recognition to automate assessment of cultural ecosystem services from social media photographs. *Ecosyst. Serv.* **2018**, *31*, 318–325. [CrossRef]
30. Callau, A.À.; Albert, M.Y.P.; Rota, J.J.; Giné, D.S. Landscape characterization using photographs from crowdsourced platforms: Content analysis of social media photographs. *Open Geosci.* **2019**, *11*, 558–571. [CrossRef]
31. Eigenbrod, F.; Armsworth, P.R.; Anderson, B.J.; Heinemeyer, A.; Gillings, S.; Roy, D.B.; Thomas, C.D.; Gaston, K.J. The impact of proxy-based methods on mapping the distribution of ecosystem services. *J. Appl. Ecol.* **2010**, *47*, 377–385. [CrossRef]
32. Gould, R.K.; Morse, J.W.; Adams, A.B. Cultural ecosystem services and decision-making: How researchers describe the applications of their work. *People Nat.* **2019**, *1*, 457–475. [CrossRef]
33. Hermes, J.; Van Berkel, D.; Burkhard, B.; Plieninger, T.; Fagerholm, N.; von Haaren, C.; Albert, C. Assessment and valuation of recreational ecosystem services of landscapes. *Ecosyst. Serv.* **2018**, *31*, 289–295. [CrossRef]
34. Retka, J.; Jepson, P.; Ladle, R.J.; Malhado, A.C.; Vieira, F.A.; Normande, I.C.; Souza, C.N.; Bragagnolo, C.; Correia, R.A. Assessing cultural ecosystem services of a large marine protected area through social media photographs. *Ocean Coast. Manag.* **2019**, *176*, 40–48. [CrossRef]
35. Ruskule, A.; Klepers, A.; Veidemane, K. Mapping and assessment of cultural ecosystem services of Latvian coastal areas. *One Ecosyst.* **2018**, *3*, e25499. [CrossRef]
36. Tieskens, K.F.; Van Zanten, B.T.; Schulp, C.J.; Verburg, P.H. Aesthetic appreciation of the cultural landscape through social media: An analysis of revealed preference in the Dutch river landscape. *Landsc. Urban Plan.* **2018**, *177*, 128–137. [CrossRef]
37. Haines-Young, R.; Potschin-Young, M. Revision of the common international classification for ecosystem services (CICES V5. 1): A policy brief. *One Ecosyst.* **2018**, *3*, e27108. [CrossRef]
38. Garcia Rodrigues, J.; Conides, A.; Rivero Rodriguez, S.; Raicevich, S.; Pita, P.; Kleisner, K.; Pita, C.; Lopes, P.; Alonso Roldán, V.; Ramos, S.; et al. Marine and Coastal Cultural Ecosystem Services: Knowledge gaps and research priorities. *One Ecosyst.* **2017**, *2*, e12290. [CrossRef]
39. Carvache-Franco, W.; Carvache-Franco, M.; Carvache-Franco, O.; Hernández-Lara, A.B. Segmentation of foreign tourist demand in a coastal marine destination: The case of Montañita, Ecuador. *Ocean Coast. Manag.* **2019**, *167*, 236–244. [CrossRef]
40. Carvache-Franco, W.; Carvache-Franco, M.; Carvache-Franco, O.; Hernández-Lara, A.B. Motivation and segmentation of the demand for coastal and marine destinations. *Tour. Manag. Perspect.* **2020**, *34*, 100661. [CrossRef]
41. Nagy, K.Z.; Tóth, K.; Gyömbér, N.; Tóth, L.; Bánhidi, M. Motives underlying water sport tourist behaviour: A segmentation approach. *World Leis. J.* **2021**, *63*, 109–127. [CrossRef]
42. Fluker, M. Riding the wave: Defining surf tourism. In Proceedings of the 13th International Research Conference of the Council for Australian University Tourism and Hospitality Education (CAUTHE), Coffs Harbour, Australia, 5–8 February 2003.
43. Elmahdy, Y.M.; Orams, M.B.; Mykletun, R.J. Exploring the Travel Behavior and Experiences of Norwegian Surfers: Cold-Versus Warm-Water Surfing. *Tour. Mar. Environ.* **2021**, *16*, 99–112. [CrossRef]
44. Boudreau, P.; Mackenzie, S.H.; Hodge, K. Flow states in adventure recreation: A systematic review and thematic synthesis. *Psychol. Sport Exerc.* **2020**, *46*, 101611. [CrossRef]
45. Houge Mackenzie, S.; Brymer, E. Conceptualizing adventurous nature sport: A positive psychology perspective. *Ann. Leis. Res.* **2020**, *23*, 79–91. [CrossRef]
46. Schmitt, A.; Bohuon, A. When women surf the world's biggest waves: Breaking gender barriers. *Sport Soc.* **2022**, *25*, 1924–1939. [CrossRef]
47. Gstaettner, A.M.; Lee, D.; Rodger, K. The concept of risk in nature-based tourism and recreation—A systematic literature review. *Curr. Issues Tour.* **2018**, *21*, 1784–1809. [CrossRef]
48. Kerr, J.H.; Houge Mackenzie, S. Multiple motives for participating in adventure sports. *Psychol. Sport Exerc.* **2012**, *13*, 649–657. [CrossRef]
49. Pomfret, G.; Bramwell, B. The characteristics and motivational decisions of outdoor adventure tourists: A review and analysis. *Curr. Issues Tour.* **2014**, *19*, 1447–1478. [CrossRef]
50. Wiersma, L.D. A phenomenological investigation of the psychology of big-wave surfing at Maverick's. *Sport Psychol.* **2014**, *28*, 151–163. [CrossRef]

51. Giddy, J.K.; Webb, N.L. The influence of the environment on adventure tourism: From motivations to experiences. *Curr. Issues Tour.* **2018**, *21*, 2124–2138. [CrossRef]
52. Buckley, R. Is adventure tourism therapeutic? *Tour. Recreat. Res.* **2021**, *46*, 553–557. [CrossRef]
53. Ewert, A.; Zwart, R.; Davidson, C. Underlying motives for selected adventure recreation activities: The case for eudaimonics and hedonics. *Behav. Sci.* **2020**, *10*, 185. [CrossRef]
54. Brymer, E.; Schweitzer, R. The search for freedom in extreme sports: A phenomenological exploration. *Psychol. Sport Exerc.* **2013**, *14*, 865–872. [CrossRef]
55. Buckley, R.C. Rush as a key motivation in skilled adventure tourism: Resolving the risk recreation paradox. *Tour. Manag.* **2012**, *33*, 961–970. [CrossRef]
56. Vidon, E.S.; Rickly, J.M.; Knudsen, D.C. Wilderness state of mind: Expanding authenticity. *Ann. Tour. Res.* **2018**, *73*, 62–70. [CrossRef]
57. Delle Fave, A.; Bassi, M.; Massimini, F. Quality of experience and risk perception in high-altitude rock climbing. *J. Appl. Sport Psychol.* **2003**, *15*, 82–98. [CrossRef]
58. Morgan, J.D.; Coutts, R.A. Measuring peak experience in recreational surfing. *J. Sport Behav.* **2016**, *39*, 202–217.
59. Swann, C.; Piggott, D.; Schweickle, M.; Vella, S.A. A review of scientific progress in flow in sport and exercise: Normal science, crisis, and a progressive shift. *J. Appl. Sport Psychol.* **2018**, *30*, 249–271. [CrossRef]
60. Martin, P.; Priest, S. Understanding the adventure experience. *J. Adventure Educ.* **1986**, *3*, 18–21.
61. Jones, C.D.; Hollenhorst, S.J.; Perna, F. An empirical comparison of the four-channel flow model and adventure experience paradigm. *Leis. Sci.* **2003**, *25*, 17–31. [CrossRef]
62. Csikszentmihalyi, M. *Beyond Boredom and Anxiety: The Experience of Play in Work and Games*; Jossey-Bass: San Francisco, CA, USA, 1975.
63. Cheng, T.M.; Lu, C.C. The causal relationships among recreational involvement, flow experience, and well-being for surfing activities. *Asia Pac. J. Tour. Res.* **2015**, *20*, 1486–1504. [CrossRef]
64. Nerothin, P.H. *A Phenomenological Investigation of Lifestyle Surfers from San Diego*; Prescott College: Prescott, AZ, USA, 2017.
65. Partington, S.; Partington, E.; Olivier, S. The dark side of flow: A qualitative study of dependence in big wave surfing. *Sport Psychol.* **2009**, *23*, 170–185. [CrossRef]
66. Clough, P.; Mackenzie, S.H.; Mallabon, L.; Brymer, E. Adventurous physical activity environments: A mainstream intervention for mental health. *Sport. Med.* **2016**, *46*, 963–968. [CrossRef]
67. Buckley, R. Nature sports, health and ageing: The value of euphoria. *Ann. Leis. Res.* **2018**, *23*, 92–109. [CrossRef]
68. Magyaródi, T.; Nagy, H.; Soltész, P.; Mózes, T.; Oláh, A. Psychometric properties of a newly established flow state questionnaire. *J. Happiness Well Being* **2013**, *1*, 89–100.
69. Houge Mackenzie, S.; Kerr, J.H. A (mis)guided adventure tourism experience: An autoethnographic analysis of mountaineering in Bolivia. *J. Sport Tour.* **2012**, *17*, 125–144. [CrossRef]
70. Fletcher, R. The emperor's new adventure: Public secrecy and the paradox of adventure tourism. *J. Contemp. Ethnogr.* **2010**, *39*, 6–33. [CrossRef]
71. Urry, J. *The Tourist Gaze*, 1st ed.; Sage: London, UK, 1990.
72. Gibson, H.J. Sport tourism: A critical analysis of research. *Sport Manag. Rev.* **1998**, *1*, 45–76. [CrossRef]
73. Hallmann, K.; Zehrer, A.; Rietz, J. Sport events as experiencescapes: The spectator's perspective. *Int. J. Sport. Mark. Spons.* **2021**, *22*, 764–779. [CrossRef]
74. Horbel, C.; Popp, B.; Woratschek, H.; Wilson, B. How context shapes value co-creation: Spectator experience of sport events. *Serv. Ind. J.* **2016**, *36*, 510–531. [CrossRef]
75. Bitner, M.J. Servicescapes: The impact of physical surroundings on customers and employees. *J. Mark.* **1992**, *56*, 57–71. [CrossRef]
76. Lee, S.; Lee, H.J.; Seo, W.J.; Green, C. A new approach to stadium experience: The dynamics of the sensoryscape, social interaction, and sense of home. *J. Sport Manag.* **2012**, *26*, 490–505. [CrossRef]
77. Kaplanidou, K.; Vogt, C. The meaning and measurement of a sport event experience among active sport tourists. *J. Sport Manag.* **2010**, *24*, 544–566. [CrossRef]
78. Kruger, M.; Saayman, M. Creating a memorable spectator experience at the two oceans marathon. *J. Sport Tour.* **2012**, *17*, 63–77. [CrossRef]
79. Wang, J.; Liu-Lastres, B.; Ritchie, B.W.; Pan, D.Z. Risk reduction and adventure tourism safety: An extension of the risk perception attitude framework (RPAF). *Tour. Manag.* **2019**, *74*, 247–257. [CrossRef]
80. Li, Y.; Pan, D.-Z.; Chanson, H.; Pan, C.-H. Tidal bore progressing on a small slope. *Exp. Therm. Fluid Sci.* **2017**, *88*, 513–518. [CrossRef]
81. Diehm, R.; Armatas, C. Surfing: An avenue for socially acceptable risk-taking, satisfying needs for sensation seeking and experience seeking. *Personal. Individ. Differ.* **2004**, *36*, 663–677. [CrossRef]
82. Harmston, R.G. *Exploratory Investigaton of the Inspirations and Motivations in the Sport of Big Wave Surfing*; California State University: Fullerton, CA, USA, 2006.
83. Zuckerman, M. *Behavioral Expressions and Biosocial Bases of Sensation Seeking*; Cambridge University Press: Cambridge, UK, 1994.
84. Ivanova, P.; Light, D. 'It's not that we like death or anything': Exploring the motivations and experiences of visitors to a lighter dark tourism attraction. *J. Herit. Tour.* **2018**, *13*, 356–369. [CrossRef]

85. Stone, P.R. Dark tourism as 'mortality capital: The case of Ground Zero and the Significant Other Dead. In *Contemporary Tourist Experience: Concepts and Consequences*; Sharpley, R., Stone, P.R., Eds.; Routledge: Abingdon, UK, 2012; pp. 71–94.
86. Light, D.; Ivanova, P. Thanatopsis and mortality mediation within "lightest" dark tourism. *Tour. Rev.* **2021**, *77*, 622–635. [CrossRef]
87. Buda, D.M. The death drive in tourism studies. *Ann. Tour. Res.* **2015**, *50*, 39–51. [CrossRef]
88. Buda, D.M.; McIntosh, A.J. Dark tourism and voyeurism: Tourist arrested for 'spying' in Iran. *Int. J. Cult. Tour. Hosp. Res.* **2013**, *7*, 214–226. [CrossRef]
89. Buda, D.M.; Shim, D. Desiring the dark: 'A taste for the unusual' in North Korean tourism? *Curr. Issues Tour.* **2015**, *18*, 1–6. [CrossRef]
90. Martini, A.; Buda, D.-M. Dark tourism and affect: Framing places of death and disaster. *Curr. Issues Tour.* 2018; *Advance online publication*. [CrossRef]
91. Stone, P. Dark Tourism as 'Spectacular Death': Towards a new era of showcasing death in the early 21st century. *Curr. Issues Dark Tour. Res.* **2017**, *1*. Available online: https://www.dark-tourism.org.uk/product-page/dark-tourism-as-spectacular-death (accessed on 31 October 2022).
92. Gordillo, F.; Mestas, L.; Arana, J.M.; Perez, M.A.; Escotto, E.A. The effect of mortality salience and type of life on personality evaluation. *Eur. J. Psychol.* **2017**, *13*, 286–299. [CrossRef] [PubMed]
93. Oren, G.; Shani, A.; Poria, Y. Mortality salience—Shedding light on the dark experience. *J. Herit. Tour.* **2019**, *14*, 574–578. [CrossRef]
94. Prayag, G.; Buda, D.-M.; Jordan, E.J. Mortality salience and meaning in life for residents visiting dark tourism sites. *J. Sustain. Tour.* **2020**, *29*, 1508–1528. [CrossRef]
95. Biran, A.; Buda, D.M. Fear of death motives in dark tourism. In *The Palgrave Handbook of Dark Tourism Studies*; Stone, P.R., Hartmann, R., Seaton, T., Sharpley, R., White, L., Eds.; Palgrave: Basingstoke, UK, 2018; pp. 515–532.
96. Xu, S.; Barbieri, C.; Stanis, S.W.; Market, P.S. Sensation-seeking attributes associated with storm-chasing tourists: Implications for future engagement. *Int. J. Tour. Res.* **2012**, *14*, 269–284. [CrossRef]
97. Wilhelm Stanis, S.A.; Barbieri, C. Niche tourism attributes scale: A case of storm chasing. *Curr. Issues Tour.* **2013**, *16*, 495–500. [CrossRef]
98. Boulais, C.M. When severe weather becomes a tourist attraction: Understanding the relationship with nature in storm-chasing tourism. *Weather Clim. Soc.* **2017**, *9*, 367–376. [CrossRef]
99. Keltner, D.; Haidt, J. Approaching awe, a moral, spiritual, and aesthetic emotion. *Cogn. Emot.* **2003**, *17*, 297–314. [CrossRef] [PubMed]
100. Lu, D.; Liu, Y.; Lai, I.; Yang, L. Awe: An important emotional experience in sustainable tourism. *Sustainability* **2017**, *9*, 2189. [CrossRef]
101. Pearce, J.; Strickland-Munro, J.; Moore, S.A. What fosters awe-inspiring experiences in nature-based tourism destinations? *J. Sustain. Tour.* **2017**, *25*, 362–378. [CrossRef]
102. Bonner, E.T.; Friedman, H.L. A conceptual clarification of the experience of awe: An interpretative phenomenological analysis. *Humanist. Psychol.* **2011**, *39*, 222–235. [CrossRef]
103. Schneider, K. *Awakening to Awe: Personal Stories of Profound Transformation*; Jason Aronson: Lanham, MD, USA, 2009.
104. Reis, P.; Caldeira, A.; Carneiro, M.J. Can surf culture foster loyalty towards surf destinations? *J. Sport Tour.* **2022**, *26*, 387–407. [CrossRef]
105. Ferreira, F.F. A Onda da Transformação. Surf, Turismo e Tradição na Nazaré. Master's Dissertation, NOVA FCSH, Universidade Nova de Lisboa, Lisbon, Portugal, 2022.
106. Ponting, J.; O'Brien, D. Regulating 'Nirvana': Sustainable surf tourism in a climate of increasing regulation. *Sport Manag. Rev.* **2015**, *18*, 99–110. [CrossRef]
107. Iliev, D. Consumption, motivation and experience in dark tourism: A conceptual and critical analysis. *Tour. Geogr.* **2021**, *23*, 963–984. [CrossRef]
108. Quico, C. Nazaré criativa: How can creative tourism initiatives contribute towards sustainable tourism? In *Creative Tourism Dynamics: Connecting Travellers, Communities, Cultures and Places*; Cabeça, S., Gonçalves, A., Marques, J., Tavares, M., Eds.; Grácio Editor: Coimbra, Portugal, 2020; pp. 133–160.
109. Carapuço, M.M.; Taborda, R.; Andrade, C. Triggers in science communication: "The Nazaré Wave: A trigger for learning". *Cont. Shelf Res.* **2022**, *244*, 104805. [CrossRef]
110. Jorgensen, D.L. Participant Observation. In *Emerging Trends in the Social and Behavioral Sciences*; Scott, R.A., Kosslyn, S.M., Eds.; Wiley: New York, NY, USA, 2015. [CrossRef]
111. Kim, H.; Stepchenkova, S. Effect of tourist photographs on attitudes towards destination: Manifest and latent content. *Tour. Manag.* **2015**, *49*, 29–41. [CrossRef]
112. Matteucci, X. Photo elicitation: Exploring tourist experiences with researcher-found images. *Tour. Manag.* **2013**, *35*, 190–197. [CrossRef]
113. Prosser, J.; Loxley, A.; Introducing Visual Methods. National Centre for Research Methods Review Paper. Available online: http://eprints.ncrm.ac.uk/420/1/MethodsReviewPaperNCRM-010.pdf (accessed on 3 July 2020).
114. Pung, J.; Yung, R.; Khoo-Lattimore, C.; Chiappa, G. Transformative travel experiences and gender: A double duoethnography approach. *Curr. Issues Tour.* **2020**, *23*, 538–558. [CrossRef]

115. Sofield, T.H.; Marafa, L.M. Revitalizing fieldtrips in tourism: Visual anthropology, photo elicitation, rapid appraisal, participant observation and Habermas. *Tour. Manag.* **2019**, *75*, 522–546. [CrossRef]
116. Mach, L.; Ponting, J.; Brown, J.; Savage, J. Riding waves of intra-seasonal demand in surf tourism: Analysing the nexus of seasonality and 21st century surf forecasting technology. *Ann. Leis. Res.* **2020**, *23*, 184–202. [CrossRef]
117. Real Watersports INC. Surgical Strike: Diaries of a Professional Recreational Surfer. Available online: http://www.realwatersports.com/news/surgical-strike-puerto-rico/ (accessed on 18 November 2022).
118. Lau, J.D.; Hicks, C.C.; Gurney, G.G.; Cinner, J.E. What matters to whom and why? Understanding the importance of coastal ecosystem services in developing coastal communities. *Ecosyst. Serv.* **2019**, *35*, 219–230. [CrossRef]
119. Vieira, I.I. O Desenvolvimento da Nazaré Através do Marketing Territorial e do Branding. Ph.D. Dissertation, Faculty of Economics, University of Coimbra, Coimbra, Portugal, 2015.
120. Müller, S. The Future Development of Surf Tourism in Coastal Destinations in Western Europe: Analysis of the Potential Development of Surf Tourism in Western Europe and How It Can Set a Benchmark for Sustainable Adventure Tourism. Bachelor's Thesis, LAB University of Applied Sciences, Lahti, Finland, 2022.

land

MDPI

Article

Urban Areas as Potential Sinks for Tropical Swallowtail Moth *Lyssa zampa*

Anuj Jain [1,2,3,*], Lin Yu Ng [1,4] and N Sivasothi [1]

[1] Department of Biological Sciences, National University of Singapore, Singapore 117543, Singapore
[2] Nature Society (Singapore), 510 Geylang Road, Singapore 389466, Singapore
[3] bioSEA Pte. Ltd., 68 Chestnut Avenue, Singapore 679521, Singapore
[4] Department of History and Cultural Studies, Free University of Berlin, 14195 Berlin, Germany
* Correspondence: anuj@biosea.sg

Abstract: (1) The tropical swallowtail moth *Lyssa zampa* received much public attention during its years of mass emergence in Singapore and Southeast Asia. However, despite its prominence, little is known about its population demographics and spatial ecology. This study aims to establish the annual abundance of *L. zampa*, determine its spatial patterns of occurrence, and examine morphological variation demonstrated by *L. zampa* with an emphasis on comparing urban vs. forest areas in Singapore. (2) Various sources (field surveys across 18 sites, citizen science datasets and expert knowledge) were used to catalogue *L. zampa* records from 2011 to 2020 and analyse its seasonal abundance. (3) We confirmed the seasonal peak of *L. zampa* emergence to be between May and July, with an unusually high mass emergence in 2014. The intensity of emergence was associated with the intensity of a dry spell in February of that year. The total number of *L. zampa* sighted in urban areas was higher despite the moth's host plant being a tree that is restricted to mature forests and is absent from urban areas. This suggests that the occurrence of *L. zampa* in urban areas is likely due to the moth's attraction to bright city lights. Our morphometric measurements further show that *L. zampa* individuals in urban areas have greater wing length and lighter body weights (smaller body widths) than their forest counterparts. (4) This implies that urban areas are not only drawing moths that are unable to find the host plants and, therefore, cannot produce offspring but are also attracting larger and better flyers out of forest areas. This situation is only likely to worsen as climate change intensifies and dry spells become longer and more intense.

Keywords: *Endospermum diadenum*; host plant; lepidoptera; mass emergence; population peak; Singapore

1. Introduction

Moths are relatively less studied in the tropics, including in Singapore. Since Murphy's seminal work on insects of Singapore in the 1980s [1], only a few ad hoc surveys have been conducted across this species-rich taxa (e.g., [2]). One exception is the tropical swallowtail moth, *Lyssa zampa* (Butler, 1869) (Uraniidae, Lepidoptera). This large, intermittently abundant species has received sporadic public attention during its years of abundant occurrence due to its size and presence in urban areas [3–5].

L. zampa [6,7] is distributed across Southeast Asia and Northeast Himalaya, and more recently, reports have extended the range to Taiwan and Japan [8,9]. It is the largest uraniid moth and second largest moth in Singapore after *Attacus atlas* (Family Saturniidae; [10]). The only host plant species recorded for the caterpillar has been *Endospermum diadenum* (Benn. & Muell. Arg) (syn. *E. malaccense*; family *Euphorbiaceae*)—itself a threatened species and limited to certain forest patches in Singapore [5,11,12].

The seasonal abundance of *L. zampa* has been documented in Singapore through recruitment of public sightings since 2005 [13–17], albeit in an ad hoc way. In May–June

2014, the largest emergence of *L. zampa* thus far known from Singapore was reported, and this resulted in numerous sightings around urban Singapore [17,18]. The emergence was also picked up by the national and international media [3,4], and a much larger emergence was reported from Malaysia, where it was reported to have disrupted a football match [19,20].

The life cycle of the *L. zampa* and mass herbivory of larval host plants during this mass emergence has been published by the lead author [5]. The 2014 study documented extensive presence (estimated to be a cluster of 15,000–20,000 individuals) of *L.zampa* caterpillars on several trees of *E. diadenum* within Singapore's Central Catchment Nature Reserve. The trees were checked for several days when silk threads were observed hanging around the main trunk of trees, and larvae were hanging from them after several days. Subsequently, a few adult moths were observed at this forested site in future visits [5].

Despite the life history documentation of *L. zampa* during the mass emergence, the abundance of the species has not been mapped spatially, and the linkages between moths in the forest and urban habitats have not been directly made. This follow-up study was initiated to:

(i) document the seasonal abundance of moths from 2011 to 2020 with an emphasis on the mass emergence in 2014.
(ii) map the distribution of adult moths in forest and urban areas during the mass emergence in 2014.
(iii) understand the movement of adult moths between forest and urban areas.
(iv) demonstrate the morphological variation in *L. zampa,* by gender, location, and across emergence batches.
(v) demonstrate the relationship between *L. zampa* abundance and rainfall patterns.

The distribution of *L. zampa* was mapped using data from public sightings and field surveys in forest and urban areas. A mark-recapture study was conducted to understand the movement between forest and urban areas. Understanding the patterns of mass emergence of insects and reasons behind them could help improve predictions of such events and, if needed, manage insect populations. This is important because insect populations are foundational to the populations of higher order organisms found in those habitats.

2. Materials and Methods

2.1. Distribution of Public Sightings from Habitatnews and NSS

Sightings of *L. zampa* were collected from the public between 2011 and 2020 through diverse sources: the National University of Singapore's Habitatnews web portal (http://habitatnews.nus.edu.sg, accessed on 7 February 2023), iNaturalist (https://www.inaturalist.org/, accessed on 7 February 2023), and Nature Society (Singapore) or NSS's members/supporters. Records from NSS members were obtained during the mass emergence of moths in 2014 using a customized Google Map (see https://goo.gl/maps/f4p5NkMhhB8QoZmTA, accessed on 7 February 2023) and were integrated with the larger database. All records were mapped and overlaid on a vegetation map of Singapore (courtesy: David Tan, National University of Singapore). Records with nonspecific location information, such as no GPS data or postal codes, were removed prior to analysis. The record locations were verified and further cleaned to exclude locations found in large water bodies, such as the Straits of Johor, or outside the borders of Singapore for analysis. Dates of sightings were categorized by month and plotted onto a graph to determine the seasonality of *L. zampa* observations.

2.2. Field Surveys during Mass Emergence

The majority of citizen science sightings during the mass emergence of *L. zampa* in 2014 came from urban areas in Singapore despite the high visitation to nature reserves, parks and nature areas in Singapore. To supplement this citizen science data, a range of natural habitats were surveyed using Pollard walks [21] in 2014 to estimate the abundance of *L. zampa* in these habitats in comparison to the urban areas.

A total of six vegetated patches, six urban parks and park connectors, and six urban areas widely spread around Singapore were visited (Figure 1). Each survey site was visited four times and once every week—twice during the observed peak emergence period between 13 and 26 July 2014 and twice during the postemergence period from 20 September to 12 October 2014.

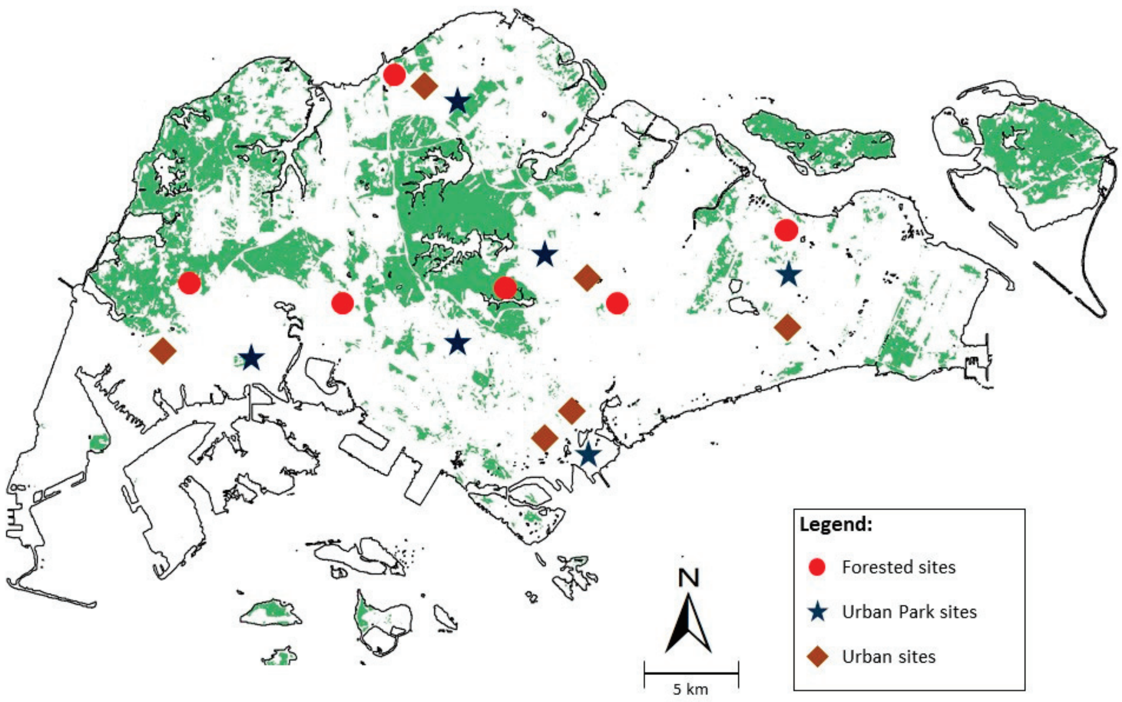

Figure 1. Field survey locations across 6 forest, 6 urban park and 6 urban sites in 2014 spread across Singapore based around sites of high occurrence of *L. zampa* as recorded on Habitatnews and NSS. One 500 metres transect was established at each site. (●) are forested survey sites at Admiralty Park forest trail, Bidadari Muslim section, Dairy Farm Pass, Jurong Eco Garden forest trail, Macritchie Nature Trail, and Pasir Ris Mangroves. (★) are urban park survey sites including Bishan Park, Fort Canning Park, Gardens by the Bay, Jurong Central Park, Mandai-Tekong Park, and Tampines Eco Green. (◆) are urban survey sites including Arcade Mall, Bishan Stadium, Jurong West Stadium, Marina Bay Financial Centre, Raffles Place, Republic Polytechnic, and Tampines Swimming Complex.

2.3. Mark Recapture of *L. zampa*

Mark recapture was conducted on 59 live individuals of *L. zampa* between June and July 2014—31 individuals from Sime Forest (forested site), nine individuals from Bidadari (also a forested site), and 19 individuals from Raffles Place (urban site) were captured, marked, and released. The capture site was revisited for two consecutive days between 10:00 and 14:00.

L. zampa were captured using standard insect nets and marked on the underside and upper side of the wing using a fine point marker pen (STAEDTLER Lumocolor permanent pen 318); each individual was marked with a specific code and then released. This method is widely used in other lepidopteran studies and, when properly executed, does not damage individuals [22] or affect recapture rates. All marked individuals were photographed for future reference. Measurements of body length, body width, wing length, as well as date, time, and GPS locations, were recorded before the release of the moths. For recaptures, if the marked code could be easily read with the naked eye or using binoculars, the individual was not netted to avoid stressing the animal.

2.4. Specimens Collection and Measurement

Fifty-nine dead specimens and sixty-one live specimens of *L. zampa* were collected and measured from both urban and forested areas with the help of volunteers across Singapore between May 2014 and July 2014. A vernier calliper was used to measure body length, body width, and wing length of all specimens (Figure 2) using standard lepidopteran measurement protocols [6,23]. The specimens were divided into two batches depending on the month of data collection. Batch 1 spanned from 23 May to 9 June 2014, whereas Batch 2 spanned from 23 June to 31 July 2014.

Figure 2. *Lyssa zampa* moths in forested and urban areas photographed during the mass emergence in 2014 across Singapore (photos by Anuj Jain). Several individual moths were seen attracted to city lights and eventually trapped in glass panels or light bulbs.

All dead specimens were photographed, numbered, and deposited in the Zoological Reference Collection at the Lee Kong Chian National History Museum, National University of Singapore.

2.5. Statistics

Significant differences in wing length, body length, and body width between sexes, batches, and locations were determined using the t-test or Wilcoxon signed rank test, depending on the normality of the datasets. The datasets were tested for normality using the Shapiro–Wilk test. The analysis was conducted using R Studio V1.2.1335.

3. Results

3.1. Seasonal Abundance of L. zampa

A total of 2547 *L. zampa* sightings were reported on Habitatnews, NSS and iNaturalist between January 2011 and December 2020. Of these, 2416 sightings (94.9%) were in 2014, and 2078 sightings (81.6%) were between April and July 2014 (Table 1). The peak emergence of *L. zampa* was identified to be in May 2014 (Table 2).

The field surveys in July 2014 were conducted during the end of the peak emergence period of *L. zampa*. Surveys in September and October 2014 were conducted during the post-peak emergence period of *L. zampa*. These surveys across 18 sites showed a total of 11 individuals of *L. zampa* (an initial high of nine *L. zampa* individuals in forested areas in week 1, i.e., 13–20 July 2014, and two individuals in the following week; Table 3). Sightings in urban areas totaled 10 individuals with an increase from 4 to 6 individuals in two weeks. Only one individual was seen in urban areas during the post-peak emergence period in September 2014 (Table 3).

Table 1. *L. zampa* sightings from 2011 to 2020 for the entire year (January–December) and during the peak emergence season (April–July).

Year	Total Sightings	Sightings (April–July)
2011	7	3
2012	19	11
2013	21	13
2014	2416	2078
2015	0	0
2016	13	4
2017	12	5
2018	33	25
2019	11	6
2020	15	4

Table 2. The total number of sightings of *L. zampa* classified by months in 2014.

Month	2014 Sightings
Jan.	1
Feb.	1
Mar.	2
Apr.	25
May	1824
Jun.	167
Jul.	62
Aug.	3
Sep.	1
Oct.	2
Nov.	0
Dec.	0

Table 3. Total number of *L. zampa* recorded through trail surveys across forested areas, urban parks, and urban areas.

Dates	Forested Areas	Urban Parks	Urban Areas
13 July–26 July 2014	11	1	10
20 September–12 October 2014	0	0	1

3.2. Spatial Distribution of L. zampa in Singapore

We recorded the highest number of sightings in areas of high human density in the central business district and southeastern regions of Singapore, namely Tampines and Bedok (Figures 2 and 3). Forested areas, such as the Central and Western Catchments, reflected few adult records, although mass emergence was documented here [5] (Figure 3). The majority of other green spaces also reported fewer than 30 sightings (Figure 3).

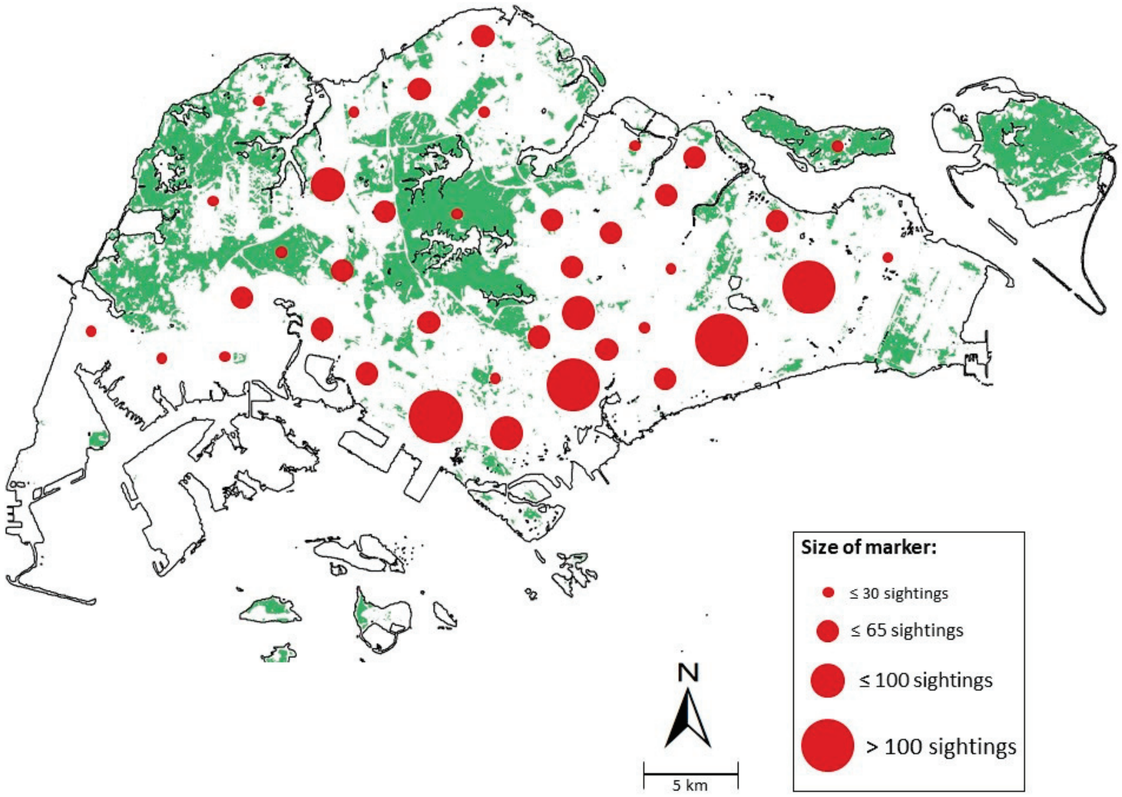

Figure 3. Number of sightings of *L. zampa* recorded in Habitatnews, iNaturalist and NSS across Singapore from 2011 to 2020 with a map scale of 1:50,000. Sightings within the Urban Redevelopment Authority Planning Zones were clustered and represented as a circle. Zones of relatively high sightings include Tampines (105 sightings) and Bedok (107 sightings) in the east, Queenstown (165 sightings) in the central west and the central business district in southern Singapore (>300 sightings). The base vegetation map was obtained from David Tan and used with permission.

3.3. Morphological Variation between Sexes, Batches, and Locations

While the results from the mark-recapture study were inconclusive, as only one of 59 marked *L. zampa* was recaptured, the dead and live specimens captured during the study and submitted by other volunteers helped us do a morphometric analysis between wing length, body length, and body width (measured in cm).

Measurements showed significant differences in wing length and body width between *L. zampa* males (n = 86) and females (n = 34; Table 4). Females have significantly longer wing lengths ($p < 0.001$, W = 757) and wider body widths ($p = 0.002$, W = 295) than male *L. zampa* (Table 4). Body lengths between male and female *L. zampa* were not significantly different. Similarly, urban moths (n = 76) have significantly longer wing lengths ($p < 0.001$, t = 2.47) and smaller body widths ($p < 0.001$, W = 517) than forest moths (n = 42).

When comparing males only, urban males (n = 47) had marginally longer wing lengths ($p = 0.045$, t = 2.05) and wider body widths ($p < 0.001$, W = 225) than forest males (n = 37). Despite the small sample size, when comparing females only, urban females (n = 29) had longer wing lengths ($p = 0.008$, W = 128) than forest females (n = 5).

Across batches, males of batch 1 (n = 27) had longer wing lengths ($p = 0.006$, W = 1092) than males of batch 2 (n = 59). Females of batch 1 (n= 21) also had longer wing lengths ($p = 0.021$, t = 2.47) than females of batch 2 (n = 13).

Table 4. Wing length, body length, and body width variation between sexes, batches and habitats (forest, urban areas) in *L. zampa*. Body length was measured from the head to the end of the abdomen. Body width was measured at the thickest point of the specimen's abdomen. Wing length was measured from the midpoint of the head to the tip of the most intact wing. 't' value refers to t-test and was used when the datasets were normally distributed. 'W' value refers to Wilcoxon signed rank test and was used when the datasets were not normally distributed. Level of significance is marked with asterisk: *** $p < 0.001$, ** $p < 0.01$, * $p < 0.05$.

All—Males & Females						
	Sex	N	Mean/cm	S.D	Test-statistic	*p*-value
Wing length	Male	86	6.29	0.62	W = 757	<0.001 ***
	Female	34	6.88	0.74		
Body length	Male	86	3.45	0.36	t = 1.37	0.177
	Female	34	3.35	0.35		
Body width	Male	86	0.55	0.16	W = 295	0.002 **
	Female	34	0.68	0.12		
	Habitat	N	Mean/cm	S.D	Test-statistic	*p*-value
Wing length	Urban	76	6.65	0.63	t = 4.27	<0.001 ***
	Forest	42	6.09	0.70		
Body length	Urban	76	3.44	0.36	t = 1.05	0.298
	Forest	42	3.37	0.36		
Body width	Urban	76	0.53	0.17	W = 517	<0.001 ***
	Forest	42	0.64	0.12		
	Batch *	N	Mean/cm	S.D	Test-statistic	*p*-value
Wing length	Batch 1	48	6.81	0.61	t = 4.92	<0.001 ***
	Batch 2	72	6.23	0.67		
Body length	Batch 1	48	3.51	0.33	t = 2.06	0.042 *
	Batch 2	72	3.37	0.38		
Body width	Batch 1	48	0.49	0.14	W = 309	0.009 **
	Batch 2	72	0.60	0.15		
Males Only						
	Habitat	N	Mean/cm	S.D	Test-statistic	*p*-value
Wing length	Urban	47	6.4	0.50	t = 2.05	0.045 *
	Forest	37	6.12	0.71		
Body length	Urban	47	3.48	0.38	W = 1012	0.2
	Forest	37	3.41	0.34		
Body width	Urban	47	0.48	0.15	W = 225	<0.001 ***
	Forest	37	0.63	0.13		
	Batch	N	Mean/cm	S.D	Test-statistic	*p*-value
Wing length	Batch 1	27	6.56	0.47	W = 1092	0.006 **
	Batch 2	59	6.17	0.64		
Body length	Batch 1	27	3.56	0.08	W = 1083	0.008 **
	Batch 2	59	3.4	0.16		
Body width	Batch 1	27	0.43	0.36	W = 141	0.001 **
	Batch 2	59	0.58	0.35		
Females Only						
	Habitat	N	Mean/cm	S.D	Test-statistic	*p*-value
Wing length	Urban	29	7.05	0.63	W = 128	0.008 **
	Forest	5	5.91	0.64		
Body length	Urban	29	3.39	0.34	t = 1.37	0.227
	Forest	5	3.13	0.40		
Body width	Urban	29	0.68	0.14	t = −0.06	0.95
	Forest	5	0.68	0.04		

Table 4. *Cont.*

Females Only						
	Batch	N	Mean/cm	S.D	Test-statistic	*p*-value
Wing length	Batch 1	21	7.12	0.63	t = 2.47	0.021 *
	Batch 2	13	6.5	0.76		
Body length	Batch 1	21	0.71	0.09	t = 1.43	0.173
	Batch 2	13	0.67	0.12		
Body width	Batch 1	21	3.42	0.26	t = 0.587	0.589
	Batch 2	13	3.22	0.46		

3.4. Relationship between L. zampa Abundance and Rainfall

A weak relationship was observed between *L. zampa*'s annual total abundance between 2011 and 2020 and rainfall (mm) in February (Pearson's R = −0.27, p = 0.41, t = −0.86; Appendix A), as well as between *L. zampa*'s annual total abundance and number of rainy days in February (Pearson's R = −0.43, p = 0.177, t = −1.47, Appendix A).

4. Discussion

Using field surveys, citizen science and expert datasets, we show the once-in-a-decade mass emergence of *Lyssa zampa* in Singapore. We also show that the highest number of *L. zampa* sightings were in areas of high human density, thus suggesting that this may have to do with moths being attracted to city lights.

4.1. Seasonal Abundance of L. zampa and Reasons behind Mass Emergence

Our observation of *L. zampa's* peak emergence from May to August and that of the *L. zampa*'s annual total abundance between 2011 and 2020 was weakly related to rainfall (mm) in February, and the number of rainy days in February corroborates with the tropical literature in which insect populations tend to peak following dry spells [24–26]. February is usually the driest month in Singapore [27]. In 2014, the mass emergence of *L. zampa* in Singapore followed a record-long dry period with only 0.2 mm of rainfall in February—the driest month on record in Singapore since 1869 [27,28]. A minor peak emergence was observed in 2021 (estimated 200 records), which was preceded by a dry spell of only 1 mm of rainfall in February —the second lowest month on record since 1869 [29]. Back in 2010, there were anecdotal records of a minor peak emergence of *L. zampa* (but only eight records submitted by citizen scientists), and this was preceded by a dry spell in February 2010 with 6.3 mm of rainfall received in that month [30]. Beyond rainfall and number of rainy days in February, there may also be other factors that determine *L. zampa* abundance and which need further investigation.

Peak abundance in tropical areas contrasts with observed insect seasonality in temperate regions ([25,26,31–33], where insects tend to be more abundant during wet seasons [25,33].

Dry spells have, in part, been observed to induce mass flowering events [34], which is true of 2005, 2010, and 2014 [13,35]. Furthermore, studies by [26] suggest that fresher green leaves are produced following the falling of older leaves during the dry season. Fresh green leaves are more nutritious for larvae [26,33], and hence their presence would provide an ideal environment for the reproduction of *L. zampa*. The dry spells may thus have triggered the mass emergence of *L. zampa*.

We also hypothesize that *L. zampa* may be exploiting a window of opportunity to feed on its toxic larval host plant, *E. diadenum,* because plant defenses are lower during the dry spells [36]. However, a longer and more rigorous study may be needed to disentangle the effect of host plant toxicity and relate it to dry spells that prompted mass emergence.

4.2. Forests as Source, Urban Areas as Sinks

The only known host plant of *L. zampa*, *E. diadenum*, is a nationally threatened tree species limited to mature forests in Singapore (A. J. pers. comm. Ali Ibrahim; [37]). Our field surveys from July to October 2014 and subsequent consultation with botanists also confirmed the lack of host plant *E. diadenum* in urban areas and parks. During the mass emergence in 2014, the mass eclosion of thousands of *L. zampa* caterpillars from a cluster of host plant trees from the Sime Forest in central Singapore was documented [5]. This location is, by far, the only known breeding source of *L. zampa* in Singapore. The finding implied that all *L. zampa* originate from Singapore's mature forests, where the host plants are present.

L. zampa is known to be nomadic and may migrate 'out of forest' in search of potential host plant clusters. Indeed, *L. zampa* host plants in Sime Forest were recorded to be nearly completely eaten away during the mass emergence in 2014 [5]. The many records of *L. zampa* in densely populated urban zones suggests that adult *L. zampa* was attracted out of the forest areas and into the brightly lit urban environment potentially in search of the larval host and/or nectar plants. Because urban areas do not have any *L. zampa* host plants, it is clear that these areas would act as population sinks, as the moths would not be able to find host plants to lay eggs and sustain their offspring.

Because light intensity and population density are shown to be positively correlated [38,39], this implies that the brightest zones in Singapore recorded the maximum number of *L. zampa* moths. However, we cannot discount that the higher reporting rates from areas of high human density may be somewhat influenced by the larger population of interested individuals there. A massive survey effort across the island would be needed to correct for potential observer bias in such citizen science-based datasets.

L. zampa have been recorded being attracted to light traps during nocturnal field surveys in Singapore [2]. *L. zampa* has also been recorded entering lit houses at night and getting trapped in building facades or bulbs. Other Uranid moths, such as *Urania fulgens* (a species phylogenetically related to *L. zampa*), are also known to be attracted to light [40].

4.3. Morphological Variations

A closer comparison of the distribution data and morphometric measurements of *L. zampa* underscores variation between wing lengths of moths found between sexes, habitats, and batches.

4.3.1. Females Larger and Heavier Than Males

Our observation of *L. zampa* females being larger (longer wing length) and heavier (wider bodies but similar body length) than males corroborates with the literature in which larger females are observed in many lepidoptera [41–45]. These morphological differences can be attributed to the sexual selection theory in which larger females have extra energy for egg production, thereby offering them a fecundity advantage [41,43,46].

4.3.2. Urban Moths Are Longer and Lighter Than Forest Counterparts

Urban *L. zampa* individuals have significantly longer wing lengths and lighter bodies (smaller body widths) than forest individuals, suggesting a greater power of flight in urban individuals. This is also true for male *L. zampa* when compared between urban and forest areas. Moths with longer and larger wings tend to be better and stronger fliers [47]. This finding suggests that larger and stronger flying *L. zampa* migrate 'out of forest' and become trapped in urban areas, leaving smaller-sized and presumably less fecund individuals in forests. This could result in population level implications for the moths in just a few generations.

4.3.3. Smaller Moths over Time

Our observation that wing length reduced with time (i.e., first batch > second batch) can be attributed to an increase in host plant defense following the emergence of the first batch of *L. zampa* in early June 2014. Plants are known to protect themselves against larvae through chemical defenses (i.e., secretion of deterrent secondary plant compounds) against predation [48]. Alkaloids, cyanogenic glycosides, terpenoids, and phenolics employed in chemical defense have been shown to increase mortality rate and decrease fecundity of insects [49–52]. In another study, the larvae of *Urania fulgens* (a species related to *L. zampa*), when fed with leaves (formerly grazed by livestock), had a significantly slower growth rate and higher mortality [49]. Due to the high costs of toxin production, such defenses against predators are generally not long running and are triggered only by herbivory [53]. It is likely that chemical defenses by *E. diadenum* were triggered after the emergence of the first batch of moths, eventually resulting in smaller moths in subsequent batches.

Another explanation for the difference in moth size between the two batches may be due to food availability. The reduced availability of fresh leaves on the host plant after the emergence of the first batch of individuals may have resulted in smaller *L. zampa* during the second batch of emergence. The authors of [54,55] reported a decrease in wing length of monarch butterflies, *Danaus plexippus,* when larvae were starved of food.

4.4. Conservation Implications

It is clear that urban areas in Singapore are acting as sinks for *L. zampa* and drawing populations of the fitter moths (i.e., larger and better-flying individuals) from the forests. The majority of *L. zampa* individuals that are attracted to urban areas would not be able to find the host plants and lay eggs and complete their life cycle. The impacts of climate change on *L. zampa* populations seem like a two-fold problem. As dry spells are likely to become longer and more intense due to climate change in the future [56], it may mean more frequent mass emergences leading to more mortality of *L. zampa* in urban areas. With fitter individuals drawn to urban areas during mass emergence events, it may mean a degraded gene pool in a possibly declining population with every such event. This is over and above the fact that insects are prone to higher extinction risk as a result of climate-mediated shifts in temperature fluctuations [56].

Urgent steps may be needed to mitigate the impact of urban population sinks for this charismatic species. An immediate first step could be to plant the host plant of *L. zampa* in urban parks adjoining forested habitats and selected streetscapes of Singapore to provide adequate host plant resources at the time of the next mass emergence. Such larval host plantings in urban parks and gardens have been shown to increase populations for another charismatic and threatened Lepidopteran species, *Pachliopta aristolochiae,* in Singapore [57]. Another useful area of research could be to examine the larval host plant preference of *L. zampa* under laboratory conditions and identify if it may use other plant species as hosts that could be planted more widely across landscapes in Singapore.

Past records show flowers of the Tembusu tree (*Cyrtophyllum fragrans*) as the only recorded nectar source for *L. zampa* in Singapore. More research should be done to document the diversity of nectar plant preferences for *L. zampa* and to determine if other nectar plant species could be planted for *L. zampa* in urban areas. Whilst our mark-recapture study failed to get enough recaptures, a longer and more intensive study may be needed to document the trajectory of the movement of *L. zampa* individuals from 'out of forest' to urban areas. Reducing urban lights by introducing appropriate lighting solutions should also be considered along migratory/flight paths of moths to mitigate the impact of urban areas as sinks.

In parallel, awareness-raising efforts about this species' unique ecology and interaction with urban areas should continue as these efforts form the bedrock of citizen science monitoring and research. Such initiatives will ensure that members of the public and experts continue to be interested and share *L. zampa* sightings across Singapore and take adequate conservation actions.

Author Contributions: Conceptualization, A.J. and N.S.; methodology, A.J. and L.Y.N.; software, A.J.; validation, A.J., L.Y.N. and N.S.; formal analysis, A.J. and L.Y.N.; investigation, A.J., L.Y.N. and N.S.; resources, A.J., and N.S.; data curation, A.J. and L.Y.N.; writing—original draft preparation, A.J. and L.Y.N.; writing—review and editing, A.J. and L.Y.N.; visualization, A.J. and L.Y.N.; supervision, A.J. and N.S.; project administration, A.J. and N.S. All authors have read and agreed to the published version of the manuscript.

Funding: This research received no external funding.

Data Availability Statement: Not applicable.

Acknowledgments: We would like to thank members of public and contributors to Habitatnews, Nature Society (Singapore)'s Google Map database. Special thanks to Gan Cheong Weei with data collection efforts. This research was carried out under the NParks permit number NP/RP14-067 and Singapore Land Authority's permit SLA/PPD/263.3.10-V5.

Conflicts of Interest: The authors declare no conflict of interest.

Appendix A

The amount of rainfall and the number of rainy days in February across Singapore from 2011 to 2020. Source: Available online: www.data.govt.sg (accessed on 7 February 2023).

Year	Feb_Rainfall_mm	Feb_Number_Rain_DAYS
2011	23	8
2012	83.6	11
2013	395.2	22
2014	0.2	1
2015	18.8	6
2016	186	10
2017	158.4	15
2018	14.8	5
2019	31.6	5
2020	65	8

References

1. Murphy, D.H. The natural history of insect herbivory on mangroves trees in and near Singapore. *Raffles Bull. Zool.* **1990**, *38*, 119–203.
2. Karam, R.; Chong, J.H. Moths of Bukit Timah Nature Reserve, Singapore. *Gard. Bull. Singap.* **2019**, *71* (Suppl. 1), 317–330. [CrossRef]
3. Ee, D. Five Things You Should Know about the *Lyssa zampa* Moth. The Straits Times. 21 May 2014. Available online: http://www.straitstimes.com/news/singapore/more-singapore-stories/story/five-things-you-should-know-about-the-lyssa-zampa-moth-2 (accessed on 7 February 2023).
4. Kwara, M. Moth Invasion in Singapore. Yahoo News. Available online: https://sg.news.yahoo.com/blogs/what-is-buzzing/moth-invasion-in-singapore-051923140.html (accessed on 7 February 2023).
5. Jain, A.; Tea, Y.-K. Mass emergence of the tropical swallowtail moth *Lyssa zampa* (Lepidoptera: Uraniidae: Uraniinae) in Singapore, with notes on its partial life history. *Trop. Lepid. Res.* **2020**, *30*, 20–27.
6. van Regteren Altena, C.O. *A Revision of the Genus Nyctalemon Dalman (Lepidoptera: Uraniidae) with Notes on the Biology, Distribution, and Evolution of Its Species*; Brill: Leiden, The Netherlands, 1953.
7. Holloway, J.D. The biogeographical analysis of a transect sample of the moth fauna of Mt. Kinabalu, Sabah, using numerical methods. *Biol. J. Linn. Soc.* **1970**, *2*, 259–286. [CrossRef]
8. Heppner, J.B.; Wang, H.Y. *Lyssa zampa* in Taiwan. *Trop. Lepid.* **1996**, *7*, 146.
9. Tokeshi, M.; Yoko-o, M. New record of the tropical swallowtail moth *Lyssa zampa* (Butler)(Lepidoptera: Uraniidae) from mainland Japan. *Entomol. Sci.* **2007**, *10*, 103–106. [CrossRef]
10. Wee, B. The Atlas Moth (*Attacus atlas*). *WETlands* 6(1). 1999. Available online: http://www.sbwr.org.sg/wetlands/text/99-6-1-7.htm (accessed on 7 February 2023).
11. Yen, S.H.; Yu, H.S.; Mu, J.H.; Tan, H.J. On *Lyssa zampa* (Butler, 1867) (Uraniidae) from Taiwan. *Jpn. Heterocerists J.* **1995**, *186*, 173–175.
12. Leong, T.M. *Metamorphosis of the Swallowtail Moth Lyssa zampa*; Singapore Biodiversity Records: Singapore, 2014; pp. 158–159.
13. Sivasothi, N. It's the Season for *Lyssa zampa*, the Large, Nocturnal, White-Striped Moth. Habitatnews. 27 May 2005. Available online: http://habitatnews.nus.edu.sg/index.php?entry=/nature/20050527-lyssa_zampa.txt (accessed on 7 February 2023).
14. Sivasothi, N. Have you Seen *Lyssa zampa* Recently? Otterman Speaks. 21 May 2009. Available online: https://otterman.wordpress.com/2009/05/21/have-you-seen-lyzza-zampa-recently/ (accessed on 7 February 2023).
15. Sivasothi, N. The Hunt for *Lyssa zampa*. Otterman Speaks. 10 June 2010. Available online: https://otterman.wordpress.com/2010/06/10/the-hunt-for-lyssa-zampa/ (accessed on 7 February 2023).

16. Sivasothi, N. Is *Lyssa zampa* Back? Send Me Your Records! Otterman Speaks. 1 May 2013. Available online: https://otterman.wordpress.com/2013/05/01/is-lyssa-zampa-back-send-me-your-records/ (accessed on 7 February 2023).
17. Sivasothi, N. Will *Lyssa zampa*, the Tropical Swallowtail Moth, Make a Big Appearance This Year? Otterman Speaks. 14 April 2014. Available online: https://otterman.wordpress.com/2014/04/14/will-lyssa-zampa-the-tropical-swallowtail-moth-make-a-big-appearance-this-year/ (accessed on 7 February 2023).
18. Mrbrown. The Myth of the Moth . . . Dude. 2014. Available online: http://www.mrbrown.com/blog/2014/05/the-myth-of-the-mothdude.html (accessed on 7 February 2023).
19. Chen, H. Malaysia Swarmed by Giant Moths. BBC News. 11 June 2014. Available online: https://www.bbc.com/news/world-asia-27758640 (accessed on 7 February 2023).
20. Wiener-Bronner, D. Giant Moths Are Swarming All Over Malaysia. The Wire. 11 June 2014. Available online: http://www.thewire.com/global/2014/06/giant-moths-malaysia/372557/ (accessed on 7 February 2023).
21. Pollard, E.; Yates, T.J. *Monitoring Butterflies for Ecology and Conservation: The British Butterfly Monitoring Scheme*; Springer: Berlin/Heidelberg, Germany, 1993.
22. Ehrlich, P.R.; Davidson, S.E. Techniques for Capture-Recapture Studies of Lepidoptera Populations. *J. Lepid. Soc.* **1960**, *14*, 227–229.
23. van Hook, T.; Williams, E.H.; Brower, L.P.; Borkin, S.; Hein, J. A Standardized Protocol for Ruler-based Measurement of Wing Length in Monarch Butterflies *Danaus plexippus* L. (Nymphalidae, Danainae). *Trop. Lepid. Res.* **2012**, *22*, 42–52.
24. Gibbs, D.G.; Leston, D. Insect phenology in a forest cocoa-farm locality in West Africa. *J. Appl. Ecol.* **1970**, *7*, 519–548. [CrossRef]
25. Wolda, H. Fluctuations in Abundance of Tropical Insects. *Am. Nat.* **1978**, *112*, 1017–1045. [CrossRef]
26. Wolda, H. Seasonal Fluctuations in Rainfall, Food and Abundance of Tropical Insects. *J. Anim. Ecol.* **1978**, *47*, 369–381. [CrossRef]
27. National Environment Agency. *Advisories: Dry Spell Advisory (4 Mar)*; National Environment Agency: Singapore, 2014. Available online: http://app2.nea.gov.sg/corporate-functions/newsroom/advisories/dry-spell-advisory-(4-mar) (accessed on 7 February 2023).
28. Ee, D. February Was the Driest Month in Singapore Since 1869, Says NEA. Straits Times. 4 March 2014. Available online: https://www.straitstimes.com/singapore/february-was-the-driest-month-in-singapore-since-1869-says-nea (accessed on 7 February 2023).
29. Samanta, D.; Horton, B.P. Commentary: 2021 Has Already Seen the Wettest and Driest Months in Decades: Is Singapore Prepared for More? Channel News Asia. 15 March 2021. Available online: https://www.channelnewsasia.com/news/commentary/weather-january-february-monsoon-rain-dry-climate-change-mss-nea-14391482 (accessed on 7 February 2023).
30. National Environment Agency. *Annual Weather Review 2010*; National Environment Agency: Singapore, 2011.
31. Owen, D.F. Species diversity and seasonal abundance in tropical Sphingidae (Lepidoptera). *Proc. R. Entomol. Soc. London. Ser. A Gen. Entomol.* **1969**, *44*, 162–168. [CrossRef]
32. Wolda, H. Insect Seasonality: Why? *Ann. Rev. Ecol. Syst.* **1988**, *19*, 1–18. [CrossRef]
33. Tanaka, L.K.; Tanaka, S.K. Rainfall and Seasonal Changes in Arthropod Abundance on a Tropical Oceanic Island. *Biotropica* **1982**, *14*, 114–123. [CrossRef]
34. Sakai, S.; Harrison, R.D.; Momose, K.; Kuraji, K.; Nagamasu, H.; Yasunari, T.; Chong, L.; Nakashizuka, T. Irregular droughts trigger mass flowering in aseasonal tropical forests in Asia. *Am. J. Bot.* **2006**, *93*, 1134–1139. [CrossRef] [PubMed]
35. Today. Dry Spell, Rain Could Have Led to Mass Flowering. 2014. Available online: http://www.todayonline.com/singapore/dry-spell-rain-could-have-led-mass-flowering (accessed on 7 February 2023).
36. Walter, J.; Hein, R.; Auge, H.; Beierkuhnlein, C.; Loffler, S.; Reifenrath, K.; Schadler, M.; Weber, M.; Jentsch, A. How do extreme drought and plant community composition affect host plant metabolites and herbivore performance? *Arthropod-Plant Interact.* **2011**, *6*, 15–25. [CrossRef]
37. Chong, K.Y.; Tan, H.T.W.; Corlett, R.T. *A Checklist of the Total Vascular Plant Flora of Singapore*; Raffles Museum of Biodiversity Research, National University of Singapore: Singapore, 2009.
38. Department of Statistics Singapore. *Geographic Distribution of the Singapore Resident Population*; Statistics Singapore Newsletter: Singapore, 2010.
39. Liu, Q.; Sutton, P.C.; Elvidge, C.D. Relationships between Nighttime Imagery and PopulationDensity for Hong Kong. *Proc. Asia-Pac. Adv. Netw.* **2011**, *31*, 79–90.
40. Calhoun, J.V. Massing of *Urania fulgens* at Lights in Belize (Lepidoptera: Uraniidae). *Trop. Lepid.* **2004**, *12*, 43–44.
41. Begum, S.; Tsukuda, R.; Fujisaki, K.; Nakasuji, F. The Effects of Wild Cruciferous Host Plants on Morphology, Reproductive Performance and Flight Activity in the Diamondback Moth, *Plutella xylostella* (Lepidoptera: Yponomeutidae). *Res. Popul. Ecol.* **1996**, *38*, 257–263. [CrossRef]
42. Tammaru, T.; Esperk, T.; Castellanos, I. No evidence for costs of being large in females of *Orgyia* spp. (Lepidoptera, Lymantriidae): Larger is always better. *Oecologia* **2002**, *133*, 430–438. [CrossRef] [PubMed]
43. Teder, T.; Tammaru, T. Sexual size dimorphism within species increases with body size in insects. *OIKOS* **2005**, *108*, 321–334. [CrossRef]
44. Stillwell, R.C.; Blanckenhorn, W.U.; Teder, T.; Davidowitz, G.; Fox, C.W. Sex Differences in Phenotypic Plasticity Affect Variation in Sexual Size Dimorphism in Insects: From Physiology to Evolution. *Annu. Rev. Entomol.* **2009**, *55*, 227–245. [CrossRef] [PubMed]

45. Allen, C.E.; Zwaan, B.J.; Brakefield, P.M. Evolution of Sexual Dimorphism in the Lepidoptera. *Annu. Rev. Entomol.* **2011**, *56*, 445–464. [CrossRef]
46. Preziosi, R.F.; Fairbairn, D.J. Lifetime Selection on Adult Body Size and Components of Body Size in a Waterstrider: Opposing Selection and Maintenance of Sexual Size Dimorphism. *Evolution* **2000**, *54*, 558–566.
47. Pinheiro, C.E.G. Palatablility and escaping ability in Neotropical butterflies: Tests with wild kingbirds (*Tyrannus melancholicus*, Tyrannidae). *Biol. J. Linn. Soc.* **1996**, *59*, 351–365. [CrossRef]
48. Young, M. Plant defence against Larvae. In *The Natural History of Moths*; T&AD Poyser Ltd.: London, UK, 1997; pp. 133–149.
49. Smith, N.G. Host plant toxicity and migration in the dayflying moth, *Urania fulgens*. *Fla. Entomol.* **1983**, *66*, 76–85. [CrossRef]
50. Kite, G.C.; Fellows, L.E.; Lees, D.C.; Kitchen, D.; Monteith, G.B. Alkaloidal Glycosidase Inhibitors in Nocturnal and Diurnal Uraniine Moths and their Respective Foodplant Genera, *Endospermum* and *Omphalea*. *Biochem. Syst. Ecol.* **1991**, *19*, 441–445. [CrossRef]
51. Scoble, M.J. Environmental and Ecological Importance of Lepidoptera. In *The Lepidoptera: Form, Function, and Diversity*; Oxford University Press: Oxford, UK, 1992; pp. 170–184.
52. Awmack, C.S.; Leather, S.R. Host Plant Quality and Fecundity in Herbivorous Insects. *Annu. Rev. Entomol.* **2002**, *47*, 817–844. [CrossRef]
53. Agrawal, A.A. Induced Responses to Herbivory and Increased Plant Performance. *Science* **1998**, *279*, 1201–1202. [CrossRef]
54. Johnson, H.; Solensky, M.J.; Satterfield, D.A.; Davis, A.K. Does Skipping a Meal Matter to a Butterfly's Appearance? Effects of Larval Food Stress on Wing Morphology and Color in Monarch Butterflies. *PLoS ONE* **2014**, *9*, e93492. [CrossRef] [PubMed]
55. Becker, C. *A Possible Size-Determined Directional Selection in Danaus plexippus (Lepidoptera: Danaidae) with Evidence from Stable Isotope Analysis*; University of Kansas: Lawrence, KS, USA, 2008.
56. Duffy, K.; Gouhier, T.C.; Ganguly, A.R. Climate-mediated shifts in temperature fluctuations promote extinction risk. *Nat. Clim. Chang.* **2022**, *12*, 1037–1044. [CrossRef]
57. Jain, A.; Zeng, Y.; Webb, E.L. Critical dependence of butterflies on a non-native host plant in the urban tropics. *Front. Ecol. Evol.* **2021**, *9*, 655012. [CrossRef]

land

MDPI

Article

Land Suitability of Urban and Industrial Development Using Multi-Criteria Evaluation (MCE) and A New Model by GIS in Fasa County, Iran

Masoud Masoudi [1,*], Mostafa Aboutalebi [2], Elham Asrari [2] and Artemi Cerdà [3,*]

[1] Department of Natural Resources and Environmental Engineering, School of Agriculture, Shiraz University, Shiraz 71441-1331, Iran
[2] Department of Civil Engineering, Payame Noor University, Tehran 19395-3697, Iran; abootalebi@shiraz.ir (M.A.); e_asrari@pnu.ac.ir (E.A.)
[3] Soil Erosion and Degradation Research Group, Department of Geography, Valencia University, 46010 Valencia, Spain
* Correspondence: masoudi@shirazu.ac.ir (M.M.); artemio.cerda@uv.es (A.C.)

Abstract: Land use planning is a science that specifies the optimized use of land based on ecological and socioeconomic characteristics. In many parts of Iran, the selection and management of land use (development, especially) is performed regardless of land capability, which causes disinvestment and reduces the environmental capacity. The main objective of this study is to evaluate and reform the ecological model of urban, rural, and industrial development in the study area. This study was conducted in Fasa County in the southern part of Iran, and the investigated methods included Weighted Linear Combination (WLC) or Multi-Criteria Evaluation (MCE), with two views, without limitation and with limitation, and the proposed geometric mean method through the integration of maps in GIS. The results showed that the geometric mean evaluation model (with kappa = 0.69) is the best and easiest compared to other models in the estimation of environmental capability. It should be mentioned that the lowest precision (with kappa = 0.59) between the methods was observed in the MCE method without a limiting factor, and it is clear that the limiting factor has a decisive role in assessing ecological capability and increasing accuracy. It is concluded that the proposed geometric mean method, due to the simplicity and high accuracy of the calculations, has a significant contribution to increasing efficiency and reducing the costs associated with the assessment of ecological capability.

Keywords: land use planning; ecological capability assessment; geometric mean; multi-criteria evaluation

1. Introduction

It is worth noting that policy assessments have gradually become more efficient in the policy-making process [1]. The Organization for Economic Co-operation and Development and other organizations have made noteworthy contributions to increasing awareness about sustainability in policy assessments. Recent research highlights the importance of assessing the potential impacts of proposed policies as a way to achieve sustainable development [2]. Sustainability and sustainable development are increasingly gaining attention from various groups, including the media, the research community, and environmental activists [3,4].

When it comes to assessing sustainability, it is crucial to consider the economic, social, and environmental dimensions [5–9]. Understanding the land's capabilities is also essential. To achieve sustainable outcomes in policies, plans, programs, or projects, utilizing indicators on different objective levels can be the key to success. Soil- and water-related elements are especially important to consider [10–13].

Sustainable development of an urban area requires urban land use planning [14]. Land use planning tries to plan optimal uses to be replaced and to protect against incompatible changes and potential changes [15,16]. Such management strategies make an urban area sustainable through land use planning. Therefore, land use planning is vital in planning a city and its suburbs [17].

Although comprehensive land use planning is a complex decision-making process, the invention of new technologies in the GIS environment has simplified such complex assessments in two ways—(1) GIS allows experts to work with a large number of datasets; (2) with several methods, techniques, or models, the analysis of land use capacity can be evaluated in GIS [18–20]. A large number of physical and environmental, social, and economic indicators have been considered for proper planning of the development of urban and industrial areas. Geographical data are used in a GIS environment by using these indicators in various complex ways in the evaluation process of urban development planning. However, to use these datasets in GIS, spatial database management is required, especially when the datasets are complex and voluminous [21,22]. To build such a spatial database, at first, it is necessary to prepare a conceptual model so that their mutual relations are well defined and the database can be used to store, edit, and query data easily. Then, some models or multi-criteria decision-making (MCDM) techniques embedded with GIS can be used to evaluate land use capability [23–25]. To weigh the indicators, the Analysis Hierarchy Process (AHP), which is a technique in MCDM, can be used for urban development planning using GIS. McHarg (1969) [26] showed that land capability assessment is an important step in land use planning. It is also very important to choose the appropriate evaluation method for land use planning [27]. Mitra and Ilangova (2004) [28] have pointed out that GIS has a very important role in the location of land uses. GIS typically stores and evaluates extensive data in the form of digital maps [29]. Pourkhbaz et al. (2014) [30] conducted a good evaluation of agriculture in the Qazvin-Takestan plain in Iran by using multi-criteria evaluation (MCE) methods and by using AHP and simple incremental weight (SAW). Their results showed that the application of MCE can be useful in evaluating agricultural potential. Jokar et al. (2021) [25] evaluated and reformed the ecological model of the development of ecotourism in Sepidan County, Iran. The results showed that the geometric mean evaluation model and its calibration are better than other models (Iranian Evaluation Model of Ecological Capability based on Boolean logic; the maximum limits proposed method (Boolean logic), and the arithmetic mean) in the estimation of environmental capability.

Parry et al. (2018) [31] were able to determine urban development potential through AHP and MCE using a set of geophysical and socio-economic criteria in urban areas of Srinagar and Jammu, India. For better urban development planning and appropriate decision making, their study provided information about the suitability of the area's lands for creating urban welfare development in the future.

A decision method for deriving combined maps using GIS is the Weighted Linear Combination (WLC) technique. It is one of the most commonly used decision-making models in the GIS field. However, the application of the method often occurs without a full understanding of the assumptions behind the approach. In many case studies, because analysts (decision makers) ignored or were unaware of the assumptions, the WLC model has been misapplied with questionable results. When it comes to the WLC method, there are specific challenges in weighting and standardizing indicators that should be taken into account. Evaluation methods face a problem with this method, as they need to consider the constraints to avoid lax evaluation and to maintain accuracy in determining the ecological range for the indicators. Weighting indicators can also lead to mistakes, and standardization of indicators can result in errors by evaluators [23]. This is why it is crucial to prepare an evaluation model that does not have these challenges to ensure reliable land evaluation.

In this research, according to the mentioned cases, two WLC evaluation methods without constraints and with constraints and considering the AHP weighting method to determine the weight of indicators were evaluated to assess the ecological capability of urban and industrial development in Fasa County in the south of Iran. Additionally, Fasa County's sufficient data and good ecological diversity made it an excellent candidate for land evaluation. Then, the accuracy of the above two methods was measured with a new and lenient evaluation method based on the evaluation of indicators based on the geometric mean. The hypothesis of this research is that the geometric mean method has higher accuracy than the WLC method without constraints and that it has equal or higher efficiency than the WLC method with constraints due to its ease of implementation. Therefore, the main objective of this study is to develop a newly proposed method in comparison to WLC or MCE (using fuzzy-AHP)-based averaging methods. This proposed method may have the ability to evaluate land for urban and industrial development more easily and accurately.

2. Materials and Methods

2.1. Study Area

Fasa County (Figure 1) is located in the southern part of Iran. Its area is 4188 Km^2. Fasa is one of the cities of the Fars province and the center of Fasa County. The city of Fasa is located at 53°40′ E and 28°58′ N at an altitude of 1370 m above sea level, and it is a city with a distance of 145 km from Shiraz, the capital of the Fars province. Fasa County is the fourth most populated city in the province, with a population of 208,000. Fasa is located in the semi-arid temperate region. The highest temperature in the summer reaches 42 °C, and the lowest in the winter reaches −8 °C; the average rainfall of the County is about 380 mm per year. The economy of this county is based on agriculture and animal husbandry. Fasa boasts of its thriving agricultural industry, particularly in wheat production, which is the highest production in Iran. The city's climate is well suited for the growth of tropical palm trees and various fruit trees, such as oranges, tangerines, pomegranates, pistachios, almonds, and walnuts. Moreover, animal husbandry contributes significantly to the local economy, with livestock and dairy products, wool, leather, and meat being among the prominent products. In general, nearly 40% of Fasa County is plain, and the rest is mountainous. The elevations in Fasa County extend from the Zagros Mountain range and follow a northwest-to-southeast direction. The mountains consist mainly of limestone and chalk, while the plains of Fasa County are relatively flat with little variation in elevation, and they are covered by alluviums from the Quaternary period. Based on the American comprehensive system, the soils in Fasa County can be categorized as either Antisol or Inceptisol. Moreover, these soils fall into three main subgroups (Arenosol, Cambisol, and Calcisol) under the international FAO system [32].

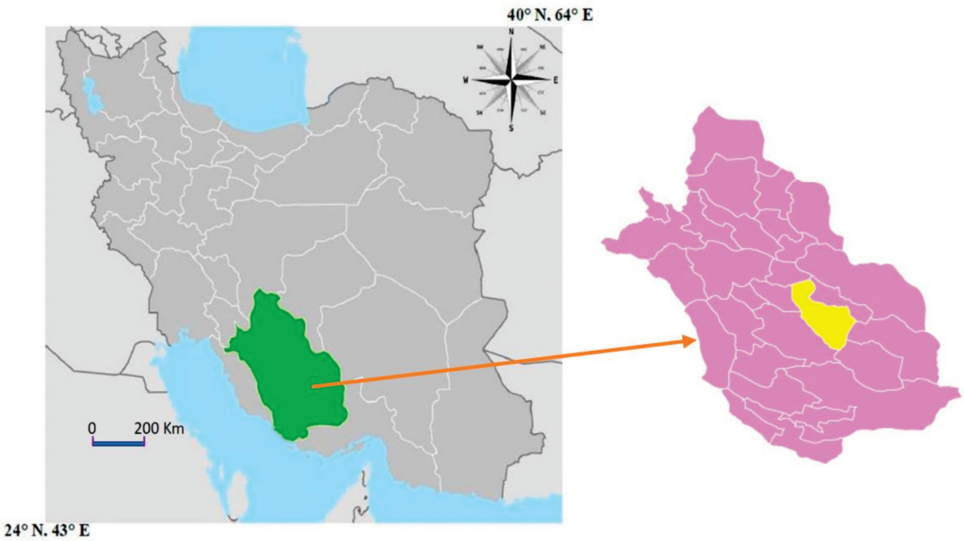

Figure 1. The map of Iran shows the location of Fars province and Fasa County in the southern region of Iran.

2.2. Methodology

The general methodology consists of two parts. (a) description and reclassification of indicators, and (b) evaluation and formulation of two models based on the geometric mean and WLC. Figure 2 shows the working method flow diagram of the programmed model. The obtained data include two types: (1) digital data and (2) map data, mainly in a vector format with the spatial reference of the UTM Zone 39N projection with semi-detailed to detailed information (with scales of 1:50,000 to 1:100,000). All of these data used by the regional and main offices of the Ministries of Energy and Agriculture of Iran have been prepared and processed using different methods in GIS to carry out this research (Table 1). The slope index was prepared from the Digital Elevation Model (DEM) map, and the land type index was prepared from the land unit map. Climate indices, like precipitation, temperature, etc., were provided from synoptic and climatology stations of the study area. Soil and geology maps with their parameters were provided based on existing maps. Also, the geometric and descriptive features of the maps were modified using Global Positioning System (GPS) tools along with fieldwork. Buffer maps of faults and rivers were obtained from the geological and stream maps. Data on the quantity of water were provided by the regional water office. It should be mentioned that we used existing maps with field surveys and modifications for vegetation parameters.

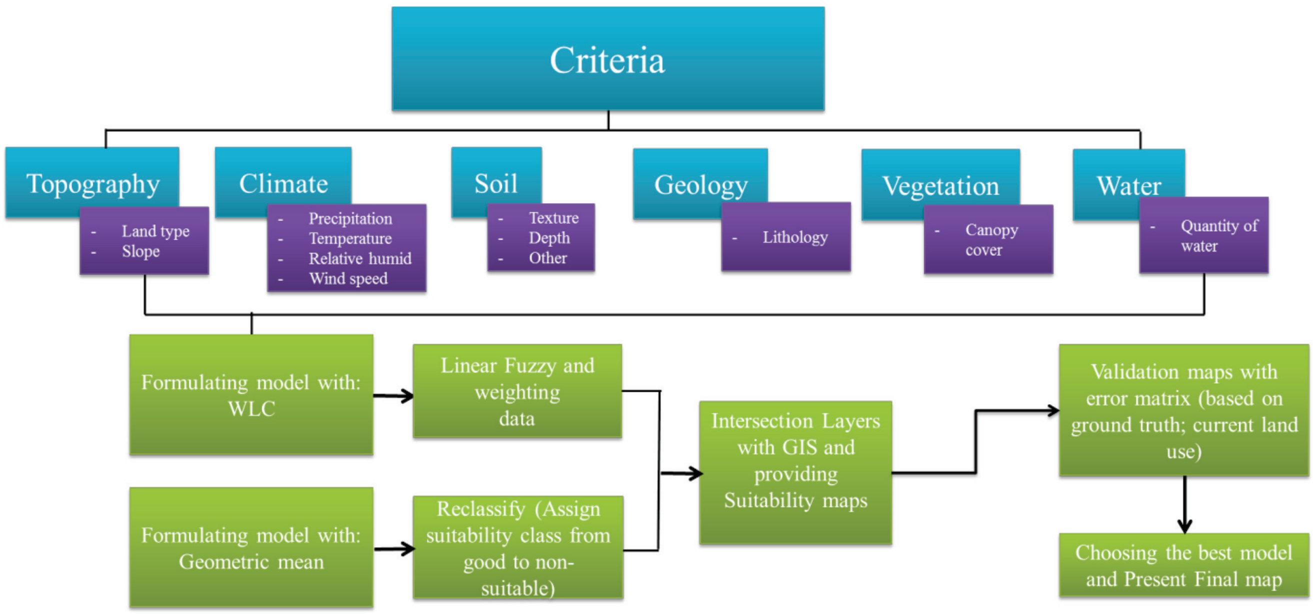

Figure 2. Flowchart of the methodology performed to assess ecological capability in this study.

Table 1. The parameter classes for the ecological capability assessment of development [23].

Criteria	Indicators	Classes of Ecological Capability and Their Rating Score		
		Highly Suitable (2)	**Moderately Suitable (1)**	**Poor to Not Suitable (0)**
TOPOGRAPHY	**Land type**	Plains except for floodplains	Plateau and upper terraces, alluvial and colluvial fans	Mountainous and hilly areas, floodplains
	Slope (%)	0–15	15–30	>30
CLIMATE	**Precipitation (mm)**	501–800	51–500 or >800	<50
	Temperature (°c)	18.1–24	24.1–30 or <18	>30
	Relative humidity (%)	40.1–70	<40 or 70–80	>80
	Wind speed (km/h)	1–35	36–60	>60

Table 1. *Cont.*

Criteria	Indicators	Classes of Ecological Capability and Their Rating Score		
		Highly Suitable (2)	**Moderately Suitable (1)**	**Poor to Not Suitable (0)**
SOIL	**Texture**	Moderate (often)	Light (often)	Heavy (often), Regosols, Lithosols
	Depth (cm)	Deep (> 80)	Semi-deep (50−80)	Shallow to very shallow (<50)
	Gravel percent	0–25	26–50	>50
	Drainage (cm/hr)	Good (2–6)	Moderate (0.1–2 or 6–25)	Poor (<0.1 or >25)
	Erosion	None to slight	Moderate	Severe to very severe
	Granulating	Moderate	Fine or coarse	Very fine
	Evolution	Perfect	Moderate	Low
GEOLOGY	**Lithology**	Sediments of the continental shelf, Ophiolite of melange color, and Sandstone	Middle Eocene pyroclastic rocks, limestone and dolomite, granite, shale, alluvial cones, conglomerate, claystone, loess, and alluvial terraces	Schist and gneiss and amphibolite, calcite marble and dolomite, quartzite, marl, salt domes, gipsum domes, sand dunes, floodplain, and Buffer maps for faults and rivers [1]
VEGETATION	**Canopy cover (%)**	0–25	26–50	>50
WATER	**Quantity of water for everyone (Lit/day)**	<225	150–225	<150

[1]—Major Fault = 1 km, Minor Fault = 300 m, River = 1 km (based on guidelines of the Department of Energy and the Department of Housing and Urban Development).

2.2.1. Description and Reclassification of Indicators

The selection of indicators and their classification method are derived from the evaluation model of the Iranian assessment of ecological capability for development use [33] based on the evaluation of Boolean logic, including three (3) classes. Of course, because the classification of indicators in the above model is not clear for the evaluators, the new classification method shown in Table 1 has been created to facilitate its use. Thus, new classes have been introduced, including highly suitable (good), moderately suitable, and poor to not suitable (Table 1). The selection of indicators in the evaluation model of the ecological capability of different utilizations in Iran is based on those indicators that are important in the evaluation of the ecological capability of residential and industrial development, such as various indicators of topography, climate, soil, geology, vegetation, and water.

Table 1 shows that the classification range of the above indices is quantitative for most of the indices and qualitative for the rest due to the descriptive nature of the index (such as land type or lithology type). Of course, as Table 1 shows, for the above two cases, the ecological capability score of the classes (0 to 2) for the averaging evaluation method is given in the form of a geometric mean. Of course, this score range for classification by the WLC method usually includes the range of 0 to 1 or 0 to 255.

2.2.2. Evaluation and Formulation of the Proposed Model Based on the Geometric Mean and WLC

Multi-criteria evaluation (MCE) or WLC: First, data or indices in vector format were converted to raster data. Then, linear fuzzy classification (0 to 1) was performed on these parameters based on their thresholds (Table 1). Linear fuzzy classification explains the fuzzy membership function based on the maximum and minimum fuzzy membership of 1 and 0. The Table 1 classification was used to classify and determine the fuzzy numbers. Suitability classes with scores of 0 and 2 will represent fuzzy values of 0 and 1, respectively.

In the next step, the mentioned indicators were weighted based on the AHP method with specialist discernment. Then, the WLC method was used to weigh the input data. With a weighted linear combination, the indices were combined by applying a weight to each index and then classifying the results to obtain a suitability map (Equation (1)).

$$\text{X1} = [(\text{W1} \times \text{Indicator1}) + (\text{W2} \times \text{Indicator2})\ldots + (\text{Wn} \times \text{Indicator n})] \times \text{Ci} \tag{1}$$

W = obtained weight for each parameter.

Ci = constraints; in this study, WLC was investigated based on both existing constraints and without constraints. Ci should be 0 (existing constraints) or 1 (without constraints) in each pixel.

Finally, a natural breaks method was performed for the final classification of the fuzzy map in 3 classes.

Geometric mean: According to the indicators listed in Table 1, each indicator in a vector format was given a weight from 0 to 2 (0 indicates poor to unsuitable ecological status, and 2 indicates suitable ecological status for development). Then, each criterion was evaluated according to the geometric mean of the indicators presented in Equation (2):

$$criterion\_x = (layer1 \times layer2 \times \ldots \times layern)^{1/n} \tag{2}$$

In this formula, *criterion_x* is a criterion, the *layer* is an indicator of the criterion (such as slope and land type parameters in the topography criterion), and *n* is the number of indicators. Next, the criteria were multiplied using the geometric mean (Equation (3)).

$$\begin{aligned} &\text{Final score of land suitability for Development} \\ &= (Topography \times Climate \times Soil \times Geology \times Vegetation \times Water)^{1/6} \end{aligned} \tag{3}$$

In this formula, the final score helped us to prepare the final suitability map. Then, the land capability classes for development use were determined using Table 2 in the GIS environment.

Table 2. Land capability classes for development use based on their points in the polygons prepared in the final map.

Suitability Classes	Good (1)	Moderate (2)	Poor to Not Suitable (3)
Scores of polygons	1.5–2	0.5–1.5	<0.5

2.2.3. Validation Models

To validate the obtained map, it should be compared with ground reality samples [34]. In the current research, the first settlement area (Fasa City as the main city) defined in the current land use map is equivalent to a good class, other cities and rural areas are equivalent to a moderate class, and the dense and semi-dense forest in the mountains and desert lands (saline and bare land) are equivalent to the poor and not suitable class (Table 3). After that, samples of these regions (Table 3) were collected in ArcGIS 9.3 environment using the "Create Fishnet" algorithm, both systematically and randomly [35]. Then, these points were placed on land capability maps for validation. The results of validation can be seen in a table called the "error matrix" or agreement matrix (Table 3). In this table, quantitative indicators of accuracy, such as the "kappa coefficient, overall accuracy, and in-class index," are estimated [36]. The in-class coefficient is an accuracy index to estimate the correct preparation of appropriate classes for each use, such as the main city in the land map [35].

Table 3. The Error matrix for development use in the region.

	Ground Reality		
Classes	Fasa City (Main)	Other cities and rural areas	The dense and semi-dense forest in the mountains, desert lands
1	*		
2		*	
3			*
Point number	510	276	675

3. Results

Table 4 shows the weight of the indicators used in WLC methods with a Consistency Ratio of CR < 0.1. According to this method, the water index has the highest weight, and the land type and lithology indices are in the next ranks.

Table 4. The weight of the indicators used in the development model based on the AHP method.

Factor	Factor Weight
Slope	0.091
Land Type	0.115
Rainfall	0.078
Temperature	0.039
Relative Humidity	0.019
Wind Speed	0.021
Soil Texture	0.039
Soil Depth	0.107
Soil Drainage	0.042
Soil Erosion	0.072
Lithology	0.114
Vegetation	0.047
Quantity of Water	0.216
CR	0.05

The capability map with the best accuracy prepared by the geometric mean is observed in Figure 3. Table 5 shows the accuracy assessment indexes in the used models. The results showed that the WLC method without constraints has the lowest accuracy, and it is clear that the limiting factor has a decisive role in assessing ecological capability and increasing the accuracy. Also, the proposed method including three classes by geo-mean is close to WLC with constraints, with high accuracy. Figure 4 also shows the proximity of the expansion of capability classes in these two methods, but it should be mentioned that the geometric mean evaluation model is simpler than WLC because this method does not need a weighting process. This issue indicates that the evaluation with a geometric mean with three final capability classes can be a suitable method for finding potential urban and industrial development areas. The final map prepared, based on the proposed method, is placed between 0 and 1. Therefore, this method has a high capability in separating classes and locating them compared to other evaluation perspectives.

Table 5. Values of validation indices, kappa coefficient, overall accuracy, and in-class coefficient in the used models.

Land Use	Model / Index	MCE (WLC) Without Constraints	MCE (WLC) With Constraints	Geometric Mean
Development	Overall Accuracy	74	82	82
	Kappa Coefficient	0.59	0.69	0.69
	In-Class Coefficient	2.18	5.29	5.13

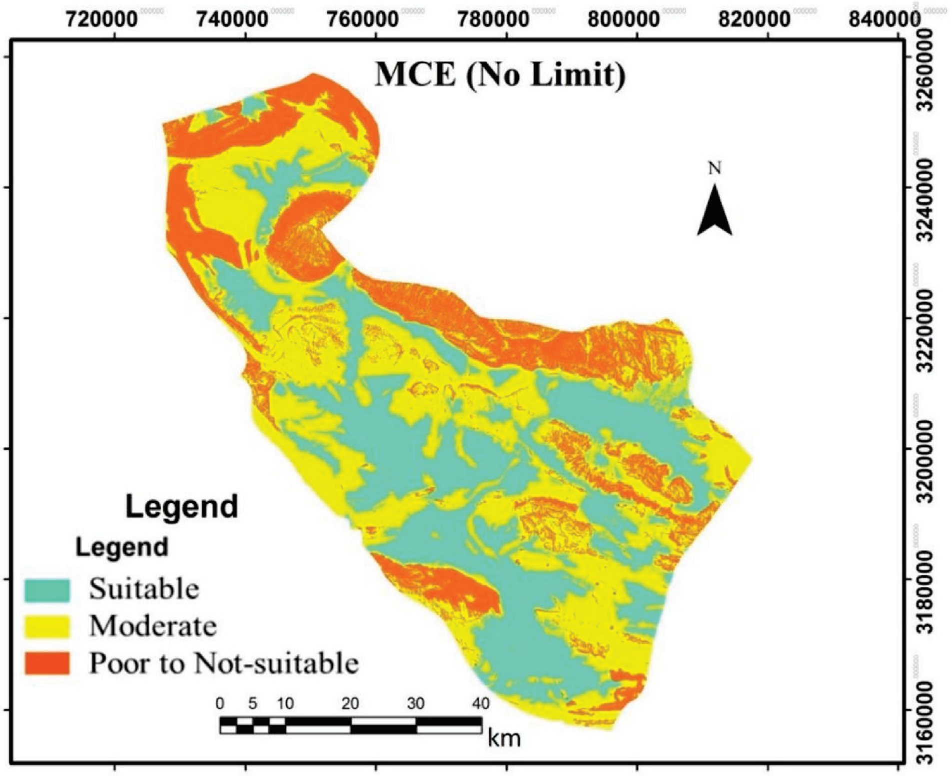

(**a**) WLC (without constraints)

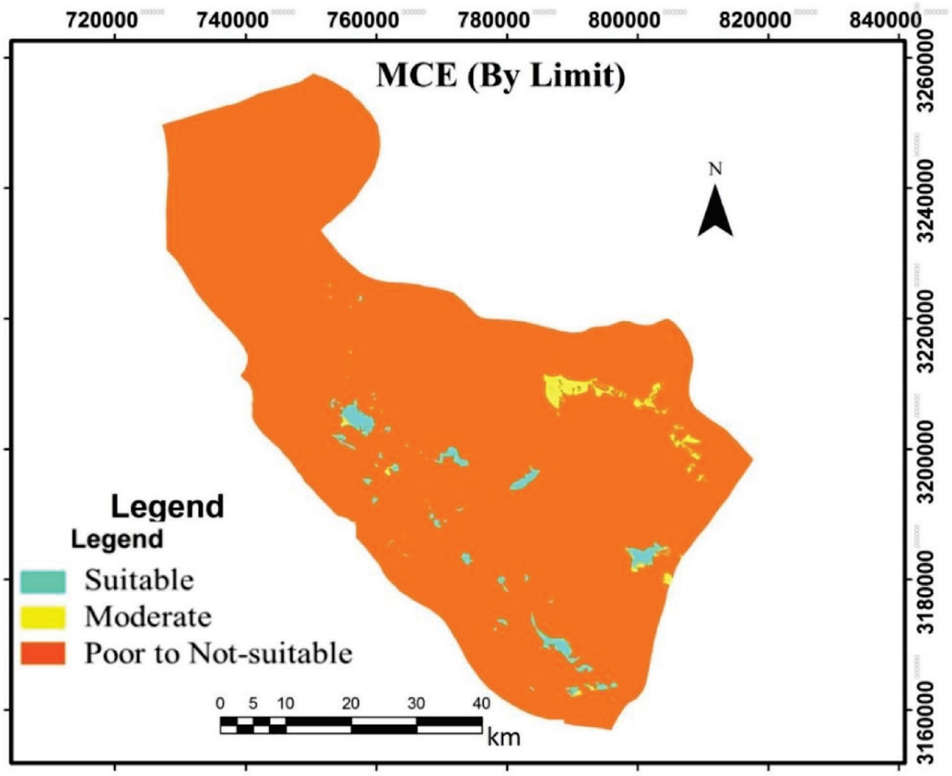

(**b**) WLC (with constraints)

Figure 3. *Cont.*

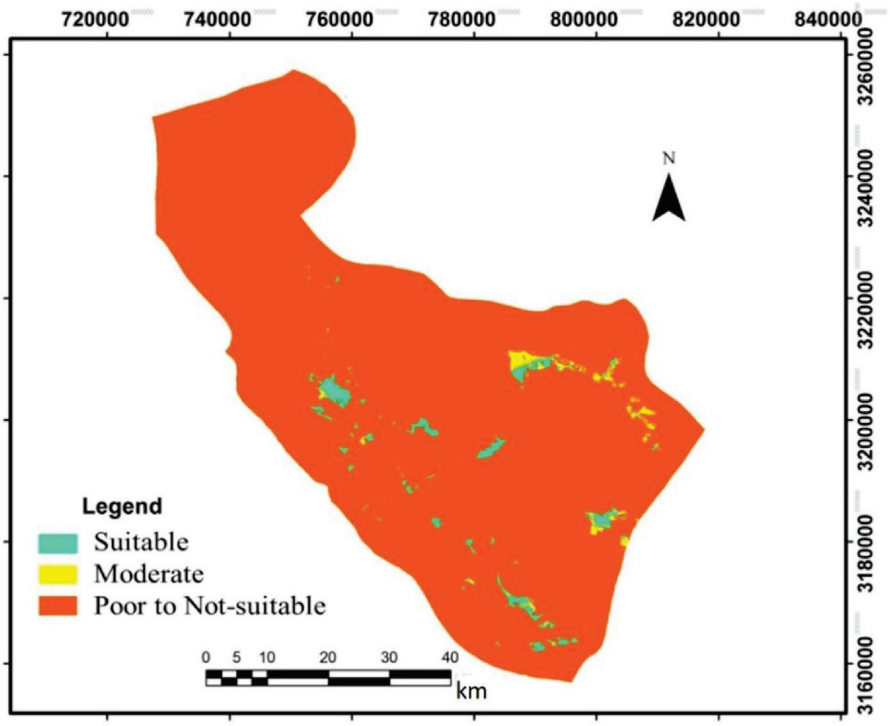

(**c**) Geometric mean method

Figure 3. Maps of the ecological capability of urban and industrial development prepared by (**a**) WLC (without constraints), (**b**) WLC (with constraints), and (**c**) geometric mean method.

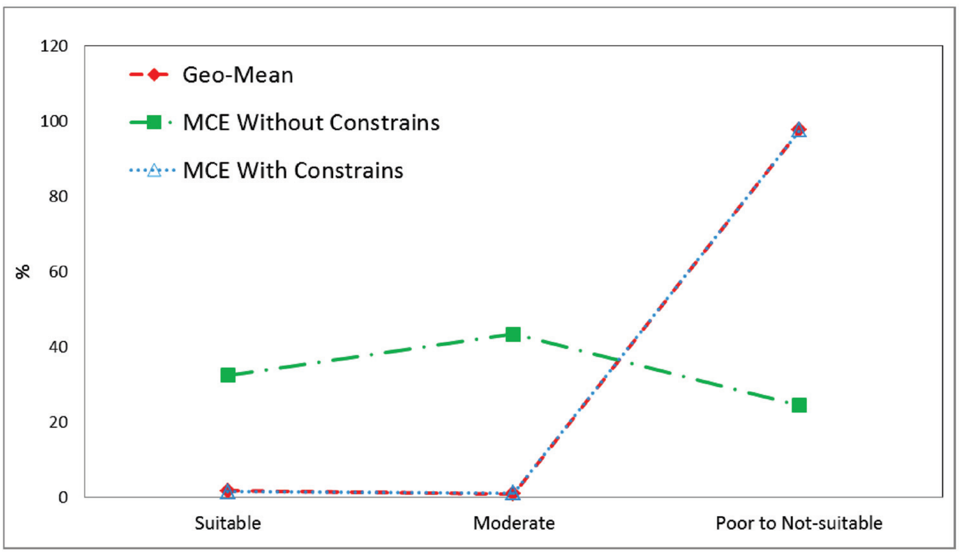

Figure 4. The percentage of lands under different capability classes for different methods of evaluating development potential in this research.

4. Discussion

Considering the ecological capacity of an area is crucial to sustainable land use planning, especially for urban and industrial zones. This approach ensures that land use is sustainable and that it caters to the needs of both the environment and humans. Urban areas play a significant role in achieving Sustainable Development Goals by providing safe and affordable housing, water, and sanitation, as well as improving transportation systems to make them accessible and sustainable for all. By prioritizing these factors, cities become safer, more resilient, and sustainable, and they contribute to a more sustainable future.

In this study, the model of the ecological capability of development use was investigated using different evaluation methods (WLC and geometric mean) and with an all-around approach to the environmental characteristics of Fasa City. It is worth mentioning that in the review of the topographic criteria for evaluating the urban development potential, changes were made compared to Iran's ecological model [33]. In this way, the land type index (based on Iran's ecological model) was added to the above model, and the height above the sea level index was removed from the above land use model. Considering that there are some suitable urban areas in the world that are at low altitudes, such as in Europe, as well as areas that are located in the plains but at high altitudes, in the current urban development model, the height index was removed. Therefore, the topography criterion was evaluated by considering the slope and land type indicators. In research conducted by Monavari et al. (2008) [37] in order to evaluate the ecological capability of the Zakhard watershed area in the northwestern part of Shiraz City in the south of Iran, the results of the study showed that upon considering all of the ecological parameters, the entire area is unsuitable for urban development. However, by removing the height index from the region, about 9% of the basin will have suitable capability for urban development.

In this research, the accuracy of the model in the geometric mean conditions was better than the WLC ecological model without considering the limiting factor and almost equal to WLC with the limiting factor considered. In relation to the evaluation method in general, it can be said that in the WLC method without considering the limiting factor or the simple WLC without weighting, which are non-strict methods, the majority of the region tends towards the appropriate classes. But, in stricter methods based on Boolean logic, such as Iran's ecological models, FAO models for evaluating agriculture and natural resources [38], and maximum limit methods, the majority of the region moves towards inappropriate classes. It is rare to find areas with suitable and moderate capability in a region. But, the evaluation methods based on the geometric mean and WLC, considering the limiting factor, are placed between these two views. However, the majority of the region tends towards the weak or medium classes due to the consideration of the limiting factor or the consideration of the zero number in the method of multiplying by the geometric mean. Therefore, the results of this research are consistent with the results of Davidson et al. (1994) [39], Baja et al. (2006) [40], Najafinejad et al. (2013) [41], and Jokar et al. (2021) [25].

In FAO models, the way to evaluate the capability of land uses is based on the maximum limit approach, which, like Iran's ecological models, has a strict decision regarding the location of land uses. This type of decision making (maximum limitation and systemic method) is based on the type of attitude towards the environment and the examination of its components, as well as estimating the capability without prejudice and only based on the inherent potential of the land [41]. However, these pure and idealistic attitudes towards the environment ignore social and economic factors and make an incomplete estimate of the real capability of the land [42]. In other words, the above methods have a limited attitude towards land evaluation. The model of ecological capability should, in addition to showing the limiting conditions, also express the climax and the peak capability of an ecosystem to create a utilization in the current conditions. This climax condition, which indicates the high capability of utilization, can be searched in its current condition. That is, if a land use has been able to settle well in the land, the possibilities and conditions of its climax have existed, and the model should be able to recognize it. This research showed that the proposed geometric mean model derived from the EMOLUP model [23,43] plays a more appropriate location approach to determining climax conditions and also involves limiting factors in land zoning.

In the EMOLUP geometric mean method, determining the evaluation criteria reduces the effect of some criteria, such as soil, with more indicators, compared to other criteria, such as topography, with fewer indicators (for example, two indicators). In this way, the weight of both the soil and topography criteria is considered equivalent, which is not seen in prominent models, such as WLC. It is worth remembering that the proposed model is also a type of multi-criteria evaluation (MCE) method. Also, by putting the number zero in the equation, the ecological intervals that create a limit or hazard for the earth (such as mountainous lands or with low water content) tend towards the wrong side with the process of geometric multiplication. With this approach, the attitude that the fans of maximum limitation have towards modeling and limiting factors is also taken into account.

It is worth mentioning that implementing the geometric mean evaluation method is easier compared to the current conventional methods (which are more difficult to implement and have ambiguities for the evaluator), such as using Boolean methods based on AND logic and the current WLC. In the current WLC, the evaluator needs to give weighting, there is a possibility that the experts estimating the weight of the indicators may make a calculation error; sometimes, there is a mistake in the standardization of the indicators (determining the ecological range between zero and one), and these are challenging cases. AHP is a broadly used weighting approach in WLC methods, and it was started by Saaty. It is easily implemented as one of the WLC techniques [44–46]. Therefore, according to the reasons mentioned and the high accuracy, and according to the equality of the kappa coefficient of the geometric mean and the weighted arithmetic mean (WLC) methods with the application of the limiting factor, the geometric mean is more convenient than this method of evaluation. It has superiority and can be recommended for evaluating other regions of the world. Some researchers, like Asadifard (2015) [47], Razaghi (2016) [48], and Jokar et al. (2023) [49], compared the methods of the geometric mean and multi-criteria evaluation in Iran. Their results showed the relative superiority of the geometric mean method for the multi-criteria evaluation.

5. Conclusions

Land preparation should be performed with a coordinated approach to development and environmental protection. Achieving this goal will lead to the sustainable development of the environment with the approach of evaluating the ecological potential and choosing the best option for the use of the land. The main goal of this research is to implement the ecological model of urban, rural, and industrial development of Fasa County in the southern part of Iran and to compare the proposed geometric mean method derived from the EMOLUP model with the weighted index arithmetic mean (WLC) with and without applying the limiting factor in the study area using GIS. The maps of land capability for urban development were prepared. Finally, the best and easiest capability assessment map was selected based on the geometric mean method derived from the EMOLUP model. It is concluded that the proposed geometric mean method, due to the simplicity and high accuracy of the calculations, has a significant contribution to increasing efficiency and reducing the costs associated with the assessment of ecological capability. To effectively implement urban and industrial development policies, it is imperative to concentrate on regions with high and medium suitability, as indicated on the production map. It is essential to avoid weak and unsuitable areas at all costs. However, it is worth noting that certain areas may become suitable with the removal of restrictions. Overall, the study results can be applied in land use planning in other regions with similar conditions. So, the results of this research can be used by different managers and other stakeholders for proper land use management.

Author Contributions: Conceptualization, M.M.; Methodology, M.M., A.C., and E.A.; Software, M.M. and M.A.; Validation, M.M. and M.A.; Formal Analysis, M.M., E.A., and M.A.; Investigation, M.A.; Resources, M.A.; Data Curation, M.M. and M.A.; Writing—Original Draft Preparation, M.M.; Writing—Review and Editing, M.M. and A.C.; Visualization, M.M.; Supervision, M.M. and E.A.; Project Administration, M.M.; Funding Acquisition, A.C. All authors have read and agreed to the published version of the manuscript.

Funding: The costs of printing the article (APC) are borne by the University of Valencia, Spain, in consideration of the grant considered for Professor Artemi Cerdà.

Data Availability Statement: The data used and analyzed throughout the present research are obtainable from the corresponding author upon sensible demand.

Acknowledgments: The authors express their honest thanks to people for their help and also the state departments, mindful advice, positive censure, efficient guidance, data generation, and preparing the maps and reports.

Conflicts of Interest: The authors announce that they do not have any conflict of interest.

References

1. Adelle, C.; Weiland, S. Policy assessment: The state of the art. *Impact Assess. Proj. Apprais.* **2012**, *30*, 25–33. [CrossRef]
2. Malmir, M.; Zarkesh, M.M.K.; Monavari, S.M.; Jozi, S.A.; Sharifi, E. Analysis of land suitability for urban development in Ahwaz County in southwestern Iran using fuzzy logic and analytic network process (ANP). *Environ. Monit. Assess.* **2016**, *188*, 447. [CrossRef] [PubMed]
3. Bond, A.; Morrison-Saunders, A.; Pope, J. Sustainability assessment: The state of the art. *Impact Assess. Proj. Apprais.* **2012**, *30*, 53–62. [CrossRef]
4. Yalew, S.G.; Van Griensven, A.; Van der Zaag, P. AgriSuit: A web-based GIS-MCDA framework for agricultural land suitability evaluation. *Comput. Electron. Agric.* **2016**, *128*, 1–8. [CrossRef]
5. Sonneveld, M.P.W.; Hack-ten Broeke, M.J.D.; Van Diepen, C.A.; Boogaard, H.L. Thirty Years of Systematic Land Evaluation in the Netherlands. *Geoderma* **2010**, *156*, 84–92. [CrossRef]
6. Elsheik, A.R.; Ahmad, N.; Shariff, A.; Balasundra, S.; Yahaya, S. An Agricultural Investment Map Based on Geographic Information System and Multi-Criteria Method. *J. Appl. Sci.* **2010**, *10*, 1596–1602. [CrossRef]
7. Pan, G.; Pan, J. Research in crop land suitability analysis based on GIS. *Comput. Comput. Technol. Agric.* **2012**, *5*, 314–325. [CrossRef]
8. Shukla, A.; Kumar, V.; Jain, K. Site suitability evaluation for urban development using remote sensing, GIS and analytic hierarchy process (AHP). In Proceedings of the International Conference on Computer Vision and Image Processing, Roorkee, India, 9–12 September 2017; Springer Science: Singapore, 2017.
9. Nengroo, Z.A.; Bhat, M.S.; Kuchay, N.A. Measuring urban sprawl of Srinagar City, Jammu and Kashmir, India. *J. Urban Manag.* **2017**, *6*, 45–55. [CrossRef]
10. Keesstra, S.D.; Bouma, J.; Wallinga, J.; Tittonell, P.; Smith, P.; Bardgett, R.D. The significance of soils and soil science towards realization of the United Nations Sustainable Development Goals. *Soil* **2016**, *2*, 111–128. [CrossRef]
11. Keesstra, S.; Mol, G.; de Leeuw, J.; Okx, J.; de Cleen, M.; Visser, S. Soil-related sustainable development goals: Four concepts to make land degradation neutrality and restoration work. *Land* **2018**, *7*, 133. [CrossRef]
12. Keesstra, S.; Sannigrahi, S.; López-Vicente, M.; Pulido, M.; Novara, A.; Visser, S.; Kalantari, Z. The role of soils in regulation and provision of blue and green water. *Philos. Trans. R. Soc. B* **2021**, *376*, 20200175. [CrossRef] [PubMed]
13. Keesstra, S.; Veraart, J.; Verhagen, J.; Visser, S.; Kragt, M.; Linderhof, V.; Groot, A. Nature-Based Solutions as Building Blocks for the Transition towards Sustainable Climate-Resilient Food Systems. *Sustainability* **2023**, *15*, 4475. [CrossRef]
14. Van Lier, H. The role of land use planning in sustainable rural systems. *Landsc. Urban Plan.* **1998**, *41*, 83–91. [CrossRef]
15. Masoudi, M.; Jokar, P.; Sadeghi, M. Land use planning using a quantitative model and geographic information system (GIS) in Darab County, Iran. *J. Mater. Environ. Sci.* **2017**, *8*, 2975–2985.
16. Jahantigh, H.R.; Masoudi, M.; Jokar, P. A quantitative approach to land use planning using GIS—A case study of Chabahar County, Iran. *Eur. J. Environ. Sci.* **2019**, *9*, 12–20. [CrossRef]
17. Masoudi, M.; Jokar, P. Development of a Quantitative Model in Land Use Planning Using GIS—A Case Study of Zarrin Dasht County, Iran. *Region* **2022**, *9*, 183–199. [CrossRef]
18. Taylor, J.C.; Wood, J.A.; Thomas, G. Mapping Yield Potential with Remote Sensing. *Précision Agric.* **1997**, *1*, 713–720.
19. Mapedza, E.; Wright, J.; Fawcett, R. An Investigation of Land Cover Change in Mafungautsi Forest, Zimbabwe, Using GIS and Participatory Mapping. *Appl. Geogr.* **2003**, *23*, 1–21. [CrossRef]
20. Pan, T.; Zhang, Y.; Su, F.; Lyne, V.; Cheng, F.; Xiao, H. Practical efficient regional land-use planning using constrained multi-objective genetic algorithm optimization. *ISPRS Int. J. Geo-Inf.* **2021**, *10*, 100. [CrossRef]
21. Malczewski, J. GIS-Based Land-Use Suitability Analysis: A Critical Overview. *Prog. Plan.* **2004**, *62*, 3–65. [CrossRef]
22. Froja, N. Fuzzy-GIS Development of Land Evaluation System for Agricultural Production in North West Libya. Ph.D. Thesis, Heriot-Watt University, Edinburgh, UK, 2013.
23. Masoudi, M. *Land Use Planning Using Computer*; Payam Noor University Publisher: Tehran, Iran, 2018.
24. Yohannes, H.; Soromessa, T. Land suitability assessment for major crops by using GIS-based multi-criteria approach in Andit Tid watershed, Ethiopia. *Cogent Food Agric.* **2018**, *4*, 147048. [CrossRef]
25. Jokar, P.; Masoudi, M.; Karimi, F. An MCE-based innovative approach to evaluating ecotourism suitability using GIS. *Cuad. Investig. Geogr.* **2021**, *47*, 545–556. [CrossRef]
26. McHarg, I.L. *Design with Nature*; Wiley: New York, NY, USA, 1969; 208p.
27. O'Neill, R.V. Perspectives in Hierarchy and Scale. In *Perspectives in Ecological Theory*; Rougharden, J., May, R.M., Levin, S.A., Eds.; Princeton University Press: Princeton, NJ, USA, 1989; pp. 140–156.

28. Mitra, D.; Ilangovan, D. Site Selection for Harbour Facilities in the Gulf of Cambay, India Using Geographic Information System. *Asian J. Geoinform.* **2004**, *4*, 81–86.
29. Lahmian, R. The use of geographical information system in identifying suitable locations for planting plants at risk of north of Iran. *J. Curr. Res. Sci.* **2016**, *4*, 27–30.
30. Pourkhabbaz, H.R.; Javanmardi, S.; Faraji Sabokbar, H.A. Suitability Analysis for Determining Potential Agricultural Land Use by the Multi-Criteria Decision Making Models SAW and VIKOR-AHP (Case study: Takestan-Qazvin Plain). *J. Agric. Sci. Technol.* **2014**, *16*, 1005–1016.
31. Parry, J.A.; Ganaie, S.A.; Sultan Bhat, M. GIS based land suitability analysis using AHP model for urban services planning in Srinagar and Jammu urban centers of J&K, India. *J. Urban Manag.* **2018**, *7*, 46–56. [CrossRef]
32. Khosravani, M.; Moemenbellah-Fard, M.; Sharafi, M.; Rafat-Panah, A. Epidemiologic profile of oriental sore caused by Leishmania parasites in a new endemic focus of cutaneous leishmaniasis, southern Iran. *J Parasit Dis.* **2014**, *40*, 1077–1081. [CrossRef]
33. Makhdoum, M. *Principles of Land Use Planning*; University of Tehran: Tehran, Iran, 2006; 289p.
34. Makhdoum, M.; Darvishsefat, A.; Jafarzadeh, H.; Makhdom, A. *Environmental Evaluation and Planning by Geographic Information System*; University of Tehran: Tehran, Iran, 2009; 304p.
35. Fallah Shamsi, S.R. Accuracy Assessment of Satellite Based Maps Using Sampling. Master's Thesis, University of Tehran, Tehran, Iran, 1997.
36. Congalton, R.G. A Review of Assessing the Accuracy of Classifications of Remotely Sensed Data. *Remote Sens. Environ.* **1991**, *37*, 35–46. [CrossRef]
37. Monavari, S.M.; Shariat, S.M.; Dashti, S.; Sabz Qobaei, G. Assessment of the environmental potential of Zakhard watershed for urban development using GIS. *Environ. Sci. Technol.* **2008**, *1*, 199–208.
38. FAO. *A Framework for Land Evaluation*; Soils Bulletin 32; Soil Resources Development and Conservation Service Land and Water Development Division: Rome, Italy, 1976; 87p.
39. Davidson, D.A.; Theocharopoulos, S.P.; Bloksma, R.J. A land evaluation project in Greece using GIS and based on Boolean and Fuzzy set methodologies. *Int. J. Geogr. Inf. Syst.* **1994**, *8*, 369–384. [CrossRef]
40. Baja, S.; Chapman, D.M.; Dragovich, D. A conceptual model for defining and assessing land management units using a Fuzzy modeling approach in GIS Environment. *Environ. Manag.* **2006**, *29*, 647–661. [CrossRef] [PubMed]
41. Najafinejad, A.; Pishdad Suleimanabad, L.; Salman Mahini, A. Comparison of the efficiency of two system methods and multi-factor land allocation in the process of land surveying using geographic information system. *J. Remote Sens. GIS Nat. Resour. Sci.* **2013**, *14*, 1–11.
42. Elaalem, M.; Comber, A.; Fisher, P. Land Suitability Analysis comparing Boolean logic with fuzzy analytic hierarchy process. In Proceedings of the Accuracy 2010 Symposium, Leicester, UK, 20–23 July 2010; pp. 245–247.
43. Masoudi, M.; Asrari, E.; Razaghi, S.; Karimi, F.; Cerdà, A. A new proposed model of EMOLUP for assessing of ecological capability of different utilizations and land use planning in Sepidan Township, Iran. *Cuad. Investig. Geográfica* **2023**, *49*. [CrossRef]
44. Saaty, T.L.; Vargas, L.G. *Models, Methods, Concepts and Applications of the Analytic Hierarchy Process*; International Series in Operations Research and Management Sciences; Kluwer Academic Publisher: New York, NY, USA, 2001.
45. Everest, T.; Sungur, A.; Özcan, H. Determination of agricultural land suitability with a multiple-criteria decision-making method in Northwestern Turkey. *Int. J. Environ. Sci. Technol.* **2021**, *18*, 1073–1088. [CrossRef]
46. Zhang, S.; Liu, X.; Wang, X.; Gao, Y. Evaluation of coffee ecological adaptability using Fuzzy, AHP, and GIS in Yunnan Province, China. *Arab. J. Geosci.* **2021**, *14*, 1366. [CrossRef]
47. Asadifard, E. Landuse Planning in Firuzabad Township Based on Modifying Method of Current Model Using GIS. Master's Thesis, Shiraz University, Shiraz, Iran, 2015.
48. Razaghi, S. Assessment and Comparison of Land Use Planning in Sepidan Region Using Models of Makhdom, MCE and EMOLUP. Master's Thesis, Shiraz University, Shiraz, Iran, 2016.
49. Jokar, P.; Masoudi, M.; Pradhan, B. A New Spatial Model for Ecological Suitability Assessment of Irrigated Farming in Jahrom County, Iran. *Rev. Caatinga* **2023**, *36*, 177–188. [CrossRef]

land

MDPI

Article

The Foundational Components of Self-Regulating (Sustainable) Economies and Ecosystems: Implications for Green Infrastructure and Economic Restoration

John H. Giordanengo

Economic Restoration Services, Fort Collins, CO 80521, USA; john@economicrestoration.org

Abstract: The current global economic system undermines sustainability efforts such as green infrastructure and circularity, while jeopardizing social and environmental values in rich and poor countries alike. These chronic failures stem in part from a poor understanding of an economy's structure. While many scientists view economic and ecological systems as homologous to one another (i.e., similar structures and processes), an understanding of the foundational components of these systems is lacking. A primary objective of this paper is to refine the understanding of those foundational components, and their interactions. Dozens of ecological processes have functional equivalents in economies, such as succession, evolution, symbiosis, and competition. The central hypothesis here is that three components—diversity, energy, and trade (i.e., resource transfers)—constitute the foundational components of self-regulating economies and ecosystems. A secondary hypothesis is that the interaction of these components regionally, rather than at a global scale, is a limiting factor to the long-term success of sustainability elements such as circularity, green infrastructure, and others. This article evaluates diversity, energy, and trade relative to measures such as net productivity, stability, resource-use efficiency, and biomass (i.e., capital) accumulation. In closing, the concept of economic restoration is summarized, as informed by principles of ecological restoration.

Keywords: complexity theory; sustainability; green infrastructure; restoration; resilience; self-reliance; energy neutrality; endogenous economy

1. Introduction

At the onset of the 2007 great recession, Simon Johnson of MIT faced a conference of American economists and criticized the failure of existing economic models [1]. In the process, he called upon a powerful analogy: significant progress in health and sanitation came only after society had discovered the structure and inner workings of the human body, and the nature of diseases that threaten it. We lack an equivalent understanding of our economies. As capitalism has grown into a truly global system, monumental efforts have been waged by dozens of nations, and countless individuals and organizations, aiming to resolve our most important social, environmental, and economic challenges. Yet one-quarter of the world's population still suffers moderate to severe food insecurity [2], soil fertility continues declining in essential food-growing regions [3–5], 70% of nations dispose of over half of their waste into landfills [6], 89% of the world's energy consumption is non-renewable [7,8], social justice remains challenged, etc. Considering the lack of sustained social and environmental progress over the past 100 years of global market expansion, we must question if important social and environmental problems can be overcome without first resolving the economic flaws responsible for their creation.

Dozens of ecological phenomena have functional equivalents in economies, such as competition, succession, symbiosis, and evolution, while innumerable components exist in both systems. This paper, though, explores the foundational components common to ecosystems and economies. *Foundational components*, as defined herein, are those capable of producing the greatest change from the slightest shifts, and are most responsible for maintaining the self-regulating nature of the system. To be considered foundational, a component must function similarly in two or more homologous systems.

The objectives of this article are to define the foundational components of self-regulating (i.e., sustainable) economies, and to examine the basic processes of economic restoration, as inferred by ecological restoration. The terms self-regulating and sustainable are used interchangeably herein, for a self-regulating economy cannot persist with activities that degrade the social and environmental resources it requires for survival. Several hypotheses are provided later, related to the boundary conditions of a sustainable economy, and the interrelationship between diversity, energy, and trade.

1.1. Ecosystems and Economies as Homologous Self-Regulating Systems

In studying the structure and functioning of self-regulating systems (e.g., human beings), such as developing a vaccine for polio, it is common to observe treatment responses in homologous systems (e.g., monkeys). Herein, economies and ecosystems are considered homologs; self-regulating systems with very high levels of complexity. A *self-regulating system* is one capable of maintaining key functions and processes in the absence of intervention (i.e., instructions) from beyond the system boundary.

Self-regulating systems exist from cells to ecosystems, where innumerable species and individuals form a web of interconnections to ensure the system's survival in the face of disturbance. For instance, roots in a forest form networks with fungi to facilitate information sharing between trees, so the forest may respond pre-emptively to an external threat such as an insect outbreak [9]. Just as self-regulating ecosystems exist via the free (i.e., unregulated) interactions between consumers, producers, and decomposers, self-regulating economies exist via the unregulated interactions between businesses and consumers across all levels of production and consumption. Systems thinking is one means to examining and understanding these complex homologs.

Systems thinking is a branch of science aimed at understanding the structures and interactions of components within living and non-living systems [10–12]. These structures, and the interactions of components, can be reflected in a system's emergent properties, such as an ecosystem's ability to maintain a *dynamic equilibrium*: a relatively steady state in the presence of outside forces [13,14]. In contrast, many modern economies require constant manipulation of policies and laws, subsidies, bailouts, and other actions to maintain a relatively steady state (i.e., stability), achieve acceptable levels of productivity, and social and environmental assets, and provide other benefits in the face of external forces. That is, these economies are not operating as self-regulating systems, and may in fact be trending toward a state of instability.

Recent examples of instability under the current global economic structure include the 2020 social justice riots in the U.S., followed by the attack on the U.S. capital; the economic collapse in Sri Lanka in 2019–2022; Argentina's economic crisis of 2023; the global economic turmoil following the Russia–Ukraine conflict of the 2022–present day; the Israel–Hamas conflict of 2023; the mass exodus of migrants from developing to developed countries; eleven unemployment spikes (i.e., >6%) in the U.S. since 1950; and the unprecedented rise in cost of living globally. Meanwhile, great degrees of wealth have become concentrated into fewer hands [15], a condition some believe threatens rather than ensures a steady state [16,17].

1.2. The Structure of Sustainable (Self-Regulating) Economies

Classic definitions of sustainability focus on efforts that improve social, environmental, and economic (i.e., industrial) conditions. This can include the recent circularity efforts, with goals such as zero waste and 100% renewable energy. However, an understanding of an economic structure that would naturally support sustainability, circularity, and related goals is lacking.

The term *highly functional* is used herein to describe an economy that can sustain the production and distribution of goods and services, without jeopardizing the social and environmental assets upon which it relies. This includes desired economic benefits such as relatively stable employment, profitability, adequate real wages, and the ability to meet basic consumer needs in the face of disturbances. That is, a highly functional economy is relatively stable, a function of resistance and resilience [18,19]. Understanding the structure of a highly functional economic system, though, requires us to look beyond unimportant details [20], such as the system's context. That context includes capital management systems such as capitalism, often blamed for poorly functioning economies. However, great resource inefficiencies, and degradation of social and environmental assets, have arisen in capitalist, socialist, and communist systems alike, suggesting that a country's capital management system is not a prerequisite to a highly functional economy. A peculiar phenomenon, though, has arisen over the evolution of global market capitalism. With each novel system, the duration of each new system has shortened (Table 1). Throughout this evolution, abundant social and environmental challenges have persisted, while the actual structure of the economic system has remained obscured.

Table 1. Epochs of capitalism. Data from Arrighi [21] and Braudel [22], with duration indicating years between signal crises. Signal crises occur in periods of comparatively stable governance.

Epoch of Capitalism	Dominant State	Approximate Time Period (AD)	Duration (Years)
Mercantile	City-states of Northern Italy (Genoa)	1340–1560	220
Mercantile	Dutch	1560–1740	180
Classical	Great Britain	1740–1870	130
Classical	United States	1870–1930	60
Keynesian	United States	1940–1970	30
Global Market	?	1970–?	?

1.2.1. Chronic Social and Environmental Challenges of the Current Economic Structure

The current epoch of global market capitalism (GMC) allows for levels of resource consumption exceeding any previous epoch, corresponding with a litany of social and environmental degradation [16,23–25]. Degradation occurs in direct forms such as social and environmental impacts, and indirect forms such as supply chain inefficiencies, where small shifts in demand can produce an increasing magnitude of interruptions for manufacturing and extractive industries at the opposite end [20].

As supply chains lengthen, or as the number of entities (i.e., links) in the chain increase, inefficiencies arise with rising uncertainty and risk for producers and consumers. To buffer against risks, producers and distributors accumulate *safety stock*, generating and storing more products than what consumers demand. Safety stock translates not only to increased financial costs of production, but increased energy and material waste. For instance, when short-lived goods (e.g., bananas and fast fashion) become safety stock, much of the stock becomes unsalable before reaching customers, leading to physical, energy, and financial waste. Another example of supply chain inefficiency is U.S. consumers who purchase food originating from an average of 1500 miles away [26], sixteen million tons of which are wasted annually [27]. Hawaii is a notable example, which ships cattle 2000 miles to the mainland for processing. The preferred shipping method is cargo planes [28], one of the least energy-efficient means of transportation [29].

Uncertainty aside, consumers at the end of long supply chains often underestimate the unintended social and environmental impacts of production and extraction at the other end (i.e., externalities). Classic examples include water pollution caused by paper manufacturing, or fertilizer run-off from industrial-scale agriculture. In 2023, a train derailment in Ohio (U.S.A.) caused an unprecedented vinyl chloride spill, an externality related to PVC pipe consumption [30]. Species extinction is another chronic externality, the leading cause being economic activity [31].

Corporate or national systems intended to improve social, economic, and environmental conditions, yet lack persistence, and thus are intrinsically unsustainable. A few examples are provided here. Victoria's Secret's corporate sustainability commitment states "We strongly believe that the quality of our merchandise begins with the treatment of the people who create our products [32]". However, during Sri Lanka's recent economic collapse, Victoria's Secret asked Sri Lanka's largest textile supplier, Mass Holdings, to shift production to their Bangladesh facility (a lower labor market), or cut costs in their Sri Lanka facilities by 30% [33]. In Germany, decades of work to reduce their carbon footprint was threatened when the country took steps to bring coal-powered plants back on-line [34]. In the U.S., decades of environmental protections were undone by a 2020 presidential signature, then partially restored by a 2022 presidential signature, and weakened again by the supreme court in 2023. Despite significant agriculture advancements in the 20th century, 33 million acres of the U.S. Corn Belt have zero topsoil remaining [35]. These persistent externalities, I posit, stem not from the form of capital management system (e.g., capitalism, socialism, or communism), but from the structure of one's economic model.

1.2.2. Economic Structure as a Function of Foundational Components and Context

Past research has indicated that the structure of an economy or ecosystem is defined by only energy flows [36–38]. While energy is certainly essential to the structure and functioning of economies and ecosystems, the central hypothesis here is that three foundational components—diversity, energy, and trade (i.e., resource transfers)—comprise the core structure of economies and ecosystems. These components form predictable interactions with one another, while being connected via feedback loops with an economy's social-environmental-industrial (SEI) context. An economy's *social context* includes its cultural values, models of governance, desired levels of productivity, etc. Its *environmental context* includes soil fertility, precipitation, the quality of natural resources, etc. Whilst, its *industrial context* includes technology, the quantity and connectivity of trade centers, infrastructure, etc. The full structure of an economy is defined herein as the balance of its foundational components—diversity, energy, and trade—in relation to the SEI context in which they exist (Figure 1).

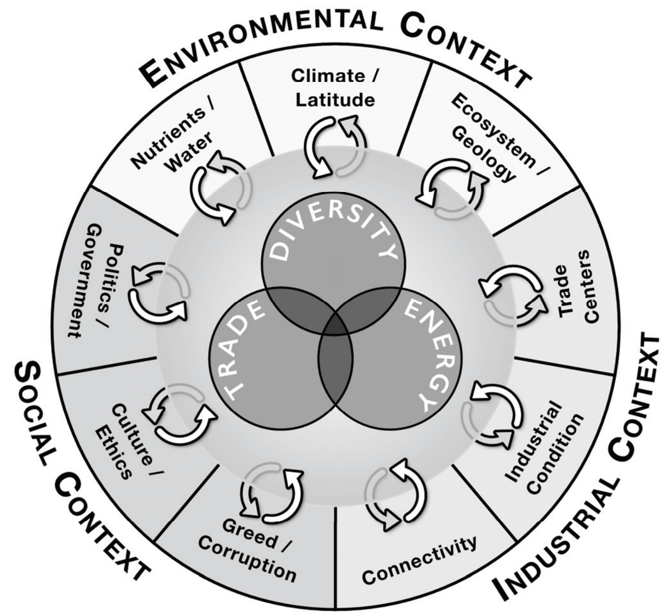

Figure 1. The structure of an economy consists of its foundational components—diversity, energy, and trade—and its context. A few contextual factors are pictured in the outer ring, with chasing arrows indicating feedback loops with the system's foundational components.

One's SEI context may be manipulated to the benefit of humans, their economies, and the environments in which they exist. The Llanos region of Colombia is one example, where human ingenuity (social context) has increased economic productivity and diversity [39].

Another example is Salinas de Guaranda, Ecuador, whose social and industrial context has been managed since the 1970s to increase the productive capacity and diversity of a high-elevation Andean economy [40,41].

1.3. Relationships between Productivity Measures and Sustainability

Relationships between economic productivity measures and sustainability are indirect but meaningful. Gross domestic product (GDP), for instance, does not account for the degradation of social and environmental conditions that result from production and extraction processes. Two productivity measures that do provide a more realistic account of system degradation, due to their positive correlation with resource-use efficiency, are productive capacity and *net* domestic production. A nation's *productive capacity* reflects its ability to produce goods and services in the future, and that capacity increases when inputs are used more efficiently (e.g., a bushel of wheat produced with less nitrogen). Such efficiencies are gained via the skill of labor, technology, political and economic stability, and other factors.

A nation's *net domestic production* (NDP) also rises with energy- and materials-use efficiency. Akin to net primary production in ecosystems, an economy's NDP accounts for system maintenance, such as the depreciation of factories, roads, and other assets. However, traditional NDP measures often fail to account for the degradation of natural resources that accompany production processes, hence NDP overestimates productivity. For example, restoring the 33 million acres of degraded farmland topsoil in the U.S. Corn Belt is estimated at U.S. $1.2 trillion [42]. That expense was unaccounted for in the years that farm outputs contributed to GDP. To more fully account for system maintenance, a measure of *real NDP* is provided here: economic productivity after accounting for the depreciation of capital assets, social assets, and ecological assets. NDP used herein represents this definition.

Indirect measures of NDP, such as valuing ecosystem services (e.g., clean water from a forested watershed), attempt to reflect the environmental costs of production. A challenge with many ecosystem service models is that they do not reflect natural supply–demand dynamics. Instead, they rely on hypothetical markets to quantify the value of services such as clean water, or the value of a species, etc. [43,44].

Real NDP must also account for the quantity of energy consumed in support of an economy's per capita productivity (Table 2). This measure reflects an economy's ability to maintain per capita productivity in a future of limited and/or uncertain energy supplies. From this measure, Iceland ranks 2nd, Italy ranks 40th, and the U.S.A. ranks 65th. Confounding variables certainly affect a nation's per capita GDP on a unit energy basis. For instance, Luxemburg has a sizable private banking industry, and Iceland harbors large supplies of geothermal energy, relative to their populations.

Table 2. Per capita GDP on a unit energy basis. A partial list of countries is presented. Energy consumption data are available for 72 countries.

Rank	Country	Per Capita GDP on Unit Energy Basis *	GDP per Capita (USD)	GDP 2021 (Billion USD)	Population 2021	Avg Energy Consumption **
1	Luxembourg	37,108	$133,590.15	$85.51	640,064	3.6
2	Iceland	13,746	$68,727.64	$25.60	372,520	5.0
3	Cyprus	8782	$22,832.46	$28.41	1,244,188	2.6
4	Ireland	6678	$100,172.16	$504.18	5,033,165	15.0
5	Latvia	5874	$21,148.16	$39.85	1,884,490	3.6
6	Estonia	4902	$27,943.70	$37.19	1,330,932	5.7
7	Slovenia	4577	$29,291.40	$61.75	2,108,079	6.4
8	Denmark	4250	$68,007.71	$398.30	5,856,733	16.0
9	Lithuania	3954	$23,723.34	$66.45	2,800,839	6.0
10	Switzerland	3593	$91,991.58	$800.64	8,703,405	25.6

Table 2. *Cont.*

Rank	Country	Per Capita GDP on Unit Energy Basis *	GDP per Capita (USD)	GDP 2021 (Billion USD)	Population 2021	Avg Energy Consumption **
12	New Zealand	2439	$48,781.09	$249.89	5,122,600	20.0
13	Norway	2286	$89,154.30	$482.18	5,408,320	39.0
16	Finland	1937	$53,654.77	$297.30	5,541,017	27.7
19	Sweden	1212	$61,028.76	$635.66	10,415,811	50.3
20	Portugal	1135	$24,567.50	$253.66	10,325,147	21.6
22	Singapore	881	$72,794.02	$396.99	5,453,566	82.6
23	Belgium	844	$51,247.00	$594.10	11,592,952	60.7
24	Greece	804	$20,192.61	$214.87	10,641,221	25.1
26	Netherlands	754	$57,768.06	$1012.85	17,533,044	76.6
30	United Arab Emirates	509	$44,315.60	$415.02	9,365,145	87.1
31	Australia	464	$60,443.21	$1552.67	25,688,079	130.3
32	Sri Lanka	441	$4013.69	$88.93	22,156,000	9.1
36	Ecuador	328	$5965.14	$106.17	17,797,737	18.2
37	United Kingdom	284	$46,510.32	$3131.38	67,326,569	163.6
39	Spain	243	$30,103.50	$1427.38	47,415,750	123.8
40	Italy	239	$35,657.45	$2107.70	59,109,668	149.4
42	France	190	$43,658.98	$2957.88	67,749,632	229.8
43	Germany	174	$51,203.50	$4259.93	83,196,078	293.8
46	Canada	167	$51,988.03	$1988.34	38,246,108	310.8
49	Argentina	134	$10,636.11	$487.23	45,808,747	79.2
50	Malaysia	119	$11,109.26	$372.98	33,573,874	93.7
51	South Korea	117	$34,997.86	$1810.96	51,744,876	300.3
53	Japan	95	$39,312.68	$4940.88	125,681,593	412.0
55	Philippines	74	$3460.53	$394.09	113,880,328	46.9
57	Bangladesh	62	$2457.93	$416.27	169,356,251	39.5
58	Mexico	61	$10,045.69	$1272.84	126,705,138	164.7
62	Ukraine	54	$4568.92	$200.09	43,792,855	84.9
64	Vietnam	36	$3756.49	$366.14	97,468,029	103.2
65	United States	32	$70,248.69	$23,315.10	331,893,745	2172.0
66	Brazil	25	$7507.15	$1608.98	214,326,223	304.2
67	Indonesia	20	$4332.70	$1186.09	273,753,191	212.0
68	Russia	17	$12,400.06	$1778.78	143,449,286	747.5
71	China	3	$12,556.36	$17,734.10	1,412,360,000	3708.6
72	India	3	$2256.59	$3176.30	1,407,563,842	886.6

* Data from World Bank, Enerdata, and BP. Energy in Mtoe. GDP in USD (production approach); ** Average of Enerdata and BP data, in Mtoe.

2. Materials and Methods

Evaluating concepts such as the foundational components of highly complex economies, or the basic operational unit of an economy (i.e., boundary conditions) requires methods other than traditional hypothesis testing. The methods herein are drawn from systems thinking, in which theoretical concepts are used to explain and predict natural phenomena [45]. This includes general systems theory, which explores concepts such as system boundaries and self-organization. For these reasons, an interpretive review was used, including the extraction and synthesis of data from selected studies.

Data were evaluated using a crosscutting approach, where the reviewer evaluates systemic patterns between two homologous systems [46]. Similar methods are used in homologs such as monkeys and humans. For instance, Rhesus Macaque (*Macaca mulatta*) was the homolog used to develop the polio vaccine for *Homo sapiens* [47]. Herein, economies and ecosystems are presumed homologous, across which several classes of information were compared: system subcomponents, theories, principles, processes, material and energy flows, concepts, functions, and other factors. Data from aquatic systems were excluded, as they differ fundamentally from terrestrial systems via energy flow and trophic pathways [48]. To understand the relationship between energy and biological diversity, this paper focused on a form of plant-available energy reported widely in the literature, which can be transferred across trophic levels: nitrogen, an energy metabolite from which glucose and other energy compounds are formed.

The interpretive review of ecological and economic literature included semantic scholar, PrimoSearch (i.e., a network of over 400 databases across economic and ecological disciplines), Econ Papers (https://econpapers.repec.org, accessed on 28 June 2023), and others. Relevant texts from prominent economists (e.g., David Ricardo, Adam Smith, Karl Marx, John Maynard Keynes, Alan Greenspan, Joseph Schumpeter, Milton Friedman, Joseph Stiglitz, Thomas Piketty, and Herman Daly), and from the career works of ecologists and evolutionary biologists, were also evaluated.

3. Results and Discussion

Abundant literature exists on the interactions between energy and ecological diversity. However, little research exists on the interactions between energy and economic diversity, or trade and economic diversity. From this integrative review, three foundational components appear to exist in both ecosystems and economies, forming equivalent interactions regardless of the context in which they occur: diversity, energy, and trade. These components, and their interactions, are summarized below, with more detail in Giordanengo [42]. Due to the natural interactions between diversity, energy, and trade, each section below will integrate some relevant information from other foundational components as appropriate.

3.1. Diversity, and Its Influence on Ecological and Economic Systems

Biological diversity has many aspects, including the quantity and distribution of species within a habitat, and the variety of habitats in an ecosystem. *Economic diversity* defined herein is simply the quantity and distribution of businesses within an economy. Economic diversity is evaluated here in terms of the economic and environmental benefits it imparts, drawing upon equivalent benefits in ecosystems. For example, ecosystems with greater plant diversity are capable of harnessing more energy from a given environment, and generating higher net productivity, compared to less diverse systems [19,36,37,49–54]. Diverse plant communities not only support a high diversity of insects, for instance, but a greater biomass of insects [55–57], from which a greater abundance of insectivores may be sustained, etc.

Research on the relationship between economic diversity and energy is sparse. Paul Templet compared national economic diversity data with the annual energy throughput of twelve countries, concluding that a positive correlation exists between economic diversity and energy-use efficiency [58]. One example of the diversity–efficiency relationship is the excess waste heat and other byproducts generated by lumber mills, which may be used to warm nearby buildings or generate biomethanol. In one Alaska (U.S.A.) community, the energy gained from a nearby mill's waste heat saved an estimated U.S. $91,500 per year [59]. At a mill in Bellemont, Arizona (U.S.A.), selective logging and milling operations produce five residual products for regional consumers, including two forms of biomass fuel [60], in part supplying Novo Power, a 27 MW biomass powerplant in northern Arizona. These specific efficiencies do not occur in an economy without a mill.

Waste heat is produced by all manufacturing and resource extraction industries. Hence, economies lacking those industries (i.e., consumption needs are met with goods extracted or manufactured outside the economy) forgo a significant form of waste heat to offset aggregate energy consumption. In the U.S., over 1500 trillion BTUs of waste heat are available for recovery from manufacturing and mining industries annually [61]. As heating the average U.S. home consumes 75,000 BTUs of energy annually, about 20 billion homes could be supplied by industrial waste heat—more homes than exist on earth. However, under the current global economic structure, industrial activities associated with U.S. consumption are concentrated in relatively few and homogenized economic spaces across the globe (i.e., diversity and trade components), often requiring exogenous energy inputs (energy component) into those spaces. Additional exogenous energy is consumed to ship manufactured goods (trade and energy components) into economies with low diversity in their manufacturing and resource extraction sectors.

In ecosystems and economies, more diverse systems are not only more energy efficient, but also more stable than low-diversity systems [62–70]. While energy efficiency and stability are directly related to high NDP and productive capacity, the relationship between diversity and NDP is less direct. Diversity in an economy promotes innovation, via knowledge and technology spillovers across sectors [71,72]. Innovation has long been recognized as a key mechanism in productivity gains, which stimulates economic growth [73].

Some economic research does show a positive correlation between diversity and economic productivity [58,74], though further research is needed. In ecosystems, a positive correlation between diversity and productivity is well known, summarized by the intermediate disturbance hypothesis [75], and to be discussed later. In economics, confounding variables in the diversity–productivity relationship arise when studies account for gross productivity, not NDP, or when they are limited in their temporal and spatial analysis, fail to use per capita GDP on a unit energy basis, or compare results across varying SEI contexts, each with a unique productive potential. A more fundamental concern is a lack of accounting for the multiple forms of diversity that exist in economies and ecosystems. Eight forms of economic diversity are described in Giordanengo [42], of which seven with functional equivalents in ecosystems. Five are described here.

3.1.1. Richness and Evenness

One of the most basic measures of biodiversity is the number of species present in an area, what ecologists refer to as *species richness*. When richness is evaluated in conjunction with the relative "dominance" of each species in the system (i.e., *evenness*), a measure of *species diversity* is provided. For instance, a meadow with a hundred species of plants is more *diverse* than a meadow with ten, assuming each species contributes equally to the biomass (i.e., capital) of the system. Species diversity is quantified by Shannon's Diversity Index [76] and other indices. Similar indices are used to measure economic diversity, only with businesses taking the place of species.

3.1.2. Functional Diversity

Every species is part of a functional group, such as producers (e.g., plants), consumers (e.g., herbivores), or decomposers (e.g., fungi), referred to as *trophic levels* in ecology. *Functional Diversity* is simply a diversity of trophic levels, and is a driver of other forms of diversity [77,78]. Systems with high functional diversity are also capable of producing more total biomass [79], as they contain a greater diversity of food chains.

In an economy, functional diversity increases when it harbors, for instance, a network of farms, mills, retailers, steel manufacturers, high tech, and recycled material processors. Economists simply use different nomenclature than ecologists, such as sectors, industry groups, and industries, in production-based hierarchies like the Nomenclature des Activités Économiques dans la Communauté Européenne (NACE), or the North American Industry Classification System (NAICS). A single-function economy, such as one in which only apples are sold, has very low functional diversity. On the contrary, an economy with a high degree of functional diversity (e.g., many sectors exist) has the potential to increase the diversity of various industry groups, each harboring multiple industries, of which each houses at least one business. In highly complex self-regulating systems, it is uncommon for a given functional group to be represented by just one business, or just one species.

3.1.3. Functional Redundancy

Within a given functional group, such as insectivorous birds, multiple species often exist (e.g., nuthatches, chickadees, and juncos), each contributing to *functional redundancy* within the group. Should the population of one species decline, other species can fill the void. In a review of 423 research articles, Biggs et al. [80] found that higher levels of functional redundancy were correlated with higher levels of ecosystem resilience and stability.

Economies are similarly diversified when multiple businesses exist to, for instance, manufacture or install wind turbines, or when multiple industries exist to generate electricity (e.g., biomethanol, hydro-electric, or solar). Should one industry falter (e.g., solar), other energy systems remain to meet demand. The American auto industry is an example of low functional redundancy. The industry became dominated by just three companies in the 1980s, then collapsed in response to a variety of external forces [81].

3.1.4. Regional Diversity

Biological diversity also exists at a landscape scale [82]—*regional diversity*—when multiple habitat patches exist in an ecological space, each shaped by differences in soils, moisture gradients, and other factors [83,84]. Patches are further diversified by disturbances that allow a variety of successional communities to exist there. Each successional community exhibits a unique species assemblage, reflecting the amount of time since the disturbance occurred (e.g., a fire occurred there 10 years ago) and the severity of the disturbance that occurred (e.g., a low-severity fire). This disturbance–diversity process is documented well by Beever [85], and regional patch diversity is a multiplier of other forms of diversity [86]. Regional diversity also exists in economies that harbor a patchwork of cities, farm communities, centers of wood production or metal recycling, energy production, and various retail centers. Based on the nature of regional diversity in ecosystems, we might expect regional diversity in an economy to be a multiplier of other forms of economic diversity.

Despite the benefits, diversity cannot simply be added to an economy, without considering its interactions with other foundational components. Evidence from economics and ecology indicates, however, that diversity may be stimulated (or suppressed) by the management of trade and energy.

3.2. Relationships between Energy and Diversity

Energy is referred to here in terms of the forms cycled within an ecosystem, such as carbohydrates (i.e., biochemical energy), or an economy, such as solar power, biogas, and coal. Economists refer to these "usable" energy forms as *primary energy*, used in energy balance equations [87]. How energy flows through economies and ecosystems affects system diversity. Diversity, in return, has an impact on energy-use efficiency.

In ecosystems, energy is often studied with respect to its flows through *trophic levels* (i.e., producer and consumer levels in a biomass pyramid). At every trophic level, energy is lost in support of growth and metabolism [37,88]. In the ecological literature [36,53], and limited economic literature [58,89], more diverse systems are reported to capture a greater quantity of energy than less diverse systems. In other words, with a fixed quantity of energy, more diverse systems support a greater level of net productivity.

While research on energy flows in economies is found in the work of Alfred Lotka [90,91], Bruce Hannon [37], Amory Lovins [92], and others, studies on the interaction between energy flows (i.e., exogenous vs. endogenous energy) and economic diversity are absent. In ecosystems, the moment primary producers transform sunlight into biochemical energy, energy becomes endogenous to the system. *Endogenous energy* is defined herein as energy consumed in the same ecological or economic space in which it is produced. To be endogenous, energy must also be produced by extant entities.

Consumers in terrestrial ecosystems obtain nearly 100% of their biochemical energy from endogenous sources. Species in each trophic level (e.g., lion) obtain energy only from the level below (e.g., gazelle), which obtains energy only from primary producers (e.g., plants). The system's biochemical energy is limited by the quantity of incoming solar radiation, which varies across the globe. That is, photosynthetically active radiation (PAR) is part of an ecosystem's environmental context, and does not become endogenous until converted to biochemical energy.

In economies, endogenous energy includes solar-generated electricity, hydropower, biofuels, etc. In contrast to ecosystems, over 80% of the energy in national economies is exogenous, mostly in the form of fossil fuels. *Exogenous energy* is that which is produced in a different place than where it is consumed, or by entities that no longer exist. Fossil fuels are one example, created hundreds of millions of years ago by extinct carboniferous forests, and usually imported into an economy from thousands of miles away. Electricity generated by wind turbines in Wyoming (U.S.A.), and then transported to New York (U.S.A.), is also exogenous to New York's economy. Imported agricultural products (e.g., cattle, grains, and fruits) also represent exogenous energy, in the form of carbohydrates and other embodied energy.

In some cases, exogenous energy can diminish an economy's capacity to produce endogenous energy. Sri Lanka, with very few fossil fuel reserves, has operated as a net energy importer for over 50 years. Today, about 25% of its GDP is expended on imported fossil fuels [93], contributing to high trade imbalance and other financial imbalances [94]. In an interview with Shihan Diddeniya in 2023, I was informed that Sri Lanka has enough renewable energy potential in wind, solar, hydroelectric, and biomass to supply over 100% of its total energy needs [95]. However, following its 2019 economic crash, Sri Lanka's capacity to develop these endogenous energy resources has diminished [96].

The terms exogenous and endogenous apply also to material resources such as protein, steel, and water. For instance, nitrogen is cycled between the atmosphere and the biosphere continuously, but does not become endogenous to an ecosystem until fungi and bacteria convert N_2 into plant-available forms such as ammonium, an energy metabolite [97]. Once assimilated by the biotic system, nitrogen, biochemical energy, and other resources are then available to be cycled across trophic levels within a food web.

3.2.1. Interactions between Exogenous Energy and System Diversity

Regions of earth receiving higher PAR tend to have higher biological diversity, as PAR peaks at the equator and diminishes toward the poles. This includes research by Wright [98] on 24 islands across the globe, noting that larger islands near the equator are richer in plants and birds than those toward the poles. At the surface, this appears to infer a positive correlation between energy and diversity. However, at least two confounding variables must be considered. The diversity gradient from the equator to the poles is more closely related to precipitation patterns than PAR [99]. Second, equatorial ecosystems were minimally impacted by the most recent glaciation events, compared to ecosystems nearer to the poles. The Laurentide ice sheet, for example, eliminated a wide range of plant communities from vast tracts of North America for thousands of years.

PAR is simply part of an economic or ecological context that becomes endogenous energy that can then be transferred across trophic levels within a specific context. Of interest here is the influence of cross-boundary transfers (e.g., between two economies, or between two ecosystems) of primary or biochemical energy on system diversity, regardless of the system's context.

Results from over 190 studies across the globe indicate that transfers of plant-available nitrogen (i.e., an energy metabolite) into an ecosystem are correlated with decreased plant community diversity [100,101]. Though economic studies on the relationship between exogenous energy and diversity are lacking, some trends are evident. Over the past 120 years, an exponential rise in exogenous energy consumption has occurred in the U.S. (Figure 2), a trend seen in many industrialized economies [29]. Diversity data from U.S. agriculture and manufacturing over this same period are presented below.

Agriculture: The 120-year rise in exogenous energy coincides with the extinction of over five million farm businesses [102]. One example comes from Oakdale in northeast Nebraska (U.S.A.), dominated today by corn (Figure 3). In the 1870s, Oakdale's economy exhibited high regional diversity, richness, and functional redundancy: dozens of different crops, barber shops, mercantilists, doctors' offices, manufacturers, etc. [103]. Trees—not children—were growing up through the playground equipment when I visited Oakdale in 2011. In 2020, "no entry" signs were posted at the entrances of schools and churches, and 20% of the population lived in poverty [104].

Besides the social and economic degradation in Oakdale, its homogenous agricultural landscape is more prone to external forces, such as those that produced the Potato Famine [105,106], the U.S. Dust Bowl, the 1970s southern corn leaf blight, etc. Additionally, future climate scenarios predict that the corn belt will experience additional stressors including increased heat stress, higher peak floods, and longer growing seasons [107]. Concurrently, US farmers are expected to experience rising costs of exogenous inputs and declining profitability [108], impairing their ability to address future stressors.

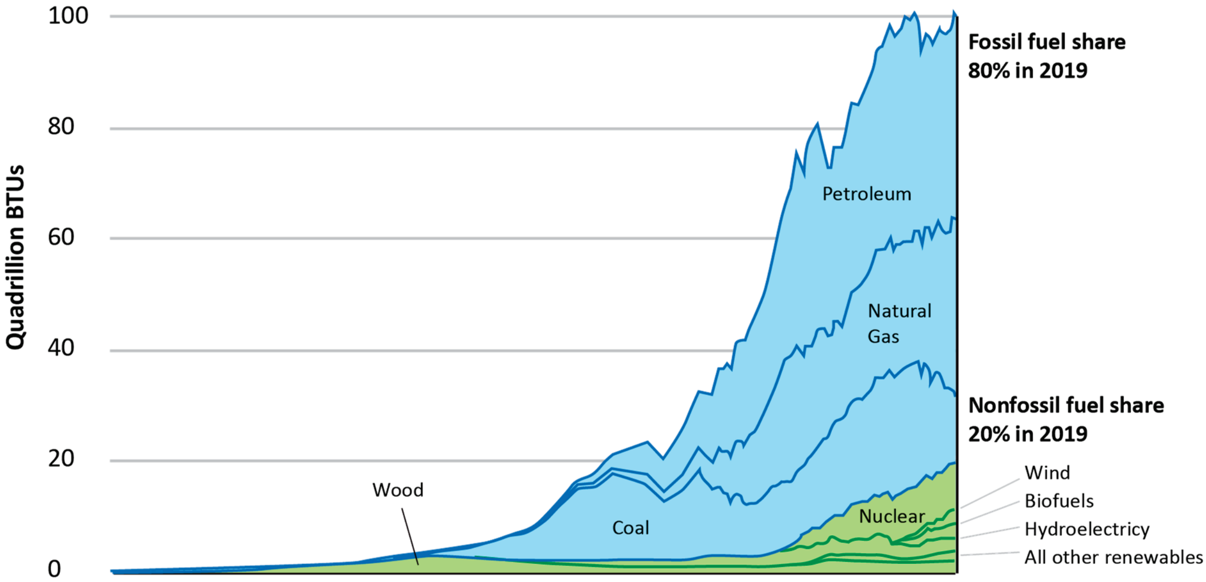

Figure 2. Energy consumption in the United States of America, from 1776 to 2020. Source: EIA, public domain [109].

Figure 3. Monoculture of corn near Oakdale, Nebraska, U.S.A.

Manufacturing: Over one hundred automobile manufacturers existed in the U.S. in the 1920s [110]. By the early 1950s, the consolidation of auto manufacturing around Detroit, MI, made this metropolis one of America's wealthiest cities [111], its prosperity hinging on the success of a single industry. In that same decade, competition began rising from Europe and Asia, while America's involvement in the Korean War redirected steel supplies and labor away from Detroit [112]. By 1980, the U.S. auto industry was dominated by three companies [83], with low richness. By the late 1990s, Detroit was described as the U.S. murder capital, with half of its real estate abandoned.

Other extinctions occurred in U.S. manufacturing in the past 120 years, with the decline in business richness estimated at 70%, on a per capita basis [42]. This amounts to a loss of about 700,000 businesses, including an estimated 318,000 bakeries, over 500 wood and paper mills, 100s of textile mills, and 100s of grain mills.

Though the inaccuracy and incompleteness of historical economics data make statistically robust analyses difficult, a correlation between diversity and exogenous energy does appear likely. For instance, exogenous energy transfers into the U.S. economy remained low between 1849 and 1899, relative to the total energy consumed, and manufacturing diversity climbed from 530 to 672 businesses per 1000 citizens [113]. This increase occurred despite the decade-long global economic recession of the 1890s. As exogenous energy consumption increased between 1900 and 1929, manufacturing diversity declined from 291 to 191 businesses per 1000 citizens. The difference in the magnitude of diversity gains and losses reflects a shift in the definition of "manufacturer" at the turn of the 20th century. The exogenous:endogenous energy ratio has continued rising since the 1930s Great Depression, with commensurate declines in the diversity of manufacturing and agricultural industries.

3.2.2. Challenges in Quantifying Economic Diversity

The lack of historical business diversity data [114] is one challenge to quantifying diversity over time. For instance, non-commercial home bakeries and artisan workshops of the 1800s were unrecorded in U.S. census data. Further, business data collected in the 1800s were biased toward specific industries, or toward urban areas where significant economic activity occurred, therefore underreporting diversity at regional scales. Other complications arise via variations in industrial classification systems over time. NACE did not exist until 1970, and NAICS was not adopted until 1997 [115]. As these classification systems evolved, so did definitions of "industry" and other basic measures.

Diversity measures like Shannon's Diversity Index provide another limitation, as they account for only two aspects of diversity, and suffer some statistical limitations [18,69]. The more recent Economic Complexity Index suffers similar limitations, and accounts for only the diversity of export-based industries [116]. Economic diversity data also ignore regional diversity patterns, and often aggregate data at the county and industry level. As a result, such studies report lower diversity in rural agricultural areas than in metropolitan areas within the same region, and can under-represent functional redundancy and regional diversity. Other limitations include the relatively short periods of economic diversity studies (e.g., 1–3 decades), or they compare regional diversity to a national benchmark, regardless if that benchmark has declined. Complications also arise from the fact that new industries have arisen over time.

3.2.3. Quantifying Net Changes in Economic Diversity

Considering the above limitations, we might ask if *net* economic diversity (i.e., the difference between gains and losses) actually increased in the U.S. over time, not decreased. For instance, thousands of new businesses have emerged in high technology, services, and others over the past century, offsetting diversity losses in manufacturing and agriculture. At the same time, new entrants in high tech (e.g., Google, Amazon, Microsoft) have followed similar diversity patterns as in manufacturing and agricultural: a tendency toward homogenization. The retail industry exhibits similar patterns, as "Big box" stores (e.g., Target, Walmart, Home Depot) have displaced thousands of businesses in some countries, and franchises such as McDonalds (37,000 storefronts globally) produce direct and indirect impacts on diversity. When standards of operation are controlled by a single entity, the tendency is for franchisees—or chains—to source tomatoes, buns, and beef from large homogenized manufacturers, placing downward pressure on diversity in agriculture and food processing. In the U.S., 773,000 franchises exist [117], half of which are in food service.

To gain a fuller understanding of diversity, and to better quantify diversity changes over time, more comprehensive measures are needed. Those measures must integrate not only richness and evenness, but functional redundancy, matrix diversity, and other diversity elements into a value that reflects system-wide diversity.

3.2.4. Relationships between Technology and Economic Diversity

Several other variables were evaluated as possible drivers of economic diversity in Giordanengo [42], including technology, one element of an economy's SEI context. For example, abundant technological advances occurred during the Industrial Revolution, such as steam power, often attributed to the homogenization of manufacturing and agriculture [118]. We might conclude, then, that technology (not energy) was the cause of economic diversity declines in that period. However, steam power was invented six centuries earlier in Greece [119]. Not until great quantities of dense energy were discovered (e.g., coal in England) did the productive potential of steam engines become realized [29,118]. It was the coal-powered steam engine that allowed the industry to manufacture larger and more precise equipment, including high-pressure boilers, a limiting factor to larger steam-powered generators [22,120]. Large-scale generators were essential to the mass production of larger machinery such as tractors and trains, which further stimulated homogenization in affected industries.

Considering the interactions between energy and diversity in both economies and ecosystems, this hypothesis is proposed: exogenous energy transfers into self-regulating ecosystems and economies, causing a reduction in diversity in those systems.

3.3. Trade (i.e., Resource Transfers) in Economies and Ecosystems

In ecosystems, resources such as fat, micronutrients, and protein begin their transfer to higher trophic levels when plants convert sunlight, CO_2, and water into biochemical energy. A notable difference between resource transfers in modern economies and in ecosystems is the origin of resources being cycled through each system. Nearly 100% of the biomass consumed and cycled within an ecosystem is produced within the system—it is endogenous, a product of primary production. In other words, the further one travels from a given habitat patch (e.g., Mediterranean scrub community in Liguria, IT), the less likely they are to encounter energy and other resources from that community. That is, the degree of resource transfers between trophic levels within an ecosystem is far greater than the resource transfers across ecosystem boundaries.

The opposite condition occurs in most modern economies. As one travels from national to local centers of consumption—nation, region, town, or home—they are more likely to encounter resources from other towns, regions, and nations. From U.S. Census Bureau import–export data, about 32% of goods consumed in the U.S. are imported, based on dollar value [42]. However, because most U.S. exports are of high value (e.g., spacecraft, airplanes), relative to imports (e.g., dolls, cookware), the quantity of imported goods is higher than 32%. In most U.S. regions, the percentage of imported goods is estimated at 60%, while many urban areas import closer to 99% of physical goods [42]. Similar trends exist globally, as the portion of global GDP attributed to foreign trade has increased from 36% in 1979 to 60% in 2019 [120]. This coincides with an approximate 100% increase in energy consumption [29].

Historically, economists have partitioned trade into three segments: domestic, foreign, and carrying [121,122]. The domestic economy (i.e., *home trade*) is the transfer of goods and services within a nation, which was the dominant form of trade through the 18th century [123]. *Foreign trade* is the transfer of goods and services across national borders. A limiting factor to foreign trade before the 18th century was fossil fuels, which were needed to increase the efficiency of long-distance transportation [29]. The *carrying trade* (i.e., carry trade) is the most nebulous echelon of global market capitalism, and includes multiple financial mechanisms used to facilitate foreign trade.

Adam Smith posited that the strength of a nation's domestic trade—not its foreign or carrying trade—forms the basis of its wealth [122]. That foundation, he argued, is sustained by a country's manufacturing and resource extraction sectors. A conceptual representation of Smith's trade paradigm, similar to the biomass pyramid of ecosystems, is the balanced trade pyramid (Figure 4). The majority of trade is domestic, and over fifty percent of domestic production is generated by agriculture, manufacturing, and other "productive" industries.

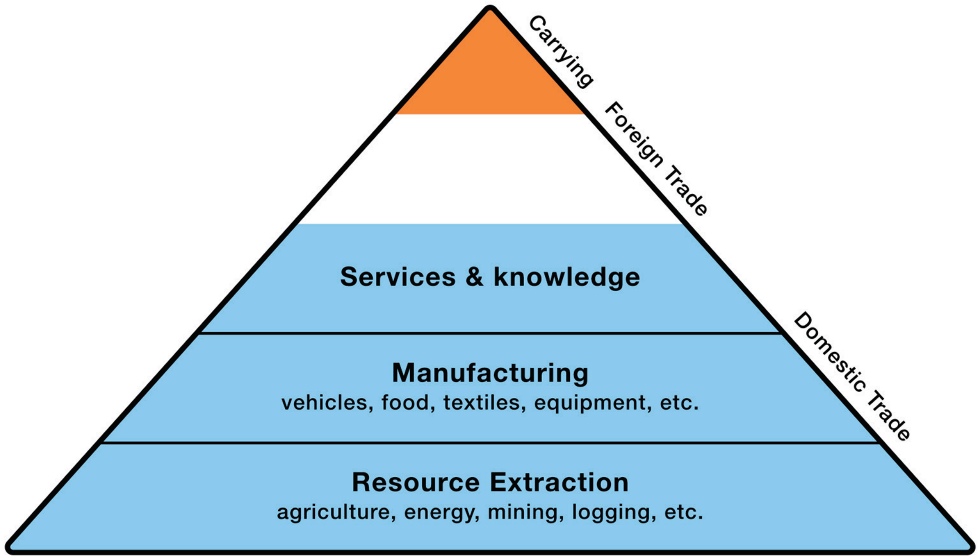

Figure 4. Balanced trade pyramid. The relative contribution of the domestic, foreign, and carrying trades in an economy. Relative GDP of various sectors within the domestic economy.

Today, U.S. agricultural and other extractive industries comprise less than 4% of GDP, and manufacturing contributes 11% of GDP [124,125]. Over 70% of GDP is derived from services, finance, IT, and other non-productive industries. Conceptually, the U.S. trade condition has shifted from a pyramid to a hot air balloon over the past 120 years (Figure 5). Carrying and foreign trades dominate the top two-thirds of the balloon. The service and knowledge sectors fill a greater volume of the domestic trade, sustained not by the productive labor of the U.S., but that of other countries. The balloon, conceptually, remains aloft by exogenous energy, the carrying trade, and imported products.

Figure 5. Trade balloon, representing the current U.S. economy. Balloon by Pixabay, public access.

3.4. Interactions between Diversity, Energy, and Trade

From this interpretive review, it appears diversity, energy, and trade form similar interactions in ecosystems and economies. Highly diverse systems are capable of extracting more energy and material resources from a given space, compared to low-diversity systems. However, transfers of energy and material resources into an economic or ecological space place downward pressure on diversity. In economies, a direct relationship exists between energy and cross-boundary trade. For instance, the use of oil in shipping resulted in a 10-fold increase in the size of cargo ships between 1871 and 1914, compared with cargo ships running coal, a lower energy-dense material [29], or those powered by wind. In turn, goods could be shipped more cheaply, increasing foreign trade profits, which were invested into greater scales of production, putting downward pressure on diversity in affected nations and industries.

3.4.1. Financial Resource Transfers, Homogenization, and Economic Productivity

Resource transfers are also facilitated by financial transfers such as loans, bailouts, and subsidies, which tend to perpetuate large homogenized industries. Hence, financial resources are also categorized as exogenous or endogenous, depending on their origin. Exogenous financial transfers can have impacts on the productive capacity and productivity of entire nations. The MOSES economic model of Sweden, for instance, revealed that regular government subsidies in specific industries in the early 1990s propped up large-scale businesses such as shipyards, which were utilizing obsolete equipment and production processes [126]. The result was to sustain low-performing businesses, which may have contributed to Sweden's economic recession in the mid-1990s.

A similar trend is evident in the U.S., where productivity growth has remained relatively flat between 1970 and 2022 [127], a period coinciding with high rates of financial transfers into the U.S. economy, agricultural subsidies of over U.S. $90 billion [128], and government bailouts of large homogenized industries such as pork producers [129], automobile manufacturers, and banks. This 52-year period also experienced increasing U.S. foreign trade and a sharp decline in manufacturing sector diversity. Economists of the '90s hypothesized that out-of-work laborers would get retrained and find jobs in the service sector or tech industry. Instead, a series of unfortunate economic events unfolded, dubbed the China Shock [130]. This included wage decline, drug and alcohol abuse, deflated housing prices, and lower tax revenues for municipalities. The impacts on unemployment and wage growth stem in part from the fact that the "economic footprint" of manufacturing is high, with each employee generating about seven indirect jobs [131]. For perspective, each service sector creates about 1.1 indirect jobs for each direct service job.

Over this same period, exporting nations such as Asia, Central America, and Sri Lanka homogenized their industries, amassing several risks. Their risks include the following: increased costs of labor, land, and other factors of production, which degrades their comparative advantage globally; low-cost exporters run the risk of tariffs, subsidies, or other counter tactics waged by importing countries to protect their industries; or global market contractions occur, rendering export-based industries "overbuilt" for their domestic markets. A combination of these risks struck Sri Lanka between 2019 and 2022, including MAS Holdings, their largest apparel manufacturer. Following Victoria's Secret's demand that MAS Holdings cut production costs steeply, MAS Holdings' best option was to increase output at their Bangladesh facility, reducing demand for Sri Lankan labor [33]. Similar cycles of industrial homogenization, boom, and bust have repeated across seven centuries of capitalist history [21], including 100 market crashes between 1985 and 2014 [132]. A connection between foreign trade and socio-economic instability was documented as far back as the late Bronze Age collapse [133].

In summary, this hypothesis is provided: an exogenous resource that transfers into or out of an economic space exerts downward pressure on economic diversity, with commensurate decreases in resistance and resilience to disturbance in affected industries and regions.

3.4.2. The Friction between Trade and Energy: The Case of New Belgium Brewing

New Belgium Brewing (NBB) is the seventh-largest brewery in the U.S., exporting tasty libations across the nation. A notable leader in sustainability, NBB has made incredible strides in alternative energy, including on-site photovoltaics, anaerobic digestion to convert organic waste to biogas, and novel energy efficiency programs [134]. As a result, their plant in Fort Collins, CO, meets 12% of its electricity demands with on-site generation. The remaining electricity needs are supplied by wind farms in Wyoming, U.S.A. [135], beyond state lines. Despite great efforts, about 88% of NBB energy consumption remains exogenous.

The NBB energy challenge is faced by countless manufacturers scaled to meet national or global consumer needs. They consume a quantity of energy that cannot be met with on-site—or even regional—endogenous energy sources. To survive, large-scale manufacturers must concentrate energy from sources far beyond their production facilities, so that water, glass, hops, and other inputs can be converted into export products. Certainly, some large-scale production facilities can produce a unit of beer, or other products, with less energy than a small-scale producer. However, such efficiencies are often outweighed by the energy required to ship a bottle of beer in refrigerated trucks from Fort Collins to, say, San Francisco. A socio-economic solution to the NBB case is offered in Giordanengo [42].

3.5. A Systems-Level Hypothesis

In summary, this systems-level hypothesis is provided: diversity, energy, and trade constitute the foundational components of an economy that, when interacting freely at a regional scale, confer a relatively stable state to an economy (i.e., relatively high resilience and resistance to disturbance). As energy and material resource transfers into or out of a regional system increase, multiple forms of diversity decline, conferring lower stability to the economy. The threshold of material and energy transfers, beyond which diversity declines, varies depending on one's SEI context.

3.6. The Basic Operational Unit of the Global Market Economy

Understanding an economy's foundational components, and their interactions, requires the appropriate boundary condition (i.e., the *basic operational unit*) to be defined. The appropriate boundary condition also depends on the complexity of the system in question. Basic operational units include organ systems, individuals (e.g., Adam Smith), and populations (e.g., the people of Scotland). Each shire in Scotland is also a basic operational unit, as is the Scottish economy, nested in the U.K. The basic operational unit of the global market economy is defined herein as an economic region, similar to the concept of ecoregions.

In nature, two adjacent ecoregions persist as basic operational units (Figure 6). Though wind and wildlife transmit pollen and seeds across ecological boundaries, and animals migrate freely across them, resulting in the exchange of genetic information, the species composition and structure of each forest remain distinct. Resource transfers within each ecoregion are greater than resource transfers between ecoregions.

Restoration ecologists recognize that ecosystems cannot persist at very small scales (e.g., one acre of prairie). Similarly, most economies cannot persist at scales as small as a single city, and maintain their self-regulating qualities. There are ecological and economic reasons for this. In a restored tallgrass prairie, for instance, the disturbance patterns and plant–animal interactions required to maintain a self-regulating ecosystem occur at scales larger than one acre. There is also a relationship between area and diversity, as richness increases in correlation with area [86], and then levels off as the sampling area increases [136]: the species–area curve.

In economics, besides the diversity factors, theories such as *comparative advantage* [137] also inform why a modern economy must operate at a scale greater than a city [42]. When an economy is large enough (e.g., several cities and counties), it can harbor multiple businesses, competing and collaborating within the economic space to gain efficiencies via unique (i.e., context-specific) compositions of skills, materials, and technology.

Figure 6. Adjacent level III ecoregions in NW California (U.S.A.): Coastal Range (redwood forest) and Klamath Mountains (mixed evergreen forest). The quantity of resource transfers within each system is far greater than the transfers between systems. Spatial data from Omernik [138].

For example, a high diversity of U.S. paper companies that existed in the Midwest in the 1800s developed means to convert recycled rags and straw to produce low-cost newsprint for regional and national consumers while yielding resource-use efficiencies [139]. As U.S. policies—Bretton Woods Agreement, Washington Consensus, etc.—shifted in favor of imported paper and other wood products from different SEI contexts (e.g., Canada and Mexico) in the 20th century, hundreds of U.S. wood and paper mill extinctions occurred. Today, the U.S. paper industry struggles to survive [139], in many cases requiring subsidies to exist. This is not to say the theory of comparative advantage is invalid. Rather, the theory may be most valid, and minimize exploitative tendencies, when applied within the correct boundary condition: regional scales, not global scales.

Another example comes from Salinas de Guaranda in the Andes mountains of Ecuador, where salt mining dominated the economy through the 1960s, primarily serving export markets; economic diversity was low. In the 1970s, Salinas de Guaranda began strengthening trade ties among twenty-four communities encompassing multiple provinces, raising their productive capacity. Today, cooperation, competition, and comparative advantage all operate in this region, which produces over 250 "Salinerito" products for only regional and national markets [41].

4. Conclusions

Many nations, regions, and cities dependent on the global marketplace can support high levels of consumption by importing relatively cheap products from different SEI contexts (trade component), facilitated by large quantities of low-cost fossil fuels (energy component). Such a model can generate financial efficiencies, but at the expense of resource-use efficiencies (e.g., waste heat and material waste), and the degradation of other system components (e.g., diversity, social conditions, or soil fertility). This can diminish a nation's or region's NDP and productive capacity, while causing an imbalance of foundational components.

The more unbalanced an economy's structure, the more amplified are the external forces acting on it over time, requiring more maintenance. This translates to more capital being allocated to combat graft, corruption, social unrest, environmental degradation, climate change, etc. That same capital is unavailable to sustain or restore an economy's productive capacity and net domestic productivity, or to provide other social, environmental, or economic benefits. Such an economy is poorly functioning, less capable of sustaining the needs of its chief beneficiaries, humans, while threatening their chief benefactor, nature. Restoring our economies according to the rules of self-regulating ecosystems has significant implications for green infrastructure, circularity, economic restoration, and other sustainable efforts.

4.1. Implications for Green Infrastructure

A common goal of green infrastructure is to protect natural resources, and provide various environmental, economic, and social benefits. This includes ecological restoration [140]. Given the interwoven nature of the earth's ecological and economic systems, and of its rural and urban capital, green infrastructure must also include economic restoration: restoring the balance of diversity, energy, and trade in regional economies. Two examples follow. In forested regions of the world, selective logging is used to provide jobs and industrial materials while improving water quality, contributing to carbon neutrality, reducing the risk of catastrophic wildfires, etc. In Bellemont, Arizona (U.S.A.), the Restoration Forest Products mill generates high-value dimensional timber (Figure 7) while yielding multiple byproducts: two forms of biomass fuel, increased understory productivity for grazing animals and pollinators, animal bedding, etc. The efficiencies gained contribute to the region's NDP and productive capacity, and integrate rural and urban capital. Critical for such green infrastructure solutions, the Bellmont mill is profitable enough to attract ample investment [58].

Figure 7. (**Left**): Restoration Forest Products mill in Bellemont, AZ. (**Center**): Primary revenue provided by engineered wood, with secondary revenue from several byproducts. (**Right**): Understory of thinned forest, increasing in blue grama (*Bouteloua gracilis*), a native grass with high protein, critical for grazing animals in late summer.

On the contrary, in states like Colorado, felled trees from thinning projects are rarely used for timber or to heat homes. Instead, logs are typically chipped on site or left in piles to burn. Since the trade liberalization policies of the '80s, decades of low-cost timber imports from Canada and elsewhere, coupled with cheap fossil fuels to heat and power buildings, have rendered Colorado's timber industry unviable, with very low diversity.

A second example comes from Sri Lanka, where a steep imbalance of payments began building in the 1980s, associated with exorbitant debt, increased reliance on imports, and other factors [98,141]. These imports included synthetic fertilizers, herbicides, and pesticides. Following Sri Lanka's 2019 economic implosion, coupled with a spike in the cost of imported farm inputs, the nation's export-based agricultural system crashed, alongside textiles and other industries. Farmers stormed the presidential palace in July 2022, sparking a global media frenzy pointing to President Rajapaksa's organic agriculture mandate as the root of the problem; the root, however, goes deeper.

Just as we gain insights into ecosystem structure and functions by observing the system's recovery following disturbance, I visited Sri Lanka in 2023 to interview organic farmers, business owners, scientists, and economists, to observe economic recovery following collapse. Sri Lankan farmers today create nitrogen from six endogenous sources, including four on-farm plant species. Endogenous fertilizers sustain not only tea plantations and subsistence farmers [142], but also profitable vegetable markets [143]. Even coconut farmers such as Gerard Gamini produce a wide range of products for regional and global markets using endogenous chicken manure, far cheaper in 2023 than exogenous fertilizers [144].

Structural diversity and richness in Sri Lankan agriculture are showcased by Ahinsa Tea, which grows over 25 agronomic species on one shade-grown plantation [142]. The plantation is located within the habitat buffer area of Sinharaja Forest Preserve, an IUCN biodiversity hotspot. A key goal of Ahinsa Tea, according to its founder, Dr. Abeygunawardana, is to increase sustainable economic use within the buffer, by developing biodiverse organic tea plantations that sustain local farm families.

Like most economies, the Sri Lankan economy requires significant restoration efforts to attain a self-regulating state, due to their trade and energy imbalances. A critical input to the economy remains imported fossil fuels, totaling U.S. $5 billion in 2022, a GDP deduction. The quantity of potential renewable energy sources (e.g., biofuels, solar, wind, hydroelectric) in Sri Lanka is estimated to exceed the nation's energy consumption [99]. However, some believe that the finances needed to develop this endogenous energy potential would require Sri Lanka to increase domestic trade while minimizing foreign trade, without amassing substantial foreign debt [96,143].

4.2. Ecological Succession: Implications for Economic Restoration

Succession, a key process that informs ecological restoration designs, has been illuminated by over a century of research [54,145–150]. *Ecological succession* is the change in plant community composition and structure over time, in response to disturbance. Disturbances such as a severe wildfire can destroy every tree in a forest, obliterating ecological niches while transforming topsoil to ash (Figure 8).

Relevant to economics, a relationship exists between productivity, diversity, and succession. During the early successional stages after wildfire, pioneer species such as annual grasses and forbs generate the bulk of productivity. As succession progresses, slower-growing species begin flourishing as the web of diversity becomes interlaced and tightened. Decades pass, and late successional plants begin to define the community, including mature shrubs and trees. Absent another wildfire, a very dense forest may develop. The economic equivalent of a very late successional stage would be an industry dominated by few large businesses. In the late stage, resources remain "locked up", largely unavailable to faster-growing species (or businesses). Inevitably, disturbances such as fire—or a major supply chain disruption—do arise, liberating resources for pioneer entities, and the succession cycle repeats.

Changes in diversity and productivity are not ever increasing over time, with a peak in the late-successional stage. Instead, a peak in biodiversity and net productivity tends to occur in mid-successional stages [52,54,151–153], shown conceptually in Figure 9. This phenomenon is known as the intermediate disturbance hypothesis (IDH), originally proposed by Connell [75]. In mid-successional stages, community structure and composition are shaped by smaller disturbances such as blowdowns of individual trees, insect outbreaks, or minor ground fires, liberating resources for other species. The increase in diversity raises the system's capacity to capture resources, contributing to greater resource-use efficiency, and hence higher net productivity.

Figure 8. Scorched forest and charred elk in the 2020 East Troublesome Fire (U.S.A.), which threatened water supplies for the regionally important Colorado–Big Thompson Project.

Though *economic* succession studies are limited, disturbance–diversity–productivity patterns similar to those observed in ecosystems are evident. In economies, disturbances that shift the system from late- to mid- or early-successional stages drive the process of creative destruction described by Joseph Schumpeter [154]. However, the connection between disturbance, creative destruction, and productivity is indirect. When disturbance strikes (e.g., recessions, industry shake-ups, or disruptive technologies), outdated business structures and processes are replaced by new business entrants and processes, which tend to yield higher rates of innovation [155–157]. Because some of the older business structures do prevail after a disturbance, the addition of new businesses can result in a rise in aggregate diversity. Hence, peak diversity co-occurs with high rates of innovation, which drives productivity gains, a basic requirement for economic growth. Other correlations between diversity and productivity were described earlier.

Countering the process of creative destruction, government programs and policies such as subsidies, bailouts, and loan programs, together with globally-oriented energy and trade policies, tend to homogenize economic landscapes, reinforcing a late successional condition.

In ecology, exceptions to the IDH are summarized by Huston [78] and Hodapp et al. [79]. Relevant to foundational components, Huston noted an ecological exception that has a functional equivalent in economics: when exogenous resources are transferred into the system. Other ecological exceptions include studies that include just one or two taxa (e.g., just upper canopy trees, or just ungulates), or are limited in their spatial or temporal scales [78,158]. Further, ecosystem management decisions such as wildfire suppression can also influence succession processes, producing very late successional communities whose biomass accumulation rates are lower than in previous stages (e.g., slower-growing trees, increased surface accumulation of wood, greater soil organic matter storage, etc.). Lacking adequate disturbance, ecosystems can cross a threshold of biomass (i.e., capital) accumulation, where diversity and net productivity begin declining (Figure 9). These late successional systems are often more susceptible to more intensive disturbances such as severe wildfires, wide-scale insect outbreaks, etc.

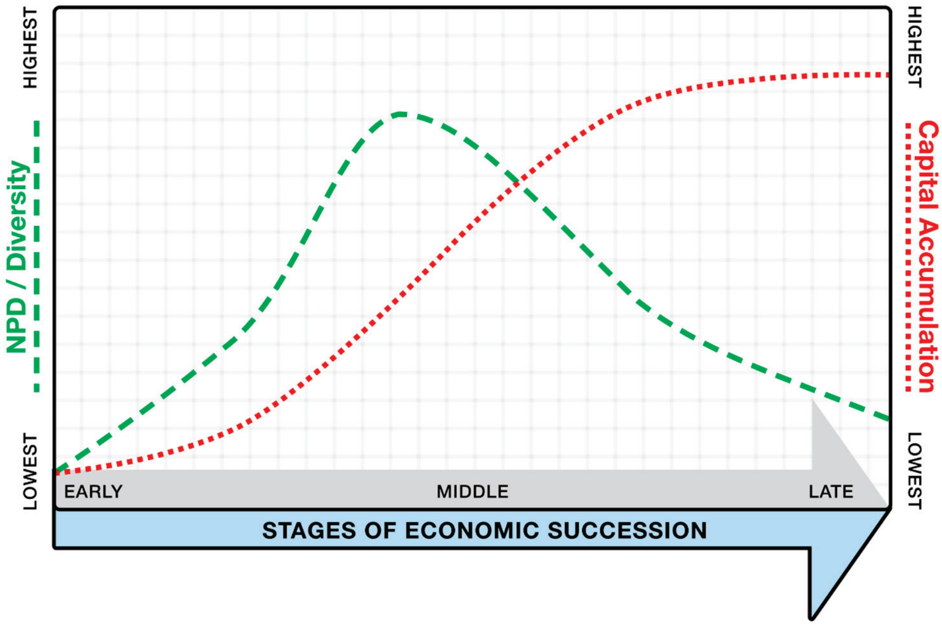

Figure 9. Estimates of aboveground net primary production (NPP), net ecosystem production (NEP), and biomass accumulation over the course of ecological succession, after Odum [52] and Gough et al. [151]. NEP can be negative following a disturbance [159].

In many regards, the U.S. economy appears to be exhibiting late-successional characteristics, where per capita GDP growth has dropped from 8% in the 1970s to less than 3% in the twenty-teens [160]. Real wages have remained flat to declining [161–164], wealth has become concentrated into fewer entities [15,17], and productivity returns on investment have declined [165]. If government bailouts, trade policies, monetary policies, and subsidies can shift economic succession to the right, can policies and programs shift succession to the middle, to stimulate diversity and its benefits?

4.3. Economic Restoration

Current use of the term economic restoration is restricted to the economic value of ecological restoration (e.g., the restoration economy), or to beautifying an urban area, rather than to restoring economic processes and functions. To clarify, I offer this definition: *Economic restoration* is the process of rebuilding economic diversity, endogenous trade, and endogenous energy systems within a regional economy. Due to this article's length, readers interested in additional data and analysis related to economic restoration, and its social, economic, and environmental implications, may contact the author for a digital copy of "Ecosystems as Models for Restoring Our Economies".

4.4. Economic Restoration Policy Implications

Several policy and program (P & P) implications stem from the results above, as related to diversity, energy, trade, and boundary conditions. Three inter-related policy implications are provided below, with others provided in Giordanengo [42]. These P & Ps are relevant not only to governments, but to NGOs, universities, and private entities working in the sustainability, green infrastructure, and circularity spaces. Specific P & Ps will vary by SEI context.

Policy implication 1: Energy security, carbon neutrality, and similar goals are facilitated not only via technology changes, but by increased economic diversity at regional scales. To stimulate diversity, P & Ps must be crafted to increase endogenous energy production and trade at regional and national scales, while minimizing exogenous energy and foreign trade. Many means exist to accomplish this, including import substitution, flexible manufacturing, cooperatives, ecological clustering, and similar system-level solutions.

Policy implication 2: Fiscal P & Ps that stimulate cross-boundary trade, such as subsidies, bailouts, loan programs, and tax breaks, have historically placed downward pressure on diversity. To facilitate the benefits of diversity described in this paper, fiscal P & Ps should be refocused to stimulate new business entrants in waste-to-resources, endogenous energy, extractive (e.g., agriculture and logging), and manufacturing industries at regional levels.

Policy implication 3: In support of policy implications above, a variety of P & Ps are available to facilitate the restoration of regional economies, such as multi-agency economic compacts, inter-agency trade and fiscal policies, regional energy development programs, and similar mechanisms. These P & Ps do not require the redrawing of jurisdictional boundaries (e.g., city, county, or state), or the creation of new currencies. Rather, regional economic zones can be established on watershed boundaries, ecological boundaries, or similar boundaries, which may cross multiple existing jurisdictions.

Funding: This research received no external funding.

Data Availability Statement: Data, tables, and additional text available at www.economicrestoration.org (accessed on 28 June 2023).

Conflicts of Interest: The author declares no conflict of interest.

References

1. Wessel, D. Why Economists Are Still Grasping to Cure Global Poverty. Section A7. *Wall Str. J.* 2007. Available online: https://www.wsj.com/articles/SB116845440351672808 (accessed on 11 November 2022).
2. FAO. The State of Food Security and Nutrition in the World 2019. Safeguarding against Economic Slowdowns and Downturns. Food and Agriculture Organization of the United Nations. 2019. Available online: https://www.wfp.org/publications/2019-state-food-security-and-nutrition-world-sofi-safeguarding-against-economic (accessed on 1 March 2022).
3. Montgomery, D. *Dirt: The Erosion of Civilizations*; University of California Press: Oakland, CA, USA, 2012.
4. Ontl, T.A.; Schulte, L.A. Soil Carbon Storage. *Nat. Educ. Knowl.* **2012**, *3*, 35.
5. Pimentel, D.; Harvey, C.; Resosudarmo, P.; Sinclair, K.; Kurz, D.; McNair, M.; Crist, S.; Shpritz, L.; Fitton, L.; Saffouri, R.; et al. Environmental and Economic Costs of Soil Erosion and Conservation Benefits. *Science* **1995**, *267*, 1117–1123. [CrossRef]
6. Tiseo, I. Global Recycling Rates of Municipal Solid Waste 2020, by Select Country. 2020. Available online: https://www.statista.com/statistics/1052439/rate-of-msw-recycling-worldwide-by-key-country/ (accessed on 21 December 2022).
7. BP. Statistical Review of World Energy. BP. 2021. Available online: https://www.bp.com/en/global/corporate/energy-economics/statistical-review-of-world-energy.html (accessed on 15 March 2023).
8. IEA (International Energy Agency). Key World Energy Statistics 2020. 2020. Available online: https://www.iea.org/reports/key-world-energy-statistics-2020 (accessed on 22 December 2022).
9. Simard, S.W. Mycorrhizal Networks Facilitate Tree Communication, Learning, and Memory. In *Memory and Learning in Plants, Signaling and Communication in Plants*; Baluska, F., Gagliano, M., Witzany, G., Eds.; Springer International Publishing AG: Cham, Switherland, 2018. [CrossRef]
10. Capra, F.; Luisi, P.L. *The Systems View of Life: A Unifying Vision*; Cambridge University Press: Cambridge, UK, 2014.
11. Emery, F. *Systems Thinking*; Penguin: London, UK, 1969.
12. Bertalanffy, L.V. *General System Theory: Foundations, Development, Applications*, Revised ed.; (17 March 1969); George Braziller Inc.: New York, NY, USA, 1969.
13. Britannica. Homeostasis: Physiology. 2022. Available online: https://www.britannica.com/science/homeostasis (accessed on 26 November 2022).
14. Daly, H. *Steady State Economics*, 2nd ed.; Island Press: Washington, DC, USA, 1991.
15. Piketty, T. *Capital in the Twenty-First Century*; Goldhammer, A., Translator; Harvard University Press: Cambridge, MA, USA, 2014.
16. Greenspan, A. *The Age of Turbulence*; Penguin Press: London, UK, 2007.
17. Stiglitz, J. *The Great Divide: Unequal Societies and What We Can Do about Them*; W.W. Norton and Company Inc.: New York, NY, USA, 2015.
18. Dissart, J.C. Regional Economic Diversity and Regional Economic Stability: Research Results and Agenda. *Int. Reg. Sci. Rev.* **2003**, *26*, 423–446. [CrossRef]
19. Tilman, D. The ecological consequences of changes in biodiversity: A search for general principles. *Ecology* **1999**, *80*, 1455–1474. [CrossRef]
20. Forrester, J.W. *Industrial Dynamics*; Martino Publishing: Eastford, CT, USA, 1961.

21. Arrighi, G. *The Long Twentieth Century: Money, Power, and the Origins of Our Time*; Verso Books: New York, NY, USA, 2010.
22. Braudel, F. *Civilization and Capitalism, 15th–18th Century: The Perspective of the World*; Harper & Row: New York, NY, USA, 1984.
23. Pew Research Center. Who Wants to Be Rich? Pew Research Center, Social and Demographic Trends Project. 2008. Available online: https://www.pewsocialtrends.org/2008/04/30/who-wants-to-be-rich/ (accessed on 7 August 2020).
24. Spash, C.L. *Routledge Handbook of Ecological Economics: Nature and Society*; Routledge: Boca Raton, FL, USA, 2017.
25. Stiglitz, J. *Globalization and Its Discontents*; W.W. Norton & Company: New York, NY, USA, 2002.
26. Hill, H. Food Miles: Background and Marketing. 2008 National Sustainable Agriculture Information Service. March 2003. Available online: https://attra.ncat.org/publication/food-miles-background-and-marketing/ (accessed on 8 April 2023).
27. RTS. Food Waste in America in 2021: Statistics and Facts. Recycle Track Systems. 2021. Available online: https://www.rts.com/resources/guides/food-waste-america/ (accessed on 8 April 2023).
28. Bechtel, W. Shipping Cattle to the Mainland. 2014. Available online: https://www.drovers.com/news/shipping-cattle-mainland (accessed on 6 December 2022).
29. Rodrigue, J.-P. *The Geography of Transport Systems*, 5th ed.; Routledge: Boca Raton, FL, USA, 2020.
30. Jindal, K. Top 10 PVC Manufacturers and Suppliers in the World. PlasticRanger. 2023. Available online: https://plasticranger.com/top-10-pvc-manufactures-and-suppliers-in-the-world/ (accessed on 26 March 2023).
31. Sodhi, N.S.; Brook, B.W.; Bradshaw, C.J.A. Chapter: V.1: Causes and Consequences of Species Extinctions. In *The Princeton Guide to Ecology*; Levin, S.A., Carpenter, S.R., Godfray, H.C.J., Kinzing, A.P., Loreau, M., Losos, J.B., Walker, B., Wilcove, D.S., Eds.; Princeton University Press: Princeton, NJ, USA, 2009; p. 515. Available online: https://assets.press.princeton.edu/chapters/s5_8879.pdf (accessed on 22 March 2023). [CrossRef]
32. Victoria's Secret. Commitment and Governance. 2023. Available online: https://www.victoriassecretandco.com/corporate-responsibility/supply-chain/commitment-and-governance (accessed on 7 May 2023).
33. David, K. (Business Manager, MAS Holdings). Interviewed by John Giordanengo, Negombo, Sri Lanka. 16 April 2023.
34. Batrawy, A. Germany's Decision to Burn Coal This Winter 'a Hard Pill to Swallow', Climate Envoy Says. Fortune.com. 2022. Available online: https://fortune.com/2022/09/20/germany-coal-power-plants-russian-war-ukraine-energy-crisis-jennifer-morgan/ (accessed on 20 March 2023).
35. Thaler, E.A.; Larsen, I.J.; Yu, Q. The extent of soil loss across the US Corn Belt. *Proc. Natl. Acad. Sci. USA* **2021**, *118*, e1922375118. [CrossRef] [PubMed]
36. Finn, J.T. Measures of ecosystem structure and function derived from analysis of flows. *J. Theor. Biol.* **1976**, *56*, 363–380. [CrossRef] [PubMed]
37. Hannon, B. The structure of ecosystems. *J. Theor. Biol.* **1973**, *41*, 535–546. [CrossRef] [PubMed]
38. Hannon, B.; Costanza, R.; Ulanowicz, R. A General Accounting Framework for Ecological Systems: A Functional Taxonomy for Connectivist Ecology. *Theor. Popul. Biol.* **1991**, *40*, 78–104. [CrossRef]
39. Weisman, A. *Gaviotas: A Village to Reinvent the World*, 2nd ed.; Chelsea Green Publishing: White River Junction, VT, USA, 2008.
40. Lupera-Martínez, M.; Zambrano-Farías, I.P. La puerta abierta "30 años de aventura misionera y social en Salinas de Bolívar Ecuador": Análisis y Revisión. *RECIAMUC* **2018**, *2*, 151–165. [CrossRef]
41. Polo, A. (President, FORNUSAL; Padre); Vascones, L. (Founder, Salinas de Guaranda oficina de turismo; Owner, La Minga Hotel); Ramirez, V. (Director, FORNUSAL). Interviewed by John Giordanengo, Guaranda, Ecuador. 21–23 January 2023.
42. Giordanengo, J.H. Ecosystems as Models for Restoring Our Economies. Economic Restoration Services. 2022. Available online: https://www.economicrestoration.org (accessed on 1 March 2023).
43. Birkhofer, K.; Diehl, E.; Andersson, J.; Ekroos, J.; Früh-Müller, A.; Machnikowski, F.; Mader, V.L.; Nilsson, L.; Sasaki, K.; Rundlöf, M.; et al. Ecosystem services—Current challenges and opportunities for ecological research. *Front. Ecol. Evol.* **2015**, *2*, 87. [CrossRef]
44. Costanza, R.; Daly, H.E.; Bartholomew, J.A. Goals, Agenda, and Policy Recommendations for Ecological Economics. In *Ecological Economics: The Science and Management of Sustainability*; Costanza, R., Ed.; Columbia University Press: New York, NY, USA, 1991.
45. Verhoeff, R.P.; Knippels, M.-C.P.J.; Gilissen, M.G.R.; Boersma, K.T. The Theoretical Nature of Systems Thinking. Perspectives on Systems Thinking in Biology Education. *Front. Educ.* **2018**, *3*, 40. [CrossRef]
46. NGSS Lead States. *Next Generation Science Standards: For States, by States*; Achieve, Inc. on Behalf of the Twenty-Six States and Partners That Collaborated on the NGSS: Washington, DC, USA, 2013; pp. 1–103. [CrossRef]
47. NASEM (National Academies of Sciences, Engineering, and Medicine). *Science, Medicine, and Animals*; The National Academies Press: Washington, DC, USA, 1991. [CrossRef]
48. Shurin, J.B.; Gruner, D.S.; Hillebrand, H. All wet or dried up? Real differences between aquatic and terrestrial food webs. *Proc. R. Soc. B Biol. Sci.* **2006**, *273*, 1–9. [CrossRef] [PubMed]
49. Cambardella, C.; Elgersma, K.; Giddens, E.; Myers, M.; Sherrard, M.; Smith, D. Prairie Power Project: Determining Maximum Sustainable Production of Biomass with a Mixture of Prairie Species. University of Northern Iowa, Tallgrass Prairie Center. 2016. Available online: https://tallgrassprairiecenter.org/sites/default/files/prairie_power_project_final_report_10-14-15.pdf (accessed on 7 November 2022).
50. Cadotte, M. Productivity Increases with Species Diversity, Just as Darwin Predicted. ScienceDaily. 2013. Available online: www.sciencedaily.com/releases/2013/05/130513152830.htm (accessed on 12 November 2022).

51. Cardinale, B.J.; Wright, J.P.; Cadotte, M.W.; Carroll, I.T.; Hector, A.; Srivastava, D.S.; Loreau, M.; Weis, J.J. Impacts of plant diversity on biomass production increase through time because of species complementarity. *Proc. Natl. Acad. Sci. USA* **2007**, *104*, 18123–18128. [CrossRef] [PubMed]
52. Odum, E.P. Strategy of ecosystem development: An understanding of ecological succession provides a basis for resolving man's conflict with nature. *Science* **1969**, *164*, 262–270. [CrossRef] [PubMed]
53. Odum, H.T.; Odum, B. Concepts and methods of ecological engineering. *Ecol. Eng.* **2003**, *20*, 339–361. [CrossRef]
54. Tilman, D.; Knops, J.; Wedin, D.; Reich, P.; Ritchie, M.; Siemann, E. The influence of functional diversity and composition on ecosystem processes. *Science* **1997**, *277*, 1300–1302. [CrossRef]
55. Borer, E.T.; Seabloom, E.W.; Tilman, D. Plant diversity controls arthropod biomass and temporal stability. *Ecol. Lett.* **2012**, *15*, 1457–1464. [CrossRef] [PubMed]
56. Hallmann, C.A.; Ssymank, A.; Sorg, M.; de Kroon, H.; Jongejans, E. Insect biomass decline scaled to species diversity: General patterns derived from a hoverfly community. *Proc. Natl. Acad. Sci. USA* **2021**, *118*, e2002554117. [CrossRef] [PubMed]
57. Welti, E.; Helzer, C.; Joern, A. Impacts of plant diversity on arthropod communities and plant–herbivore network architecture. *Ecosphere* **2017**, *8*, e01983. [CrossRef]
58. Templet, P.H. Energy, diversity and development in economic systems; an empirical analysis. *Ecol. Econ.* **1999**, *30*, 223–233. [CrossRef]
59. Nicholls, D.L.; Zerbe, J.I.; Bergman, R.D.; Crimp, P.M. *Use of Wood Energy for Lumber Drying and Community Heating in Southeast Alaska*; General Technical Report FPL−GTR−152; U.S. Department of Agriculture: Washington, DC, USA, 2004.
60. Edwards, R. (Procurement Forester, Restoration Forest Products). Interviewed by John Giordanengo, Bellemont, Arizona. 26 April 2023.
61. USDE. Quadrennial Technology Review 2015 Chapter 6: Innovating Clean Energy Technologies in Advanced Manufacturing. U.S. Department of Energy. 2015. Available online: https://www.energy.gov/sites/prod/files/2016/02/f30/QTR2015-6M-Waste-Heat-Recovery.pdf (accessed on 8 May 2023).
62. Cleland, E.E. Biodiversity and Ecosystem Stability. *Nat. Educ. Knowl.* **2011**, *3*, 14.
63. Loranger, J.; Violle, C.; Shipley, B.; Lavorel, S.; Bonis, A.; Cruz, P.; Louault, F.; Loucougaray, G.; Mesléard, F.; Yavercovski, N.; et al. Recasting the dynamic equilibrium model through a functional lens: The interplay of trait-based community assembly and climate. *J. Ecol.* **2016**, *104*, 781–791. [CrossRef]
64. Moretti, M.; Duelli, P.; Obrist, M.K. Biodiversity and resilience of arthropod communities after fire disturbance in temperate forests. *Oecologia* **2006**, *149*, 312–327. [CrossRef]
65. Oliver, T.H.; Heard, M.S.; Isaac, N.J.B.; Roy, D.B.; Procter, D.; Eigenbrod, F.; Freckleton, R.P.; Hector, A.L.; Orme, C.D.L.; Petchey, O.; et al. Biodiversity and Resilience of Ecosystem Functions. *Trends Ecol. Evol.* **2015**, *30*, 673–684. [CrossRef] [PubMed]
66. McLaughlin, G.E. Industrial Diversification in American Cities. *Q. J. Econ.* **1930**, *45*, 131–149. [CrossRef]
67. Brown, L.; Greenbaum, R.T. The role of industrial diversity in economic resilience: An empirical examination across 35 years. *Urban Stud.* **2016**, *54*, 1347–1366. [CrossRef]
68. Felix, A. Industrial Diversity, Growth, and Volatility in the Seven States of the Tenth District. Federal Reserve Bank of Kansas City. 2012. Available online: https://www.kansascityfed.org/ (accessed on 3 January 2021).
69. Tran, H.P.D. Industrial Diversity and Economic Performance: A Spatial Analysis. Dissertations, Theses, and Student Research from the College of Business. University of Nebraska, Lincoln. 2011. Available online: https://digitalcommons.unl.edu/businessdiss/19 (accessed on 12 June 2021).
70. OECD; WTO. Economic Diversification—Lessons from Practice. In *Aid for Trade at a Glance 2019: Economic Diversification and Empowerment*; OECD Publishing: Paris, France, 2019; pp. 135–160. [CrossRef]
71. Feldman, M.; Audretsch, D. Innovation in Cities: Science-Based Diversity, Specialization and Localized Competition. *Eur. Econ. Rev.* **1999**, *43*, 409–429. [CrossRef]
72. Jacobs, J. *The Economy of Cities*; Random House: New York, NY, USA, 1969.
73. Ortega-Argiles, R.; McCann, P. The Innovation-Productivity Paradox. In *Background Paper for the OECD-EC High-Level Expert Workshop Series "Productivity Policy for Places"*; OECD: Paris, France, 2021.
74. Templet, P.H. The energy transition in international economic systems: An empirical analysis of change during development. *Int. J. Sustain. Dev. World Ecol.* **1996**, *3*, 13–30. [CrossRef]
75. Connell, J.H. Diversity in Tropical Rain Forests and Coral Reefs. *Science* **1978**, *199*, 1302–1310. [CrossRef] [PubMed]
76. Shannon, C.E. A Mathematical Theory of Communication. *Bell Syst. Tech. J.* **1948**, *27*, 379–423. [CrossRef]
77. Schuldt, A.; Assmann, T.; Brezzi, M.; Buscot, F.; Eichenberg, D.; Gutknecht, J.; Härdtle, W.; He, J.-S.; Klein, A.-M.; Kühn, P.; et al. Biodiversity across trophic levels drives multifunctionality in highly diverse forests. *Nat. Commun.* **2018**, *9*, 2989. [CrossRef] [PubMed]
78. Huston, M.A. *Biological Diversity: The Coexistence of Species on Changing Landscapes*; Cambridge University Press: Cambridge, UK, 1995.
79. Hodapp, D.; Hillebrand, H.; Striebel, M. "Unifying" the Concept of Resource Use Efficiency in Ecology. *Front. Ecol. Evol.* **2019**, *6*, 233. [CrossRef]

80. Biggs, C.R.; Yeager, L.A.; Bolser, D.G.; Bonsell, C.; Dichiera, A.M.; Hou, Z.; Keyser, S.R.; Khursigara, A.J.; Lu, K.; Muth, A.F.; et al. Does functional redundancy affect ecological stability and resilience? A review and meta-analysis. *Ecosphere* **2020**, *11*, e03184. [CrossRef]
81. Ingrassia, P.; White, J.B. *Comeback: The Fall and Rise of the American Automobile Industry*; Touchstone, a Trademark of Simon and Schuster Inc.: New York, NY, USA, 1995.
82. Urban, D.L.; O'Neill, R.V.; Shugart, H.H., Jr. A hierarchical perspective can help scientists understand spatial patterns. *BioScience* **1987**, *37*, 119–127. [CrossRef]
83. Whittaker, R.; Levin, S. The Role of Mosaic Phenomena in Natural Communities. *Theor. Popul. Biol.* **1977**, *12*, 117–139. [CrossRef]
84. Scheiner, S.M. Measuring Pattern Diversity. *Ecology* **1992**, *73*, 1860–1867. [CrossRef]
85. Beever, E.A.; Prange, S.; DellaSalla, D.A. *Disturbance Ecology and Biological Diversity: Scale, Context, and Nature*; CRC Press, Taylor & Francis Group: Boca Raton, FL, USA, 2020.
86. Harner, R.F.; Harper, K.T. The Role of Area, Heterogeneity, and Favorability in Plant Species Diversity of Pinyon-Juniper Ecosystems. *Ecology* **1976**, *57*, 1254–1263. [CrossRef]
87. IEA. *World Energy Statistics 2019*; International Energy Agency: Paris, France, 2019.
88. Odum, H.T. Trophic Structure and Productivity of Silver Springs, Florida. *Ecol. Monogr.* **1957**, *27*, 55–112. [CrossRef]
89. Odum, H.T. Energy in Society: A Special Issue (1973). *Ambio* **1973**, *2*, 220–227. Available online: https://www.jstor.org/stable/4312030 (accessed on 17 June 2022).
90. Lotka, A.J. Contribution to the energetics of evolution. *Proc. Natl. Acad. Sci. USA* **1922**, *8*, 147–151. [CrossRef] [PubMed]
91. Lotka, A.J. Natural selection as a physical principle. *Proc. Natl. Acad. Sci. USA* **1922**, *8*, 151–154. [CrossRef] [PubMed]
92. Lovins, A. Reinventing Fire: Physics + Markets = Energy Solutions. Rocky Mountain Institute. 2014. Available online: www.rmi.org (accessed on 6 August 2021).
93. Mawatha, A.C. *Sri Lanka Energy Balance 2020*; No. 72; Sri Lanka Sustainable Energy Authority: Colombo, Sri Lanka, 2020; ISSN 2386-172X.
94. Gunaruwan, T.L. (Professor, University of Colombo, Department of Economics). Interviewed by John Giordanengo, Virtual Meeting. 8 May 2023.
95. Diddeniya, S.C. (Retired Electrical Engineer, Ceylon Electricity Board). Interviewed by John Giordanengo, Colombo, Sri Lanka. 3 April 2023.
96. Lo, J. Sri Lanka Can't Afford Fossil Fuels but Can't Afford to Get Off Them Either. Climate Home News. 2022. Available online: https://www.climatechangenews.com/ (accessed on 1 May 2023).
97. González-Moro, M.B.; González-Moro, I.; de la Peña, M.; Estavillo, J.M.; Aparicio-Tejo, P.M.; Marino, D.; González-Murua, C.; Vega-Mas, I. A Multi-Species Analysis Defines Anaplerotic Enzymes and Amides as Metabolic Markers for Ammonium Nutrition. *Front. Plant Sci.* **2021**, *11*, 632285. [CrossRef] [PubMed]
98. Wright, D.H. Species-Energy Theory: An Extension of Species-Area Theory. *Oikos* **1983**, *41*, 496. [CrossRef]
99. Saupe, E.E.; Myers, C.E.; Peterson, A.T.; Soberón, J.; Singarayer, J.; Valdes, P.; Qiao, H. Spatio-temporal climate change contributes to latitudinal diversity gradients. *Nat. Ecol. Evol.* **2019**, *3*, 1419–1429. [CrossRef] [PubMed]
100. Midolo, G.; Alkemade, R.; Schipper, A.M.; Benítez-López, A.; Perring, M.P.; De Vries, W. Impacts of nitrogen addition on plant species richness and abundance: A global meta-analysis. *Glob. Ecol. Biogeogr.* **2018**, *28*, 398–413. [CrossRef]
101. Soons, M.B.; Hefting, M.M.; Dorland, E.; Lamers, L.P.M.; Versteeg, C.; Bobbink, R. Nitrogen effects on plant species richness in herbaceous communities are more widespread and stronger than those of phosphorus. *Biol. Conserv.* **2017**, *212*, 390–397. [CrossRef]
102. USDA. Ag and Food Statistics: Charting the Essentials. U.S. Department of Agriculture, Economic Research Service. Administrative Publication Number 083. 2020. Available online: https://www.ers.usda.gov/data-products/ag-and-food-statistics-charting-the-essentials/ (accessed on 23 March 2021).
103. Leach, A.J. *A History of Antelope County Nebraska: From Its First Settlement in 1868 to the Close of the Year 1883*; The Lakeside Press: Chicago, IL, USA; R.R. Donnelley & Sons Company: Chicago, IL, USA, 1909.
104. Data USA. Oakdale, NE. Data USA. 2022. Available online: https://datausa.io/profile/geo/oakdale-ne (accessed on 12 February 2023).
105. Baker, N. The Great Hunger—What Was the Irish Potato Famine? How Was Queen Victoria Involved, How Many People Died and When Did It Happen? The Sun. 2017. Available online: https://www.thesun.co.uk/news/4321971/irish-potato-famine-queen-victoria-death-toll-when/ (accessed on 25 August 2017).
106. Mokyr, J. Great Famine. Encyclopedia Britannica, Inc. 2020. Available online: https://www.britannica.com/event/Great-Famine-Irish-history (accessed on 7 August 2020).
107. Pryor, S.C.; Scavia, D.; Downer, C.; Gaden, M.; Iverson, L.; Nordstrom, R.; Patz, J.; Robertson, G.P. Chapter 18: Midwest. Climate Change Impacts in the United States: The Third National Climate Assessment. In *U.S. Global Change Research Program*; Melillo, J.M., Richmond, T.C.T., Yohe, G.W., Eds.; U.S. Global Change Research Program: Washington, DC, USA, 2014; pp. 418–440. Available online: https://nca2014.globalchange.gov/report/regions/midwest (accessed on 6 January 2023). [CrossRef]
108. Dreibus, T. Farmers Got Older, Income Fell, Ag Census Shows. Successful Farming. 2019. Available online: https://www.agriculture.com/news/business/farmers-got-older-income-fell-ag-census-data-shows (accessed on 3 August 2021).

109. EIA. Use of Energy Explained: Energy Use for Transportation. U.S. Energy Information Administration. 2020. Available online: https://www.eia.gov/energyexplained/use-of-energy/transportation.php (accessed on 7 February 2021).
110. Scott, R. 1922 Car Prices. 1920-30.com. 2012. Available online: http://www.1920-30.com/automobiles/1922-car-prices.html (accessed on 7 August 2021).
111. Sugrue, T. From Motor City to Motor Metropolis: How the Automobile Industry Reshaped Urban America. Automobile in American Life and Society. University of Michigan—Dearborn. 2004. Available online: http://www.autolife.umd.umich.edu/ (accessed on 8 August 2021).
112. Clark, D.J. Separating Truth from Myth in the So-Called 'Golden Age' of the Detroit Auto Industry. 2019. Available online: https://www.smithsonianmag.com/history/separating-truth-myth-so-called-golden-age-detroit-auto-industry-180972139/ (accessed on 19 May 2019).
113. U.S. Census Bureau. 1930 Census: Manufactures, 1929 Volume 2. Reports by Industries. U.S. Census Bureau, Produced 1933. 1930. Available online: https://www.census.gov/library/publications/1933/dec/1930f-vol-02-manufactures.html (accessed on 1 May 2023).
114. de Zwart, P.; van Leeuwen, B.; van Leeuwen-Li, J. Real wages since 1820. In *How Was Life?: Global Well-Being since 1820*; van Zanden, J.L., Baten, J., d'Ercole, M.M., Rijpma, A., Smith, C., Timmer, M., Eds.; OECD Publishing: Paris, France, 2014. [CrossRef]
115. NAICS. *North American Industry Classification System*; United States Executive Office of the President, Office of Management and Budge: Washington, DC, USA, 2022.
116. Hidalgo, C.A.; Hausmann, R. The building blocks of economic complexity. *Proc. Natl. Acad. Sci. USA* **2009**, *106*, 10570–10575. [CrossRef] [PubMed]
117. Swift, D.; Niu, C.; Despradel, L.; Li, C. Franchise Business Economic Outlook 2020. Prepared for the International Franchise Association. 2019. Available online: https://franchiseeconomy.com/assets/26604.pdf (accessed on 16 January 2023).
118. Marshall, A.M. *Industry and Trade: Two Volumes in One*; Original Work Published in 1919; Cosimo Classics: New York, NY, USA, 2011.
119. Fisher, K. Steam Engine, Alexandria, 100 CE. Smith College Museum. 2022. Available online: https://www.smith.edu/hsc/museum/ancient_inventions/steamengine3.html (accessed on 3 January 2022).
120. UNCTAD. Evolution of the World's 25 Top Trading Nations. United Nations Conference on Trade and Development. 2022. Available online: https://unctad.org/topic/trade-analysis/chart-10-may-2021 (accessed on 11 December 2022).
121. North, D. *Discourses Upon Trade*; The Johns Hopkins Press: Baltimore, MD, USA, 1692.
122. Smith, A. *The Wealth of Nations*, 5th ed.; Original Work Published in 1776; Ixia Press: Calabasas, CA, USA, 2019.
123. Spufford, P. *Power and Profit: The Merchant in Medieval Europe*; Thames & Hudson, Inc.: New York, NY, USA, 2002.
124. BEA. Industry Economic Accounts. U.S. Department of Commerce, Bureau of Economic Analysis. 2019. Available online: https://apps.bea.gov/iTable/index_industry_gdpIndy.cfm (accessed on 10 January 2020).
125. Statista. Share of Value Added to the Gross Domestic Product (GDP) of the United States in 2021, by Industry. Statista. 2022. Available online: https://www.statista.com/statistics/248004/percentage-added-to-the-us-gdp-by-industry/ (accessed on 16 December 2022).
126. Eliasson, G.; Johansson, D.; Taymaz, E. Chapter VI: Firm Turnover and the Rate of Macro Economic Growth—Simulating the macroeconomic effects of Schumpeterian creative destruction. In *The Birth, the Life, and the Death of Firms: The role of Entrepreneurship, Creative Destruction and Conservative Institutions in a Growing and Experimentally Organized Economy*; Eliasson, G., Ed.; Ratio: Stockholm, Sweden, 2005.
127. BLS. The U.S. Productivity Slowdown: An Economy-Wide and Industry-Level Analysis. U.S. Bureau of Labor Statistics. 2021. Available online: https://www.bls.gov/opub/mlr/2021/article/the-us-productivity-slowdown-the-economy-wide-and-industry-level-analysis.htm (accessed on 8 March 2023).
128. Foley, J. It's Time to Rethink America's Corn System. Scientific American. 2013. Available online: https://www.scientificamerican.com/article/time-to-rethink-corn (accessed on 7 November 2021).
129. Bunge, J.; Maltais, K. Pork Industry, USDA Discuss Euthanizing Hogs after Coronavirus Closes Plants. The Wall Street Journal. 2020. Available online: https://www.wsj.com/articles/pork-industry-usda-discuss-euthanizing-hogs-after-coronavirus-closes-plants-11588015611 (accessed on 27 April 2020).
130. Autor, D.; Dorn, D.; Hanson, G.H. On the Persistence of the China Shock. National Bureau of Economic Research. Working Paper 29401. 2021. Available online: http://www.nber.org/papers/w29401 (accessed on 12 August 2022).
131. Bivens, J. Updated Employment Multipliers for the U.S. Economy. Economic Policy Institute. 2019. Available online: https://files.epi.org/pdf/160282.pdf (accessed on 12 August 2022).
132. Stiglitz, J. Trickle Down Economics Has Failed: Stiglitz. CNBC. 2015. Available online: https://www.cnbc.com/2015/04/22/trickle-down-economics-has-failed-stiglitz.html (accessed on 22 April 2021).
133. Cline, E.H. *1177 B.C.: The Year Civilization Collapsed*; Walter de Gruyter GmbH: Berlin, Germany, 2014; ISBN 9781400849987.
134. New Belgium. Climate: Our Commitments. New Belgium Brewing. 2021. Available online: https://www.newbelgium.com/company/mission/climate/ (accessed on 5 December 2021).
135. Fort Collins Gov. Green Energy Program. Fort Collins Utilities Public Information. 2021. Available online: https://www.fcgov.com/utilities/residential/renewables/green-energy/ (accessed on 12 August 2021).
136. Wilson, E.O. *The Diversity of Life*; W. W. Norton & Co. Inc.: New York, NY, USA, 1992.

137. Ricardo, D. *The Principles of Political Economy and Taxation*; Original Work Published in 1817; Dover Publications: Mineola, NY, USA, 2004.
138. Omernik, J.M. Ecoregions of the Conterminous United States (map supplement). *Ann. Assoc. Am. Geogr.* **1987**, *77*, 118–125. [CrossRef]
139. Wisconsin Historical Society. Paper Industry in Wisconsin. Wisconsin Historical Society. 2020. Available online: https://www.wisconsinhistory.org/Records/Article/CS2055 (accessed on 7 August 2020).
140. Semeraro, T.; Turco, A.; Arzeni, S.; La Gioia, G.; D'armento, R.; Taurino, R.; Medagli, P. Habitat Restoration: An Applicative Approach to "Biodiversity Heritage Relicts" in Social-Ecological Systems. *Land* **2021**, *10*, 898. [CrossRef]
141. Gunaruwan, L.T.; Wickremeratne, N. Sri Lankan Economic Sovereignty: Insights of Potentially Alarming Trends. *Sri Lanka J. Econ. Res.* **2018**, *6*, 111–124. [CrossRef]
142. Abeygunawardana, P. (Director and Founder, Ahinsa Tea Company). Interviewed by John Giordanengo, Morawaka, Sri Lanka. 13 April 2023.
143. Ishikawa, N. (President, Kenko 1st Organic). Interviewed by John Giordanengo, Colombo, Sri Lanka. 5 April 2023.
144. Shewa, R. (President, Inter Coir Limited). Interviewed by John Giordanengo, Colombo, Sri Lanka. 3 April 2023.
145. Bazzaz, F.A. The physiological ecology of plant succession. *Annu. Rev. Ecol. Syst.* **1979**, *10*, 351–371. [CrossRef]
146. Clements, F.E. Nature and structure of the climax. *J. Ecol.* **1936**, *24*, 252. [CrossRef]
147. Cowles, H.C. The ecological relations of the vegetation on the sand dunes of Lake Michigan. *Bot. Gaz.* **1899**, *27*, 95–117, 167–202, 281–308, 361–391. [CrossRef]
148. Gleason, H.A. The Individualistic Concept of the Plant Association. *Bull. Torrey Bot. Club* **1926**, *53*, 7–26. [CrossRef]
149. Grime, J.P. *Plant Strategies and Vegetation Processes*; John Wiley and Sons: Hoboken, NJ, USA, 1979.
150. Tilman, G.D. The resource-ratio hypothesis of plant succession. *Am. Nat.* **1985**, *125*, 827–852. [CrossRef]
151. Gough, C.M.; Curtis, P.S.; Hardiman, B.S.; Scheuermann, C.M.; Bond-Lamberty, B. Disturbance, complexity, and succession of net ecosystem production in North America's temperate deciduous forests. *Ecosphere* **2016**, *7*, e01375. [CrossRef]
152. Kira, T.; Shedei, T. Primary production and turnover of organic matter in different forest eco-systems of the Western Pacific. *Jpn. J. Ecol.* **1967**, *17*, 70–87. [CrossRef]
153. Tang, J.; Luyssaert, S.; Richardson, A.D.; Kutsch, W.; Janssens, I.A. Steeper declines in forest photosynthesis than respiration explain age-driven decreases in forest growth. *Proc. Natl. Acad. Sci. USA* **2014**, *111*, 8856–8860. [CrossRef] [PubMed]
154. Schumpeter, J.A. *Capitalism, Socialism, and Democracy*, 3rd ed.; Harper and Brothers: New York, NY, USA, 1950.
155. Eliasson, G. Deregulation, Innovative Entry and Structural Diversity As a Source of Stable and Rapid Economic Growth. *J. Evol. Econ.* **1991**, *1*, 49–63. [CrossRef]
156. Haltiwanger, J.C.; Jarmin, R.S.; Miranda, J. Who Creates Jobs? Small vs. Large vs. Young. NBER Working Paper no. 16300. 2010. Available online: http://www.nber.org/papers/w16300 (accessed on 12 August 2022).
157. Schumpeter, J.A. *The Theory of Economic Development: An Inquiry into Profits, Capital, Credit, Interest, and the Business Cycle*; Harvard University Press: Cambridge, MA, USA, 1934.
158. Nijs, I.; Impens, I. Underlying effects of resource use efficiency in diversity-productivity relationships. *Oikos* **2000**, *91*, 204–208. [CrossRef]
159. Lovett, G.M.; Cole, J.J.; Pace, M.L. Is Net Ecosystem Production Equal to Ecosystem Carbon Accumulation? *Ecosystems* **2006**, *9*, 152–155. [CrossRef]
160. Macrotrends. U.S. per Capita GDP 1960–2021. Macrotrends. 2020. Available online: https://www.macrotrends.net/countries/USA/united-states/gdp-per-capita (accessed on 2 August 2022).
161. BLS. *Real Earnings News Release*; U.S. Bureau of Labor Statistics, Division of Current Employment Statistics: Washington, DC, USA, 2023. Available online: https://www.bls.gov/news.release/realer.htm# (accessed on 14 March 2023).
162. Desilver, D. For Most U.S. Workers, Real Wages Have Barely Budged in Decades. Pew Research Center. 2018. Available online: https://www.pewresearch.org/fact-tank/2018/08/07/for-most-us-workers-real-wages-have-barely-budged-for-decades/ (accessed on 8 November 2020).
163. Gould, E. State of Working America Wages 2019: A Story of Slow, Uneven, and Unequal Wage Growth over the Last 40 Years. Economic Policy Institute. 2020. Available online: https://www.epi.org/publication/swa-wages-2019/ (accessed on 8 November 2021).
164. CRS. Real Wage Trends, 1979 to 2019. U.S. Congressional Research Service. CRS Reports, R45090. 2020. Available online: https://crsreports.congress.gov (accessed on 12 December 2021).
165. Romer, P.M. The Origins of Endogenous Growth. *J. Econ. Perspect.* **1994**, *8*, 3–22. [CrossRef]

land

MDPI

Article

Landscape Composition and Crop Border Vegetation Diversity Effect on Pollinators, Auxiliary Fauna, and Phytophagous Arthropods of Leguminous Cropland in Araba (Basque Country)

Ainhoa Urkijo [1,*], Ibone Ametzaga-Arregi [2,*], Eneko Elkano [1] and Isabel Albizu [1]

[1] Department of Conservation of Natural Resources, NEIKER—Basque Institute of Agricultural Research and Development, Basque Research and Technology Alliance (BRTA), 48160 Derio, Bizkaia, Spain
[2] Department of Plant Biology and Ecology, University of the Basque Country (UPV/EHU), 48940 Leioa, Bizkaia, Spain
* Correspondence: aurkijo@neiker.eus (A.U.); ibone.ametzaga@ehu.eus (I.A.-A.)

Abstract: Many strategies and directives are starting to address the importance of an appropriate landscape for agricultural biodiversity, such as pollinators and auxiliary fauna. Therefore, it is necessary to identify which landscape features are more important for agricultural biodiversity conservation and the ecosystem services they offer, like pollination and pest control. Thus, the main objective of this study was to assess the effect of landscape composition, configuration, connectivity, and crop border vegetation on arthropod diversity. The arthropod community was sampled in eight legume crops located across a gradient of landscape complexity. Additionally, the border vegetation of each plot was characterized, and the surrounding landscape was analyzed at a small and a large scale. For the statistical analysis, Generalized Linear Mix Models and redundancy analyses were applied. Pollinators were positively affected mainly by landscape connectivity. Pest control agents were less influenced by the landscape and only before harvest were they positively affected by riparian forests. Finally, phytophagous arthropod richness increased with border vegetation diversity and cropland in the surroundings. In conclusion, in the leguminous crops of Araba landscape connectivity together with cropland extension in the surroundings should be considered to promote ES-offering fauna diversity.

Keywords: complexity; connectivity; biodiversity; ecosystem services; hedgerow

1. Introduction

In 2024, the European Union (EU) approved a new law for Nature Restoration [1] in order to cease the accelerated biodiversity loss and ecosystem misfunctioning that have been occurring recently [2] due to anthropogenic landscape simplification [3] and a reduction in microhabitats for arthropods [4,5], among other causes. This law aims to restore 20% of the EU's land and sea ecosystems that are in bad condition for 2030 and 90% of all the areas in need for 2050.

In agricultural landscapes, food production depends on the supply of different ecosystem services (ES), such as pollination and pest control, both performed by mobile fauna that inhabit surrounding natural habitats. Thus, there is wide evidence that more ES are expected in agricultural areas with the presence of natural habitats in the landscape [6–10], like for example meadows or pastures [11,12] and native forests [12]. Similarly, increasing the heterogeneity within the plot [9,13–17] and adopting biodiversity-friendly measures like diversifying crop species or decreasing plot size [18] have also been observed to promote pollinator and auxiliary fauna community conservation and to increase yield. In addition to these measures, green infrastructure alone has also been claimed to be insufficient, suggesting that habitat connection should be equally important [12]. Therefore, agricultural landscapes must be multifunctional [19] and bioredundant [20] to guarantee food security.

For that reason, the Nature Restoration law (EU 2024/191) [1] considers the presence of agriculture in high-diversity landscapes as an indicator for agricultural landscape restoration and urges pollination conservation and agricultural landscape restoration.

However, there is a certain debate about how natural habitats could also function as reservoirs of pests and different phytophagous arthropods [21–23]. Similarly, landscape complexity and connectivity also play a crucial role in disease dispersal. For instance, although agricultural matrixes with a high diversity of crops have been proven to decrease aphid richness, they have also been observed to increase virus diseases [24]. The high variability of the interactions between the landscape and biodiversity makes local studies completely necessary to promote the local populations of pollinators and auxiliary fauna.

Therefore, the main objective of this study was to identify key features of the landscape to contribute to the knowledge of agricultural biodiversity and the ES they may provide in the province of Araba (Basque Country). For that purpose, the effects of landscape composition, configuration, and connectivity were assessed, as well as crop border vegetation, on arthropod functional groups of legume crops to evaluate biodiversity associated with two of the most important ES for agriculture, namely pollination and pest control. Legumes were selected as the crop because of their greater resource offer for different arthropod groups, especially when they are in flower [25,26]. Thus, landscape connectivity and configurational complexity, together with natural or semi-natural habitats like pastures, natural forests, or riparian forests, were expected to benefit these arthropod groups, which could lead to better pollination and pest control ES. On the contrary, phytophagous arthropods were expected to decrease in complex landscapes, due to the richer auxiliary fauna community.

2. Material and Methods

2.1. Survey Area

The sampling was carried out in the province of Araba in the Basque Country (northeastern of the Iberian Peninsula, Spain) (Figure 1a). In this province, the climate is Subatlantic- Mediterranean and there is a mixture of more intensive agriculture in a more simplified landscape and a more natural agriculture placed in a more natural and complex landscape. In the province of Araba, agriculture has great importance on the economy, as 92% of its land surface is under agricultural use [27]. The main management model in the province is intensive agriculture of potatoes, cereals, and diverse legumes, while organic farming still has little impact on the market since it only occupies 4.2% of the whole agricultural land [28]. Natural or semi-natural vegetation patches consist of *Quercus robur* and *Q. faginea* forests.

In total, 8 sites were sampled in May 2021 (before harvest) and 7 in August 2021 (after harvest, 1 of them was not harvested) to see the effect of the landscape when crops were present and when they were not. The sites were located in different landscape matrixes with different levels of naturalness. All the crops were leguminous, they were organically managed, and they followed a similar management calendar. Due to the low presence of organic farming in the province, it was not possible to select a single crop species for the whole study and different organic leguminous croplands were sampled: pea, vetch, lentil, and chickpea. For the same reason, not all crops were in the same phenological development state (4 of them were in flower, while 4 of them were not), which had to be considered when applying the models.

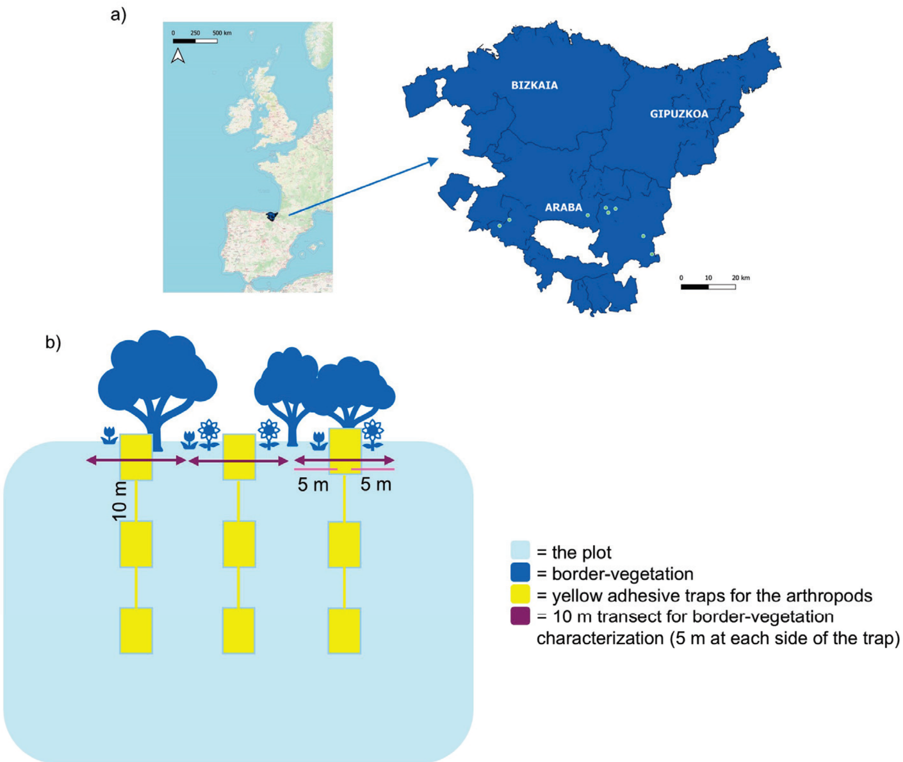

Figure 1. (**a**) On the left: map of Europe taken from © OpenStreetMap [29] with the Autonomous Community of the Basque Country (CABC) highlighted in dark blue; and on the right: map of the CABC with the eight sample plots colored in light green; (**b**) drawing of the sampling-design, where the location of the adhesive traps for the arthropods (yellow rectangles) and the transects for the border vegetation characterization (purple arrows) are displayed.

2.2. Arthropod Sampling

Arthropods were sampled before harvest (May 2021) and after harvest (August 2021). For that purpose, a plot of at least 1 ha was selected at each site and adhesive yellow traps of 10 × 25 cm were placed at a height of 1 m. Nine traps were set at each plot, forming 3 transects of 3 positions, the first one on the border vegetation, the second one at 10 m toward the center of the plot from the border, and the third one at 20 m toward the center of the plot from the border (Figure 1b). Between transects, a minimum of 10 m was left. The traps stayed in the field for 14 days. Arthropods were then identified at the family level at the laboratory using the following keys: Goulet and Huber (1993) [30], Oosterbroek (2006) [31], and Bellmann (2018) [32]. In addition, they were classified into 3 different groups depending on their functional role: pollinators (small pollinators and flower-visiting insects (according to Oosterbroek (2006) [31] and Bellmann (2018) [32])), predators and pest control agents (also known as auxiliary fauna), and phytophagous arthropods. It should be highlighted that as identifications were not conducted to the species level, generalizations for each family were conducted and "one single family"-"one single group" associations were made. For each group, richness (number of taxa) was calculated.

2.3. Border Vegetation Characterization

The border vegetation of each plot was only characterized in May 2021 by sampling 3 transects in each plot (Figure 1b). In each transect, the trap placed on the border was established as the center of the 10 m transect (5 m to one side and another 5 m to the other side) and 1.5 m width into the hedgerow. This vegetation transect was perpendicular to the transect of the arthropod traps. All the plants were identified to the smallest level possible, differentiating 5 strata (0–0.2 m, 0.2–1 m, 1–2 m, 2–5 m and >5 m) and giving each plant species a cover-value with a semi-quantitative scale (+ = 0–5%, 1 = 5–20%, 2 = 20–40%, 3 = 40–60%, 4 = 60–80%, 5 = 80–100%). This way, the Shannon diversity of border vegetation was calculated [33].

2.4. Landscape Analysis

The landscape surrounding each plot was analyzed by the QGIS program 3.28.3 version [34] using the EUNIS vegetation layer as a base. For landscape composition pasture, natural forest (*Quercus* spp., mixed forests), riparian forest (*Populus* spp., *Fraxinus* spp.), and cropland percentage were calculated [12]. Moreover, for landscape complexity, the next indexes were calculated based on the same cartography: the richness of different land uses (S) and the Shannon diversity index of the different land uses (SHDI) [35,36]. Then, landscape configuration patch density (PD) and edge density (as the sum of all patch perimeters in the buffer) (EDG) [35,36] were calculated. Finally, for landscape connectivity, the Effective Mesh Size Index (EMS) was calculated [37]. Considering previous analysis with larger scales and seeing that only small arthropods were sampled and that larger ones (better dispersal abilities) like bees, hoverflies, or butterflies were not caught by the traps, for the landscape assessment, two scales were used: a small scale of a 500 m radius buffer and a large scale of a 1000 m radius buffer (Table 1) [6,12,38].

Table 1. A buffer of 500 m and 1000 m radius, percentages of pasture, natural forest, riparian forest and cropland, land-use diversity as the Shannon index of different land-uses (SHDI), land-use richness as the number of different vegetation types (S), patch density as patches per ha (PD), edge density as the sum of border perimeters (EDG), and Effective Mesh Size (EMS) for each site.

Site	Buffer	Pasture	Natural Forest	Riparian Forest	Cropland	SHDI	S	PD	EDG	EMS
1	500	0.00	0.67	0.71	87.76	0.54	8	0.19	181.73	0.01
	1000	0.17	1.08	1.41	94.07	0.30	6	0.08	121.66	0.03
2	500	0.00	0.07	2.32	96.26	0.19	4	0.13	168.03	0.02
	1000	0.47	9.89	2.50	84.41	0.60	6	0.08	162.48	4.36
3	500	0.00	0.00	0.00	98.10	0.11	3	0.04	55.01	0.00
	1000	0.00	0.00	2.03	94.75	0.27	7	0.06	104.38	0.07
4	500	0.00	19.97	2.21	48.72	1.58	11	0.67	556.28	4.64
	1000	3.39	30.43	1.27	48.47	1.35	10	0.16	165.39	51.88
5	500	28.00	14.50	0.00	52.24	1.24	10	0.61	434.19	15.68
	1000	26.56	20.24	0.07	45.49	1.33	9	0.49	433.96	72.44
6	500	4.03	28.19	0.19	33.56	1.92	15	0.40	429.65	9.91
	1000	18.39	35.07	0.29	20.83	1.51	8	0.25	283.29	75.21
7	500	0.00	0.00	1.65	95.08	0.23	3	0.09	133.24	0.01
	1000	0.78	13.46	2.44	75.95	0.89	10	0.16	165.39	7.26
8	500	4.54	23.50	2.11	45.04	1.41	9	0.31	283.41	12.23
	1000	4.36	36.56	1.49	44.55	1.27	8	0.13	192.54	71.71

2.5. Statistical Analysis

Statistical analyses were performed with R program 4.2.2 version [39]. Generalized Linear Mix Models (GLMMs) were made with "lme4" package. First, the correlation between the different land uses and landscape complexity indexes was assessed to avoid autocorrelation effects. This way, the cropland percentage in 500 m and 1000 m buffer, riparian forest percentage in 500 m buffer, Effective Mesh Size in 500 m and 1000 m buffer, and border vegetation diversity were selected (Table 2). Pollinator, pest control agent, and phytophagous richness were defined as response variables. To select the explanatory variables avoiding autocorrelation, all the compositional, configurational, and connectivity variables at the two scales and border vegetation diversity were defined as explanatory variables. *Gamma* distribution was used for building the models, and due to the differences in the phenological development state of the crops, this was defined as a random factor (less developed vs. in flower). Additionally, trap position and sampling time were also defined as random factors. For each arthropod variable, the best models were selected (smallest AIC value). The same methodology was followed to assess the response of the most abundant taxa of each group to landscape features. These taxa were Empididae (pollinator), Muscidae (pest control), and Thysanoptera (phytophagous).

Table 2. Correlations between land uses and landscape complexity indexes at two scales: 500 m and 1000 m radius buffer. R^2 and *p* values are expressed. Land-use diversity (SHDI), land-use richness (S), patch density (PD), and edge density (EDG). *Statistically significant values.

Variables		500		1000	
		R^2	*p*	R^2	*p*
Cropland	Natural forest	−0.97	<0.001 *	−0.93	<0.001 *
	Riparian forest	0.12	0.443	0.55	<0.001 *
	Pastures	−0.66	<0.001 *	−0.90	<0.001 *
Effective Mesh Size	SHDI	0.61	<0.001 *	0.89	<0.001 *
	R	0.65	<0.001 *	0.51	<0.001 *
	EDG	0.69	<0.001 *	0.95	<0.001 *
	PD	0.69	<0.001 *	0.83	<0.001 *

The cycle of the crop itself and the surrounding ones are factors to be considered in understanding the dynamics of the arthropod community [40]. Because of that, the interaction between the sampling moment and the explanatory variables was also analyzed, and GLMM models were made separately before and after harvest when the interaction was significant (using *Gamma* distribution and defining trap position and crop development (only before harvest) as random factors). However, since the community of the trapped pollinators was mainly composed of smaller pollinators or flower visitors and leguminous crops are mainly pollinated by bees and large pollinators [26], this group was not analyzed separately before and after harvest.

Finally, a Redundancy Analysis (RDA) was performed to observe the effect of the landscape variables on the community composition of each group.

3. Results

3.1. General Results

In total, 11,639 arthropods were identified and 51 taxa were observed before harvest, in May. Among them, 17 taxa were classified as pollinators or small flower visitors, 17 as pest control fauna, and 17 as phytophagous. Meanwhile, after harvest (in August), 23,450 arthropods and 92 taxa were counted and identified: 32 taxa were classified as pollinators, 27 as pest control fauna, and 33 as phytophagous arthropods. Most of them were dipters and small hymenopters, together with some heteropters and coleopters (Table S1). Other important taxa (mainly for the pollinator group) like bees and butterflies, however, were not caught. When it comes to the vegetation, 172 species were identified in total.

3.2. Pollinators

Among cropland percentage (negatively related to pastures and natural forests), riparian forests, landscape connectivity (represented by Effective Mesh Size), and border vegetation diversity, the best predictor for pollinator richness was Effective Mesh Size (EMS) in 500 m buffer (Table 3; Figure 2a). This variable had a positive relationship with pollinator richness. This landscape complexity variable is representative of the connectivity of the natural habitats and refuges in the surroundings of the site.

Table 3. The best Generalized Linear Mix Model with significant results ($p < 0.05$) for pollinator richness depending on different landscape parameters and indexes, at two scales (500 m and 1000 m radius buffers) and at both sampling moments. The following values are expressed: AIC value, Estimate, Standard error, T value, and p-value. *EMS* = Effective Mesh Size.

	AIC	Variables	Buffer	Estimate	Std. Error	t Value	Pr
Pollinator richness	125.6	Intercept		0.36	0.1	3.74	<0.001
		EMS	500	−0.00	0.00	−3.28	0.001
Empididae abundance (before harvest)	177.3	Intercept		−0.13	0.06	2.08	0.038
		Cropland	500	0.00	0.00	3.10	0.002
		EMS	500	−0.01	0.00	−3.12	0.002

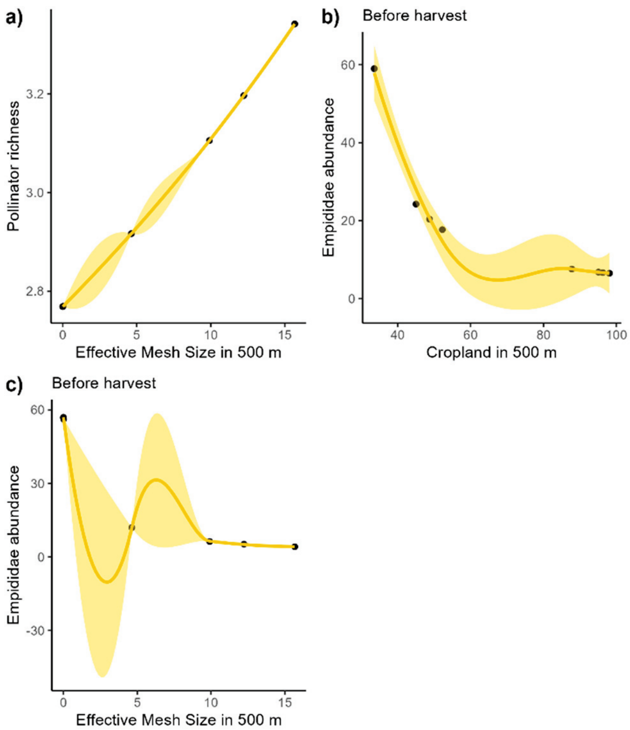

Figure 2. Relationship between pollinator richness and (**a**) Effective Mesh Size (ha) in 500 m buffer, representing the best Generalized Linear Mix Model for this variable. Relationship between Empididae abundance and (**b**) cropland in 500 m buffer before harvest, (**c**) Effective Mesh Size in 500 m buffer before harvest. Standard error is represented as a ribbon in light yellow.

The sampled pollinators were principally small Diptera and Hymenoptera taxa, as well as some Coleoptera. However, larger pollinators like bees and butterflies did not adhere to the traps. As the RDA analysis showed, the pollinator community was clearly differentiated by the sampling moment since the overlapping between before and after community composition is very small. Moreover, among the assessed landscape variables, the most influential one was the Effective Mesh Size in a 500 m buffer ($R^2 = 0.04$; $p = 0.002$) (Figure 3). Empididae was one of the most abundant pollinator families in both sampling moments and every site. The abundance of this family decreased with cropland percentage in the landscape before harvest (Table 3; Figure 2b. Moreover, the Effective Mesh Size also had a negative effect on their abundance (Figure 2c), although it was more subtle than cropland extension.

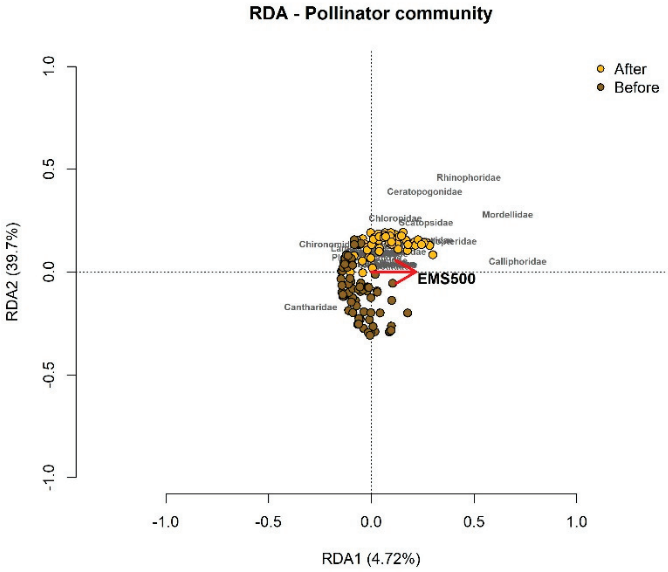

Figure 3. Redundancy Analysis (RDA) plot for pollinator community before and after harvest. The red arrow shows the most influential variable. EMS500 = Effective Mesh Size in 500 m buffer.

3.3. Pest Control Agents

The riparian forest percentage in 500 m buffer (t = 2.62; $p = 0.008$) showed significant interactions with the sampling moment. Thus, when assessing this variable separating the sampling moment, it had a significant effect before harvest. This way, the best predictor for pest control agent richness was riparian forest percentage in 500 m buffer (Table 4; Figure 4) with a positive effect.

Table 4. The best Generalized Linear Mix Models with significant results ($p < 0.05$) for pest control agent richness and Muscidae family only before harvest, depending on different landscape parameters and indexes, at two scales (500 m and 1000 m radius buffers). The following values are expressed: AIC value, Estimate, Standard error, T value, and *p*-value. EMS = Effective Mesh Size.

	AIC		Buffer	Estimate	Std. Error	t Value	Pr
Pest control richness	84.1	Intercept		0.26	0.02	12.04	<0.001
(before harvest)		Riparian forest	500	−0.03	0.01	−2.16	0.031
Muscidae abundance	−284.6	Intercept		5.05	3.68	1.37	0.170
(before harvest)		EMS	500	−0.3	0.24	−1.26	0.208

Similar to the pollinator community, the RDA analysis showed a clear separation between the community composition before and after harvest. Moreover, the most influential landscape variable was also the Effective Mesh Size in a 500 m buffer ($R^2 = 0.0098$; $p = 0.04$), although it explained a smaller part of the differentiation (1.76%) compared to the pollinator community (Figure 5). Among these families, only Muscidae showed as being affected by the assessed variables. However, even if the best GLMM (lower AIC value) included the Effective Mesh Size in a 500 m buffer as an explanatory variable, its effect was not significant (Table 4).

Among the landscape parameters that showed a significant effect on the richness of this group and Muscidae before harvest, both of them were defined at a 500 m buffer scale.

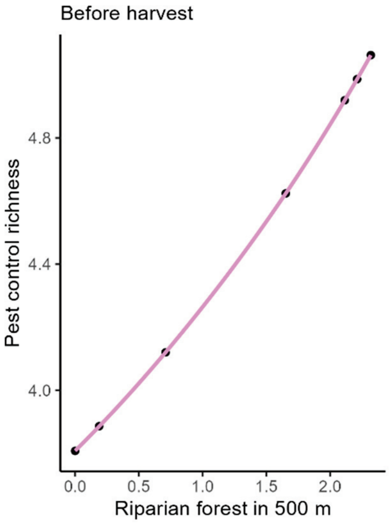

Figure 4. Only before harvest, the relationship between pest control agent richness and riparian forest percentage in 500 m buffer. Standard error is represented as a ribbon in light purple.

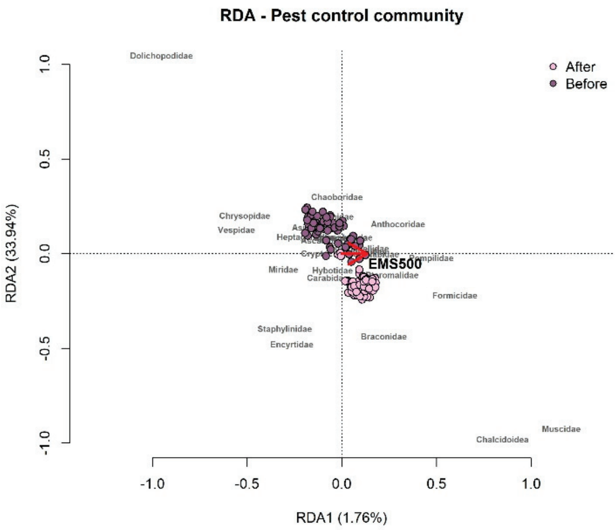

Figure 5. Redundancy Analysis (RDA) plot for pest control community before and after harvest. The red arrow shows the most influential variable. EMS500 = Effective Mesh Size in 500 m buffer.

3.4. Phytophagous

Phytophagous richness was positively affected by cropland percentage in 500 m buffer (Table 5; Figure 6a) and border vegetation diversity (Figure 6b). Although the best GLMM also incorporated the riparian forest percentage in a 500 m buffer, this variable was not significant.

Border vegetation diversity showed interactions with the sampling moment (t = 2.5; $p = 0.012$). This way, harvest phytophagous richness also increased with border vegetation diversity (Table 5).

Finally, the RDA analysis showed that the phytophagous community was well differentiated by the sampling moment and that its composition was most affected by the border vegetation diversity ($R^2 = 0.03$; $p = 0.003$) (Figure 7 "Border-vegetation"). Thysanoptera was one of the most abundant taxa in the community, which showed a tendency to be more abundant with the increase in cropland in 500 m buffer (Table 5; Figure 6c).

Table 5. The best Generalized Linear Mix Model with significant results ($p < 0.05$) for phytophagous arthropod richness, depending on different landscape parameters and indexes. The following values are expressed: AIC value, Estimate, Standard error, T value, and *p*-value.

	AIC		Buffer	Estimate	Std. Error	t Value	Pr
Phytophagous richness	135.2	Intercept		0.33	0.05	6.50	<0.001
		Cropland	500	−0.00	0.00	−2.81	0.004
		Border vegetation diversity		−0.05	0.02	−2.76	0.005
		Riparian forest	500	−0.01	0.00	−1.93	0.054
Phytophagous richness (before harvest)	61.2	Intercept		0.30	0.02	14.73	<0.001
		Border vegetation diversity		−0.06	0.02	−2.98	0.003
Thysanoptera abundance (after harvest)	176.2	Intercept		0.07	0.02	4.03	<0.001
		Cropland	500	−0.00	0.00	2.82	0.005

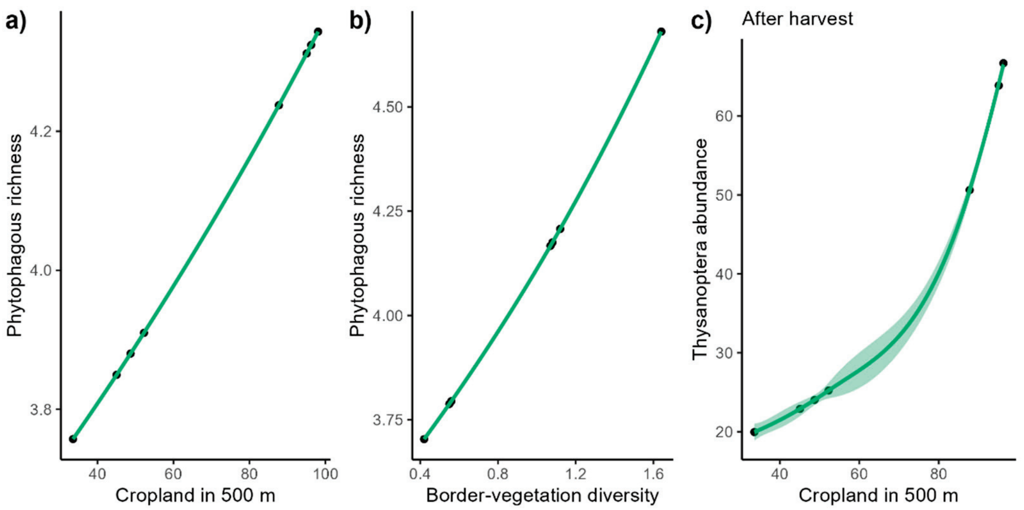

Figure 6. Relationship between phytophagous richness and (**a**) cropland in 500 m buffer and (**b**) border vegetation diversity. Relationship between (**c**) Thysanoptera abundance and cropland in 500 m buffer. Standard error is represented as a ribbon in light green.

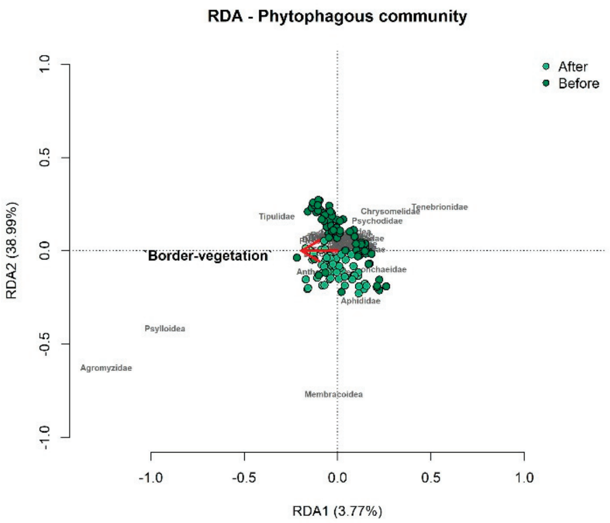

Figure 7. Redundancy Analysis (RDA) plot for the phytophagous community before and after harvest. The red arrow shows the most influential variable. 'Border vegetation´ = Border vegetation diversity.

4. Discussion

Spatial and temporal changes in a system can cause sudden changes in its biodiversity, affecting, at the same time, its functionality [41], which means that the dynamics of crops can shadow the effect of landscape complexity on the arthropod community [40]. In this study, the pollinator community was affected by the landscape, despite the presence of the crop. However, pest control and phytophagous arthropods were less affected by the landscape, suggesting that other factors must be affecting them at the same time.

4.1. Pollinators

Different variables are known to be beneficial for arthropod richness, and especially for pollinators, such as overall landscape diversity and complexity [6–9], extensive meadows or pastures [11,12], the vicinity of the forest, woody elements and deadwood [8,9,11,12,42–44], and riparian forests [45,46].

In our study, among all, the best predictor for pollinator richness in the legume crops was found to be landscape connectivity. On the one hand, these results highlight the importance of natural habitats and resources being connected across the landscape matrix, even to a larger scale, to allow the dispersal of pollinators [12]; and on the other hand, they can be indicators of the importance of adopting small scale measures to promote this connectivity within the plot [9,13,16,17,42]. Therefore, not only is it important to promote habitats and resources for pollinators, but it is equally relevant to arrange them correctly to enable pollinators to disperse.

As expected, the proportion of intensive cropland extension on the landscape was not the best predictor for pollinator richness, even if a lower percentage of cropland in the landscape was representative of a higher percentage of pastures and natural forests. It is true that very intensive agricultural matrixes can be detrimental to the diversity of these arthropods, due to the loss and fragmentation of natural or semi-natural habitats [6,47]. However, considering that pollinator-friendly legumes took an important extension of the "intensive cropland" category on the buffers, such a negative effect was not expected to be observed. Legumes are mainly pollinated by bees and larger pollinators [26], which can be better competitors for these resources and do not depend on landscape naturalness as opportunistic or non-crop pollinators [48]. Since the pollinators we sampled were small, other crop pollinators like bees might have left the smaller pollinators to feed on poorer resources, such as small wildflowers in the borders [8]. This coincides with the results for Empididae, which was the most abundant pollinator family. Their abundance was lower when cropland extension was higher, which could indicate that this small Diptera family is more benefited by other natural habitats than by the crops themselves. This family, however, was, at the same time, slightly negatively affected by landscape connectivity, which could be a consequence of facilitated dispersal to more suitable habitats since this family is often associated with aquatic or highly humid habitats [49,50]. This highlights the importance of landscape complexity and natural vegetation for the richness of the pollinator community, even in crops with dense floral resources.

The 500 m radius buffer was observed to be best for landscape assessment for pollinator richness. Thus, to evaluate the features of the landscape and its suitability for hosting, a rich pollinator community using a buffer of a 500 m radius should be sufficient.

4.2. Pest Control Agents

Several studies have proved that predators, pest control agents, or auxiliary fauna benefit from a higher complexity of the landscape [51–53], and there is wide evidence that borders increase in-farm biodiversity [6,9,17,54,55]. This way, a well-connected matrix [12] with natural habitats like pastures [56–58], for example, should be necessary to enhance pest control in crops. However, this study failed to prove a clear positive effect of landscape connectivity. This variable only influenced their community composition, but it did not promote auxiliary fauna richness. In addition, cropland extension did not have a negative effect on this group, and neither did landscape configuration and complexity indexes, contrary to what other studies show [13,59,60]. This lack of significance could be indicative of crops resulting in an important food source for pest control agents since they feed on the phytophagous arthropod community that grows on plants. Thus, other factors like crop cycle and pest dynamics should be considered to assess pest control arthropods.

Moreover, the presence of riparian forests in the landscape before harvest was identified as the only variable that had a positive effect on the pest control agent community. These habitats have been claimed to be refuges for auxiliary fauna since pest control services can be higher in crops near riparian forests [61,62]. Therefore, their conservation could be key for the promotion of pest control services in rural Araba and more studies should be made on these ecosystems.

Equally to the pollinators, this group was more related to the smaller scale. Therefore, it would be better to use the 500 m buffer for landscape assessment in relation to this group. However, more studies should be made about the interactions between the dynamics of pests and auxiliary fauna in crops and the landscape.

4.3. Phytophagous Arthropods

There is a certain controversy on whether landscape complexity increases pest pressure or contributes to diminishing it. Some authors claim that natural habitats function as a source of phytophagous arthropods, causing heavier pest pressure and more damage to crops [22,23]. However, others suggest that the effects of this group decrease in complex landscapes due to a higher pest control or a higher availability of alternative resources for the phytophagous in the landscape [17,24].

In this case, cropland extension in the landscape was one of the drivers for phytophagous richness, which means that when the percentage of pastures and natural forests was higher, phytophagous richness was lower. This coincides with the latter authors. In addition, Thysanoptera abundance was also higher with cropland extension. Being potential pests of legume crops and other species of crops, it was expected to find an increase in this group with the increase in cropland [63].

Additionally, and similarly to auxiliary fauna, riparian forests also increased phytophagous richness. As said before, riparian forests are an important source of biodiversity [61,62,64]. Because of that, it is logical to observe an augment in phytophagous arthropod richness with their presence. Moreover, riparian forests in agricultural landscapes are commonly cut, so that the riparian habitat becomes limited to the stream flow and some associated vegetation. Consequently, the conservation of these forests could bring an increase in biodiversity in general.

At the same time, border vegetation diversity also contributed to a higher phytophagous richness due to two possible options: first, that a higher plant diversity hosted a higher phytophagous diversity, and second, that crops, being monospecific, could host a less diverse phytophagous community. This result should not be considered only as a threat to crop health but also as an opportunity for border vegetation to absorb part of the phytophagous community as an alternative food source, especially for native phytophagous when the vegetation is natural [65]. Thus, the controversy of these results could be related to the fact that phytophagous arthropods also depend on other factors that were not assessed in this study, like crop cycle and its structural complexity [66,67]. Because of that, more studies should be conducted on how phytophagous arthropod populations change depending on crop cycles and their interaction with the landscape in Araba.

Regarding the landscape scale, the smaller scale could be more appropriate, which suggests that the analysis of the nearest vegetation could be more important to assess this community and approach landscape evaluation and management. Since many of the phytophagous arthropods are very small and they might not be good dispersers [68], the adjacent vegetation would play an essential role in conditioning their presence or absence.

5. Conclusions

In closing, the Effective Mesh Size Index for landscape connectivity could be a key feature of the landscape as an indicator of the pollinator and pest-control arthropod communities in the leguminous cropland of the Mediterranean region of Araba. Therefore, sustainable agricultural management should consider this index to assess the conservation of biodiversity in agricultural contexts. Moreover, cropland extension for phytophagous arthropods, and riparian forests both for phytophagous and pest control agents could also be interesting indicators for their richness. Additionally, based on the present results, a radius of 500 m could be a good measure to evaluate landscape suitability for the assessed arthropod communities.

Thus, this work not only contributes to the knowledge of the arthropod communities in the agricultural landscape of Araba, but it is also a starting point for the introduction of landscape characteristics as a feature to be considered in agricultural management. Therefore, more studies should be made to advance the study of sustainable landscape designs.

All these results highlight the importance that landscape complexity and natural vegetation have for ES offering groups in an agricultural context. Therefore, the first step in the management of the leguminous crops of the region should be to analyze the landscape within the area in order to improve biodiversity conservation, which goes in line with a lot of sustainable strategies and with the focus of the recent Nature Restoration law (2024/191) [1] on agrarian landscapes. Moreover, more studies should be made on the real capacity of the fauna on ES delivery and on the production of the crops.

Supplementary Materials: The following supporting information can be downloaded at https://www.mdpi.com/article/10.3390/land13122128/s1: Table S1: Mean values of the assessed arthropod taxa abundance in each site before and after harvest.

Author Contributions: Conceptualization, A.U., I.A.-A. and I.A.; Data curation, A.U., E.E. and I.A.; Formal analysis, A.U. and E.E.; Funding acquisition, I.A.; Investigation, A.U., I.A.-A., E.E. and I.A.; Methodology, A.U., I.A.-A., E.E. and I.A.; Project administration, I.A.-A. and I.A.; Resources, I.A.-A. and I.A.; Supervision, I.A.-A. and I.A.; Visualization, A.U. and E.E.; Writing—original draft, A.U.; Writing—review and editing, I.A.-A. and I.A. All authors have read and agreed to the published version of the manuscript.

Funding: This work was supported by the Basque Government, Agriculture, Fishing and Food Policy Deputy Council: POLITA—Contribution of Agroecosystems to Biodiversity and Ecosystem Services. This work was supported by the Basque Government, Agriculture, Fishing and Food Policy Deputy Council: A training program for investigators and technologists in the scientific, technologic, and corporate ambit of the farming–fishing and food sector (2020). This work was supported by the Basque Government research group GIC21/201-IT1648-22.

Data Availability Statement: Data will be made available upon request.

Acknowledgments: We thank all the farmers from Araba who welcomed us, let us sample their cropland, and provided all the information we needed. We also thank all the NEIKER staff who helped select the methodology and worked on the samplings.

Conflicts of Interest: The authors declare no conflicts of interest.

References

1. EU. Regulation (EU) 2024/1991 of the European Parliament and of the Council of 24 June 2024 on nature restoration and amending Regulation (EU) 2022/869. 2024. Available online: https://eur-lex.europa.eu/legal-content/EN/TXT/?uri=CELEX:32024R1991#document1 (accessed on 6 December 2024).
2. IPBES. *Global Assessment Report on Biodiversity and Ecosystem Services of the Intergovernmental Science-Policy Platform on Biodiversity and Ecosystem Services*; Brondizio, E.S., Settele, J., Díaz, S., Ngo, H.T., Eds.; IPBES: Bonn, Germany, 2019.
3. Meehan, T.D.; Werling, B.P.; Landis, D.A.; Gratton, C. Agricultural landscape simplification and insecticide use in the Midwestern United States. *Proc. Natl. Acad. Sci. USA* **2011**, *108*, 11500–11505. [CrossRef]
4. IPBES. *The Assessment Report of the Intergovernmental Science-Policy Platform on Biodiversity and Ecosystem Services on Pollinators, Pollination and Food Production*; Potts, S.G., Imperatriz-Fonseca, V.L., Ngo, H.T., Eds.; IPBES: Bonn, Germany, 2016.
5. FAO. *Why Bees Matter. The Importance of Bees and Other Pollinators for Food and Agriculture*; FAO: Rome, Italy, 2018.

6. Steffan-Dewenter, I.; Münzenberg, U.; Bürger, C.; Thies, C.; Tscharntke, T. Scale-dependent effects of landscape context on three pollinator guilds. *Ecology* **2002**, *83*, 1421–1432. [CrossRef]
7. Klein, A.M.; Vaissière, B.E.; Cane, J.H.; Steffan-Dewenter, I.; Cunningham, S.A.; Kremen, C.; Tscharntke, T. Importance of pollinators in changing landscapes for world crops. *Proc. R. Soc. B Biol. Sci.* **2007**, *274*, 303–313. [CrossRef] [PubMed]
8. Lautenbach, S.; Seppelt, R.; Liebscher, J.; Dormann, C.F. Spatial and temporal trends of global pollination benefit. *PLoS ONE* **2012**, *7*, e35954. [CrossRef] [PubMed]
9. Shackelford, G.; Steward, P.R.; Benton, T.G.; Kunin, W.E.; Potts, S.G.; Biesmeijer, J.C.; Sait, S.M. Comparison of pollinators and natural enemies: A meta-analysis of landscape and local effects on abundance and richness in crops. *Biol. Rev.* **2013**, *88*, 1002–1021. [CrossRef]
10. Galpern, P.; Vickruck, J.; Devries, J.H.; Gavin, M.P. Landscape complexity is associated with crop yields across a large temperate grassland region. *Agric. Ecosyst. Environ.* **2020**, *290*, 106724. [CrossRef]
11. Maurer, C.; Sutter, L.; Martínez-Núñez, C.; Pellisier, L.; Albrecht, M. Different types of semi-natural habitat are required to sustain diverse wild bee communities across agricultural landscapes. *J. Appl. Ecol.* **2022**, *59*, 2604–2615. [CrossRef]
12. Vujanović, D.; Losapio, G.; Mészáros, M.; Popov, S.; Ristić, Z.M.; Stojnić, S.M.; Jović, J.; Vujić, A. Forest and grassland habitats support pollinator diversity more than wildflowers and sunflower monoculture. *Ecol. Entomol.* **2023**, *48*, 421–432. [CrossRef]
13. Holzschuh, A.; Steffan-Dewenter, I.; Tscharntke, T. How do landscape composition and configuration, organic farming and fallow strips affect the diversity of bees, wasps and their parasitoids? *J. Anim. Ecol.* **2010**, *79*, 491–500. [CrossRef]
14. Garbach, K.; Long, R.F. Determinants of field edge habitat restoration on farms in California's Sacramento Valley. *J. Environ. Manag.* **2017**, *189*, 134–141. [CrossRef]
15. Duarte, G.T.; Santos, P.M.; Cornelissen, T.G.; Ribeiro, M.C.; Paglia, A.P. The effects of landscape patterns on ecosystem services: Meta-analyses of landscape services. *Landsc. Ecol.* **2018**, *33*, 1247–1257. [CrossRef]
16. Kleijn, D.; Bommarco, R.; Fijen, T.P.M.; Garibaldi, L.A.; Potts, S.G.; van der Putten, W.H. Ecological Intensification: Bridging the Gap between Science and Practice. *Trends Ecol. Evol.* **2019**, *34*, 154–166. [CrossRef] [PubMed]
17. Martin, E.A.; Dainese, M.; Clough, Y.; Báldi, A.; Bommarco, R.; Gagic, V.; Garratt, M.P.D.; Holzschuh, A.; Kleijn, D.; Kovács-Hostyánszki, A.; et al. The interplay of landscape composition and configuration: New pathways to manage functional biodiversity and agroecosystem services across Europe. *Ecol. Lett.* **2019**, *22*, 1083–1094. [CrossRef] [PubMed]
18. Magrach, A.; Giménez-García, A.; Allen-Perkins, A.; Garibaldi, L.A.; Bartomeus, I. Increasing crop richness and reducing field sizes provide higher yields to pollinator-dependent crops. *J. Appl. Ecol.* **2023**, *60*, 77–90. [CrossRef]
19. Parron, L.M.; Villanueva, A.J.; Glenk, K. Estimating the value of ecosystem services in agricultural landscapes amid intensification pressures: The Brazilian case. *Ecosyst. Serv.* **2022**, *57*, 101476. [CrossRef]
20. Puma, M.J.; Bose, S.; Chon, S.Y.; Cook, B.I. Assessing the evolving fragility of the global food system. *Environ. Res. Lett.* **2015**, *10*, 024007. [CrossRef]
21. Jauker, F.; Diekötter, T.; Schwarzbach, F.; Wolters, V. Pollinator dispersal in an agricultural matrix: Opposing responses of wild bees and hoverflies to landscape structure and distance from main habitat. *Landsc. Ecol.* **2009**, *24*, 547–555. [CrossRef]
22. Chaplin-Kramer, R.; O'Rourke, M.E.; Blitzer, E.J.; Kremen, C. A meta-analysis of crop pest and natural enemy response to landscape complexity. *Ecol. Lett.* **2011**, *14*, 922–932. [CrossRef]
23. Karp, D.S.; Chaplin-Kramer, R.; Meehan, T.D.; Martin, E.A.; DeClerck, F.; Grab, H.; Gratton, C.; Hunt, L.; Larsen, A.E.; Martínez-Salinas, A.; et al. Crop pests and predators exhibit inconsistent responses to surrounding landscape composition. *Proc. Natl. Acad. Sci. USA* **2018**, *115*, E7863–E7870. [CrossRef]
24. Pitt, W.J.; Kairy, L.R.; Mora, V.; Peirce, E.; Jensen, A.S.; Bradford, B.; Groves, R.; Christensen, T.; MacRae, I.; Nachappa, P. Landscapes with higher crop diversity have lower aphid species richness but higher plant virus prevalence. *J. Appl. Ecol.* **2024**, *61*, 1573–1586. [CrossRef]
25. Altieri, M.A.; Nicholls, C.I. An agroecological basis for designing diversified cropping systems in the tropics. In *New Dimensions in Agroecology*; Clements, D.R., Shrestha, A., Eds.; Haworth Press: New York, NY, USA, 2004.
26. Murphy-Bokern, D.; Stoddard, F.L.; Watson, C. *Legumes in Cropping Systems*; CAB International: Oxfordshire, UK, 2017.
27. Eustat. Producción Final Agraria de la C.A. de Euskadi por Sectores Según Territorio Histórico (Miles de Euros). 2016(*). 2016. Available online: https://www.eustat.eus/elementos/ele0000200/produccion-final-agraria-de-la-ca-de-euskadi-por-sectores-segun-territorio-historico-miles-de-euros/tbl0000245_c.html (accessed on 10 June 2024).
28. Ekolurra. Ekolurra.Cifras.Estadísticas 2020. *Estadísticas 31/12/2020—Operadores de Producción Agroalimentaria Ecológica de EUSKADI*. 2020. Available online: https://ekolurra.eus/wp-content/uploads/2022/07/ENEEK_Estatistika-2020.pdf (accessed on 7 May 2021).
29. Open Street Map. 2022. Available online: https://www.openstreetmap.org (accessed on 15 June 2022).
30. Goulet, H.; Huber, J.T. *Hymenoptera of the World: An Identification Guide to Family*; Centre for Land and Biological Resources Research, Agriculture Canada: Ottawa, ON, Canada, 1993.
31. Oosterbroek, P. *The European Families of the Diptera. Identification, Diagnosis, Biology*; KNNV Publishing: Utrecht, The Netherlands, 2006.
32. Bellmann, H. *Guía de Campo de los Insectos*; Ediciones OMEGA BCN, S.L.: Barcelona, Spain, 2018.
33. Magurran, A.E. *Measuring Biological Diversity*; John Wiley & Sons: New York, NY, USA, 2003.
34. QGIS Development Team. QGIS Geographic Information System; Open Source Geospatial Foundation Project; 2021. Available online: http://qgis.org (accessed on 20 February 2023).

35. Plexida, S.G.; Sfougaris, A.I.; Ispikoudis, I.P.; Papanastasis, V.P. Selecting landscape metrics as indicators of spatial heterogeneity-Acomparison among Greek landscapes. *Int. J. Appl. Earth Obs. Geoinf.* **2014**, *26*, 26–35.
36. Morelli, F.; Benedetti, Y.; Šímová, P. Landscape metrics as indicators of avian diversity and community measures. *Ecol. Indic.* **2018**, *90*, 132–141. [CrossRef]
37. Jaeger, J.A.G. Landscape division, splitting index, and effective mesh size: New measures of landscape fragmentation. *Landsc. Ecol.* **2000**, *15*, 115–130. [CrossRef]
38. Zhang, Y.; Haan, N.L.; Landis, D.A. Landscape composition and configuration have scale-dependent effects on agricultural pest suppression. *Agric. Ecosyst. Environ.* **2020**, *302*, 107085. [CrossRef]
39. R Core Team. *A Language and Environment for Statistical Computing*; R Foundation for Statistical Computing: Viena, Austria, 2022.
40. Tscharntke, T.; Karp, D.S.; Chaplin-Kramer, R.; Batáry, P.; DeClerck, F.; Gratton, C.; Hunt, L.; Ives, A.; Jonsson, M.; Larsen, A.; et al. When natural habitat fails to enhance biological pest control—Five hypotheses. *Biol. Conserv.* **2016**, *204*, 449–458. [CrossRef]
41. Tscharntke, T.; Tylianakis, J.M.; Rand, T.A.; Didham, R.K.; Fahrig, L.; Batáry, P.; Bengtsson, J.; Clough, Y.; Crist, T.O.; Dormann, C.F.; et al. Landscape moderation of biodiversity patterns and processes—Eight hypotheses. *Biol. Rev.* **2012**, *87*, 661–685. [CrossRef]
42. Šálek, M.; Hula, V.; Kipson, M.; Daňková, R.; Niedobová, J.; Gamero, A. Bringing diversity back to agriculture: Smaller fields and non-crop elements enhance biodiversity in intensively managed arable farmlands. *Ecol. Indic.* **2018**, *90*, 65–73. [CrossRef]
43. Proesmans, W.; Bonte, D.; Smagghe, G.; Meeus, I.; Decocq, G.; Spicher, F.; Kolb, A.; Lemke, I.; Diekmann, M.; Bruun, H.H.; et al. Small forest patches as pollinator habitat: Oases in an agricultural desert? *Landsc. Ecol.* **2019**, *34*, 487–501. [CrossRef]
44. Elisante, F.; Ndakidemi, P.; Arnold, S.E.J.; Belmain, S.R.; Gurr, G.M.; Darbyshire, I.; Xie, G.; Stevenson, P.C. Insect pollination is important in a smallholder bean farming system. *PeerJ* **2020**, *8*, e10102. [CrossRef]
45. Cunningham, S.A.; Schellhorn, N.A.; Marcora, A.; Batley, M. Movement and phenology of bees in a subtropical Australian agricultural landscape. *Austral Ecol.* **2013**, *38*, 456–464. [CrossRef]
46. Santos, A.; Fernandes, M.R.; Aguiar, F.C.; Branco, M.R.; Ferreira, M.T. Effects of riverine landscape changes on pollination services: A case study on the River Minho, Portugal. *Ecol. Indic.* **2018**, *89*, 656–666. [CrossRef]
47. Seibold, S.; Gossner, M.M.; Simons, N.K.; Blüthgen, N.; Müller, J.; Ambarlı, D.; Ammer, C.; Bauhus, J.; Fischer, M.; Habel, J.C.; et al. Arthropod decline in grasslands and forests is associated with landscape-level drivers. *Nature* **2019**, *574*, 671–674. [CrossRef] [PubMed]
48. Fijen, T.P.M.; Scheper, J.A.; Boekelo, B.; Raemakers, I.; Kleijn, D. Effects of landscape complexity on pollinators are moderated by pollinators' association with mass-flowering crops. *Proc. R. Soc. B Biol. Sci.* **2019**, *286*, 20190387. [CrossRef] [PubMed]
49. Delettre, Y.R.; Morvan, N.; Tréhen, P. Local biodiversity and multi-habitat use in empidoid flies (Insecta: Diptera, Empidoidea). *Biodivers. Conserv.* **1998**, *7*, 9–25. [CrossRef]
50. Słowińska, I.; Jaskuła, R. Distributional patterns of aquatic Empididae (Diptera) along an elevational diversity gradient in a low mountain range: An example from Central Europe. *Insects* **2021**, *12*, 165. [CrossRef] [PubMed]
51. Gurr, G.M.; Wratten, S.D.; Michael Luna, J. Multi-function agricultural biodiversity: Pest management and other benefits. *Basic Appl. Ecol.* **2003**, *4*, 107–116. [CrossRef]
52. Schmidt, M.H.; Tscharntke, T. The role of perennial habitats for Central European farmland spiders. *Agric. Ecosyst. Environ.* **2005**, *105*, 235–242. [CrossRef]
53. Rusch, A.; Chaplin-Kramer, R.; Gardiner, M.M.; Hawro, V.; Holland, J.; Landis, D.; Thies, C.; Tscharntke, T.; Weisser, W.W.; Winqvist, C.; et al. Agricultural landscape simplification reduces natural pest control: A quantitative synthesis. *Agric. Ecosyst. Environ.* **2016**, *221*, 198–204. [CrossRef]
54. Vickery, J.; Carter, N.; Fuller, R.J. The potential value of managed cereal field margins as foraging habitats for farmland birds in the UK. *Agric. Ecosyst. Environ.* **2002**, *89*, 41–52. [CrossRef]
55. Fahrig, L.; Girard, J.; Duro, D.; Pasher, J.; Smith, A.; Javorek, S.; King, D.; Lindsay, K.F.; Mitchell, S.; Tischendorf, L. Farmlands with smaller crop fields have higher within-field biodiversity. *Agric. Ecosyst. Environ.* **2015**, *200*, 219–234. [CrossRef]
56. Bianchi, F.J.J.A.; Booij, C.J.H.; Tscharntke, T. Sustainable pest regulation in agricultural landscapes: A review on landscape composition, biodiversity and natural pest control. *Proc. R. Soc. B Biol. Sci.* **2006**, *273*, 1715–1727. [CrossRef] [PubMed]
57. Botha, M.; Siebert, S.J.; van den Berg, J. Grass abundance maintains positive plant–arthropod diversity relationships in maize fields and margins in South Africa. *Agric. For. Entomol.* **2017**, *19*, 154–162. [CrossRef]
58. Nagy, R.K.; Bell, L.W.; Schellhorn, N.A.; Zalucki, M.P. Role of grasslands in pest suppressive landscapes: How green are my pastures? *Austral Entomol.* **2020**, *59*, 227–237. [CrossRef]
59. Hendrickx, F.; Maelfait, J.P.; Van Wingerden, W.; Schweiger, O.; Speelmans, M.; Aviron, S.; Augenstein, I.; Billeter, R.; Bailey, D.; Bukacek, R.; et al. How landscape structure, land-use intensity and habitat diversity affect components of total arthropod diversity in agricultural landscapes. *J. Appl. Ecol.* **2007**, *44*, 340–351. [CrossRef]
60. Martin, E.A.; Seo, B.; Park, C.R.; Reineking, B.; Steffan-Dewenter, I. Scale-dependent effects of landscape composition and configuration on natural enemy diversity, crop herbivory, and yields. *Ecol. Appl.* **2016**, *26*, 448–462. [CrossRef]
61. Gray, C.L.; Lewis, O.T. Do riparian forest fragments provide ecosystem services or disservices in surrounding oil palm plantations? *Basic Appl. Ecol.* **2014**, *15*, 693–700. [CrossRef]

62. Heimoana, V.; Pilkington, L.J.; Raman, A.; Mitchell, A.; Nicol, H.I.; Johnson, A.C.; Gurr, G.M. Integrating spatially explicit molecular and ecological methods to explore the significance of non-crop vegetation to predators of brassica pests. *Agric. Ecosyst. Environ.* **2017**, *239*, 12–19. [CrossRef]
63. Madeira, F.; Clemente-Orta, G.; Alomar, O.; Batuecas, I.; Sossai, S.; Albajes, R. Land use alters the abundance of herbivore and predatory insects on crops: The case of alfalfa. *J. Pest Sci.* **2022**, *95*, 473–491. [CrossRef]
64. Popescu, C.; Oprina-Pavelescu, M.; Dinu, V.; Cazacu, C.; Burdon, F.J.; Forio, M.A.E.; Kupilas, B.; Friberg, N.; Goethals, P.; McKie, B.G.; et al. Riparian vegetation structure influences terrestrial invertebrate communities in an agricultural landscape. *Water* **2021**, *13*, 188. [CrossRef]
65. Tamburini, G.; Santoiemma, G.; O'Rourke, M.E.; Bommarco, R.; Chaplin-Kramer, R.; Dainese, M.; Karp, D.S.; Kim, T.N.; Martin, E.A.; Petersen, M.; et al. Species traits elucidate crop pest response to landscape composition: A global analysis. *Proc. R. Soc. B Biol. Sci.* **2020**, *287*, 20202116. [CrossRef]
66. Stinson, C.S.; Brown, V.K. Seasonal changes in the architecture of natural plant communities and its relevance to insect herbivores. *Oecologia* **1983**, *56*, 67–69. [CrossRef] [PubMed]
67. Montero, G. Ecología de las interacciones entre malezas y artrópodos. In *Malezas e Invasoras de la Argentina: Ecología y Manejo. Tomo I*; Fernández, O., Acciaresi, H.A., Leguizamón, E., Eds.; Editorial Universidad Nacional del Sur: Bahía Blanca, Argentina, 2014; pp. 267–305.
68. Mkenda, P.A.; Ndakidemi, P.A.; Stevenson, P.C.; Sarah, S.E.; Belmain, S.R.; Chidege, M.; Gurr, G.M. Field margin vegetation in tropical african bean systems harbours diverse natural enemies for biological pest control in adjacent crops. *Sustainability* **2019**, *11*, 6399. [CrossRef]

land

MDPI

Article

Multi-Scenario Simulation of Ecosystem Service Value in Beijing's Green Belts Based on PLUS Model

Ziying Hu [1,†] and Siyuan Wang [1,2,3,*,†]

[1] School of Landscape Architecture, Beijing Forestry University, Beijing 100083, China; huziying6053@bjfu.edu.cn

[2] Beijing Laboratory of Urban and Rural Ecology and Environment, Beijing Forestry University, Beijing 100083, China

[3] National Forestry and Grassland Administration Key Laboratory of Urban and Rural Landscape Construction, Beijing Forestry University, Beijing 100083, China

* Correspondence: wangsyuan@bjfu.edu.cn

† These authors contributed equally to this work.

Abstract: Urbanization and economic growth have substantially modified the land utilization structure, affecting ecosystem services and their spatial distribution. As a crucial component of Beijing's urban framework, the city's green belts, located at the periphery of its core metropolitan area, play a vital role in supplying urban ecosystem services. They also represent a focal point for land use transformation conflicts, making them an important study area. This research utilizes land utilization data from 2000, 2005, 2010, 2015, and 2020 as the primary dataset. It adopts a modified standard equivalent factor and integrates it with the Patch-Generaling Land Use Simulation (PLUS) model to model land utilization in Beijing's green belts for 2035 under three scenarios: the natural development scenario (NDS), ecological protection scenario (EPS) and cultivated protection scenario (CPS). The study aims to analyze and project the spatial and temporal evolution of ecosystem service values (ESVs) in 2035 under different scenarios in the green belts of Beijing. The results indicate that (1) land use in Beijing's green belts is dominated by cropland and construction land. Construction land has expanded significantly since 2000, increasing by 500.78 km^2, while cropland has decreased by 488.47 km^2. Woodland, grassland, and water have also seen a reduction. Overall, there is a trend of woodland and water being converted into cropland, with cropland subsequently transitioning into construction land. (2) In the NDS, construction land increases by 91.76 km^2, while cropland, grassland, and water decrease. In EDS, the growth of construction land decelerates to 22.09 km^2, the reduction in cropland decelerates, and the conversion of cropland to construction land is limited. Grassland and water remain largely unchanged, and woodland experiences a slight increase. In CPS, the conversion of cropland to construction land is notably reduced, with construction land increasing by 11.97 km^2, woodland increasing slightly, and grassland and water decreasing slightly. (3) The ESV ranking across scenarios is as follows: EPS 1830.72 mln yuan > CPS 1816.23 mln yuan > NDS 1723.28 mln yuan. Hydrological regulation and climate regulation are the dominant services in all scenarios. ESV in EPS attains the greatest economic gains. This study contributes to understanding the effects of land utilization changes on ESV, offering valuable empirical evidence for sustainable development decision-making in swiftly urbanizing areas.

Keywords: land use; green belt; PLUS model; driving factors; multi-scenario modeling; ecosystem service values

1. Introduction

Urbanization continues to accelerate globally, driven by the concentration of populations in cities, which fosters the expansion of urban boundaries and infrastructure development. While this process contributes to economic growth and social development, it also results in the encroachment of ecological and agricultural lands [1]. Ecosystem services (ES) form the foundation of the resources and environmental systems that sustain human life and sustainable development [2,3]. Frequent human activities, however, are continually altering the land use/land cover (LULC) patterns, which in turn affect the supply and distribution of these services [4,5].

In recent years, scholars have conducted extensive investigations into ecosystem services from diverse perspectives. Regarding research scope, since Costanza's [6] pioneering global-scale ES valuation in 1997, subsequent studies have progressively refined their focus to regional scales, examining specific ecosystems including forests [7–9], grasslands [10–12], agricultural lands [13,14], wetlands [15–17] and coastal environments [18–20]. The research paradigm has evolved from static assessments of single ecosystems like forests and wetlands to dynamic analyses of complex systems such as urban–rural ecotones. Current research dimensions encompass multiple aspects: quantitative methodologies for ecosystem service evaluation [21–24], the spatiotemporal pattern analysis of ecosystem services [25], and the investigation of service trade-offs and synergies [26]. Methodologically, the application of specialized tools such as the InVEST model [27,28] and SolVES model [29,30] has facilitated significant advancements from basic spatial mapping to sophisticated quantitative assessments. These methodological developments provide crucial insights for understanding the complexity of urban ecosystem services and their multidimensional impacts on human well-being.

International precedents such as the London Metropolitan Green Belt [31,32] and Seoul Green Belt [33,34] demonstrate the perpetual tensions between urban expansion imperatives and ecological conservation in peri-urban transitional zones. Functioning as critical buffer areas between urban and rural landscapes, these greenbelts maintain vital ecological functions while playing important socio-economic roles. This study's selection of the Beijing Greenbelt Area as its research focus addresses both empirical and theoretical imperatives. As China's capital undergoing rapid urbanization, Beijing presents the prototypical urban ecological challenges prevalent among global megacities [35]. The research outcomes possess significant generalizability, offering methodological references for comparable regions worldwide.

The methodological framework of this study involves employing the Patch-Generaling Land Use Simulation (PLUS) model for future land use simulation, followed by ecosystem service value (ESV) assessment utilizing the equivalent value factor method. Current spatial simulation models for land use change, including the CA-Markov [36,37], ANN-CA [38], CLUS-S [39], Dyna-CLUE [40], and FLUS [41] models, etc., exhibit limitations in simulating land use patch transformation processes. These models demonstrate insufficient accuracy in ecological condition assessment due to their failure to account for temporal and spatial variations [42]. Compared with alternative models, the PLUS model demonstrates significant advantages by better elucidating the relationship between land use changes and their driving factors, thereby enhancing the precision of regional land use simulations. To address the inherent limitation of the equivalent value method in capturing ESV's spatiotemporal dynamics, Xie [43] enhanced this methodology by integrating the characteristics of China's ecosystems. In this research, we have adopted Xie's improved framework as a theoretical foundation and have further refined the equivalent factor table through the incorporation of Beijing's grain price data and Net Primary Productivity (NPP) data, consequently improving the accuracy of ESV assessment.

2. Materials and Methods

2.1. Study Area

Beijing is the capital of the People's Republic of China. It is located on the northern edge of the North China Plain (115°25′–117°35′ E, 39°28′–41°05′ N) and spans a total land area of 1.68×10^4 km^2. With four distinct seasons, the city has a warm temperate continental monsoon climate. The annual precipitation is 595 mm, with the majority occurring from June to September. Beijing, as the capital city of China and a megacity, features a unique urban planning approach characterized by a "decentralized group approach". From the outset of urban planning, Beijing's green belts served as an ecological buffer zone between the core urban areas and the surrounding built-up regions. They have also been a focal point for land use conflict during the process of urban development.

The Greenbelt Area of Beijing covers approximately 1220 square kilometers. The First Greenbelt Area, encompassing a policy-defined scope of approximately 310 square kilometers, is designed to safeguard the ecological security framework of the central urban area. The Second Greenbelt Area, covering around 910 square kilometers, extends beyond the First Greenbelt's policy boundary to the outer edge of the Sixth Ring Road. This zone provides extensive green space and serves as a strategic reserve to enhance urban ecological resilience and consolidate the ecological security structure of the plain region. Although the Second Greenbelt Area is delimited based on the urban ecological structure during planning, its implementation is coordinated with township administrative units, leading to a certain degree of policy mismatch. The scope of this study encompasses all township administrative units involved in the relevant planning of the Greenbelt Area, covering an area of 2058.19 km^2, as shown in Figure 1.

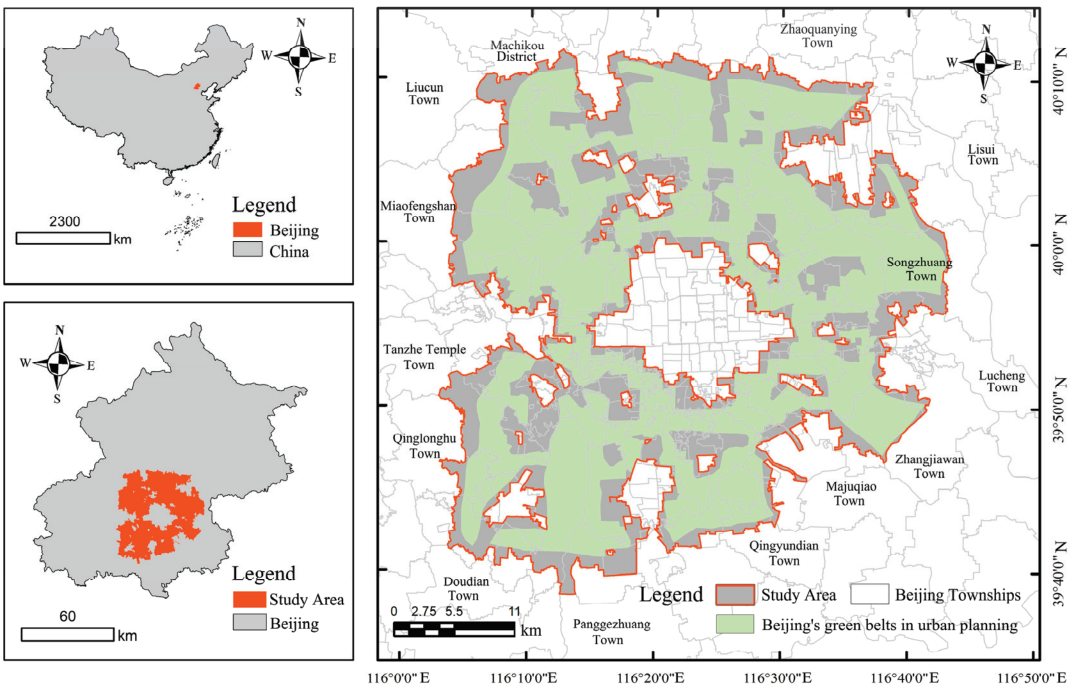

Figure 1. Location and study area.

2.2. Data Sources

The data utilized in this study consist of land use data and driving factors data. The land utilization data were obtained from the China Land Cover Dataset (CLCD), covering five time periods, with a spatial resolution of 30 m: 2000, 2005, 2010, 2015, and 2020. In the selection of driving factors, this paper considered the combined effects of natural, social, and economic [44] conditions. Thirteen driving factors were chosen (Figure 2) based on the principles of data accessibility, spatial characteristics, and comprehensiveness. The data types and their origins are outlined in Table 1.

Table 1. Data information.

Data	Subdata	Year	Format	Resolution	Institution	Website
Land use data	Land use	2000–2020	Grid	30 m	China Land Cover Dataset (CLCD)	https://zenodo.org/records/12779975 (accessed on 20 December 2024).
Climate and environmental data	Annual precipitation	2022	Grid	1000 m	National Earth System Science Data Center (NESSDC)	http://www.geodata.cn/ (accessed on 20 December 2024).
	Annual temperature	2022	Grid	1000 m	NESSDC	http://www.geodata.cn/ (accessed on 20 December 2024).
	Elevation	2024	Grid	30 m	Geospatial data cloud	https://www.gscloud.cn/ (accessed on 20 December 2024).
	Slop	2024	Grid	30 m	calculated from DEM	/
	Soil type	2018	Shpfile	-	NESSDC	http://www.geodata.cn/ (accessed on 20 December 2024).
	Distance to water	2024	Shpfile	-	Open Street Map (OSM)	https://www.openstreetmap.org/ (accessed on 20 December 2024).
Socio-economic data	GDP	2020	Grid	1000 m	Resources and Environmental Science and Data Center, Chinese Academy of Sciences	https://www.resdc.cn/ (accessed on 20 December 2024).
	Population	2020	Grid	100 m	WorldPop	https://www.worldpop.org/ (accessed on 20 December 2024).
	Railway	2024	Shpfile	-	OSM	https://www.openstreetmap.org/ (accessed on 20 December 2024).
	Motorway	2024	Shpfile	-	OSM	https://www.openstreetmap.org/ (accessed on 20 December 2024).
	Primary road	2024	Shpfile	-	OSM	https://www.openstreetmap.org/ (accessed on 20 December 2024).
	Secondary road	2024	Shpfile	-	OSM	https://www.openstreetmap.org/ (accessed on 20 December 2024).
	Tertiary roads	2024	Shpfile	-	OSM	https://www.openstreetmap.org/ (accessed on 20 December 2024).

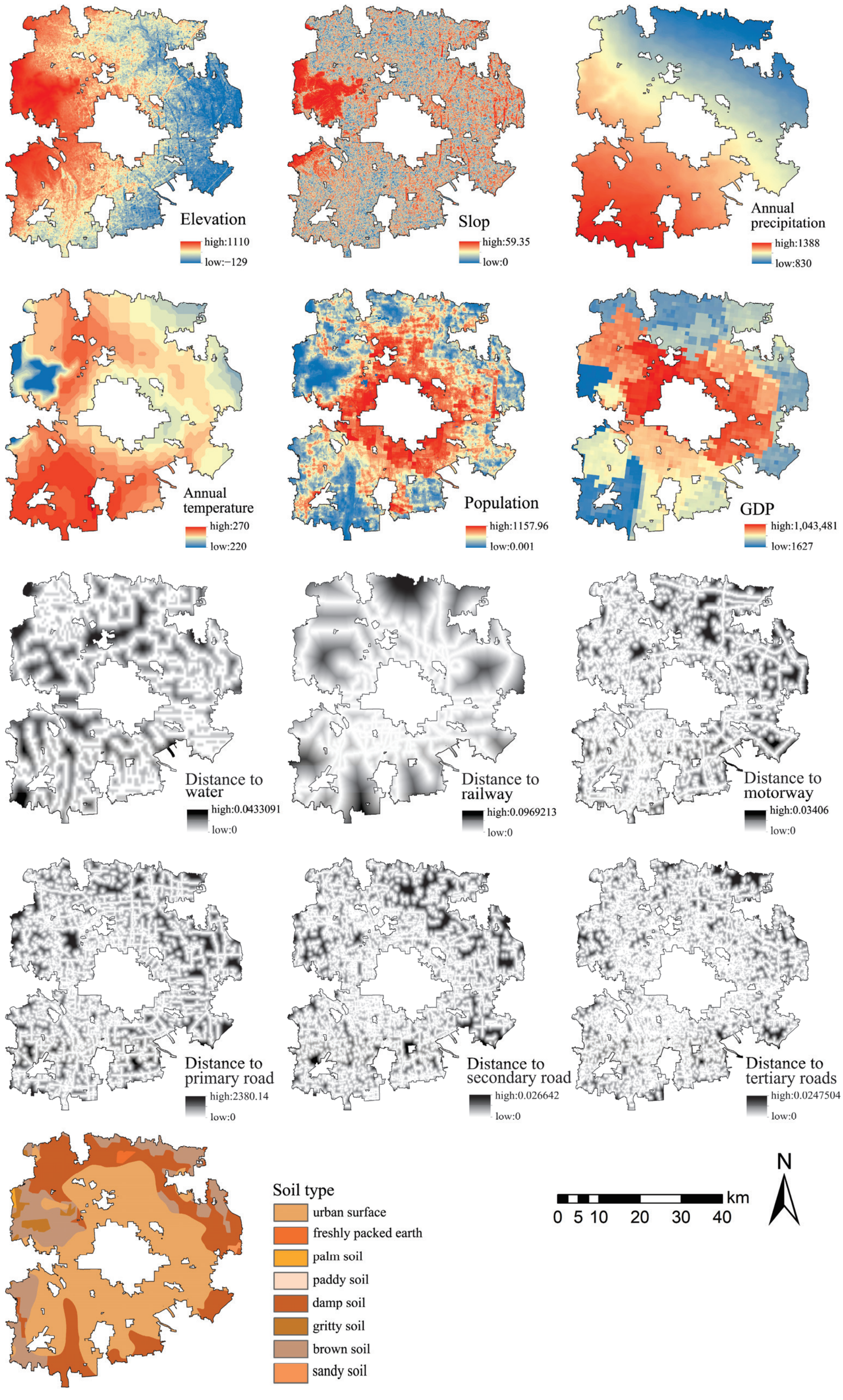

Figure 2. Driving factors.

3. Methodology

The research framework was divided into three parts, as shown in Figure 3. The first part was data preparation, including the CLCD dataset, the data of the 13 driving factors, and the relevant policies on land use in Beijing. The second part was the simulation of land use in Beijing's green belts in 2035 under the NDS, EPS, and CPS, using the PLUS model. The third part involved analyzing and predicting the spatial and temporal evolution of ESV in Beijing's green belts using the modified standard equivalent factor.

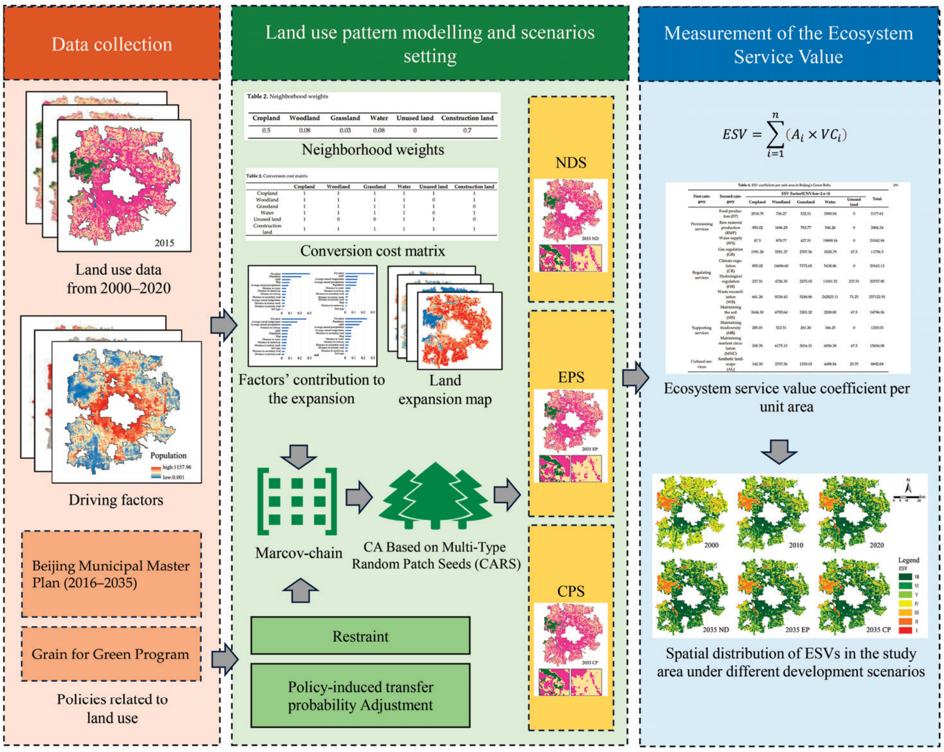

Figure 3. The framework of the study.

3.1. Land Use Change (LUC) Analysis

In this research, the land use transfer matrix approach [45] was employed to present the variations in different land utilization types in the study area between 2000 and 2020, as well as the transitions between these types. The formula used for constructing the transfer matrix is as follows:

$$S_{ij} = \begin{bmatrix} S_{11} & S_{12} & \dots & S_{1n} \\ S_{21} & S_{22} & \dots & S_{2n} \\ \dots & \dots & \dots & \dots \\ S_{n1} & S_{n2} & \dots & S_{nn} \end{bmatrix} \tag{1}$$

In the formula: S_{ij} represents the area of each land use type, i denotes the initial land use type, j is the terminal land use type and n is the number of land use types.

The single land use dynamics (K), which indicate the rate of the quantitative change for a specific land use type within the study area over a given time frame, is expressed using the following formula:

$$K = \frac{U_b - U_a}{U_a} \times \frac{1}{T} \times 100\% \tag{2}$$

In the formula, K represents the single land use dynamics of a land use type in the study area; U_a and U_b are the areas of the land use type at the beginning and at the end of the study period; and T denotes the number of years between the beginning and the end periods.

3.2. PLUS Model

3.2.1. A Rule-Mining Framework Based on a Land Expansion Analysis Strategy (LEAS)

The LEAS module can investigate the relationship between the expansion among land use types and its driving factors [46,47]. The formula used in this process is as follows:

$$P_{i,k}^{d}(x) = \frac{\sum_{n=1}^{M} I(h_x(x) = d)}{M} \tag{3}$$

In the formula, the value of d is 0 or 1, with a value of 1 indicating a shift from other land use types to k land use types, and a value of 0 indicating other shifts; x is a vector consisting of multiple driving factors; $I(\cdot)$ is an indicator function for the set of decision trees; $h_x(x)$ represents the prediction type of the nth decision tree for vector x; and M denotes the total number of decision trees.

3.2.2. Markov-Based Land Use Quantity Projections

The Markov model is a prediction method [48] that estimates the probability of an event occurring based on its initial state and the matrix of state transition probabilities. It predicts the likelihood of various states occurring in the future. The transfer probability P_{ij} at moment n is calculated as follows:

$$P_{ij} = \begin{bmatrix} P_{11} & P_{12} & \cdots & P_{n1} \\ P_{21} & P_{22} & \cdots & P_{n2} \\ \vdots & \vdots & \cdots & \vdots \\ P_{1n} & P_{2n} & \cdots & P_{nn} \end{bmatrix} \tag{4}$$

$$S_{t+1} = P_{ij} \times S_t \tag{5}$$

In the formula, P_{ij} denotes the probability of land use type i converting to land use type j; n represents the number of land use types; and S_t and S_{t+1} are the states of land use types at moments t and $t+1$, respectively.

3.2.3. CARS-Based Spatial Modelling of Land Use

The CARS module [49] was also developed based on the CA theory to study LUC spatial simulations. The formula for calculating the overall transition probability $OP_{i,k}^{d-1,t}$ of land use type k is represented as follows:

$$OP_{i,k}^{d-1,t} = P_{i,k}^{d} \times \Omega_{i,k}^{t} \times D_{k}^{t} \tag{6}$$

In the formula, $P_{i,k}^{d}$ represents the probability of land use type k growing for the i -th cell; $\Omega_{i,k}^{t}$ represents the neighborhood effect for cell i; and D_{k}^{t} represents the influence of the future demand for land use type k, expressed as an adaptive driving coefficient that depends on the gap between the current land quantity and the target demand for land use type k at iteration t.

3.2.4. Different Scenario Settings

The design of land use scenarios establishes competitive conditions and defines conversion constraints for land use changes under varying policy frameworks. This is achieved by adjusting neighborhood weights and land use transition matrices [50]. In multi-scenario simulations, changes in neighborhood weights affect the overall transition probabilities of land use types, while transition matrices impose specific restrictions on the transitions between certain land use categories. This paper is informed by key Chinese land management policies, including the "Beijing Municipal Master Plan (2016–2035)", the "14th Five-Year

Plan" for development, the national policy to prevent the "non-agriculturalization" of cultivated land, and the "Grain for Green" ecological restoration initiative. Based on these guiding frameworks, three distinct land use scenarios were formulated: natural development, ecological priority, and cultivated land protection. The settings for neighborhood weights and land use transition matrices corresponding to these scenarios are detailed in Tables 2 and 3.

Table 2. Neighborhood weights.

Cropland	Woodland	Grassland	Water	Unused Land	Construction Land
0.5	0.08	0.03	0.08	0	0.7

Table 3. Conversion cost matrix.

	Cropland	Woodland	Grassland	Water	Unused Land	Construction Land
Cropland	1	1	1	1	1	1
Woodland	1	1	1	1	0	1
Grassland	1	1	1	1	1	0
Water	1	1	1	1	0	1
Unused land	1	0	0	1	1	0
Construction land	1	1	1	1	1	1

The natural development scenario (NDS) assumes that land use changes proceed in accordance with historical trends, without being directly influenced by specific planning policies. In this scenario, neighborhood weights are derived from historical land use expansion data, and the land use transition matrix is designed without incorporating external interventions or imposing conversion restrictions.

The ecological protection scenario (EPS) prioritizes ecological protection and sustainable development. Under this scenario, the strict enforcement of ecological protection red lines is required, with a focus on gradually expanding ecological spaces, strengthening water conservation measures, and establishing a stable, high-quality ecological security barrier. Specific measures include prohibiting the conversion of forests and grasslands to agricultural land, orchards, or other land uses. The probability of agricultural land transforming into construction land is decreased by 30% [51], while the probability of forest and grassland converting to construction land is reduced by 50%; additionally, the probability of agricultural land and grassland converting to forest is increased by 30%. With a 15-year interval, the land use configuration for 2035 under the ecological priority scenario is predicted based on 2020 data.

The cultivated protection scenario (CPS) is dedicated to ensure national food security by strictly preventing the "non-agriculturalization" and "non-food crop cultivation" of agricultural land. This scenario emphasizes stringent control over the conversion of agricultural land, and aims to guarantee the effective protection of agricultural land. Compared to the natural growth scenario, the probability of agricultural land converting to construction land is reduced by 60% [52]. Using a 15-year interval, the land use configuration under the CPS in 2035 is predicted based on 2020 data.

3.2.5. Accuracy Validation of PLUS Model Results

The validation method involved simulating the land use in 2020 based on 2015 at 5-year intervals, and then calculating the kappa coefficients by comparing the simulation results with the real 2020 land use data. The accuracy evaluation was based on the Kappa coefficient and overall accuracy, where values closer to 1 indicate a higher simulation accuracy. A Kappa coefficient exceeding 0.8 signifies that the simulation accuracy of the model is statistically satisfactory [53]. For the simulation results, the Kappa coefficient was 0.87 and the overall accuracy was 0.94. This shows a strong resemblance between the simulation results for 2020 and the spatial pattern of the modelling results, further validating the model's reliability.

3.3. Measurement of the ESV

In this study, a grid resolution of 300 m × 300 m [54,55] was used as the unit of analysis to quantify the ESV within the study area, employing the equivalent factor method. Originally proposed by Costanza [6] et al., this method was later improved by Xie [43] et al., who derived the equivalent ESV for China. Based on Xie's equivalent values for various land use types, this study further revised the equivalent factor table using findings from relevant research, as well as data on grain prices and the net primary productivity (NPP) specific to Beijing. The revision formulas are provided in Equations (7) and (8), and the calculation formula for ESV is given in Formula (9). The ESV coefficients for the study area are presented in Table 4.

$$E_t = \frac{1}{7} \times \frac{T_t}{X_t} \quad (7)$$

Table 4. ESV coefficient per unit area in Beijing's Green Belts.

First Category	Second Category	ESV Factor/(CNY·hm^{-2}·a^{-1})					Total
		Cropland	Woodland	Grassland	Water	Unused Land	
Provisioning services	Food production (FP)	2018.79	736.27	522.51	1900.04	0	5177.61
	Raw material production (RMP)	950.02	1686.29	783.77	546.26	0	3966.34
	Water supply (WS)	47.5	878.77	427.51	19,689.16	0	21,042.94
Regulating services	Gas regulation (GR)	1591.28	5581.37	2707.56	1828.79	47.5	11,756.5
	Climate regulation (CR)	855.02	16,696.60	7172.65	5438.86	0	30,163.13
	Hydrological regulation (HR)	237.51	4726.35	2375.05	13,181.53	237.51	20,757.95
	Waste reconciliation (WR)	641.26	8336.43	5248.86	242,825.11	71.25	257,122.91
Supporting services	Maintaining the soil (MS)	2446.30	6792.64	3301.32	2208.80	47.5	14,796.56
	Maintaining biodiversity (MB)	285.01	522.51	261.26	166.25	0	1235.03
	Maintaining nutrient circulation (MNC)	308.76	6175.13	3016.31	6056.38	47.5	15,604.08
Cultural services	Aesthetic landscape (AL)	142.50	2707.56	1330.03	4488.84	23.75	8692.68

In the formula, E_t represents the economic value of grain yield per unit area (yuan/hm^2); T_t represents the total annual value of grain in the study area (yuan); and X_t represents the annual sown area of grain in the study area (hm^2).

$$Q_t = \frac{NPP}{NPP_{mean}} \quad (8)$$

In the formula, Q_t represents the regional difference coefficient in year t, and NPP_{mean} represents the NPP of an average level of natural vegetation in China (t·hm^{-2}·a^{-1}).

$$ESV = \sum_{i=1}^{n}(A_i \times VC_i) \tag{9}$$

In the formula, A_i represents the area of land use type i and VC_i represents the ecosystem service value per unit area for the ith land use type.

In order to investigate the spatial differentiation characteristics of ESV in the green belts of Beijing, the ESV of the study area was divided into 7 classes according to the geometric segmentation method [56] in the ArcGIS 10.8 standard classification system. The value intervals of classes I to VII were [0, 8479), [8479, 28,707), [28,707, 76,963), [76,963, 192,086), [192,086, 466,726), [466,726, 1,121,919), [11,121,919, 2,684,970).

4. Results

4.1. LUC from 2000 to 2020

LUC in Beijing's green belts is predominantly characterized by cropland and construction land (Table 5). Since 2000, significant construction land expansion has been observed, increasing by 500.78 km^2. Conversely, the cropland area has decreased by 488.47 km^2, while woodland and grassland have decreased by 9.67 km^2, 2.37 km^2, respectively. A substantial amount of cropland has been converted into construction land, with a transfer volume of 497.86 km^2. Additionally, woodland and water have been converted into cropland, with transfer volumes of 14.52 km^2, and 5.89 km^2, respectively. Meanwhile, some cropland has transitioned to woodland and water, with transfer volumes of 6.89 km^2 and 5.69 km^2, respectively. Overall, the region exhibits a trend of woodland and water being converted into cropland, and cropland being converted into construction land. In terms of the spatial distribution, construction land is concentrated in the central region, cropland dominates the peripheral areas, and woodland is primarily distributed in the northwestern areas near Beijing's shallow mountainous regions and along the Yongding River (Figure 4). Between 2000 and 2020, construction land in the central urban area expanded significantly, reflecting the ongoing process of urbanization. This expansion of construction land was accompanied by a decrease in cropland, woodland, grassland, and watersheds.

Table 5. Land use area and single land use dynamics.

Land Use Type		Cropland	Woodland	Grassland	Water	Unused Land	Construction Land
Area/km^2	2000	1091.27	124.86	3.48	21.28	0.05	817.26
	2005	885.92	121.26	2.84	18.31	0.03	1029.82
	2010	730.35	123.38	3.61	17.33	0.03	1183.50
	2015	637.85	113.63	1.60	21.62	0.02	1283.47
	2020	602.80	115.18	1.11	21.00	0.05	1318.04
K/%	2000–2005	−3.76	−0.58	−3.65	−2.78	−9.12	5.20
	2005–2010	−3.51	0.35	5.38	−1.08	0.00	2.98
	2010–2015	−2.53	−1.58	−11.14	4.95	−5.16	1.69
	2015–2020	−1.10	0.27	−6.10	−0.57	26.96	0.54
	2000–2020	−2.24	−0.39	−3.40	−0.06	−0.26	3.06

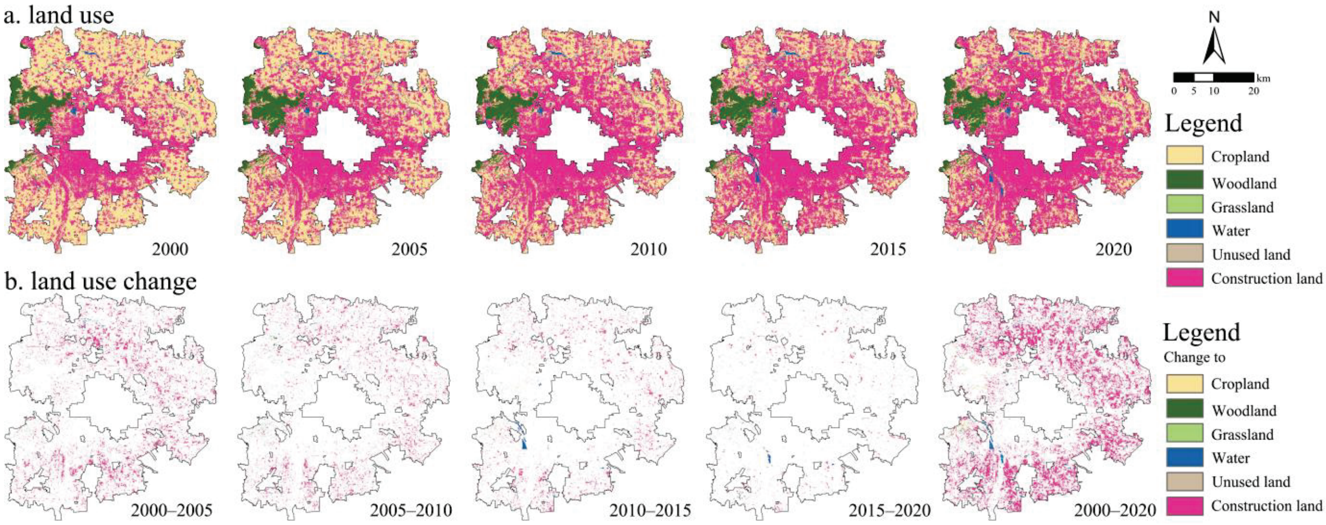

Figure 4. LUC from 2000 to 2020. (**a**) Land use; (**b**) Land use change.

4.2. Probability of Expansion of LUC

The contribution of driving factors to the main land cover types (cropland, woodland, water, construction land) and the spatial probabilities of land use development are presented in Figure 5. Significant differences were observed in the contribution of each driving factor to the distribution of various land cover types. For cropland, DEM and POP exhibited the highest explanatory contributions. In contrast, for forest land dynamics, the DEM and average temperature demonstrated the greatest driving contributions. These findings highlight the varying degrees of influence that different drivers exert on the spatial distribution of specific land cover types.

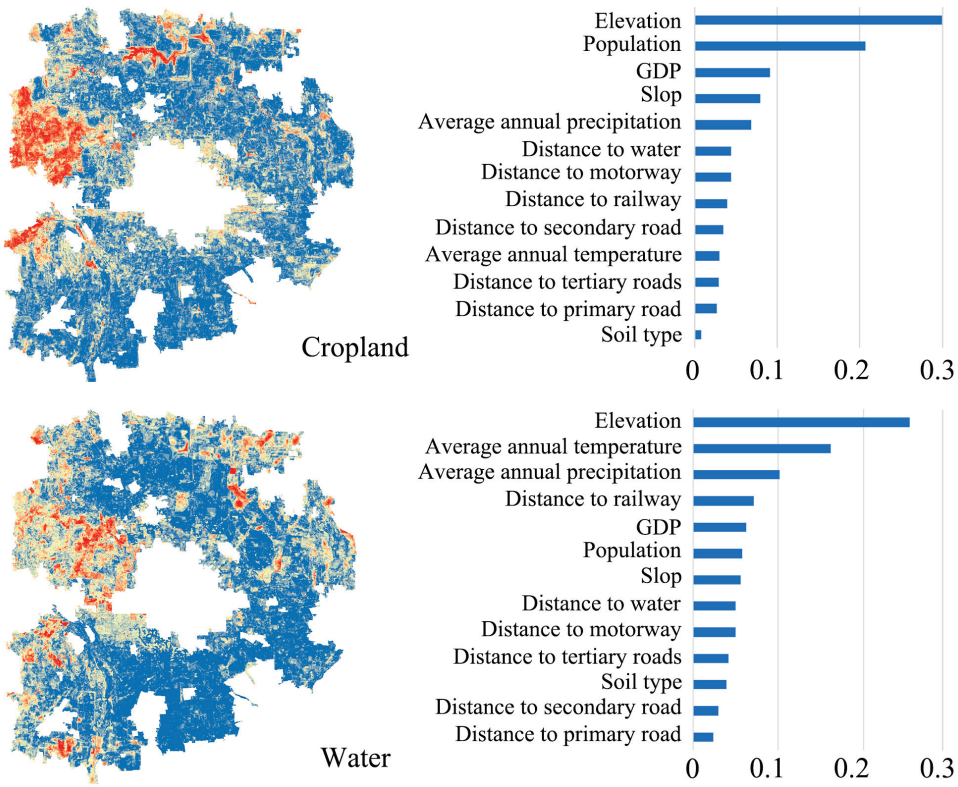

Figure 5. *Cont.*

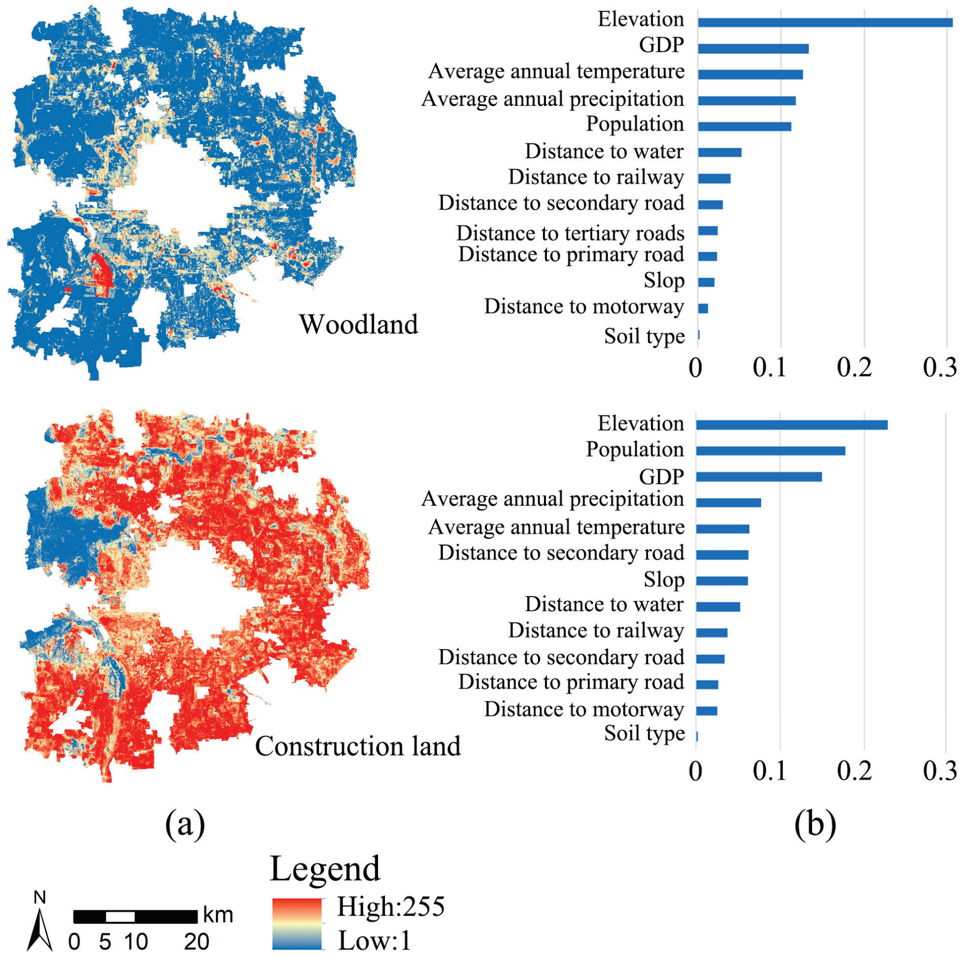

Figure 5. (**a**) Atlas of expansion probability; (**b**) Contribution of drivers to expansion.

4.3. LUC Simulation Results for Different Scenarios in 2035

Figure 6 illustrates the spatial distribution of projected land use types for 2035. Table 6 presents the corresponding quantitative data, including the area and the percentage change relative to the baseline year 2020, demonstrating notable shifts and trends in land use dynamics.

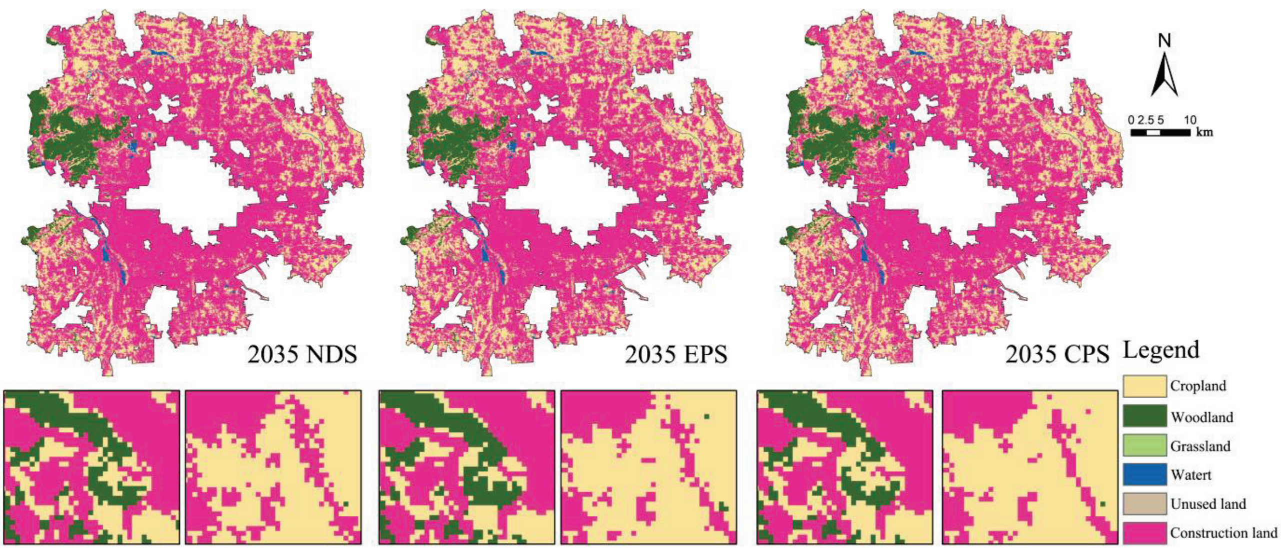

Figure 6. Simulation of spatial distribution of land use under different scenarios in 2035.

Table 6. Prediction of land use structure under different scenarios.

Year	Index	Cropland	Woodland	Grassland	Water	Unused Land	Construction Land
2020	Area/km^2	602.80	115.18	1.11	21.00	0.05	1318.04
2035 NDS	Area/km^2	510.33	117.69	0.53	19.79	0.05	1409.80
	change	−92.47	2.51	−0.58	−1.21	0.00	91.76
2035 EPS	Area/km^2	578.54	117.63	0.83	21.00	0.05	1340.13
	change	−24.26	2.45	−0.28	0.00	0.00	22.09
2035 CPS	Area/km^2	590.23	116.54	0.82	20.54	0.05	1330.01
	change	−12.57	1.36	−0.29	−0.47	0.00	11.97

In NDS, land use changes are projected to continue along the trends observed between 2015 and 2020. Construction land is expected to expand by 91.76 km^2, primarily in the northern part of Haidian District, the eastern part of Chaoyang District, the northwestern part of Daxing District, and the northeastern part of Fangshan District. Meanwhile, cropland is projected to decrease by 92.47 km^2. Grassland and water bodies are also anticipated to decrease by 0.58 km^2 and 1.21 km^2, respectively.

In EPS, the expansion of construction land will slow down, and the decrease in cultivated land will decelerate. The rate at which cultivated land is converted into construction land will diminish. Grassland and water bodies are expected to remain largely unchanged, while woodland will experience a slight increase. Specifically, construction land will expand by 22.09 km^2, cultivated land will decrease by 24.26 km^2, and forestland will increase by 2.45 km^2. Furthermore, 0.7 km^2 of grassland and 0.42 km^2 of water bodies will be converted into woodland. Land use conversions from cropland, grassland and water will occur in the eastern Fangshan District, the eastern Mentougou District, and the western Haidian District.

In CPS, the conversion of cropland to construction land will decrease significantly. Construction land will increase by 11.97 km^2, while cropland will decrease by 12.57 km^2. Woodland will experience a slight increase of 1.36 km^2, and both grassland and water bodies will decrease slightly, by 0.29 km^2 and 0.47 km^2, respectively.

4.4. ESV Simulation Results for Different Scenarios

Figure 7 and Table 7 illustrate the ESV of Beijing in different years (2000, 2010, 2020), along with projections for 2035 under the NDS, EPS, and CPS in 2035.

Table 7. ESV for each ecological service type under multi-scenario modeling/million yuan.

First Category	Second Category	2000	2010	2020	2035		
					NDS	EPS	CPS
Provisioning services	FP	233.72	160.01	134.22	115.48	129.60	131.68
	RMP	126.16	91.42	77.92	69.45	76.18	76.91
	WS	58.20	48.59	54.38	51.75	54.56	53.52
Regulating services	GR	248.17	189.23	164.35	150.66	162.37	162.95
	CR	315.85	280.46	256.07	251.28	259.44	256.81
	HR	113.81	99.36	96.70	93.96	97.73	96.37
	WR	692.63	572.40	645.19	611.67	646.67	634.20
Supporting services	MS	357.62	267.49	230.71	209.33	227.06	228.36
	MB	38.07	27.64	23.58	21.04	23.06	23.27
	MNC	124.73	110.32	102.79	100.58	104.12	102.88
Cultural services	AL	59.37	52.07	49.35	48.09	49.92	49.29
Total		2368.35	1899.00	1835.26	1723.28	1830.72	1816.23

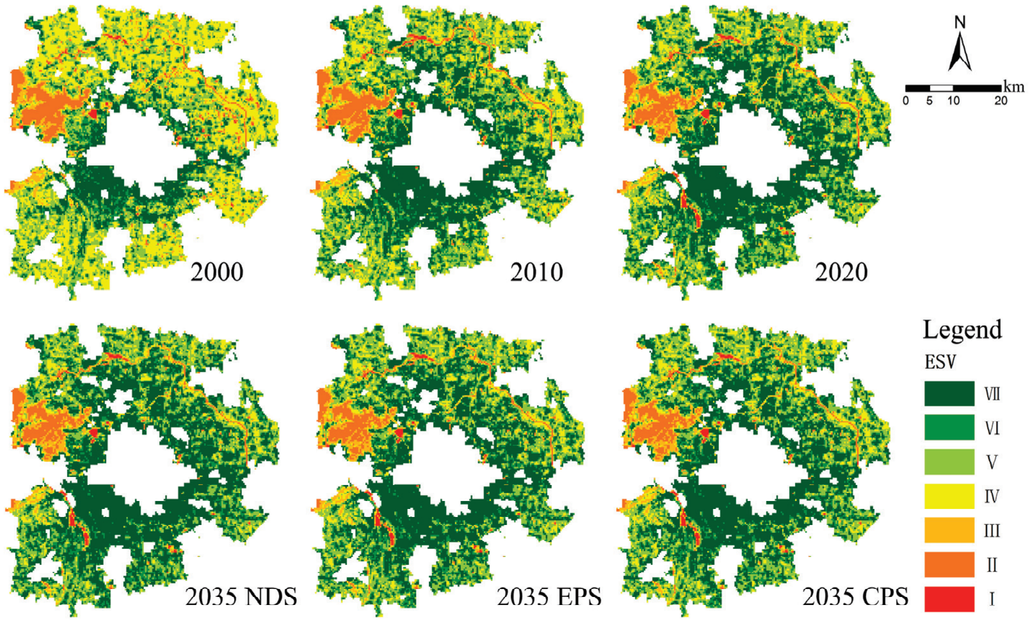

Figure 7. ESV simulation results.

In terms of provisioning services, the value of FP, RMP and WS have all decline between 2000 and 2020. For example, the value of FP will decline from CNY 233.72 million in 2000 to CNY 134.22 million in 2020. Under the projected scenarios for 2035, these values are expected to differ, with the NDS showing the lowest values, and the EPS indicating relatively higher values.

In regulating services, the values of GR, CR, HR, and WR are also projected to exhibit a downward trend. Among these, WR maintains the highest value, with the most significant differences anticipated across the forecasted scenarios for 2035. Specifically, under EPS, the value of WR is projected to reach CNY 646.67 million, but under the NDS, it is forecasted to be only CNY 611.67 million.

For supporting services, the values associated with MS, MB and MNC have also declined. For instance, the value of MS was CNY 357.62 million in 2000, decreasing to CNY 230.71 million by 2020. When considering the projected scenarios for 2035, these values are expected to vary according to different development scenarios. However, the overall magnitude of change is likely to be relatively small.

The aesthetic landscape value within cultural services has also exhibited a downward trend, dropping from CNY 59.37 million in 2000 to CNY 49.35 million in 2020. For the projected scenarios in 2035, the differences in these values across various development scenarios are expected to be relatively small.

Overall, farmland in Beijing has demonstrated a downward trend from 2000 to 2020. In the projected scenarios for 2035, these values will vary depending on the chosen development scenarios. However, in general, the ESV will be relatively higher under the EP development scenario. This indicates that while promoting economic and social development, prioritizing ecological environmental protection plays a crucial role in enhancing the ESV.

5. Discussion

5.1. Comparison with Previous Studies

The rapid urbanization of Beijing's greenbelt areas has triggered significant land use transitions and ecosystem service degradation over the past two decades. Our findings revealed a pronounced shift from ecological and agricultural land such as forests, water bodies, and croplands to urban construction, aligning with global patterns of peri-urban land conversion under urban sprawl pressures [57]. Notably, the net loss of 488.47 km^2 of cropland and 497.86 km^2 of cropland-to-construction conversion between 2000 and 2020 underscore the dominance of economic development priorities, reflecting China's broader urbanization trajectory [58]. The divergent contributions of driving factors, including DEM, population and temperature, to land cover changes highlight the complexity of urbanization processes. The prominent role of DEM in shaping the distribution of croplands and forests aligns with previous findings from Wuhan [59]. In our study, the distance to roads exhibited a relatively low contribution to land use transitions, diverging from observations in Wuhan's urban context. This discrepancy can be attributed to Wuhan's implementation of a transit-oriented development (TOD) strategy, emphasizing transportation corridors along metro lines and major highways, whereas Beijing's central urban area follows a monocentric outward expansion pattern characterized by radial development from its historical core. Meanwhile, population emerged as a key driver of cropland conversion, reinforcing the role of population growth in land use conflicts—a phenomenon well documented in the rapidly developing Chongqing [60] region. Scenario analyses revealed stark contrasts in ESV trajectories. The natural development scenario's 91.76 km^2 construction land gain and associated ESV decline exemplified the environmental costs of unregulated urban growth. In contrast, the EPS's moderated land conversion and partial ESV recovery demonstrated the viability of targeted conservation policies. These results resonate with analogous studies [42].

5.2. Discussion on Land Use and Ecological Conservation Policies

The study revealed that from 2000 to 2020, approximately 497.86 km^2 of cropland underwent conversion into construction land. This rapid transformation underscores the urgent need for land use policy optimization. Future urban development strategies should prioritize brownfield redevelopment over cropland encroachment. Implementation approaches could include land consolidation and intensive utilization strategies, specifically through spatial optimization measures such as green space restoration, industrial structure adjustment, old village renovation, and illegal structure demolition to achieve construction land conservation.

Under the EPS, the research demonstrated significantly enhanced ESV, with the hydrological regulation value reaching CNY 646.67 million compared to 611.67 million under NDS. This divergence emphasizes the necessity of proactive ecological conservation measures. A "negative list" system could be established to restrict construction activities in ecologically sensitive zones, particularly critical forest–water interface areas near mountainous regions and the Yongding River watershed. Expanding protected areas along northwestern riparian corridors would facilitate wetland rehabilitation and urban green space expansion, thereby enhancing the capacity of climate regulation and biodiversity conservation to offset the 1.21 km^2 water body loss projected under natural development patterns.

The quantitative analysis of ESV revealed substantial losses: grain production declined by 49% and the soil retention capacity decreased by 35% between 2000 and 2020. These outcomes emphasize the imperative of integrating ESV assessments into urban and regional planning processes. It is recommended that ESV metrics be adopted to quantify cross-regional ecological responsibilities, ensuring compensation mechanisms where beneficiaries compensate ecosystem service providers. Predictive models utilizing drivers such as DEM and population data should be developed to provide early warnings of detrimental land use conversions. Furthermore, establishing an interdepartmental committee—encompassing agricultural, ecological, and urban planning authorities—would align policies with the

Sustainable Development Goals and ensure the transparent management of trade-offs between construction demands and ESV preservation.

5.3. Limitations

This research has some constraints. In research utilizing multi-source data, the simulation accuracy was constrained by the driving factor data limitations imposed by data providers. Future investigations could employ updated, higher-precision data with unified temporal consistency for prediction, which would significantly enhance the forecasting accuracy. Moreover, the three scenario configurations adopted in this research may not comprehensively capture the potential impacts of future policy changes, suggesting that subsequent studies could establish additional policy scenarios for comparative analysis. Additionally, future research might also integrate more advanced methodologies, such as the GMOP [61] approach, to refine the mathematical modeling of policy elements' influence on land use scenarios, which might yield more precise predictive outcomes.

6. Conclusions

This study utilized data from 2000 to 2020, adopted revised standard equivalent factors, and integrated the PLUS model to simulate land use in Beijing's Green Belt Area under three scenarios—NDS, EPS, and CPS—for the year 2035. The analysis focused on predicting the spatiotemporal evolution of ESV under these scenarios.

The study shows that from 2000 to 2020, land use in Beijing's Green Belt Area was dominated by cropland and construction land. Construction land expanded significantly, increasing by 500.78 km^2, while cultivated land decreased by 488.47 km^2. Additionally, woodland, grassland, and water bodies also declined. The overall trend indicated the conversion of woodland and water bodies into cropland, and subsequently, the transformation of cropland to construction land. By 2035, under the NDS, construction land is projected to increase by 91.76 km^2, accompanied by decreases in cropland, grassland, and water bodies. In contrast, under the EPS, the growth of construction land is expected to slow down, with an increase of 22.09 km^2. The decrease in cropland will also decelerate, and the rate of conversion from cropland to construction land will decrease. Grassland and water bodies are anticipated to remain largely unchanged, while woodland will experience a slight increase. Similarly, under the CPS, the conversion of cropland to construction land will decrease significantly, resulting in an increase in construction land of 11.97 km^2. Woodland will increase, while grassland and water bodies will decrease slightly. In terms of ecosystem service assessment, the projected ESV for 2035 is CNY 1830.72 million under the EPS, exceeding CNY 1816.23 million for the CPS and CNY 1723.28 million for the NDS. Among the individual ESV components, WR and CR will remain dominant. The EPS demonstrates the potential to achieve higher economic benefits in terms of ESV.

The innovations of this study are mainly reflected in the following aspects: First, it focuses on the Beijing Green Separation Area, a representative region of land use conflict. By collecting and analyzing land use data at five time points (2000, 2005, 2010, 2015, and 2020), the study constructed a detailed temporal basis for land use change, providing a robust foundation for understanding long-term trends and transitions. Thirteen key driving factors were selected by comprehensively considering both natural and socio-economic dimensions, allowing for an in-depth analysis of the intrinsic driving forces and likelihood of land use transformation. Secondly, the study integrates the PLUS model, a cutting-edge tool in land use simulation. By designing scenarios for NDS, EPS, and CPS, it simulated the land use status of the Green Separation Area in 2035 under different policy orientations. These simulations offer a scientific basis for effective land management and policy formulation. Finally, the study enhances the accuracy of ESV, by using the equivalent value factor method of Xie as the theoretical basis. The equivalence factor table was revised using Beijing-specific data, such as its food price and NPP, thereby improving the precision of the valuation.

Author Contributions: Conceptualization, Z.H. and S.W.; methodology, Z.H.; software, Z.H.; validation, Z.H.; formal analysis, Z.H.; investigation, Z.H.; resources, Z.H.; data curation, Z.H.; writing—original draft preparation, Z.H.; writing—review and editing, Z.H. and S.W.; visualization, Z.H.; supervision, Z.H.; project administration, Z.H.; funding acquisition, S.W. All authors have read and agreed to the published version of the manuscript.

Funding: This research was funded by the National Natural Science Foundation of China (grant number: 52108038), Beijing High-Precision Discipline Project-Discipline of Ecological Environment of Urban and Rural Human Settlements and Territorial Spatial Planning and Design Project (project number: YJSY-DSTD2022008).

Data Availability Statement: The datasets generated during or analyzed during the current study are available from the corresponding author upon reasonable request.

Acknowledgments: We hereby thank the National Natural Science Foundation of China, Beijing High-Precision Discipline Project-Discipline of Ecological Environment of Urban and Rural Human Settlements and Territorial Spatial Planning and Design Project for financial support for this research. We extend our sincere gratitude to researchers Wenzhuo Rong and Xinyang Liu for their contributions to language polishing and literature review refinement in this paper.

Conflicts of Interest: The authors declare no conflicts of interest.

References

1. d'Amour, C.B.; Reitsma, F.; Baiocchi, G.; Barthel, S.; Guneralp, B.; Erb, K.-H.; Haberl, H.; Creutzig, F.; Seto, K.C. Future urban land expansion and implications for global croplands. *Proc. Natl. Acad. Sci. USA* **2017**, *114*, 8939–8944. [CrossRef]
2. Fu, H.; Yan, Y. Ecosystem service value assessment in downtown for implementing the "Mountain-River-Forest-Cropland-Lake-Grassland system project". *Ecol. Indic.* **2023**, *154*, 110751. [CrossRef]
3. Liu, J.; Pei, X.; Zhu, W.; Jiao, J. Understanding the intricate tradeoffs among ecosystem services in the Beijing-Tianjin-Hebei urban agglomeration across spatiotemporal features. *Sci. Total Environ.* **2023**, *898*, 165453. [CrossRef] [PubMed]
4. Bateman, I.J.; Harwood, A.R.; Mace, G.M.; Watson, R.T.; Abson, D.J.; Andrews, B.; Binner, A.; Crowe, A.; Day, B.H.; Dugdale, S.; et al. Bringing Ecosystem Services into Economic Decision-Making: Land Use in the United Kingdom. *Science* **2013**, *341*, 45–50. [CrossRef]
5. Cao, Y.; Kong, L.; Zhang, L.; Ouyang, Z. The balance between economic development and ecosystem service value in the process of land urbanization: A case study of China's land urbanization from 2000 to 2015. *Land Use Policy* **2021**, *108*, 105536. [CrossRef]
6. Costanza, R.; de Groot, R.; Sutton, P.; van der Ploeg, S.; Anderson, S.J.; Kubiszewski, I.; Farber, S.; Turner, R.K. Changes in the global value of ecosystem services. *Glob. Environ. Change Hum. Policy Dimens.* **2014**, *26*, 152–158. [CrossRef]
7. García-Ontiyuelo, M.; Acuña-Alonso, C.; Valero, E.; Álvarez, X. Geospatial mapping of carbon estimates for forested areas using the InVEST model and Sentinel-2: A case study in Galicia (NW Spain). *Sci. Total Environ.* **2024**, *922*, 171297. [CrossRef] [PubMed]
8. Bai, Z.; Wang, W.; Li, H.; Liu, R.; Guo, Z.; Liu, H. Evaluation of Forest Ecosystem Service Function of Kanas National Nature Reserve. *J. Northwest For. Univ.* **2018**, *33*, 292–296. [CrossRef]
9. Li, Q. Analysis on Dynamic Change, Regional Decomposition and Influencing Factors of Forest Ecosystem Service Value in Zhejiang Province. Master's Thesis, Zhejiang A&F University, Hangzhou, China, 2020.
10. Zheng, X.; Zhang, J.; Cao, S. Net value of grassland ecosystem services in mainland China. *Land Use Policy* **2018**, *79*, 94–101. [CrossRef]
11. Sawut, R.; Manlik, A.; Li, H.; Kasim, N.; Zheng, F.; Li, X.; Abdukerim, R.; Qahar, Y. Spatio-temporal changes of grassland ecosystem service values in Urumgi Citybased on the RS and GIS. *Acta Ecol. Sin.* **2020**, *40*, 522–539. [CrossRef]
12. Li, L.; Lin, H.; Gao, Y. Emergy analysis of the value of grassland ecosystem services in the Three Rivers Source Region. *Acta Prataculturae Sin.* **2016**, *25*, 34–41. [CrossRef]
13. Botzas-Coluni, J.; Crockett, E.T.H.; Rieb, J.T.; Bennett, E.M. Farmland heterogeneity is associated with gains in some ecosystem services but also potential trade-offs. *Agric. Ecosyst. Environ.* **2021**, *322*, 107661. [CrossRef]
14. Xu, H. Market failure and loss of ecosystem service value of farmlandin the process of farmland conversionA case study of Jiangsu Province. *Chin. J. Eco-Agric.* **2010**, *18*, 1366–1371. [CrossRef]

15. Athukorala, D.; Murayama, Y.; Bandara, C.M.M.; Lokupitiya, E.; Hewawasam, T.; Gunatilake, J.; Karunaratne, S. Effects of urban land change on ecosystem service values in the Bolgoda Wetland, Sri Lanka. *Sustain. Cities Soc.* **2024**, *101*, 105050. [CrossRef]
16. Han, Z.; Meng, Q.; Yan, X.; Zhao, W. Spatial and temporal relationships between land use intensity and the value ofEcosystem Services in northern Liaodong Bay over the past 30 years. *Acta Ecol. Sin.* **2020**, *40*, 2555–2566. [CrossRef]
17. Xie, C.; Wang, K.; Chen, H.; Zhang, M. Impact of land use change on the value of ecosystem services in the Dongting Lake area. *Resour. Environ. Yangtze Basin* **2006**, *15*, 191–195. [CrossRef]
18. Arkema, K.K.; Field, L.; Nelson, L.K.; Ban, N.C.; Gunn, C.; Lester, S.E. Advancing the design and management of marine protected areas by quantifying the benefits of coastal ecosystems for communities. *One Earth* **2024**, *7*, 989–1006. [CrossRef]
19. Xu, L.; Xu, X.; Luo, T.; Zhu, G.; Ma, Z. Services based on land use: A case study of Bohai Rim. *Geogr. Res.* **2012**, *31*, 1775–1784. [CrossRef]
20. Shi, Y.; Lv, X.; Hang, X.; Yu, M. Cultivated land use transition and its ecosystem service value change response in Jiangsu coastal area. *J. Nat. Resour.* **2017**, *32*, 961–976. [CrossRef]
21. Fu, B.-J.; Su, C.-H.; Wei, Y.-P.; Willett, I.R.; Lue, Y.-H.; Liu, G.-H. Double counting in ecosystem services valuation: Causes and countermeasures. *Ecol. Res.* **2011**, *26*, 1–14. [CrossRef]
22. Tang, X.; Liu, Y.; Pan, Y. An Evaluation and Region Division Method for Ecosystem Service Supply and Demand Based on Land Use and POI Data. *Sustainability* **2020**, *12*, 2524. [CrossRef]
23. Hanna, D.E.L.; Tomscha, S.A.; Dallaire, C.O.; Bennett, E.M. A review of riverine ecosystem service quantification: Research gaps and recommendations. *J. Appl. Ecol.* **2018**, *55*, 1299–1311. [CrossRef]
24. Shi, W.; Cheng, K.-M.; Wang, J.-S. Progress on the accounting purpose-based ecosystem service valuation methods. *J. Appl. Ecol.* **2021**, *32*, 1518–1530. [CrossRef]
25. Chen, W.; Chi, G. Ecosystem services trade-offs and synergies in China, 2000–2015. *Int. J. Environ. Sci. Technol.* **2023**, *20*, 3221–3236. [CrossRef]
26. Shen, J.; Li, S.; Wang, H.; Wu, S.; Liang, Z.; Zhang, Y.; Wei, F.; Li, S.; Ma, L.; Wang, Y.; et al. Understanding the spatial relationships and drivers of ecosystem service supply-demand mismatches towards spatially-targeted management of social-ecological system. *J. Clean. Prod.* **2023**, *406*, 136882. [CrossRef]
27. Turkay, Z.; Tezer, A. Utilizing ecosystem services for spatial decision-making with trade-off&synergy analysis in Istanbul. *Environ. Dev. Sustain.* **2024**. [CrossRef]
28. Wang, Q.; Bai, X. Spatiotemporal characteristics of human activity and land use on ecosystem service functions in mountainous areas of Northeast Guizhou, Southwest China. *Ecol. Eng.* **2025**, *212*, 107473. [CrossRef]
29. Hu, B.; Zhou, S.; Luo, P.; Chen, H. Assessment of Habitat Services and Gradient Zoning Optimization in Coal Mining Subsidence Areas from a Social-Ecological Coupling Perspective. *Sustainability* **2025**, *17*, 17. [CrossRef]
30. Guan, D.; Ran, B.; Zhou, L.; Jin, C.; Yu, X. Assessing and transferring social value of ecosystem services in wetland parks based on SolVES model. *Ecol. Indic.* **2023**, *157*, 111300. [CrossRef]
31. Amati, M.; Yokohari, M. Temporal changes and local variations in the functions of London's green belt. *Landsc. Urban Plan.* **2006**, *75*, 125–142. [CrossRef]
32. Tan, M.; Guy, M.R.; Li, X. Urban spatial development and land use in Beijing: Implications from London's experiences. *J. Geogr. Sci.* **2011**, *21*, 49–64. [CrossRef]
33. Xie, X.; Kang, H.; Behnisch, M.; Baildon, M.; Krueger, T. To What Extent Can the Green Belts Prevent Urban Sprawl?-A Comparative Study of Frankfurt am Main, London and Seoul. *Sustainability* **2020**, *12*, 679. [CrossRef]
34. Jun, M.-J. Simulating Seoul's greenbelt policy with a machine learning-based land-use change model. *Cities* **2023**, *143*, 104580. [CrossRef]
35. Zhang, H.; Zhou, Q.; Yang, J.; Xiang, H. Change and driving factors of eco-environmental quality in Beijing green belts: From the perspective of Nature-based Solutions. *Ecol. Indic.* **2024**, *166*, 112581. [CrossRef]
36. Zhao, M.; He, Z.; Du, J.; Chen, L.; Lin, P.; Fang, S. Assessing the effects of ecological engineering on carbon storage by linking the CA-Markov and InVEST models. *Ecol. Indic.* **2019**, *98*, 29–38. [CrossRef]
37. Chu, L.; Sun, T.; Wang, T.; Li, Z.; Cai, C. Evolution and Prediction of Landscape Pattern and Habitat Quality Based on CA-Markov and InVEST Model in Hubei Section of Three Gorges Reservoir Area (TGRA). *Sustainability* **2018**, *10*, 3854. [CrossRef]
38. Yang, X.; Chen, R.; Zheng, X.Q. Simulating land use change by integrating ANN-CA model and landscape pattern indices. *Geomat. Nat. Hazards Risk* **2016**, *7*, 918–932. [CrossRef]
39. Xu, K.; Chi, Y.; Ge, R.; Wang, X.; Liu, S. Land use changes in Zhangjiakou from 2005 to 2025 and the importance of ecosystem services. *PeerJ* **2021**, *9*, 12122. [CrossRef]
40. Tizora, P.; le Roux, A.; Mans, G.; Cooper, A.K. Adapting the Dyna-CLUE model for simulating land use and land cover change in the Western Cape Province. *S. Afr. J. Geomat.* **2018**, *7*, 190–203. [CrossRef]
41. Liang, X.; Liu, X.; Li, X.; Chen, Y.; Tian, H.; Yao, Y. Delineating multi-scenario urban growth boundaries with a CA-based FLUS model and morphological method. *Landsc. Urban Plan.* **2018**, *177*, 47–63. [CrossRef]

42. Yan, X.; Huang, M.; Tang, Y.; Guo, Q.; Wu, X.; Zhang, G. Study on the Dynamic Change of Land Use in Megacities and Its Impact on Ecosystem Services and Modeling Prediction. *Sustainability* **2024**, *16*, 5364. [CrossRef]
43. Xie, G.; Lu, C.; Leng, Y.; Zheng, D.; Li, S. Value assessment of ecological assets on the Qinghai-Tibet Plateau. *J. Nat. Resour.* **2003**, *18*, 189–196. [CrossRef]
44. Wu, A.; Zhang, J.; Zhao, Y.; Shen, H.; Guo, X. Simulation and Optimization of Supply and Demand Pattern of Multiobjective Ecosystem Services-A Case Study of the Beijing-Tianjin-Hebei Region. *Sustainability* **2022**, *14*, 2658. [CrossRef]
45. Liu, Y.; Ma, C.; Ma, L. Dynamics of the Oasis-Desert-Impervious Surface System and Its Mechanisms in the Northern Region of Egypt. *Land* **2024**, *13*, 1480. [CrossRef]
46. Jiang, F.; Xu, S.; Liu, C.; Zhao, J.; Jiang, B.; Fan, F. Assessment and prediction of habitat risk on the Qinghai-Xizang plateau under multiple scenarios. *Ecol. Indic.* **2024**, *168*, 112804. [CrossRef]
47. Guo, H.; Cai, Y.; Li, B.; Tang, Y.; Qi, Z.; Huang, Y.; Yang, Z. An integrated modeling approach for ecological risks assessment under multiple scenarios in Guangzhou, China. *Ecol. Indic.* **2022**, *142*, 109270. [CrossRef]
48. Zhao, L.; Liu, G.; Xian, C.; Nie, J.; Xiao, Y.; Zhou, Z.; Li, X.; Wang, H. Simulation of Land Use Pattern Based on Land Ecological Security: A Case Study of Guangzhou, China. *Int. J. Environ. Res. Public Health* **2022**, *19*, 9281. [CrossRef] [PubMed]
49. Zhou, H.; Tang, M.; Huang, J.; Mei, X.; Zhao, H. Driving mechanisms and multi-scenario simulation of land use change based on National Land Survey Data: A case in Jianghan Plain, China. *Front. Environ. Sci.* **2024**, *12*, 1422987. [CrossRef]
50. Yang, S.; Su, H. Multi-Scenario Simulation of Ecosystem Service Values in the Guanzhong Plain Urban Agglomeration, China. *Sustainability* **2022**, *14*, 8812. [CrossRef]
51. Wang, Y.; Li, M.; Jin, G. Exploring the optimization of spatial patterns for carbon sequestration services based on multi-scenario land use/cover changes in the changchun-Jilin-Tumen region, China. *J. Clean. Prod.* **2024**, *438*, 140788. [CrossRef]
52. Zhang, J.; Ding, H.; Xu, J.; Zheng, B. A Simulation-Based Prediction of Land Use Change Impacts on Carbon Storage from a Regional Imbalance Perspective: A Case Study of Hunan Province, China. *Land* **2024**, *13*, 1721. [CrossRef]
53. Ma, G.; Li, Q.; Zhang, J.; Zhang, L.; Cheng, H.; Ju, Z.; Sun, G. Simulation and Analysis of Land-Use Change Based on the PLUS Model in the Fuxian Lake Basin (Yunnan-Guizhou Plateau, China). *Land* **2023**, *12*, 120. [CrossRef]
54. Li, S.; Zhao, Y.; Xiao, W.; Yellishetty, M.; Yang, D. Identifying ecosystem service bundles and the spatiotemporal characteristics of trade-offs and synergies in coal mining areas with a high groundwater table. *Sci. Total Environ.* **2022**, *807*, 151036. [CrossRef] [PubMed]
55. Chen, S.; Fu, H.; Fu, G.; Chen, J. Spatial and Temporal Evolution of Wetland Ecosystem Service Value and ltsResponse to Landscape Pattern Changes in Haikou. *J. Northwest For. Univ.* **2023**, *38*, 236–242. [CrossRef]
56. Zhao, H.; Xu, X.; Tang, J.; Wang, Z.; Miao, C. Understanding the key factors and future trends of ecosystem service value to support the decision management in the cluster cities around the Yellow River floodplain area. *Ecol. Indic.* **2023**, *154*, 110544. [CrossRef]
57. Seto, K.C.; Fragkias, M.; Gueneralp, B.; Reilly, M.K. A Meta-Analysis of Global Urban Land Expansion. *PLoS ONE* **2011**, *6*, 0023777. [CrossRef]
58. Wei, Y.D.; Ye, X. Urbanization, urban land expansion and environmental change in China. *Stoch. Environ. Res. Risk Assess.* **2014**, *28*, 757–765. [CrossRef]
59. Wu, H.; Lin, A.; Xing, X.; Song, D.; Li, Y. Identifying core driving factors of urban land use change from global land cover products and POI data using the random forest method. *Int. J. Appl. Earth Obs. Geoinf.* **2021**, *103*, 102475. [CrossRef]
60. Wu, F.; Mo, C.; Dai, X. Analysis of the Driving Force of Land Use Change Based on Geographic Detection and Simulation of Future Land Use Scenarios. *Sustainability* **2022**, *14*, 5254. [CrossRef]
61. Zhu, L.; Huang, Y. Multi-Scenario Simulation of Ecosystem Service Value in Wuhan Metropolitan Area Based on PLUS-GMOP Model. *Sustainability* **2022**, *14*, 13604. [CrossRef]

land

Article

Are We Satisfied with the Achievements of New Eco-City Construction in China? A Case Study of the Sino-Singapore Tianjin Eco-City

Xuan Sun [1,2], Tao Sun [3,*], Jingchuan Hou [4], Zhuoruo Yue [1,2] and Xiaomeng Li [5]

1 Zhou Enlai School of Government, Nankai University, Tianjin 300350, China; sunxuan@nankai.edu.cn (X.S.); yuezhuoruo@mail.nankai.edu.cn (Z.Y.)
2 Laboratory of Digital City Governance, Nankai University, Tianjin 300350, China
3 School of Humanities and Social Science, Harbin Institute of Technology, Shenzhen 518055, China
4 School of Architecture and Planning, Massachusetts Institute of Technology, Cambridge, MA 02139, USA; hjc66@mit.edu
5 Management Committee of the Sino-Singapore Tianjin Eco-City, Tianjin 300480, China
* Correspondence: suntao2020@hit.edu.cn

Abstract: With the goal of sustainable urbanization, eco-cities have garnered significant global attention in recent decades. Unlike eco-city renovation or renewal, the construction of a new eco-city represents a comprehensive urbanization process that integrates environmental sustainability with livability. To evaluate the outcomes of new eco-city construction in China, this study employs a dual approach combining objective achievements and residents' subjective satisfaction to systematically examine the Sino-Singapore Tianjin Eco-City. The analysis encompasses five dimensions: environmental amenity, life safety, residential functionality, traffic capability, and economic well-being, with the relative weights of specific indicators determined through the entropy method, expert scoring, and analytic hierarchy process. The findings reveal that based on objective indicators, the eco-city's overall performance nearly doubled during its first phase of development, with life safety showing the most notable improvements. However, subjective assessments revealed that overall resident satisfaction remained below 70%, with residential functionality receiving the highest rating. The annual progress of the eco-city did not consistently align with residents' needs, and no clear correlation was found between the eco-city's current state and public sentiment. For sustainable development, the eco-city must address its shortcomings and better cater to residents' demands across various dimensions through targeted and effective strategies.

Keywords: eco-city; achievements; satisfaction; China; Sino-Singapore Tianjin Eco-City

1. Introduction

Recent decades have witnessed rapid urbanization alongside worsening environmental conditions in numerous countries [1]. With half of the world's population now residing in urban areas, city development often prioritizes short-term economic gains and relies on intrusive consumption and production practices, significantly undermining environmental sustainability [2]. High emissions, extensive land use, and uncontrolled urban sprawl are key drivers of unsustainable urbanization. To address these challenges, various solutions, such as the green economy, smart growth, and compact development, have been proposed [3–5]. Among these approaches, the concept of the eco-city, an integration of multiple strategies for sustainable urbanization, has garnered particular attention [6,7].

Regarded as a "technological fix", eco-city initiatives have been implemented worldwide, focusing primarily on environmental regeneration, economic transformation, and sustainable urban development [8]. Examples include the development of green buildings and clean energy industries in Freiburg, Germany, and the ecological redevelopment of industrial areas in Hammarby, Sweden [9,10]. Some eco-cities have emphasized social sustainability and public welfare, such as community rebuilding programs in Aswan, Egypt [11]. Others have prioritized ecological construction methods, such as the U-City plan in Songdo, South Korea, which integrates smart city technologies with eco-city principles [12]. Based on different ideas, most eco-cities worldwide have expanded from existing urban areas or retrofitted existing infrastructure, while only a small fraction have been constructed on undeveloped land [13]. Notable among these is Masdar City in Abu Dhabi, a solar-powered eco-city built in the desert [14].

China's eco-city projects, though late to start, have developed rapidly [15]. Over the past 30 years, China has established more than 100 eco-cities, incorporating advanced planning concepts, a strong emphasis on human–nature relationships, and a focus on improving livability [16–19]. The turning point for eco-city construction in China came in 2002 during the Fifth International Conference on Eco-Cities in Shenzhen, which marked the transition from theoretical discussion to practical implementation. Building on this momentum, several landmark projects have emerged, each showcasing unique approaches to eco-city development. The Dongtan Eco-City and the Chongming Eco-Island in Shanghai, for instance, feature forward-looking planning for self-sufficient development with green technologies [20]. The Caofeidian International Eco-City highlighted the use of technology in urban construction, embodying several characteristics of techno-cities [21]. Suzhou focused on eco-industrial park development with strict environmental regulations and an increased emphasis on the tertiary sector in economic growth [22]. Rizhao pursued a circular economy eco-city model, enhancing resource efficiency and reducing environmental burdens [23]. Notably, the Sino-Singapore Tianjin Eco-City, the first state-level cooperative project of its kind, has been a pioneer in environmental protection, resource conservation, and improving living conditions. However, these eco-city projects have also faced critical discussions regarding multiple aspects, such as insufficient social resilience, unfulfilled spatial rights for urban poor populations, lack of concrete pathways for public participation and democratic decision-making mechanisms, raising concerns about the actual effectiveness of eco-city construction [24–26].

To evaluate the effectiveness of eco-city construction, various index systems have been proposed [27,28]. Unlike traditional urban indices, which emphasize economic growth, eco-city indices focus on the sustainable development of entire urban systems [29–31]. These assessments typically consider ecological, social, and economic dimensions [32]. Many eco-cities have developed their own Key Performance Indicators (KPIs) to measure progress and environmental changes [33,34]. While these indices effectively capture objective achievements, they often fail to reflect residents' satisfaction.

In the meantime, for a better understanding of the public perceptions of eco-city construction, studies have also examined subjective assessments of ongoing projects. Surveys in European cities have shown that residents' perceptions correlate with eco-efficiency, reflecting the integration of ecological and socio-economic practices [35]. In China, field surveys have explored community-level perceptions of eco-urbanization and investigated residents' needs and satisfaction through questionnaires [36,37]. Recent years have seen increasing attention to the social impacts of eco-cities, yet no universal standard for people-oriented eco-city construction has been established [38].

To fill these gaps, this study attempts to amplify the otherwise muted voices of residents by incorporating public feedback into the eco-city evaluation framework. By systematically juxtaposing subjective satisfaction with objective performance metrics, it assesses both the actual efficacy of newly constructed eco-city projects and the limitations of technocratic indicators. In addition, this study identifies key challenges and offers policy recommendations to advance the sustainable development of eco-cities. In doing so, it refines critical discussions on eco-city models under authoritarian contexts and contributes context-sensitive insights to the broader international debates on sustainable urbanism.

The remainder of this paper is organized as follows. Section 2 outlines the research materials and methods, evaluating the efficacy of new eco-city development through a dual analytical framework: objective achievement and subjective satisfaction. Section 3 visually synthesizes the empirical findings, presenting comparative results for both objective and subjective indicators. Section 4 critically examines the (dis)parities between these indicators, highlighting systemic challenges in current eco-city planning and offering policy-relevant recommendations to enhance urban sustainability. Finally, Section 5 concludes by consolidating key insights and their implications for future research and practice.

2. Materials and Methods

2.1. Materials

The Sino-Singapore Tianjin Eco-City is located in the Binhai New Area of Tianjin, 45 km away from the central city, and adjacent to the Coastal Tourist Area (CTA), the Tianjin Port (TP), and the Tianjin Economic–Technological Development Area (TEDA) (see Figure 1). With the goal of building an ecological and livable city on deserted land, the planning scheme was triggered in 2007. It has been planned to cover an area of 30 square kilometers and accommodate a population of 350,000, and the advantageous transportation with high-speed, aviation, railway, and sea routes laid a good foundation for the economic and social development of the city.

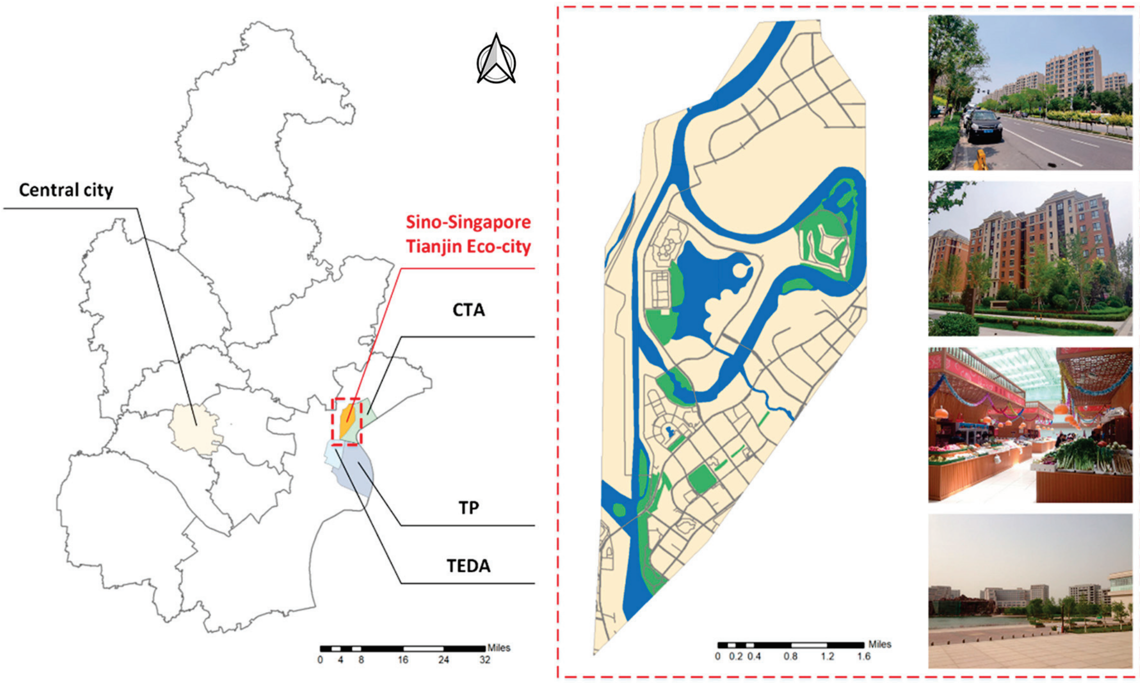

Figure 1. Location and spatial extent of the Sino-Singapore Tianjin Eco-City.

With an emphasis on sustainable development and ecological environment protection, the Sino-Singapore Tianjin Eco-City is committed to green economy in industry development, and special priority is given to the enterprises with high-tech content and high added values. By 2018, the number of market entities had surpassed 8300, around 50% of which were Internet, technological, cultural, and creative companies. Meanwhile, the number of financial enterprises had reached 1198, along with the registered capital of CNY 159.3 billion.

For the enhancement of living conditions and ecosystem stability, the Sino-Singapore Tianjin Eco-City upholds the basic idea of human and natural harmony in the whole process of urban development. On the one hand, it adopts Singapore's "neighborhood unit" concept and establishes a three-level residential system, within which public facilities are allocated at different scales of space to satisfy the diversified needs of residents in daily life. On the other hand, it enforces strict controls on energy use and emissions and promotes a number of ecological restoration projects during these years. By 2018, 13 kindergartens, 6 primary schools, 2 middle schools, 1 large general hospital, and several commercial centers and parks had been constructed and put into use. The proportion of green buildings in the eco-city has reached 100%, along with the ratio of green travel reaching 90%. It has successfully built a complex ecosystem of lake, river, wetland, and green space, and the total green area of the city has reached 7 million square meters. Furthermore, the garbage classification has been carried out, fulfilling the harmless treatment of household waste there.

However, setting aside the positive works above, the development of the new eco-city also faces many challenges nowadays. Among all of them, the slow population growth is one of the most prominent, where its current population of 100,000 is still far less than the anticipated number of 350,000. In this context, the subjective satisfaction of residents has been gaining more and more attention in recent years. Therefore, this study seeks to amplify residents' voices by adopting a mutual-validation approach that cross-examines subjective satisfaction data and objective achievement data to assess the actual performance of eco-city construction. On the one hand, we conducted a 20-day random sampling survey, distributing and collecting over 1000 questionnaires to gather residents' subjective evaluations. On the other hand, objective achievement data were obtained from statistical yearbooks and government portals. All the raw data—both subjective and objective—underwent standardized preprocessing prior to analysis.

2.2. Methods

To investigate the actual efficacy of new eco-city construction, we developed an analytical framework to visualize the methodological sequencing (see Figure 2).

Multidimensional analysis serves as a robust methodological approach for evaluating the performance of eco-city construction. Guided by the principles of sustainability and livability, this study evaluates the outcomes of new eco-city construction through both objective achievements and residents' subjective satisfaction across five key dimensions: environmental amenity, life safety, residential functionality, traffic capability, and economic well-being. Environmental amenity, a fundamental component of eco-cities, embodies the harmonious integration between the urban environment and the society [39]. While life safety and residential functionality demonstrate the livability of a city in people's daily life, traffic capability and economic well-being largely determine the living conditions of residents with respect to economic and social life [40–43]. The specific indicators and surveyed elements corresponding to each dimension will be elaborated on in subsequent sections.

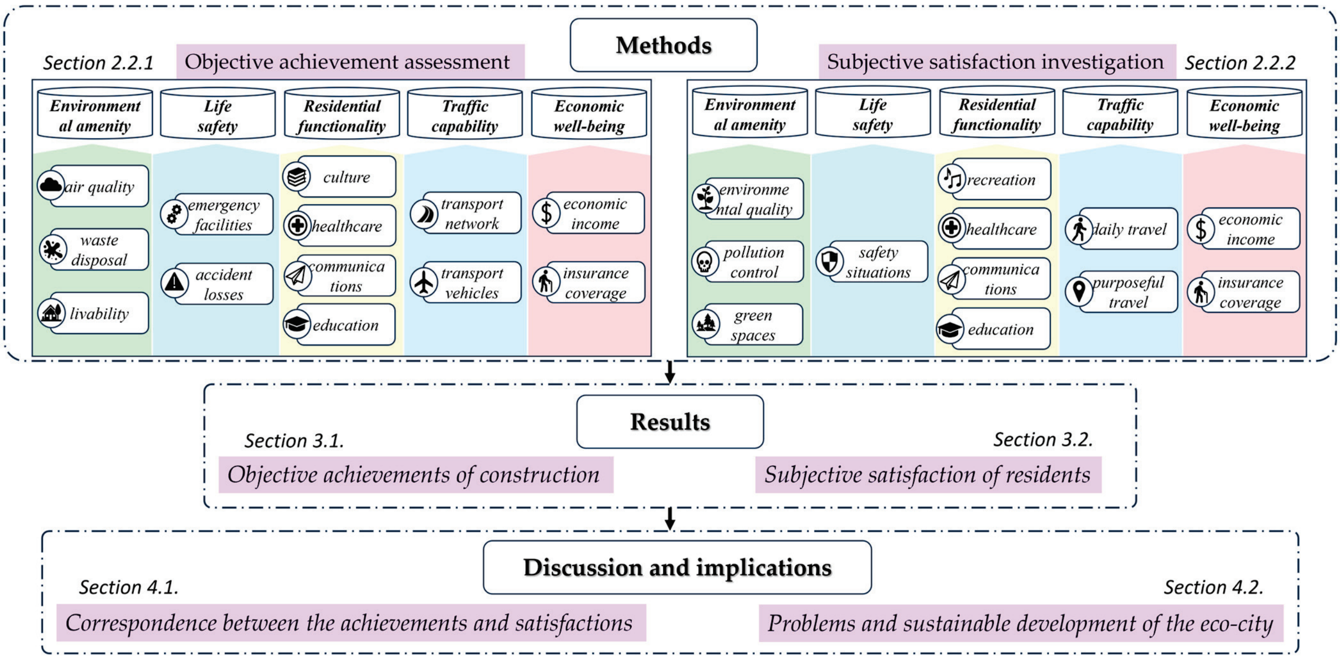

Figure 2. Methodological workflow of analytical framework.

2.2.1. Objective Achievement Assessment

Drawing upon existing evaluation frameworks documented in statistical yearbooks and the scholarly literature [44–46], this study selects specific indicators from the aforementioned five dimensions (see Table 1) to objectively assess the outcomes of eco-city construction. This research comprehensively incorporates both positive and negative indicators, standardizing the data to ensure comparability across metrics. Furthermore, the entropy method is employed to determine the relative weights of each indicator.

Table 1. Indicators for the objective assessment of the eco-city's achievements.

First-Level Indicators	Second-Level Indicators	Unit
Environmental amenity (X_1)	Days with good air quality (X_{11})	days
	Urban sewage treatment rate (X_{12})	%
	Industrial solid waste disposal and utilization rate (X_{13})	%
	Household waste disposal rate (X_{14})	%
	Green coverage rate in built-up areas (X_{15})	%
	Green park area per capita (X_{16})	m^2/person
	Population density of built-up areas (X_{17})	persons/km^2
Life safety (X_2)	Emergency shelter area per capita (X_{21})	m^2/person
	Criminal cases registered (X_{22})	cases/10,000 persons
	Deaths in traffic accidents (X_{23})	deaths/10,000 vehicles
	Deaths in fire accidents (X_{24})	deaths/10,000 persons
	Deaths in production accidents (X_{25})	deaths/CNY 100 million
Residential functionality (X_3)	Number of kindergartens (X_{31})	kindergartens/10,000 persons
	Number of fundamental education schools (X_{32})	schools/10,000 persons
	Number of hospital beds (X_{33})	beds/10,000 persons
	Number of cultural centers (X_{34})	centers/10,000 persons
	Business volume of post and telecommunications (X_{35})	CNY/person
	Internet fiber optic cable to the household rate (X_{36})	%

Table 1. *Cont.*

First-Level Indicators	Second-Level Indicators	Unit
Traffic capability (X_4)	Density of public transport network (X_{41})	km/km^2
	Road network area per capita (X_{42})	km^2/person
	Rail transit mileage (X_{43})	km/10,000 persons
	Number of buses (X_{44})	buses/10,000 persons
	Number of taxis (X_{45})	taxis/10,000 persons
Economic well-being (X_5)	Average salary of people (X_{51})	CNY/year
	Average disposable income (X_{52})	CNY/year
	Social assistance expenditure ratio (X_{53})	%
	Unemployment insurance coverage (X_{54})	%
	Endowment insurance coverage (X_{55})	%
	Medical insurance coverage (X_{56})	%

Specifically, environmental amenity indicators focus on measuring environmental improvement and protection outcomes, primarily encompassing three aspects: air quality, waste disposal rate, and livability. Life safety is operationalized through various metrics related to socio-economic activities, including emergency facilities and accident-related losses. Residential functionality indicators capture multifaceted living conditions, incorporating education, healthcare, cultural amenities, and social interaction opportunities. Traffic capability indicators primarily reflect the development and operational status of public transit systems, including both transportation networks and specific modes of transport. Economic well-being, meanwhile, is measured through indicators such as income levels, expenditure patterns, and coverage rates of various social welfare programs.

Due to the different data types and units, the selected indicators are not comparable in their original forms. Thus, it is required that the indicators be normalized before data treatments. Distinguishing between the indicators with positive meanings (e.g., X_{11}, X_{12}) and indicators with negative meanings (e.g., X_{22}, X_{23}), a dichotomous approach for data normalization is adopted here.

Assuming that there are n indicators for evaluation, the states of the eco-city in m years can be expressed as a matrix $C = \{c_{ij}\}_{m\times n}$ $(i = 1, 2, \ldots, m; j = 1, 2, \ldots, n)$, and the normalized dataset $Q = \{q_{ij}\}_{m\times n}$ is able to be calculated with the following formula:

Positive Indicator:

$$q_{ij} = \frac{c_{ij}}{s_j}(i = 1, 2, \ldots, m; j = 1, 2, \ldots, n) \tag{1}$$

Negative Indicator:

$$q_{ij} = \frac{s_j}{c_{ij}}(i = 1, 2, \ldots, m; j = 1, 2, \ldots, n) \tag{2}$$

where c_{ij} and q_{ij} are the original value and the normalized value of the jth indicator in the ith year, respectively, and s_j is the standard value of the jth indicator.

After data normalization, the entropy method is then employed to determine the relative weights of the indicators. Different from subjective weighting methods, the entropy method is purely based on the data themselves and has a sound theoretical basis for the evaluation of objective changes [47]. The higher the degree of the value change is, the bigger the weight of the corresponding indicator would be, reflecting a greater contribution to the ultimate result; otherwise, it is smaller. Mathematically, the weight of each indicator can be calculated with the following formula:

$$p_{ij} = \frac{Ind_{ij}}{\sum\limits_{i=1}^{m} Ind_{ij}} \tag{3}$$

$$\mathrm{e}_j = -k\sum_{i=1}^{m} p_{ij}\ln(p_{ij}) \tag{4}$$

$$w_j = \frac{1-e_j}{\sum\limits_{j=1}^{n}(1-e_j)} \tag{5}$$

where Ind_{ij} stands for the index value of the jth indicator in the ith year, p_{ij} is the proportion of the jth indicator's index value on the basis of the accumulative value of all the related indicators in the ith year, e_j is the entropy of the jth indicator, and w_j is the jth indicator's relative weight. k is the Boltzmann constant, which satisfies $k = 1/\ln(m)$. As for the index value Ind_{ij}, when it corresponds to a second-level indicator, $Ind_{ij} = q_{ij}$.

According to the grouping and layered relationships of indicators, the index values were calculated hierarchically for the assessment of the eco-city's achievements at different levels. First, with the index values and the weights of the second-level indicators in different groups, the index values of the first-level indicators were calculated. Second, based on the indexes of all the first-level indicators and their relative weights calculated with the entropy method, a comprehensive index was obtained as the overall assessment of the eco-city. The numerical calculation process of the indexes is as follows:

$$Ind_{iu} = \sum_{j=1}^{Num(u)} (w_j(u) \times Ind_{ij}(u)) \tag{6}$$

$$Ind_i = \sum_{u=1}^{D} (w_u \times Ind_{iu}) \tag{7}$$

where Ind_{iu} and Ind_i stand for the index value of the uth first-level indicator and the comprehensive index value of the eco-city in the ith year, respectively, Num (u) represents the number of subordinate second-level indicators of the uth first-level indicator, Ind_{ij} (u) is the ith year's index value of the jth subordinate indicator of the uth first-level indicator, w_j (u) is the weight of the jth indicator among all the subordinate indicators of the uth first-level indicator, and w_u is the relative weight of the uth indicator among all the D number of first-level indicators of the eco-city. In our study, $D = 5$.

2.2.2. Subjective Satisfaction Investigation

To evaluate residents' subjective satisfaction with the new eco-city construction, this study conducted a comprehensive random sampling survey (20-day duration) covering five representative residential communities in the Sino-Singapore Tianjin Eco-City, collecting 1000 valid responses from 1152 distributed questionnaires (86.81% response rate). Aside from the personal attributes of respondents, the topics and elements of the survey were designed in accordance with the indicators for objective assessment (see Table 2). Each topic involved several elements, and each element could be rated in five grades, which were "very satisfied", "satisfied", "neutral", "dissatisfied", and "very dissatisfied". For specialized urban performance indicators beyond general public knowledge, the study employed adapted measurement approaches—assessing "life safety" through safety situation indicators and evaluating "traffic capability" via both purposeful travel and non-commuting daily travel. This methodological design ensures the subjective investigation maintains conceptual consistency with the objective assessment framework while effectively capturing residents' lived experiences of eco-city construction.

Table 2. Topics and elements of the subjective survey.

Surveyed Topic	Surveyed Elements
Environmental amenity	Atmosphere environment quality (AEQ) Water environment quality (WEQ) Ecological environment quality (EEQ) Emission pollution control (EPC) Noise pollution control (NPC) Community green space (CGS) Green activity space (GAS)
Life safety	Urban safety situation (USS) Community safety situation (CSS) Traffic safety situation (TSS) Accident safety situation (ASS)
Residential functionality	Convenience of children's education (CCE) Convenience of medical treatment (CMT) Convenience of recreation and entertainment (CRE) Convenience of social communication (CSC)
Traffic capability	Traveling in daily life (TDL) Traveling to city center (TCC) Traveling to study and work (TSW)
Economic well-being	Family income status (FIS) Material life level (MLL) Endowment insurance level (EIL) Medical insurance level (MIL)

As a reflection of subjective demand intensities, the weights of factors (topics or elements) in different levels were determined by means of expert scoring and the analytic hierarchy process (AHP) method. Through pairwise comparison of related factors, the corresponding judgement matrix of experts $A = \{a_{ij}\}_{N\times N}$ was established. When the judgement matrix passed the consistency test, the weights of the elements $W = \{w_i\}_N$ could be calculated with the following formula:

$$\overline{a_i} = \sqrt[N]{\prod_{j=1}^{N} a_{ij}} \tag{8}$$

$$w_i = \frac{\overline{a_i}}{\sum\limits_{i=1}^{N} \overline{a_i}} \tag{9}$$

where N is the number of related factors for discussion, a_{ij} represents the relative importance of the ith factor compared with the jth factor, $\overline{a_i}$ stands for the average importance of the ith factor, and w_i is the weight of the ith factor.

According to the grouping and layered relationships of different factors, several judgement matrices were determined by experts independently at different levels, and a hierarchical set of weights was able to be calculated. With the surveyed results and the hierarchical weights obtained, the satisfaction of residents was summarized in different dimensions and also as a whole. For the integrity of the results, the fuzzy comprehensive evaluation (FCE) method was adopted in the process of satisfaction summarization, which can be expressed as the following functions:

$$B_u = W(u) \times \begin{bmatrix} B_1(u) \\ B_2(u) \\ \vdots \\ B_{Num(u)}(u) \end{bmatrix} = (w_1(u), w_2(u), \ldots, w_{Num(u)}(u)) \times \begin{bmatrix} b_{11}(u) & b_{11}(u) & \ldots & b_{1G}(u) \\ b_{21}(u) & b_{21}(u) & \ldots & b_{2G}(u) \\ \vdots & \vdots & \ldots & \vdots \\ b_{Num(u)1}(u) & b_{Num(u)2}(u) & \ldots & b_{Num(u)G}(u) \end{bmatrix} \tag{10}$$

$$B = W \times \begin{bmatrix} B_1 \\ B_2 \\ \vdots \\ B_D \end{bmatrix} = (w_1, w_2, \ldots, w_D) \begin{bmatrix} b_{11} & b_{12} & \ldots & b_{DG} \\ b_{21} & b_{22} & & b_{2G} \\ & & & \\ b_{D1} & b_{D2} & & b_{DG} \end{bmatrix} \tag{11}$$

where $B = \{b_i, b_2,..., b_G\}$ and $B_u = \{b_{u1}, b_{u2},..., b_{uG}\}$ stand for the fuzzy sets of the overall satisfaction value and the satisfaction of residents in the dimension of the *u*th topic, respectively. G is the number of grades for subjective scoring, $Num\ (u)$ represents the number of surveyed elements of the *u*th topic, $B_i\ (u) = \{b_{i1}\ (u), b_{i2}\ (u),..., b_{iG}\ (u)\}$ is the fuzzy set of the assessment of the *i*th subordinate element of the *u*th topic, $W\ (u) = \{w_1\ (u), w_2\ (u), ..., w_{Num\ (u)}\ (u)\}$ is the weight vector of the subordinate elements of the *u*th topic, and $W = \{w_1, w_2, ..., w_D\}$ is the weight vector of all the D number of topics for investigation. In our study, $G = 5$, $D = 5$.

Furthermore, with the grade-score mapping vector $M = \{m_1, m_2,..., m_G\}$, each fuzzy set $B_i = \{b_{i1}, b_{i2},..., b_{iG}\}$ can be converted to a specific score, intuitively reflecting the subjective satisfaction degree of residents. The calculation process is as follows:

$$v_i = M \times B_i^T = (m_1, m_2, \ldots, m_G) \begin{bmatrix} b_{i1} \\ b_{i2} \\ \vdots \\ b_{iG} \end{bmatrix} \tag{12}$$

where v_i stands for the score of residents' satisfaction in some i dimension, corresponding to a certain topic of the subjective survey or the overall state of the eco-city. In our study, the grade-score mapping vector M was set as {100, 75, 50, 25, 0}, representing differentiated degrees of satisfaction with equal intervals. Based on the specified vector M, v_i will fall in the range of [0, 100]. A score of 0 means being totally dissatisfied, a score of 100 means being totally satisfied, and a score of 50 indicates a neutral attitude.

3. Results

3.1. Objective Achievements of Eco-City Construction

The original data for objective achievement assessment were collected from the Tianjin Statistics Yearbook, the Statistics Yearbook of Tianjin Binhai New Area, and government websites. Taking the statistics in 2010 as the standard values of indicators, the original data were normalized by means of the method presented in Section 2.2.1, and the results during the first phase of the city construction, from 2010 to 2017, are shown in Table 3.

Table 3. Normalized data for objective achievement assessment.

Indicators	2010	2011	2012	2013	2014	2015	2016	2017
X_{11}	1.00	1.02	1.09	1.26	1.50	1.35	1.26	1.17
X_{12}	1.00	1.01	1.03	1.01	1.00	1.41	1.33	1.17
X_{13}	1.00	1.19	1.49	1.19	1.08	1.28	1.72	1.78
X_{14}	1.00	1.07	1.07	1.11	1.13	1.22	1.28	1.32
X_{15}	1.00	1.06	1.00	1.06	1.05	1.06	1.07	1.08
X_{16}	1.00	1.29	1.42	1.53	1.62	1.68	1.85	1.96
X_{17}	1.00	1.09	1.19	1.29	1.28	1.27	1.28	1.30
X_{21}	1.00	1.47	1.59	1.72	1.83	2.20	2.31	2.35
X_{22}	1.00	1.12	1.32	1.21	1.55	1.63	1.82	2.00
X_{23}	1.00	1.36	1.25	1.82	1.71	1.65	1.85	2.00
X_{24}	1.00	1.33	1.55	1.66	1.78	1.62	1.55	1.92
X_{25}	1.00	1.19	1.32	1.45	1.52	1.63	1.85	1.98
X_{31}	1.00	1.00	1.00	1.00	1.32	1.41	1.52	1.63
X_{32}	1.00	1.00	1.00	1.00	1.00	1.00	1.50	2.00
X_{33}	1.00	1.24	1.32	1.42	1.48	1.59	1.68	2.00
X_{34}	1.00	1.21	1.36	1.41	1.58	1.63	1.71	1.92
X_{35}	1.00	1.01	0.99	1.01	1.02	1.03	1.04	1.08
X_{36}	1.00	1.01	1.00	1.01	1.02	1.03	1.04	1.08
X_{41}	1.00	1.11	1.18	1.33	1.42	1.50	1.55	1.63
X_{42}	1.00	1.19	1.59	1.49	1.29	1.42	1.66	1.96
X_{43}	1.00	1.01	1.11	1.31	1.44	1.61	1.80	1.98
X_{44}	1.00	1.00	1.00	1.00	1.02	1.03	1.05	1.17
X_{45}	1.00	1.08	1.15	1.23	1.36	1.54	1.32	1.76
X_{51}	1.00	1.01	1.02	1.02	1.03	1.06	1.07	1.08
X_{52}	1.00	1.07	1.11	1.13	1.22	1.22	1.26	1.32
X_{53}	1.00	1.21	1.32	1.24	1.36	1.42	1.52	1.68
X_{54}	1.00	1.23	1.02	1.41	1.32	1.52	1.32	1.50
X_{55}	1.00	1.17	1.26	1.41	1.63	1.80	1.85	1.92
X_{56}	1.00	1.35	1.27	1.68	1.74	1.88	2.02	2.04

Based on the normalized dataset, the entropies and weights of indicators at different levels were calculated (see Table 4). According to the entropy weights obtained, the improvement of life safety (X_2) and residential functionality (X_3) actually played a prominent role in the eco-city construction during 2010–2017. By contrast, the effects of environmental amenity (X_1) improvement were relatively weak, especially in the aspects of household waste disposal rate (X_{14}), green coverage rate in built-up areas (X_{15}), and population density of built-up areas (X_{17}).

Table 4. Entropies and weights of indicators for objective achievement assessment.

First-Level Indicator	First-Level Indicator Entropy	First-Level Indicator Weight	Second-Level Indicator	Second-Level Indicator Entropy	Second-Level Indicator Weight
X_1	0.9950	0.115	X_{11}	0.9958	0.135
			X_{12}	0.9956	0.142
			X_{13}	0.9903	0.312
			X_{14}	0.9980	0.064
			X_{15}	0.9998	0.006
			X_{16}	0.9913	0.282
			X_{17}	0.9982	0.059

Table 4. *Cont.*

First-Level Indicator	First-Level Indicator Entropy	First-Level Indicator Weight	Second-Level Indicator	Second-Level Indicator Entropy	Second-Level Indicator Weight
X_2	0.9894	0.244	X_{21}	0.9853	0.268
			X_{22}	0.9877	0.223
			X_{23}	0.9896	0.189
			X_{24}	0.9926	0.134
			X_{25}	0.9898	0.186
X_3	0.9896	0.239	X_{31}	0.9903	0.211
			X_{32}	0.9817	0.401
			X_{33}	0.9911	0.195
			X_{34}	0.9915	0.186
			X_{35}	0.9998	0.004
			X_{36}	0.9999	0.003
X_4	0.9912	0.203	X_{21}	0.9940	0.162
			X_{22}	0.9911	0.238
			X_{23}	0.9858	0.381
			X_{24}	0.9994	0.017
			X_{25}	0.9925	0.202
X_5	0.9914	0.199	X_{51}	0.9998	0.005
			X_{52}	0.9982	0.050
			X_{53}	0.9950	0.141
			X_{54}	0.9949	0.144
			X_{55}	0.9887	0.320
			X_{56}	0.9880	0.340

With the normalized data and the weights of the indicators, the objective achievements of the Sino-Singapore Tianjin Eco-City in different dimensions were able to be quantitatively assessed, and an integrated assessment was obtained in the end. Judging from the results, the new eco-city has obviously made significant improvements in the recent decade. With a steady growth, the integrated assessment had almost doubled during 2010–2017 (see Table 5).

Table 5. Objective achievement assessments during 2010-2017.

	X_1	X_2	X_3	X_4	X_5	Integrated Assessment
2010	1.00	1.00	1.00	1.00	1.00	1.00
2011	1.16	1.30	1.09	1.08	1.24	1.18
2012	1.30	1.41	1.13	1.24	1.23	1.26
2013	1.27	1.57	1.16	1.33	1.46	1.37
2014	1.29	1.68	1.27	1.38	1.56	1.45
2015	1.41	1.79	1.32	1.52	1.70	1.56
2016	1.58	1.93	1.58	1.62	1.75	1.71
2017	1.60	2.08	1.90	1.86	1.83	1.89

However, in different dimensions, the developments actually progressed at different paces (see Figure 3). Under continuous development, the eco-city obtained the most notable achievements in life safety. While the traffic capability was improved at a relatively uniform pace during these years, the developments in residential functionality mainly happened in the later stage. Except for the universal growth in the period of 2010–2011, the developments in economic well-being alternated with those in environmental amenity, but the achievements in environmental amenity generally lagged behind due to the slowing down and stagnation of developments in 2013, 2014, and 2017.

Figure 3. Progress of the eco-city construction in different dimensions.

3.2. Subjective Satisfaction of Residents

To ensure the representativeness of the subjective investigation, the questionnaire survey was conducted by means of random sampling in different residential communities of the Sino-Singapore Tianjin Eco-City. From 10 April 2019 to 30 April 2019, 1152 copies of the questionnaire were sent out, and 1096 responses were received. Removing incomplete ones from the received questionnaires, 1000 valid samples were ultimately obtained.

Overall, the surveyed population showed specific demographic characteristics (see Figure 4). Among the 1000 valid respondents, males and females were roughly balanced, young ages made up the majority, and well-educated people were the mainstream. While most of the respondents were from a family of three or four people, the ones from a family of one or two people also accounted for more than one-third of the surveyed population. Almost half of the residents were able to make a salary of CNY 4000–6000, and only 3% of the population earned less than CNY 2000.

According to the respondents' answers, most of the residents were generally satisfied with the eco-city's current state (see Figure 5). Except for the endowment insurance level (EIL), all the other elements' satisfaction ratios (satisfied and very satisfied) were over 50%. Especially for the ecological environment quality (EEQ), community green space (CGS), community safety situation (CSS), and convenience of medical treatment (CMT), the satisfaction ratios were even over 80%. The convenience of medical treatment (CMT) won the most positive votes. However, there were also elements with high dissatisfaction ratios. Over 10% of people were very dissatisfied with the traffic in daily life (TDL), traveling to study and work (TSW), and endowment insurance level (EIL).

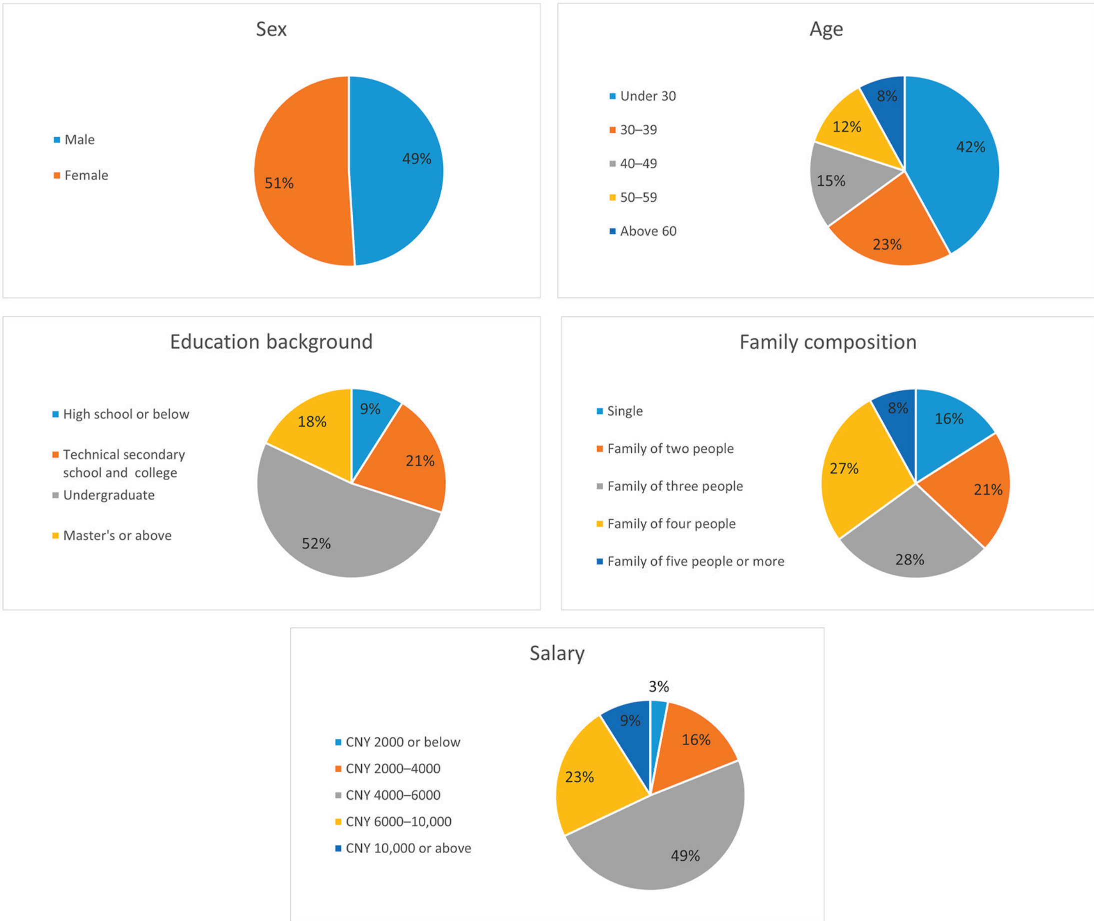

Figure 4. Demographic characteristics of the surveyed population.

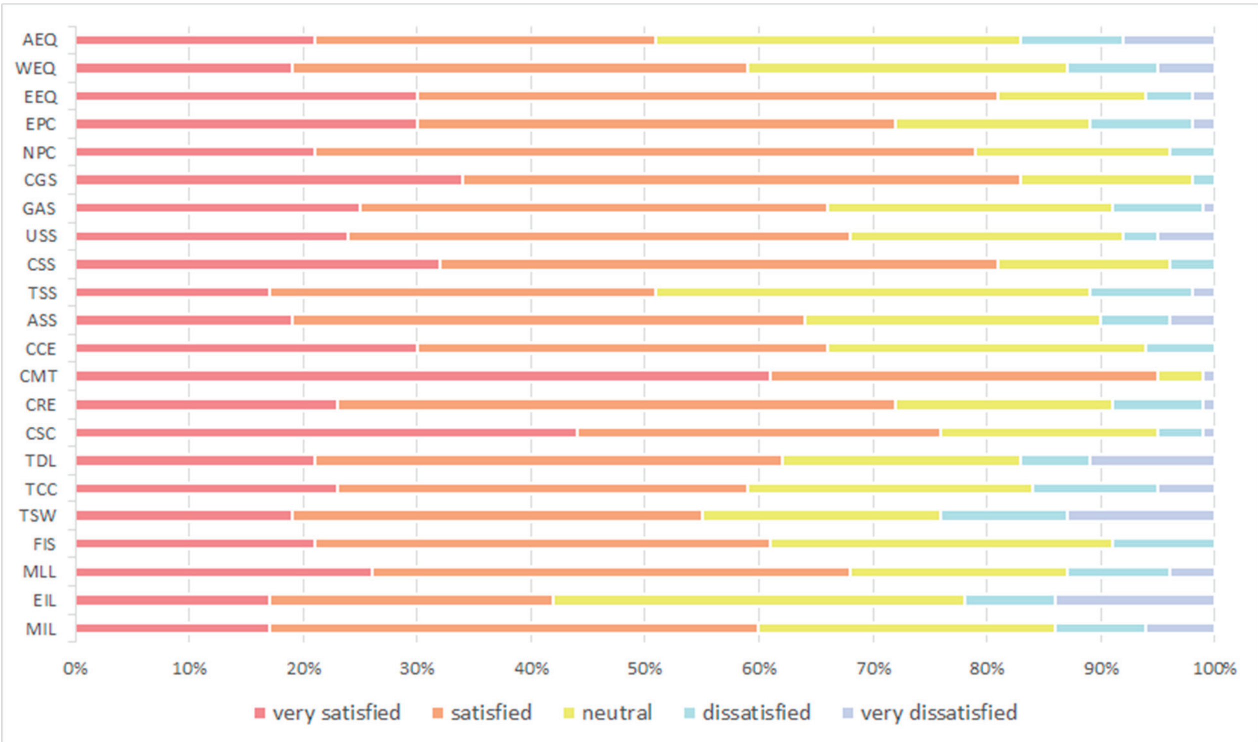

Figure 5. Surveyed results of the residents' satisfaction with different elements.

Following the AHP method, 15 scholars in urban planning and 10 experts involved in the eco-city construction were invited to decide the relative importance of each factor in the subjective survey. The factors in different levels were compared through the Saaty 1–9 scaling approach, and judgement matrices of the surveyed topics and elements were constructed. With the formula presented in Section 2.2.2, the hierarchical weights were then calculated (see Table 6).

Table 6. The weights of different topics and elements.

Surveyed Topics	Weight	Surveyed Elements	Weight
Environmental amenity	0.18	AEQ	0.11
		WEQ	0.10
		EEQ	0.19
		EPC	0.10
		NPC	0.11
		CGS	0.22
		GAS	0.17
Life safety	0.32	USS	0.22
		CSS	0.30
		TSS	0.28
		ASS	0.20
Residential functionality	0.22	CCE	0.38
		CMT	0.26
		CRE	0.19
		CSC	0.17
Traffic capability	0.17	TDL	0.35
		TCC	0.20
		TSW	0.45
Economic well-being	0.11	FIS	0.26
		MLL	0.27
		EIL	0.24
		MIL	0.23

Based on the surveyed results and the hierarchical weights obtained, the satisfaction levels of residents with different topics and the overall state of the eco-city were calculated with the FCE method (see Figure 6). Judging from the overall satisfaction, a ratio of over 60% were satisfied and very satisfied with the current state of the eco-city. While environmental amenity and residential functionality received relatively high marks, traffic capability and economic well-being were not very satisfactory.

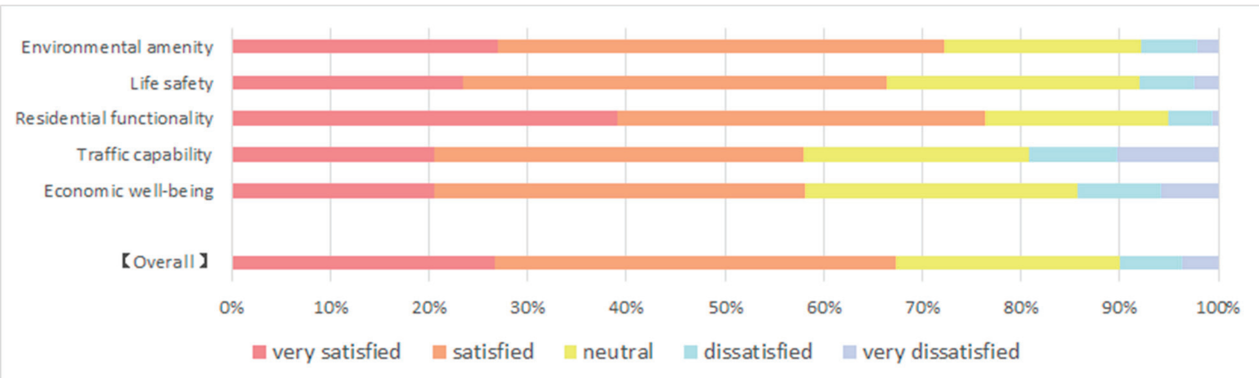

Figure 6. Satisfaction levels of residents with different topics and the overall state of the eco-city.

Converting the fuzzy results to specific scores, the subjective satisfaction of residents was intuitively measured (see Figure 7). The overall score was 70.08, indicating that there was still a lot of room for progress in the future. While the score of residential functionality was near 80, significantly above the overall score, the scores of traffic capability and economic well-being were just over 60, obviously below the overall score. Furthermore, the scores of life safety and environmental amenity were similar to the overall score.

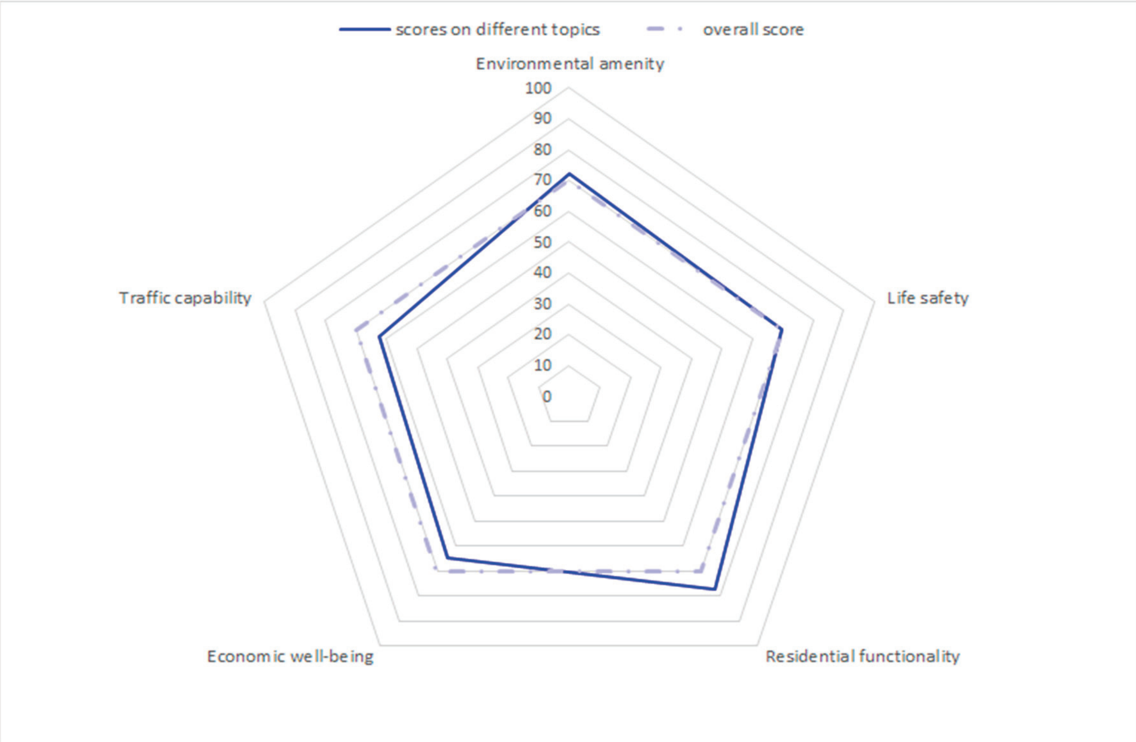

Figure 7. The scores measuring the subjective satisfaction of residents.

4. Discussion and Implications

4.1. Correspondence Between the Achievements and People's Satisfaction

With reference to the objective indicators, the Sino-Singapore Tianjin Eco-City attained enormous achievements during 2010–2017. However, judging from the results of the subjective survey, the satisfaction of residents was not as good as the achievements obtained. There was a poor correspondence between the two in many aspects.

4.1.1. Annual Developments and Demands

In terms of the construction process, the eco-city's annual developments did not well conform with people's demands, which was represented by the subjective weights in different dimensions (see Figure 8). Numerically, the correlation coefficient between the changes in the objective indicators and the subjective weights never exceeded 0.50 during 2010–2017.

In 2015–2016, the objective developments and the subjective weights fitted best, where the corresponding correlation coefficient was 0.45. However, just one year prior, in 2014–2015, the two fitted worst, and the correlation coefficient was −0.43. Although the development focus varied over time, the ultimate achievements in different dimensions were relatively balanced by 2017. Among all the dimensions, life safety occupied the highest subjective weight, but it achieved the biggest improvement only in 2010–2011. Comparatively, economic well-being received the lowest weight, but its objective achievement increased significantly in 2010–2011 and 2012–2013. Not restricted by the biased demands, the eco-city generally developed with a shift in focus from environmental amenity to life safety and economic well-being, and then to residential functionality and traffic capability.

Figure 8. Annual developments of the eco-city versus people's demands.

4.1.2. Current States and Feelings

In terms of the construction results, there was also no uniform relationship between the current states of the eco-city and people's feelings (see Figure 9), where the correlation coefficient between the objective assessments and the subjective scores was just −0.05. More notable achievements in certain dimensions did not necessarily mean a correspondingly higher satisfaction of residents.

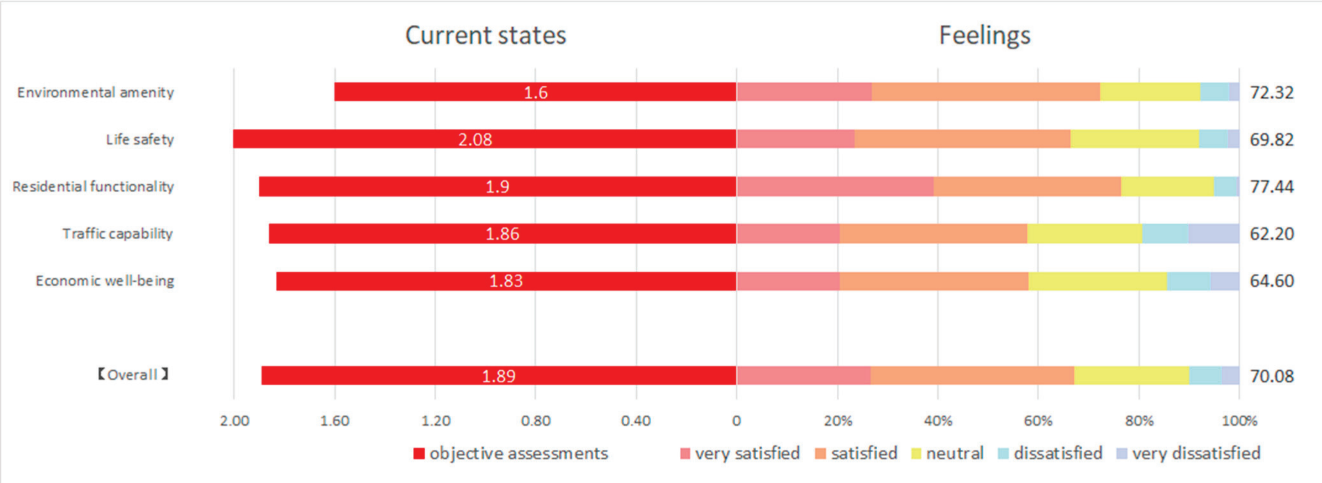

Figure 9. Current state of the eco-city and people's feelings.

The eco-city had the worst objective assessment in the dimension of environmental amenity, but the subjective score was high. Conversely, the eco-city had the most outstanding achievements in the dimension of life safety, but people's subjective satisfaction was only at a medium level. Referring to the quantitative relationship between the overall objective assessment and the corresponding subjective score, the achievement of the eco-city in life functionality had a strong positive effect on the satisfaction of residents. However, as for traffic capacity and economic well-being, the positive effects of the objective achievements on people's satisfaction were limited.

This case demonstrates a pronounced disjunction between subjective perceptions and objective developments. Residents exhibited relatively higher satisfaction perceptions toward environmental amenity but lower perceptions toward life safety. Existing research suggests such perception–development mismatch is a common challenge in eco-city construction: subjective satisfaction with sanitation and greenery tends to be inflated, whereas development initiatives potentially harming environmental conditions may trigger significant discontent [35,36]. This implies that life safety, belonging to basic demand hierarchies, elicits limited sensitivity to objective improvements; in contrast, environmental amenity, representing higher-level needs, triggers more acute perceptual responses to changes.

4.2. Problems and Sustainable Development of the Eco-City

In fact, the deviations between the objective achievements and subjective satisfaction indicated a variety of unsolved problems in the eco-city's construction. Facing these problems, the sustainable development of the eco-city should make up for the deficiencies and meet the needs of residents, improving development quality.

First, from the aspect of environmental amenity, the objective achievements were not very good, and it seemed to have entered a bottleneck in the later stage. As a restricting factor of social and economic development, the improvements in environment indicators always struggled to reach a high level. Most notably, the indicator values of days with good air quality (X_{11}), urban sewage treatment rate (X_{12}), and green coverage rate in built-up areas (X_{15}) had all experienced ups and downs during these years and remained at a low level in the end. The Sino-Singapore Tianjin Eco-City had implemented a comprehensive environmental indicator system within its KPI framework [25]. Notably, substantial progress in industrial waste disposal and utilization (X_{13}) coupled with significant park and green space development (X_{16}) contributed to residents' relative satisfaction with the current conditions. However, from the perspective of sustainable development, it is necessary to introduce as many low-emission, high-tech, high-value-added projects and enterprises as possible in the future, optimizing the ways of economic development and controlling pollution from the source. Meanwhile, to further improve the ecological environment in urban areas, it is necessary to build diversified environmental protection mechanisms and carry out more projects on the efficiency enhancement of smoke and sewage treatments.

Second, from the aspect of life safety, the objective achievements were most prominent, but given China's longstanding reputation as one of the world's safest countries, residents' subjective perceptions remained relatively muted. To effectively enhance people's sense of life safety, the eco-city needs to focus on the traffic safety situation (TSS) and accident safety situation (ASS) in the future. On the one hand, scientific urban safe operation plans ought to be formulated among multiple sectors, to reduce the occurrence of traffic and production accidents in daily life; on the other hand, different types of public safety facilities need to be set up in densely populated areas to improve the disaster prevention and response capabilities in emergencies. Furthermore, it is also necessary to build an advanced early warning, prevention, and control system with intelligent technologies to improve the safety management level of the eco-city overall.

Third, regarding the aspect of residential functionality, the rapid development of education (X_{32}), medical care (X_{33}), and culture (X_{34}) facilities caused the eco-city to be highly regarded by the public. Based on the concept of the "neighborhood unit" in the eco-city construction, all the public facilities were located within walkable distances from dwellings, greatly improving the convenience of activities of residents in daily life (CCE, CMT, CRE, and CSC). However, after nearly two decades of development, the social infrastructure configuration in this new eco-city remains less mature than that of Tianjin's central urban area. It has yet to fully incorporate human-scale design principles, resulting in an ecological enclave lacking social sustainability—a phenomenon well-documented in prior studies highlighting deficiencies in social interaction, employment opportunities, and consumption facilities [26,38]. To fully satisfy people's needs in residential functionality, the Sino-Singapore Tianjin Eco-City needs to further improve the diversity and quality of public service provision in the future. Only by continuously improving the quality of life of residents can the eco-city attract more people to settle in and achieve the anticipated population eventually.

Finally, regarding the aspects of traffic capacity and economic well-being, people's subjective satisfaction levels were both not very high. Although objective assessments of the former showed significant improvement in recent years, many residents remained dissatisfied with current conditions regarding traveling in daily life (TDL), traveling to the city center (TCC), and traveling to study and work (TSW). Notably, despite the consistent promotion of green mobility options, bicycles and walking failed to gain popularity due to lifestyle constraints and middle-class preferences, leaving private vehicles as the persistently dominant transportation mode [26]. As for economic well-being, the objective evaluations were merely average, and the core problem was the limited improvements in people's salary (X_{51}) and disposable income (X_{52}). Even as a state-led flagship project, the eco-city appears inevitably constrained by market logic [43]. So, for sustainable development, the eco-city construction should focus more on the improvement in the socio-economic environment in the future. On the one hand, attention needs to be given to the improvement in urban transportation systems, optimizing the existing public transportation routes and enhancing the transportation capability across regions; on the other hand, the economic lives of residents should be of concern, promoting scientific and technological innovation in economic development and providing more high-end job opportunities for people.

5. Conclusions

New eco-city construction represents a comprehensive urbanization process aimed at balancing environmental sustainability with urban livability. As a flagship initiative of China's eco-city development, the Sino-Singapore Tianjin Eco-City has made remarkable progress over the past two decades, particularly in environmental protection, resource efficiency, and urban functionality. In performance evaluations, national and local governments typically favor standardized indicators that offer clarity and comparability. However, the inherent complexity and contextuality of real-world urban processes often render such metrics inadequate in fully capturing urban realities. Beyond top-down macro-level assessments, it is imperative to incorporate residents' lived experiences to validate the efficacy and authenticity of these objective measurements. This study seeks to amplify the otherwise muted voices of ordinary residents within academic discourse, aiming to prevent the eco-city from devolving into a disembodied utopian imagination.

The findings reveal a pronounced divergence between objective performance evaluations and residents' subjective satisfaction. Despite near-doubling of the eco-city's performance during its first development phase according to official indicators, the overall resident satisfaction rate has remained below 70%, with 10% of respondents expressing dissatisfaction or strong dissatisfaction. This gap necessitates a more nuanced investigation into the determinants of public perception and their alignment—or lack thereof—with planning objectives. Inadequate environmental amenities, deficiencies in life safety provisions, suboptimal residential functionality, constrained traffic capacity, and underlying economic difficulties have all undermined the city's ability to fulfill its residents' diverse and evolving needs.

For decades, Chinese urban governance has been critiqued as a form of state-led elite urbanism. Under this paradigm, major urban decisions are negotiated behind closed doors by technocrats and sectoral elites. In the case of the Sino-Singapore Tianjin Eco-City, the technocratic indicators employed as instruments of spatial regulation are far from infallible, while residents' subjective feedback—lacking substantive avenues for civic participation—is often reduced to survey data at best. Notably, although policy documents frequently invoke terms such as "democratic decision-making" and "public participation", they largely fail to offer concrete and actionable mechanisms for implementation. In most cases, public participation remains a symbolic and ceremonial gesture. For the majority of residents, the so-called "right to the city" becomes a rhetorical assertion rather than a lived reality, as they are rarely granted genuine opportunities to shape urban development according to their own aspirations.

To bridge the disconnect between developmental achievements and lived satisfaction, targeted strategies must be adopted to realize the sustainable transformation of eco-cities. First, environmental public services should be significantly enhanced to foster greener, healthier, and more aesthetically appealing urban environments that promote well-being and social cohesion. Second, safety and resilience must be prioritized through improved disaster preparedness, robust public safety infrastructure, and overall urban resilience. Third, residential functions need to be optimized to ensure that housing and community services are attuned to daily needs and expectations. Fourth, transport infrastructure should be upgraded to enhance accessibility, reduce congestion, and support sustainable mobility systems. Fifth, economic vitality must be reinforced through industrial diversification, expanded employment opportunities, and inclusive economic policies that distribute benefits more equitably across social groups. All of these improvements require an integrated planning and governance framework that incorporates resident feedback, adapts to dynamic urban demands, remedies the current lack of actionable mechanisms for democratic participation, and aligns technological innovation with human-centered development goals.

Future research should focus on refining eco-city evaluation frameworks to incorporate broader and more nuanced metrics of resident well-being and satisfaction while also expanding the spatial and demographic scope of sampling. Moreover, longitudinal studies tracking the evolving relationship between resident satisfaction and urban development will provide critical insights into the dynamic mechanisms that underlie sustainable urban transformation. Only through such efforts can the vision of eco-cities as harmonious and inclusive urban spaces be genuinely realized.

Author Contributions: Conceptualization, X.S.; Methodology, X.S.; Writing—review and editing, X.S.; Project administration, T.S.; funding acquisition, T.S.; Writing—original draft, J.H.; Charting—original draft, J.H.; Charting—review and editing, Z.Y.; Data collection, X.L. All authors have read and agreed to the published version of the manuscript.

Funding: This research was jointly supported by the Chey Institute's ISEF program, the National Natural Science Foundation of China (Grant No. 72074127, 72442029), and the ESRC Global Challenges Research Fund (Grant No. ES/P011020/1).

Data Availability Statement: The original contributions presented in the study are included in the article, further inquiries can be directed to the corresponding author.

Conflicts of Interest: The authors declare that they have no potential conflicts of interest with respect to the research, authorship, or publication of this article.

References

1. Uttara, S.; Bhuvandas, N.; Aggarwal, V. Impacts of urbanization on environment. *Int. J. Res. Eng. Appl. Sci.* **2012**, *2*, 1637–1645.
2. Cui, X. How can cities support sustainability: A bibliometric analysis of urban metabolism. *Ecol. Indic.* **2018**, *93*, 704–717. [CrossRef]
3. Bailey, I.; Caprotti, F. The green economy: Functional domains and theoretical directions of enquiry. *Environ. Plan. A* **2014**, *46*, 1797–1813. [CrossRef]
4. Ibrahim, M.; El-Zaart, A.; Adams, C. Smart sustainable cities roadmap: Readiness for transformation towards urban sustainability. *Sustain. Cities Soc.* **2018**, *37*, 530–540. [CrossRef]
5. Bibri, S.E.; Krogstie, J.; Kärrholm, M. Compact city planning and development: Emerging practices and strategies for achieving the goals of sustainability. *Dev. Built Environ.* **2020**, *4*, 100021. [CrossRef]
6. Roseland, M. Dimensions of the eco-city. *Cities* **1997**, *14*, 197–202. [CrossRef]
7. Joss, S.; Cowley, R.; Tomozeiu, D. Towards the 'ubiquitous eco-city': An analysis of the internationalisation of eco-city policy and practice. *Urban Res. Pract.* **2013**, *6*, 54–74. [CrossRef]
8. Caprotti, F. Eco-urbanism and the Eco-city, or, Denying the Right to the City? *Antipode* **2014**, *46*, 1285–1303. [CrossRef]
9. Rohracher, H.; Späth, P. The interplay of urban energy policy and socio-technical transitions: The eco-cities of Graz and Freiburg in retrospect. *Urban Stud.* **2014**, *51*, 1415–1431. [CrossRef]
10. Mahzouni, A. The 'policy mix'for sustainable urban transition: The city district of Hammarby Sjöstad in Stockholm. *Environ. Policy Gov.* **2015**, *25*, 288–302. [CrossRef]
11. Elnokaly, A.; Elseragy, A. Eco-cities: Strategies of rebuilding communities for resilient and sustainable development in Egypt with particular emphasis on Aswan. In Proceedings of the International Conference on Changing Cities III: Spatial, Design, Landscape & Socio-Economic Dimensions, Mykonos, Greece, 26–30 June 2017.
12. Yoo, J.S.; Shin, D.B. Utilizing urban facility sensor information in U-City: Multi-dimensional scaling approach. *Spat. Inf. Res.* **2016**, *24*, 53–64. [CrossRef]
13. Joss, S. Eco-cities: A global survey 2009. *WIT Trans. Ecol. Environ.* **2010**, *129*, 239–250.
14. Grey, F.A. Masdar City as a Prototype for Eco-Cities. *Dig. Middle East Stud.* **2018**, *27*, 261–277. [CrossRef]
15. Jiang, Y.; Liu, C.; Zhou, C.; Chen, M. Overview of theoretical research and practical considerations on eco-cities of China. *Geogr. Res.* **2015**, *34*, 2222–2237.
16. Xie, L.; Cheshmehzangi, A.; Tan-Mullins, M.; Flynn, A.; Heath, T. Urban entrepreneurialism and sustainable development: A comparative analysis of Chinese eco-developments. *J. Urban Technol.* **2020**, *27*, 3–26. [CrossRef]

17. Liu, H.; Wennersten, R.; Luo, P.; Jiang, L.; Dong, W. Conceptual Sustainability Framework for Eco-City Development in the City Core of Xuzhou. *J. Urban Plan. Dev.* **2016**, *142*, 05016003. [CrossRef]
18. Zhuang, Y. Confucian ecological vision and the Chinese eco-city. *Cities* **2015**, *45*, 142–147. [CrossRef]
19. Gong, F.; Chen, X. Study on the Evaluation of Ecological Livable City in Anhui Based on Intuitionistic Fuzzy Theory. In *IOP Conference Series: Earth and Environmental Science*; IOP Publishing: Bristol, UK, 2020; Volume 555, p. 012089.
20. Chang, I.C.C.; Sheppard, E. China's eco-cities as variegated1 urban sustainability: Dongtan eco-city and Chongming eco-island. *J. Urban Technol.* **2013**, *20*, 57–75. [CrossRef]
21. Joss, S.; Molella, A.P. The eco-city as urban technology: Perspectives on Caofeidian international eco-city (China). *J. Urban Technol.* **2013**, *20*, 115–137. [CrossRef]
22. Yu, C.; Dijkema, G.P.; De Jong, M.; Shi, H. From an eco-industrial park towards an eco-city: A case study in Suzhou, China. *J. Clean. Prod.* **2015**, *102*, 264–274. [CrossRef]
23. Li, J.; Sun, W.; Song, H.; Li, R.; Hao, J. Toward the construction of a circular economy eco-city: An emergy-based sustainability evaluation of Rizhao city in China. *Sustain. Cities Soc.* **2021**, *71*, 102956. [CrossRef]
24. Caprotti, F. Critical research on eco-cities? A walk through the Sino-Singapore Tianjin Eco-City, China. *Cities* **2014**, *36*, 10–17. [CrossRef]
25. Caprotti, F.; Springer, C.; Harmer, N. 'Eco'For Whom? Envisioning Eco-urbanism in the Sino-Singapore Tianjin Eco-city, China. *Int. J. Urban Reg. Res.* **2015**, *39*, 495–517. [CrossRef]
26. Flynn, A.; Yu, L.; Feindt, P.; Chen, C. Eco-cities, governance and sustainable lifestyles: The case of the Sino-Singapore Tianjin Eco-City. *Habitat Int.* **2016**, *53*, 78–86. [CrossRef]
27. Zhou, N.; He, G.; Williams, C.; Fridley, D. ELITE cities: A low-carbon eco-city evaluation tool for China. *Ecol. Indic.* **2015**, *48*, 448–456. [CrossRef]
28. Liu, L. A sustainability index with attention to environmental justice for eco-city classification and assessment. *Ecol. Indic.* **2018**, *85*, 904–914. [CrossRef]
29. Murakami, S.; Kawakubo, S.; Asami, Y.; Ikaga, T.; Yamaguchi, N.; Kaburagi, S. Development of a comprehensive city assessment tool: CASBEE-City. *Build. Res. Inf.* **2011**, *39*, 195–210. [CrossRef]
30. Wong, C. A framework for 'City Prosperity Index': Linking indicators, analysis and policy. *Habitat Int.* **2015**, *45*, 3–9. [CrossRef]
31. Yao, J.; Yan, H.; Shao, J. Study on Evaluation of Eco-city Construction Based on Sustainable Development. In *IOP Conference Series: Earth and Environmental Science*; IOP Publishing: Bristol, UK, 2020; Volume 571, p. 012096.
32. Dong, H.; Fujita, T.; Geng, Y.; Dong, L.; Ohnishi, S.; Sun, L.; Fujii, M. A review on eco-city evaluation methods and highlights for integration. *Ecol. Indic.* **2016**, *60*, 1184–1191. [CrossRef]
33. Liu, J.; Low, S.P.; Wang, L.F. Critical success factors for eco-city development in China. *Int. J. Constr. Manag.* **2018**, *18*, 497–506. [CrossRef]
34. Sharifi, A. From Garden City to Eco-urbanism: The quest for sustainable neighborhood development. *Sustain. Cities Soc.* **2016**, *20*, 1–16. [CrossRef]
35. Gudipudi, R.; Lüdeke, M.K.; Rybski, D.; Kropp, J.P. Benchmarking urban eco-efficiency and urbanites' perception. *Cities* **2018**, *74*, 109–118. [CrossRef]
36. Zeng, C.; Deng, X.; Yang, J.; Cheng, Y.; Zhao, T.; Wang, P. The exploration of residents' perception of eco-urbanization at community and driving factors in China. *Cities* **2022**, *122*, 103513. [CrossRef]
37. Li, J.; Wang, Q.; Xuan, Y.; Zhou, H. User demands analysis of Eco-city based on the Kano model—An application to China case study. *PLoS ONE* **2021**, *16*, e0248187. [CrossRef]
38. Caprotti, F.; Gong, Z. Social sustainability and residents' experiences in a new chinese eco-city. *Habitat Int.* **2017**, *61*, 45–54. [CrossRef]
39. Mersal, A. Eco city Challenge and opportunities in transferring a city in to green city. *Procedia Environ. Sci.* **2017**, *37*, 22–33. [CrossRef]
40. Surjan, A.K.; Shaw, R. 'Eco-city'to 'disaster-resilient eco-community': A concerted approach in the coastal city of Puri, India. *Sustain. Sci.* **2008**, *3*, 249–265. [CrossRef]
41. Mouratidis, K.; Yiannakou, A. What makes cities livable? Determinants of neighborhood satisfaction and neighborhood happiness in different contexts. *Land Use Policy* **2022**, *112*, 105855. [CrossRef]
42. Kenworthy, J.R. The eco-city: Ten key transport and planning dimensions for sustainable city development. *Environ. Urban* **2006**, *18*, 67–85. [CrossRef]
43. Cugurullo, F. Urban eco-modernisation and the policy context of new eco-city projects: Where Masdar City fails and why. *Urban Stud.* **2016**, *53*, 2417–2433. [CrossRef]
44. Reis, I.F.; Ferreira, F.A.; Meidutė-Kavaliauskienė, I.; Govindan, K.; Fang, W.; Falcão, P.F. An evaluation thermometer for assessing city sustainability and livability. *Sustain. Cities Soc.* **2019**, *47*, 101449. [CrossRef]

45. Giles-Corti, B.; Lowe, M.; Arundel, J. Achieving the SDGs: Evaluating indicators to be used to benchmark and monitor progress towards creating healthy and sustainable cities. *Health Policy* **2020**, *124*, 581–590. [CrossRef] [PubMed]
46. Chen, Y.; Zhang, D. Evaluation and driving factors of city sustainability in Northeast China: An analysis based on interaction among multiple indicators. *Sustain. Cities Soc.* **2021**, *67*, 102721. [CrossRef]
47. Al-Aomar, R. A combined ahp-entropy method for deriving subjective and objective criteria weights. *Int. J. Ind. Eng. Theory Appl. Pract.* **2010**, *17*, 12–24.

land

MDPI

Article

Socio-Ecological Outcomes of Forest Landscape Mutations in the Congo Basin: Learning from Cameroon

Pontien Kuma Nyongo [1,2] and Jude Ndzifon Kimengsi [2,3,*]

[1] Centre for International Postgraduate Studies of Environmental Management (CIPSEM), Technische Universität Dresden, Zellescher Weg 41c, 01217 Dresden, Germany; pony364g@tu-dresden.de
[2] Forest Institutions and International Development Research Group, Technische Universität Dresden, Cotta-Bau, Pienner Str. 7, 01737 Tharandt, Germany
[3] Department of Geography, The University of Bamenda, Bambili P.O. Box 39, Cameroon
* Correspondence: jude_ndzifon.kimengsi@tu-dresden.de or pontiano4@gmail.com or kimengsi.jude@uniba.cm

Abstract: Globally, the mutations around forest landscapes continue to draw significant scientific interest, despite fragmented evidence on the socio-ecological outcomes linked to this process. This knowledge gap is evident in the Congo Basin—one of the world's major ecosystems. To contribute towards addressing the knowledge gap, this study analyzed two decades of forest landscape mutations and the socio-ecological transformation-cum-outcomes linked to the process in Cameroon. A mixed-methods approach was employed, combining remote sensing-based land use/land cover (LULC) analysis (using multi-date Landsat imagery at 30 m resolution) with household surveys involving 100 randomly selected forest-dependent households across three forest blocks: Ebo, Ndokbou, and Makombé for ground truthing. Survey data were analyzed using descriptive statistics and combined spatial analysis to reveal the following. Firstly, forest cover has significantly increased within the 20-year period; this involved a 104.01% increase between 2004 and 2014, and an additional 47.27% between 2014 and 2024. In that vein, agricultural land declined by more than 20%, whereas settlement and water bodies increased by 226.4% and 376.2%, respectively. Secondly, forest landscape mutations in the Yabassi Forest Area were primarily driven by a convergence of social (notably population growth at 57% and livelihood diversification), economic (agricultural expansion and timber exploitation), political (tenure ambiguity and development-driven land conversion), and environmental (climate variability at 36% and ecological restoration efforts) forces. These interwoven drivers shaped the land use change process, revealing how the human-environment feedback defines landscape trajectories in complex and non-linear ways. Thirdly, while the ecological outcomes of forest mutations were largely positive—with significant gains in forest cover, the social outcomes were skewed towards the negative. Communities experienced both improvements in livelihoods and infrastructure (66%), but also faced land conflicts (67%), the loss of traditional access (69%), and resource-based insecurity. By applying the socio-ecological systems (SES) framework, this study provides novel insights on how governance, ecological processes, and human behavior co-evolve in forest landscapes. The findings do not only edify the SES framework but also challenge the mainstream position about forest decline by highlighting areas of recovery. The evidence informs adaptive forest governance processes in the Congo Basin and similar contexts. Further research should investigate the institutional and adaptive mechanisms that influence these dynamics across the Congo Basin.

Keywords: forests; mutations; drivers' socio-ecological outcomes; Congo Basin

1. Introduction

Forest ecosystems worldwide are undergoing profound transformations driven by a complex interplay of anthropogenic pressures and environmental changes. At the heart of these transformations are forest management institutions (FMIs), which play a pivotal role in mediating the access, use and conservation of forest resources. The functionality, design, and enforcement capacities of these institutions remain central themes in academic discourse as scholars seek to unravel the dynamics that underpin compliance and sustainability in forest governance systems [1–3]. Expanding global comparative research remains vital to enhance our understanding of how FMIs are formulated and how they respond to socio-ecological challenges [4].

A key concern within this context is forest landscape mutation. This term encapsulates the long-term transformation of forested areas through substantial land use, ecological structures and land cover changes. These shifts, primarily triggered by logging, agricultural expansion, mining, infrastructural development and climate change, undermine forest integrity and ecosystem service functions [5–7]. Globally, forest degradation and deforestation is alarming; recent data reveals an unsettling reversal in conservation gains. In 2023, 6.37 million hectares of forest was cleared. This renders the target to halt global deforestation by 2030 quite daunting [7]. With carbon emissions from deforestation reaching 3.8 billion metric tons of CO_2 equivalent and more than 62 million hectares of ecological downgraded, forest mutation now constitutes a global ecological emergency.

Agricultural expansion remains the foremost driver of forest change worldwide. In the Congo Basin, which has the second-highest forest cover after the Amazon, more than 90% of deforestation is attributed to land conversion for agricultural purposes [8]. Although similar processes occur in Latin America and Southeast Asia, Africa is considered as the region with the highest net forest loss globally, averaging 3.94 million hectares annually between 2010 and 2020 [9]. In sub-Saharan Africa (SSA), small-scale agriculture for domestic markets, along with informal logging and mining, exacerbates forest fragmentation and ecological degradation [10,11].

The outcomes of forest landscape mutations in SSA are intimately linked to structural governance deficits that affect the ecological change process and limit community adaptation. According to [9], we experienced the highest net forest loss globally between 2010 and 2020. This intensified soil erosion, leading to an increase in water insecurity and degradation of ecosystems that are crucial for livelihoods and climatic moderation. Beyond biophysical degradation, these transformations jeopardize progress towards attaining global environmental commitments. Ref. [12] argues that unchecked forest mutations across SSA derail efforts to meet climate mitigation goals and biodiversity conservation targets, particularly under frameworks such as the REDD+ and the Aichi Targets.

In another dimension, the negative socio-ecological impacts of forest landscape mutations are not uniform. A growing body of research highlights the role of local resilience and community innovations in adapting to and mitigating landscape disruptions. For instance, Ref. [13] documents how communities under secured forest tenureship engage in ecologically beneficial practices such as agroforestry, selective harvesting, and community reforestation. These adaptive responses underscore the fact that outcomes do not hinge solely on environmental issues but equally manifest through institutional arrangements. When governance systems are locally embedded, participatory, and responsive, they can act as buffers against the adverse impacts of forest degradation. Nonetheless, persistent challenges such as institutional fragmentation, overlapping jurisdictions, and elite capture continue to weaken governance capacity [13]. These obstacles dilute accountability and limit the effectiveness of community-based interventions. Therefore, understanding the interplay between governance quality and forest mutation outcomes is essential for designing regionally tailored, equity-oriented forest conservation strategies in the Congo Basin, with Cameroon being a classical example.

Cameroon exemplifies the tensions between the conservation of forest landscapes and socio-economic development, with forests covering approximately 42% of its territory [6]. Smallholder farming, illegal logging, and artisanal mining have led to an annual forest loss of 1.3% between 2010 and 2020 [6,7]. The Yabassi forest, part of the ecologically significant Ebo Forest landscape, has witnessed accelerated degradation as exemplified by is significant natural forest cover decline [14]. Cameroon's 1994 Forestry Law introduced progressive mechanisms such as Community Forest Management (Section 37) and Logging Rights for Local Populations (Section 57), designed to align sustainable resource use with local development. Even the recent 2024 Forestry and Wildlife Law further emphasized these issues. Although these frameworks have shaped positive socio-ecological outcomes, challenges linked to weak enforcement, exclusionary regulations, and inequitable benefit sharing still exacerbate forest governance [15–17]. The above issues validate the need for context-specific evidence to uncover governance questions in the context of forest landscape mutations, with the Yabassi Forest Area being a valid case.

Questions on forest landscape mutations in the Yabassi Forest Area remain less understood with emphasis on its spatiotemporal dynamics and the socio-ecological transformation-cum-outcomes linked to the process. The evidence is useful in providing insights to edify the SES framework and challenges the mainstream position on forest decline by highlighting areas of recovery. The evidence also informs forest management policy with emphasis on adaptive forest governance processes in the Congo Basin and similar contexts.

2. Research Methods

2.1. Analytical Framework

This study is grounded in the socio-ecological systems (SES) framework, which provides a holistic lens for analyzing the dynamic interactions between human and ecological subsystems [18]. The SES framework integrates ecological processes, resource use patterns, governance structures, and social behaviors into a single analytical structure. By adapting the SES framework to the context of the Yabassi Forest Area, the study conceptualizes forest landscape mutation not merely as physical land cover change but as a multi-scalar and multidimensional transformation shaped by interlinked ecological, socio-economic, institutional, and governance drivers.

The analytical model employed (Figure 1) maps the interplay between core components of the SES resource systems (forests), resource units (timber, NTFPs, biodiversity), actors (local communities, loggers, state agencies), and governance systems (formal forestry laws, customary norms, NGOs). This also captures both proximate and underlying drivers of landscape mutations. The drivers interact with biophysical feedback and institutional responses, resulting in distinct socio-ecological outcomes—both negative and positive.

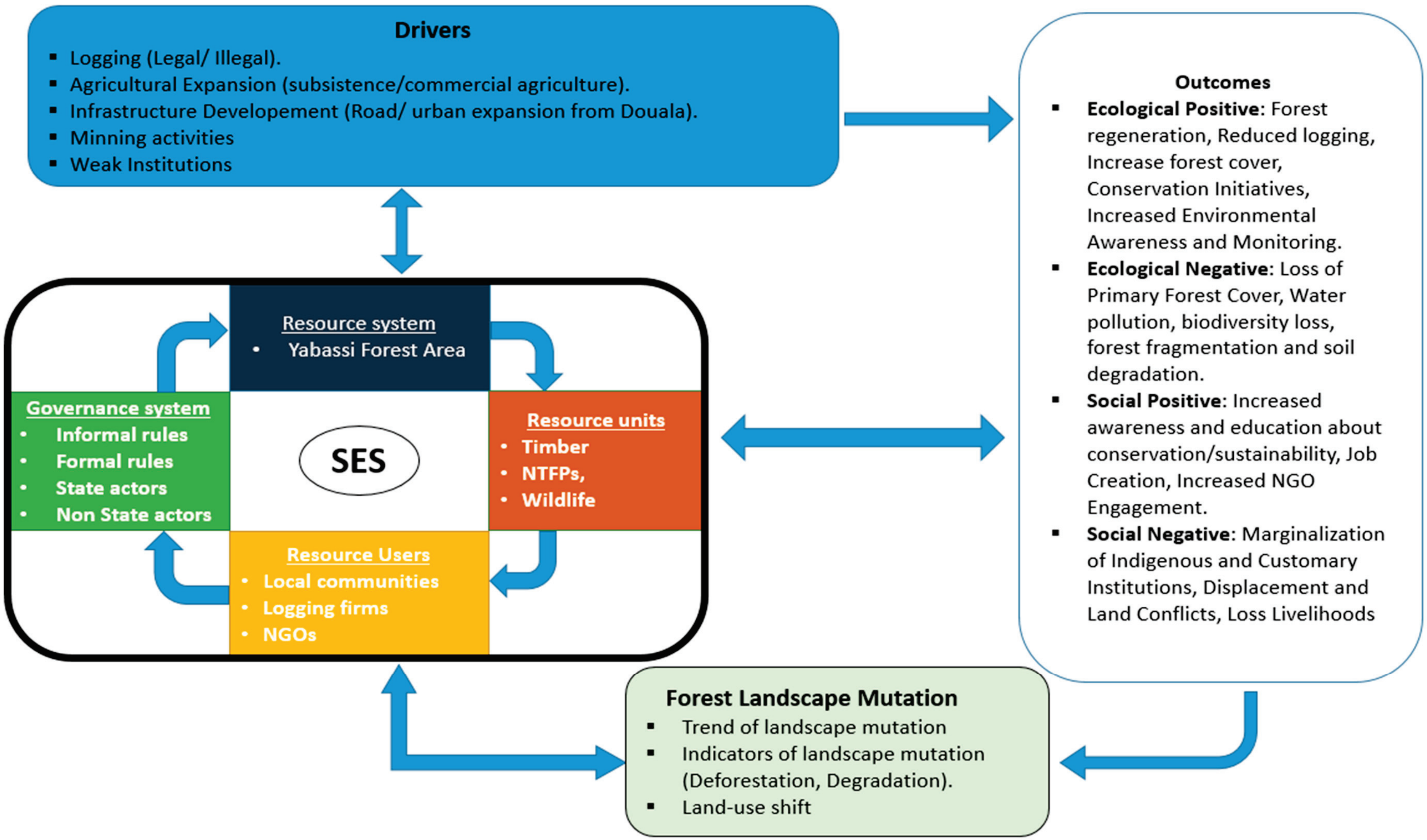

Figure 1. Application of Ostrom's social-ecological systems (SES) framework to the Yabassi Forest Area. Blue arrows indicate the interactions and feedback loops between SES components, external drivers, forest landscape mutation processes, and socio-ecological outcomes (developed based on [18]) [4].

The Yabassi Forest Area has experienced significant structural and functional shifts in land cover due to logging, agricultural encroachment, mining, and infrastructural development [19]. Forest cover declined by more than 30% between 1990 and 2020, with an estimated annual deforestation rate of 1.3% between 2010 and 2020, primarily in the southern and eastern zones adjacent to the Douala–Yabassi corridor [20–22]. These zones are marked by expanding road networks, illegal logging routes, and encroaching settlement frontiers.

The SES framework allows for a nuanced exploration of the drivers of forest landscape mutations, including:

- Logging (legal and illegal): More than 60% of the residents perceive illegal logging as the dominant threat, driven by enforcement failures and corruption [23,24].
- Agricultural expansion: Both subsistence and commercial farming (cassava, cocoa, oil palm) have led to a 45% increase in cultivated area, replacing vital forest cover in high-pressure zones [23].
- Infrastructural development: Logging firms and urban sprawl from Douala have tripled the regional road network since 2000, facilitating deeper forest penetration [24].
- Mining: Informal gold and gravel extraction led to river sedimentation, ecological fragmentation, and biodiversity loss, particularly affecting freshwater ecosystems [22].
- Governance fragmentation: Weak institutional capacity, overlapping mandates, and elite capture reduce policy effectiveness and allow unsustainable land use practices to flourish [25].

The interactions yield varied socio-ecological outcomes. Some of the ecological outcomes include deforestation, biodiversity loss (e.g., *Kupeantha yabassi*, *Louisea yabassi*), soil erosion, and hydrological disruption [22,25,26]. However, secondary forest regeneration and increased conservation awareness are championed by NGO campaigns to counter these threats in zones with reduced disturbance. The social outcomes include livelihood disruption, cultural erosion (especially loss of access to sacred groves), gendered inequalities in resource access, and land use conflicts among stakeholders. The influx of labor migrants linked to extractive industries led to an increase in social fragmentation. However, some communities have benefited from short-term employment in logging and agriculture and have engaged in participatory governance through village forest management committees (VFMCs) and NGO partnerships (e.g., AJESH).

By embedding these dynamics within the SES framework, the study captures the nonlinear, feedback-driven nature of forest landscape mutation in Yabassi. It emphasizes that the outcomes are not simply a product of environmental pressures but are fundamentally shaped by governance quality, actor interactions, and institutional adaptability. Thus, the framework provides an integrated platform for evaluating the resilience or vulnerability of forest landscapes, offering insights that can inform policy reform and community-led conservation strategies in the Congo Basin and similar contexts.

2.2. Study Area

This study was conducted in the Yabassi Forest Area, a 300,000-hectare landscape located in Cameroon's Littoral and Central Regions, specifically in the Nkam and Mbam Divisions (Figure 2). The area comprises three ecologically significant forest blocks: the Ebo Forest (141,700 ha), the Ndokbou Forest (100,000 ha), and the Makombe Forest (60,000 ha) [23]. As part of the Guineo–Congolian rainforest belt, the region is recognized as a Key Biodiversity Area, home to more than 310 bird species and several endangered mammals, including the western gorilla (*Gorilla gorilla*), chimpanzee (*Pan troglodytes*), drill monkey (*Mandrillus leucophaeus*), and forest elephant (*Loxodonta africana*) [22,25]. The forests span an altitudinal gradient of 9 to 1304 m and are characterized by high rainfall and a mosaic of microhabitats. Despite its ecological value, the region faces growing development pressure, though conservation victories such as suspending a proposed logging concession in Ebo Forest in 2020 have highlighted its strategic importance [27]. The forest landscape is bordered by more than 40 communities, including indigenous Banen populations, whose livelihoods are based primarily on subsistence agriculture. As of 2018, the area had a population of 17,127. Poor infrastructure and limited road access have contributed to the area's conservation value and governance challenges in the forest [28].

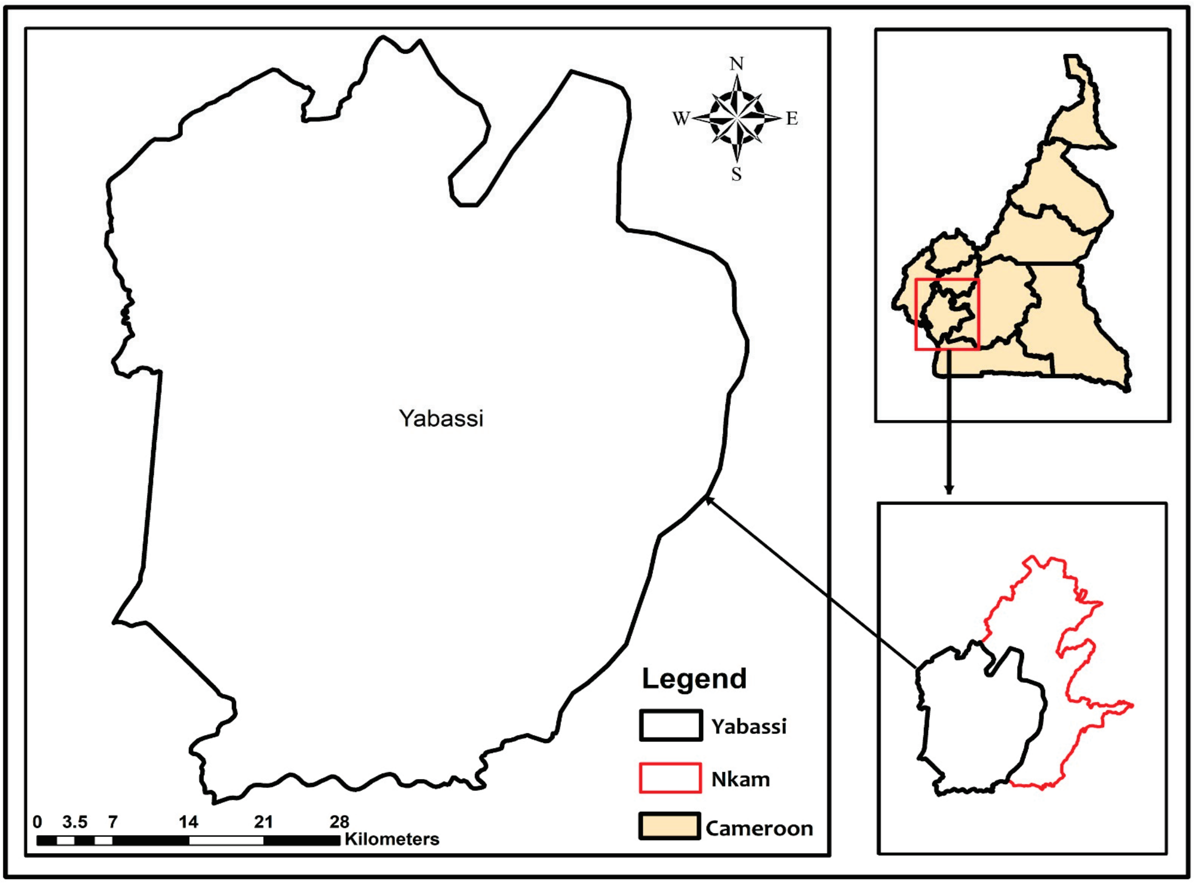

Figure 2. Study area map. **Source:** QGIS 3.28 (QGIS Development Team 2023).

The study area covers approximately 300,000 hectares, representing the generalized boundary of the target landscape. However, the total area analyzed varies slightly across different components of the study due to the application of specific data masks and inclusion criteria. During land use/land cover (LULC) classification, all valid pixels within the defined study boundary were included, resulting in a total classified area of approximately 308,765 hectares. This slightly exceeds the nominal study area due to pixel-level inclusion along boundaries and within an irregular geographic extent. In contrast, the transition matrix analysis includes only pixels with valid classification in both time periods. As a result, unclassified, cloud-covered, or masked pixels—due to sensor limitations or quality filtering—were excluded, reducing the total analyzed area to approximately 268,701 hectares. Such variation is common in remote sensing-based landscape analysis, where differing pixel availability and data quality across time periods necessitate conservative inclusion criteria to ensure reliable change detection. All area-based calculations and percentage changes reported are internally consistent within each analysis.

2.3. Research Design and Data Collection

The study adopts a mixed-methods design guided by an explanatory sequential model to examine the patterns and impacts of forest landscape mutations. The research began with a spatial analysis to quantify forest change over 20 years (2004–2024), followed by household surveys to assess local perceptions and socio-ecological outcomes. This integration allowed for triangulation between observed land use dynamics and community experiences, providing a more robust and policy-relevant understanding of the phenomena under study.

Spatial data were derived from Landsat satellite imagery (Landsat 7 ETM+ for 2004, Landsat 8 OLI for 2014, and Landsat 9 OLI-2 for 2024), sourced from the USGS Earth Explorer. Supervised image classification was conducted using ArcGIS 10.8 to categorize land cover into five classes: dense forest, degraded forest, agricultural land, settlements, and water bodies. Google Earth Pro was used to extract geographic control points (GCPs) for classification support. The land use and land cover analysis was conducted using Landsat imagery obtained from the United States Geological Survey (USGS). Each image had a spatial resolution of 30 m, which is suitable for detecting medium-scale landscape changes in forested environments. The selected images corresponded to the dry season months, thus reducing cloud interference and cover for 2004 (Landsat 5 TM), 2014 (Landsat 8 OLI), and 2024 (Landsat 9 OLI-2). At the same time, field verification was carried out between March and May 2024 across selected communities in the three forest blocks. These observations, combined with historical land use narratives, improved classification reliability. Ground truthing was employed to enhance accuracy in mapping complex land cover transitions, as recommended by Foody [29], while change detection analysis was subsequently applied to quantify forest loss and gains, and to identify the spatial patterns of landscape mutation.

To complement the geospatial analysis, a structured household survey was implemented to assess community-level socio-ecological outcomes. The survey instrument contained 18 closed-ended questions across four domains: demographics, environmental changes, ecological impacts, and social impacts. The survey targeted residents of the Yabassi Forest Area who are actively engaged in forest-dependent activities such as farming, hunting, and NTFP collection.

The sample was selected using a stratified random sampling approach to improve representativeness. Eight villages were selected across the three forest blocks—Ebo (Iboti, Bekob, Logdeng), Ndokbou (Ndokbou I, Ndokbou II), and Makombe (Milombe, Balam, Moya)—based on their proximity to the forest and active reliance on forest resources (Table 1). Within each village, households were randomly selected using a raffle-draw method adapted to linear settlement patterns. The number of households surveyed in each village was proportional to its estimated population and settlement density, helping to ensure equitable spatial coverage. A total of 100 households were surveyed, representing approximately 0.6% of the estimated population. While this proportion may appear low, the sampling fraction of 5–10% was assured for each community.

Data collection occurred in two phases. In March 2024, preliminary visits and interviews with two traditional leaders were carried out to identify key forest governance structures and validate the survey design. From March to May 2025, the second phase involved the full deployment of surveys by two research assistants who could communicate in English and French. Before administering the questionnaire, community sensitization sessions were held to explain the study's purpose and ensure informed consent. Participation was voluntary, and confidentiality was maintained throughout the process.

Table 1. Community and village allocation with number of questionnaires.

Community	Village Allocation	Number of Questionnaires
Ebo	Iboti	10
	Bekob	5
	Logdeng	18
Ndokbou	Ndokbou I	11
	Ndokbou II	8
Makombe	Milombe	11
	Balam	11
	Moya	26
		Total: 100

To ensure contextual relevance and adaptation to logistical constraints, the survey design process included a pre-testing phase conducted in December 2024. During this period, the research team visited selected communities within the Yabassi Forest Area to pre-test survey instruments, engage with local leaders, and assess the feasibility of various distribution methods. This process informed the refinement of the data collection instrument and the choice of the online survey approach. The online survey was conducted with the support of community focal points and civil society organizations who helped circulate the survey and assist less digitally literate participants. To reduce sampling bias, the study targeted forest-dependent households with known engagement in farming, hunting, and/or non-timber forest products (NTFPs) collection. While some remote households may have been underrepresented due to digital access limitations, outreach was broadened through local mobilization and the involvement of trained field assistants who provided guidance where needed. Survey results were triangulated with spatial analysis and key informant interviews, strengthening the validity of the findings.

2.4. Data Analysis

This study adopted a mixed-methods approach combining spatial analysis and household survey data. Land use and land cover (LULC) classifications were derived from multi-temporal satellite imagery using supervised classification techniques. Accuracy assessment was performed using the ENVI 4.5 software, with standard metrics such as overall accuracy and Cohen's kappa coefficient applied to evaluate classification performance across 2004, 2014, and 2024. For the household survey, responses were coded and analyzed using Microsoft Excel. Descriptive statistics (frequencies and percentages) were used to summarize trends related to forest changes, socio-ecological impacts, and governance perceptions. Graphs and charts were used to visualize patterns, while thematic analysis guided the interpretation of open-ended responses.

All results were interpreted using the socio-ecological systems (SES) framework [18], which enabled the structured analysis of four key components: resource systems (forest landscapes), resource units (timber, wildlife, NTFPs), users (households, traditional authorities, private firms), and governance systems (customary laws, state regulations, community forest committees). Through this integrative and systems-oriented approach, the study offers a grounded understanding of the ecological and social outcomes of forest landscape mutations, generating theoretical and action-oriented insights for conservation and rural development in the Congo Basin.

2.5. Accuracy Assessment of Image Classification

To assess the accuracy of land use and land cover (LULC) classifications, the classified outputs were validated using ground control points from preliminary field visits and remote validation with high-resolution satellite imagery. Accuracy assessment was conducted with the ENVI 4.5 software using standard metrics, including overall accuracy and Cohen's kappa coefficient [30]. The results indicated moderate classification performance, with kappa values of 0.54, 0.46, and 0.65 and overall accuracies of 73.02%, 60.44%, and 73.85% for the years 2004, 2014, and 2024, respectively (Table 2). Earlier years exhibited a significant fraction of unclassified pixels—41.87% in 2004 and 32.16% in 2014. This was mainly due to cloud cover, image noise, and spectral confusion. However, improvements in image resolution and classification techniques by 2024 eliminated the unclassified category entirely, enhancing reliability. In addition to remote sensing data, the study incorporated ancillary socio-economic, demographic, and policy information sourced from government agencies, research institutions, and existing literature. These contextual datasets provided insights on the drivers of land use and land cover change such as governance reforms, evolving livelihood practices, and infrastructural growth in the Yabassi Forest Area, in line with the recommendations of [31].

Table 2. Accuracy assessment metrics for land cover classification in the Yabassi Forest Area for 2004, 2014, and 2024, including per-class producer and user accuracy, overall accuracy, kappa coefficient, and unclassified area percentage.

Land Cover Mutation Classes	2004 Producer Accuracy (%)	2004 User Accuracy (%)	2014 Producer Accuracy (%)	2014 User Accuracy (%)	2024 Producer Accuracy (%)	2024 User Accuracy (%)
Agriculture	88.00	73.17	40.00	50.00	36.36	72.73
Forest	55.56	55.56	60.71	58.62	90.90	45.45
Settlement	60.00	81.82	75.00	60.00	80.00	80.00
Water	40.00	100.00	80.95	73.91	100.00	100.00
Unclassified	–	–	–	–	–	–
Overall Accuracy (%)	73.02	–	60.44	–	73.85	–
Kappa Coefficient (κ)	0.54	–	0.46	–	0.65	–
Unclassified Area (%)	41.87	–	32.16	–	0.00	–

Land Cover Mutation Classes	2004		2014		2024	
	Producer Accuracy (%)	User Accuracy (%)	Producer Accuracy (%)	User Accuracy (%)	Producer Accuracy (%)	User Accuracy (%)
Agriculture	88.00	73.17	40.00	50.00	36.36	72.73
Forest	55.56	55.56	60.71	58.62	90.90	45.45
Settlement	60.00	81.82	75.00	60.00	80.00	80.00
Water	40.00	100.00	80.95	73.91	100.00	100.00
Unclassified	-	-	-	-	-	-
Kappa Coefficient	0.54		0.46		0.65	
Overall Accuracy	73.02		60.44		73.85	

Year	Overall Accuracy (%)	Kappa Coefficient (κ)	Unclassified Area (%)
2004	73.02	0.54	41.87
2014	60.44	0.46	32.16
2024	73.85	0.65	0.00

3. Results

3.1. Forest Landscape Mutations

Forest landscape mutations were analyzed using land use/land cover maps for the periods between 2004 and 2024 as follows:

3.1.1. Land Use Land Cover Situation in 2004

The period 2004 recorded unclassified areas as the most dominant in terms of land use (41.87%) followed by agricultural land (33.84%), with the least being water bodies (0.50%). The dominance of unclassified areas is largely due to the inability to accurately recognize land use, coupled with cloud cover, which rendered classification very difficult. In recognition of this, agriculture dominated the land use classes, signifying the encroachment of farmland into forest areas (Table 2 and Figure 3). This may partly explain the limited coverage of forest areas (22.85%). Settlements in 2004 were not significant, as the population was limited at the time. This probably caused the few inhabitants to construct buildings for shelter (0.94%), as seen in (Table 3). It is also important to note that the image had scan lines that could be attributed to how satellite captures the area within the analysis period, as Landsat 7 is affected by scan line corrector (SLC) failure.

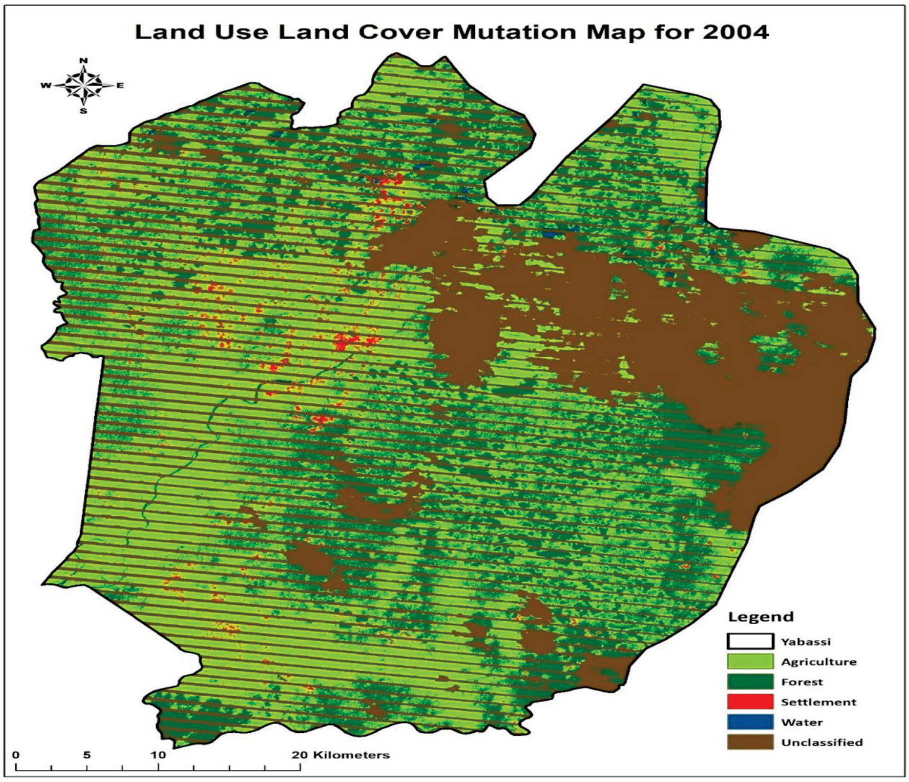

Figure 3. Supervised classification map of Yabassi 2004. Source: USGS Landsat 8; ground truthing (March–May 2024).

Table 3. Area (ha) and percentage coverage of LULC mutation classes for 2004.

LULC Mutation Classes	Area (ha)	Percentage (%)
Agriculture	104,486.686164	33.84
Forest	70,552.291268	22.85
Settlement	2892.831775	0.94
Water	1547.167395	0.50
Unclassified	129,286.17359	41.87
Total	308,765.15019	100

3.1.2. Land Use Land Cover Situation in 2014

As of 2014, forest cover increased substantially by 46.63%, representing the most dominant land cover classes in the landscape. Although a similar pattern of unclassified land cover class exists in the 2014 images, covering a significant area (32.16%), it highlights the difficulty during the classification process in identifying this land cover class. Water bodies and settlements recorded the least land cover classes, with 2.48% and 2.06%, respectively, representing the fourth and fifth land cover classes. It was expected that with population growth, more land would be exploited for agricultural purposes (Table 4 and Figure 4). However, by 2014, agricultural land declined from 33.84% in 2004 to 16.69%, revealing a probable mismatch in the classification. Areas classified as unclassified may be productive for agriculture; however, since there were difficulties identifying and classifying these areas as potentially productive agricultural lands, the land cover for agriculture decreased drastically.

Table 4. Area (ha) and percentage coverage of LULC mutation classes for 2014.

LULC Mutation Classes	Area (ha)	Percentage (%)
Agriculture	51,507.786547	16.69
Forest	143,953.3177	46.63
Settlement	6346.582301	2.06
Water	7668.268628	2.48
Unclassified	99,287.735788	32.16
Total	308,763.690965	100

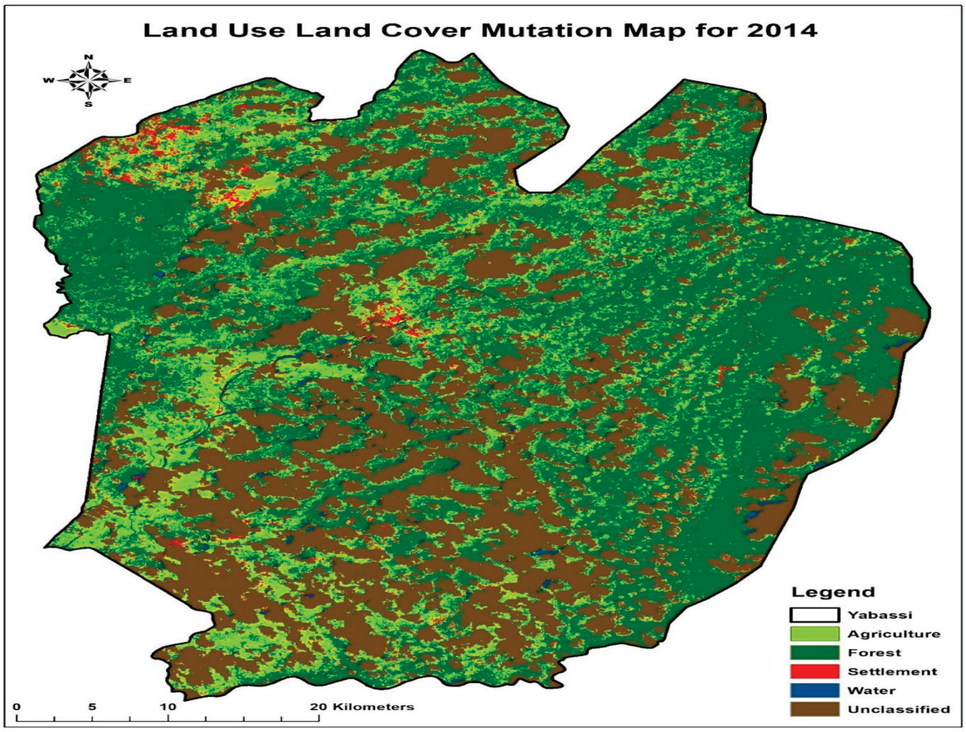

Figure 4. Supervised classification map of Yabassi 2014. Source: USGS Landsat 8; ground truthing (March–May 2024).

3.1.3. Land Use Land Cover Situation in 2024

The 2024 land cover map places forest as the most dominant land cover class, with a total area of 211,982.271101 ha, representing 68.65% of the total landscape. This increase may be attributed to several interventions in the region, including but not limited to enrichment planting, agroforestry systems, and farmer-managed natural regeneration. These activities were implemented by government agencies such as the Delegation of Forestry and Wildlife and some environmental conservation NGOs. In 2024, images were clear enough to facilitate the distinction between the various land cover classes. This eliminated the unclassified category due to improved image quality. Agriculture became the second most dominant land cover class, with a total area of 80,120.52 ha, representing 25.91% of the total landscape. Population increase along with its attendant demand for resources led to the expansion of agricultural land (Table 5 and Figure 5). Although settlement and water bodies increased by 3.05% and 2.39% in the landscape, they remain the least recorded land cover classes within the landscape. The increase in population has forced people to convert land classes, such as forests or agricultural areas, to pave the way for other land uses.

Table 5. Area (ha) and percentage coverage of LULC mutation classes for 2024.

LULC Mutation Classes	Area (ha)	Percentage (%)
Agriculture	80,012.520766	25.91
Forest	211,982.271101	68.65
Settlement	9410.935624	3.05
Water	7369.197745	2.39
Total	308,774.925237	100

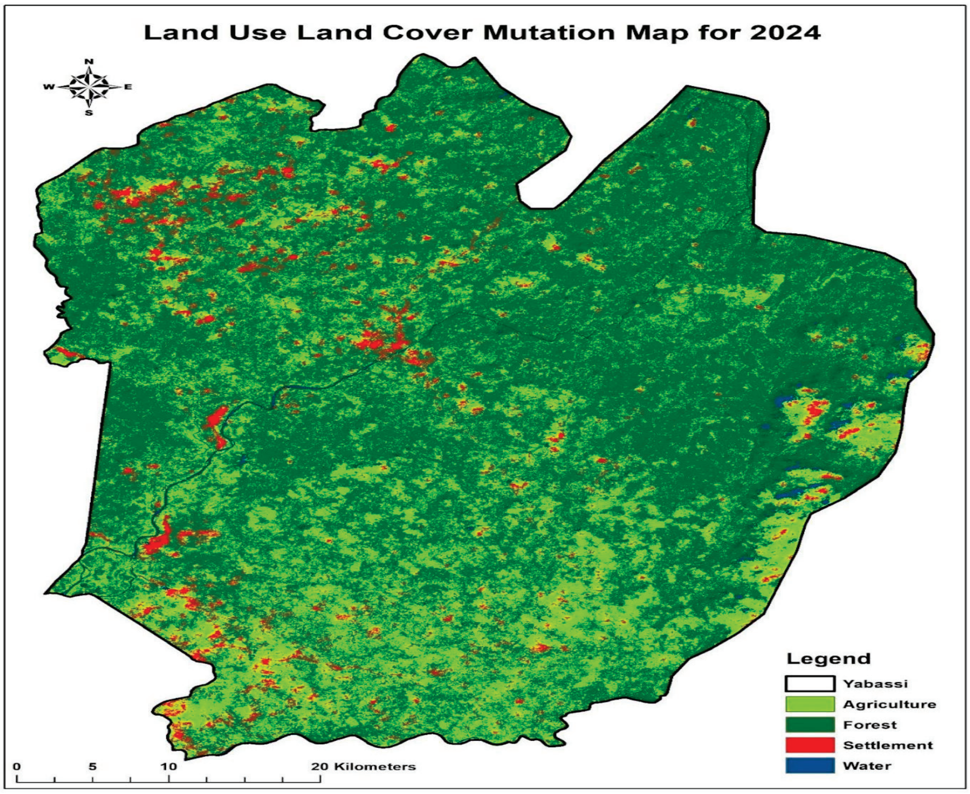

Figure 5. Supervised classification map of Yabassi, 2024. Source: USGS Landsat 8; ground truthing (March–May 2024).

Between 2004 and 2014, the landscape underwent significant transformations (Table 6). A substantial 40.9% of the land originally under agriculture in 2004, equivalent to 41,743.73 hectares, transitioned into forest by 2014, suggesting either widespread reforestation or potential reclassification due to improved spectral resolution and classification techniques. However, this greening was offset by 9156.90 hectares of forest converted to agriculture, representing 12.9% of the forest area in 2004. These shifts underscore a pattern of land use flux driven by both environmental management interventions and ongoing agricultural expansion. Additionally, 38,675.50 hectares (or 41.9%) of previously unclassified areas contributed to forest cover in 2014. While this indicates improved image clarity, it could also underscore the challenge of cloud cover and spectral confusion in earlier classifications. These issues are commonly reported in remote sensing in the tropics [29].

Table 6. LULC mutation matrix of the Yabassi Forest Area showing the overall transition in land use classes from 2004 to 2014.

	2014						
	LULC Classes	**Agriculture**	**Forest**	**Settlement**	**Water**	**Unclassified**	**Total (ha)**
2004	Agriculture	21,764.639088	41,743.732875	2356.469593	2528.440193	36,069.114439	104,462.396188
	Forest	9156.904288	35,165.75245	1260.313862	1912.301475	23,040.731832	70,536.003907
	Settlement	547.337363	1018.147443	169.379734	90.597952	1067.064001	2892.526493
	Water	238.13694	728.118938	42.16421	118.90013	419.300533	1546.620751
	Unclassified	19,789.478084	65,267.65669	2515.956245	3015.045938	38,675.497044	129,263.634001
	Total (ha)	51,496.495763	103,923.408396	6344.283644	7665.285688	99,271.707849	268,701.18134

Table 7. LULC mutation matrix of the Yabassi Forest Area showing the overall transition in land use classes from 2014 to 2024.

	2024						
	LULC Classes	**Agriculture**	**Forest**	**Settlement**	**Water**	**Unclassified**	**Total (ha)**
2014	Agriculture	14,779.651417	34,087.081191	2062.270619	566.920719	-	51,495.923946
	Forest	29,299.318649	108,596.384953	2634.278284	3397.778932	-	143,927.760818
	Settlement	1622.125297	3833.065688	749.099956	139.990615	-	6344.281556
	Water	1849.346489	4497.960899	232.194471	1085.906103	-	7665.407962
	Unclassified	32,423.845596	60,917.467946	3759.360243	2174.159415	-	99,274.8332
	Total (ha)	79,974.287448	211,931.960677	9437.203573	7364.755784	-	268,708.207482

Between 2014 and 2024, further landscape transformation was observed (Table 7); 108,596.38 hectares, which is 75.5% of the 2014 forest area remained forested in 2024, reflecting relative stability and ecological continuity. In contrast, 34,087.08 hectares (approximately 66.2% of agriculture from 2014) were reclassified as forest, potentially due to successful conservation efforts such as community forest management, agroforestry, and reforestation programs supported by NGOs such as AJESH and local governance structures [32]. Despite this, deforestation persisted, with 29,299.32 hectares of forest converted to agricultural land. Around 20.4% of the forest area in 2014 was converted, highlighting continued land pressure, particularly from subsistence and commercial farming [12]. Additionally, 2634.28 hectares of forest were lost to settlements, likely due to population growth and urban expansion associated with proximity to Douala. Importantly, the total landscape area remained consistent at around 268,701 hectares, allowing for accurate inter-period comparison. A key improvement in the 2024 dataset was the elimination of unclassified land, reflecting enhanced data quality, classification accuracy, and ground validation efforts through field surveys conducted between January and April 2024.

The transition matrices illustrate a highly dynamic system, with agriculture emerging as the most volatile class, constituting both a driver and a consequence of land use change. These patterns reflect broader African forest trends, where shifting cultivation, population growth, and weak governance contribute to land use change [9]. In Yabassi, such changes are associated with socio-ecological outcomes including habitat loss and biodiversity decline to altered livelihood systems, land tenure conflicts, and shifts in resource access. Such outcomes require adaptive forest governance strategies [28].

3.1.4. Change Analysis of Land Use/Land Cover

From the data, it is observed that between 2004 and 2014, forest cover in the Yabassi Forest Area expanded significantly by 104.01%, rising from 70,536 ha to 143,927.76 ha (Table 8). This rise is the result of natural regeneration or increased conservation initiatives. This growth continued, albeit moderately, between 2014 and 2024, with a further 47.27% increase. This brings the forest area to 211,931.96 ha and marks a total increase of +151.28% over the past two decades. In contrast, agricultural land dropped by 50.72% between 2004 and 2014, declining from 104,462.40 ha to 51,495.92 ha. However, it showed a partial rebound by 55.33% in 2024, totaling 79,974.29 ha. Despite this recovery, the overall agricultural footprint recorded a net loss of −23.46%, reflecting a dynamic cycle of land use influenced by abandonment, classification limitations, and/or changing livelihood strategies.

Table 8. Change analysis of key metrics over time.

LULC Class	2004 Area (ha)	2014 Area (ha)	2024 Area (ha)	% Change (2004–2014)	% Change (2014–2024)	% Change (2004–2024)
Agriculture	104,462.40	51,495.92	79,974.29	−50.72%	+55.33%	−23.46%
Forest	70,536.00	143,927.76	211,931.96	+104.01%	+47.27%	+151.28%
Settlement	2892.53	6344.28	9437.20	+119.47%	+48.75%	+226.43%
Water	1546.62	7665.41	7364.76	+396.00%	−3.92%	+376.20%
Unclassified	129,263.63	99,274.83	N/A	−23.23%	N/A	N/A

Settlement witnessed consistent expansion in both decades, increasing from 2892.53 ha in 2004 to 6344.28 ha in 2014 (+119.47%). This reached 9437.20 ha in 2024 (+48.75%), representing an overall increase of +226.43%. Water bodies showed an initial sharp change. This was characterized by a +396.00% increase from 1546.62 ha to 7665.41 ha between 2004 and 2014, then a slight decline in 2024, indicating a net gain of +376.20% over the 20 years. Meanwhile, the unclassified land area recorded a decrease from 129,263.63 ha in 2004 to 99,274.83 ha in 2014 (−23.23%). By 2024, this class was eliminated due to advancements in image clarity and classification techniques. Overall, the results highlight a complex yet instructive pattern of landscape transformation, driven by both ecological restoration and human activities that shape the socio-ecological trajectory of the Yabassi Forest Area.

3.2. Drivers of Forest Landscape Mutations

The results reveal that forest landscape mutations in the Yabassi Forest Area are driven by a combination of socio-economic and environmental pressures, as seen in Figure 6 below. Population growth (57%) and deforestation for agriculture or farming (56%) emerged as the leading drivers, highlighting the growing demand for land amid limited alternative livelihoods. Logging activities (48%) and urban expansion (48%) further contributed to forest degradation, particularly near rapidly growing settlements such as Solle and Dimbong. These pressures were compounded by the perceived effects of climate change (36%), which affects vegetation patterns and exacerbates land vulnerability. Though less frequently cited, mining activities (20%), government projects (16%), and infrastructural development (14%), including the construction of roads and schools, also played a role in altering the landscape. These findings point to a complex interplay of local land use decisions and broader development agendas, underscoring the need for integrated forest governance approaches that address both immediate livelihood needs and long-term environmental sustainability.

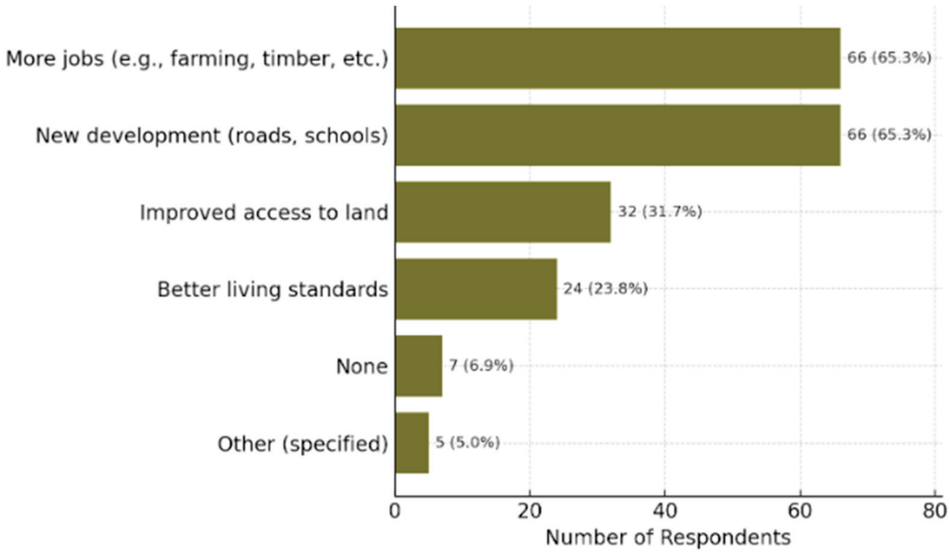

Figure 6. Drivers of FLSM. Source: field work 2025.

3.3. Socio-Ecological Outcomes of Forest Landscape Mutations

Table 9 captures the dual nature of forest landscape mutations, which are structured under positive and negative ecological and social outcomes. The most significant positive ecological outcome was forest regeneration (30%), followed by improvements in biodiversity conservation (25%). The least reported was the emergence of ecotourism opportunities (8%). From the negative perspective, the perceived decline in biodiversity (76%) and wildlife loss (75%) were the most significant, while other aspects of ecological stress (2%) featured the least.

The significant positive social outcomes included the provision of job opportunities (66%) and infrastructural development (66%), while the least reported ones included access to forest products and mobility (5%). The loss of traditional forest access (69%) and land conflicts (67%) stood as the significant negative social outcomes, while the disruption of the social fabric (2%) was the least reported (Table 6).

Table 9. Socio-ecological outcomes of forest landscape mutations in the Yabassi Forest Area (2004–2024).

Dimension	Positive Outcomes	Negative Outcomes
Ecological	- Forest regeneration (30%) - Biodiversity conservation (25%) - Reforestation/afforestation interventions (18%) - Emerging ecotourism opportunities (8%)	- Wildlife loss (75%) - Hotter, drier local climate (52%) - Decline in wood and medicinal plants (42%) - Soil erosion and flooding (34%) - Diminished water sources (14%) - Other ecological stress (2%) - Perceived decline in biodiversity (76%)
Social	- Job opportunities (66%) - Infrastructure development (66%) - Improved access to land (32%) - Better living standards (24%) - Other social benefits, e.g., access to forest products and mobility (5%)	- Loss of traditional forest access (69%) - Land conflicts (67%) - Food and water shortages (23%) - Decline in income from forest resources (14%) - Migration due to worsening conditions (13%) - Other social disruptions (2%)

4. Discussion

The Yabassi Forest Area, situated within the Congo Basin, offers an insightful case of socio-ecological transformations shaped by two decades of dynamic forest landscape mutations. Using the socio-ecological systems (SES) as analytical framework [18], this study illustrates how interactions between resource systems (forests), resource units (biodiversity and land cover types), governance systems (local and state institutions), and users (communities and actors such as NGOs) collectively produce a set of positive and negative socio-ecological outcomes.

To deepen the SES framework, this study anchored its findings to the core components of the SES framework. The forest landscapes of Ebo, Ndokbou, and Makombé serve as distinct resource systems (RS), each exhibiting different forest cover trends and land use pressures. Within these systems, households engage with various resource units (RU)—including timber, NTFPs, wildlife, and medicinal plants—based on livelihood needs and cultural practices. These interactions are mediated by a diverse array of actors (A) such as herbalists, hunters, and women, many of whom face limitations in access and decision-making power. The governance system (GS) encompasses both formal institutions (e.g., forestry laws and NGO interventions) and informal mechanisms (e.g., traditional rules and community bylaws). Reported participation in conservation activities (66%) alongside low perceived governance effectiveness (29%) highlight tensions within this system. Through activities like farming, hunting, and forest product collection, these actors engage in interactions (I) that lead to key outcomes (O) such as perceived forest decline (95%), biodiversity loss (90%), land conflicts (67%), and importantly local observations of forest regeneration (30%). The core contribution centers on the observed positive and negative ecological and social outcomes linked to the changes in the resource system (socio-ecological system). This enhances the understanding of how governance failures, livelihood dependencies, and ecological pressures have co-evolved in shaping the Yabassi forest landscape.

Between 2004 and 2024, Yabassi experienced a notable increase in forest cover, from 22.85% to 68.65%, representing a net gain of more than 45%. This net gain is accounted for, in part, by the sustained ecological interventions such as agroforestry, enrichment planting, and farmer-managed natural regeneration of state actors and NGOs. This affirms the SES proposition that resilient outcomes are possible when institutional arrangements (e.g., community forestry) align with local ecological knowledge and incentives. These findings align with the work of the author of [33], who observed that community-led forest governance in Cameroon enhances the success of reforestation and ecological stewardship. However, this contrasts with that in [34], which argued that conservation interventions often fail to deliver long-term environmental benefits in Central Africa due to institutional fragmentation and inconsistent policy enforcement. The Yabassi case, however, suggests that where multi-actor governance is coordinated and socio-ecological feedback is recognized, achieving significant recovery is possible.

While the study recorded a +151% increase in forest cover between 2004 and 2024, it is important to note that this finding does not align with regional and global trends, which generally report net forest loss across Cameroon and other parts of the Congo Basin. For instance, Refs. [6,9] highlight persistent deforestation in the Congo Basin due to agricultural expansion, logging, and infrastructure development. However, the results reflect localized landscape dynamics within the Yabassi Forest Area and should not be generalized as indicative of national or continental trends.

Several contextual factors help explain the observed forest gains. First, passive regeneration of formerly cultivated or abandoned farmland—particularly in areas affected by shifting livelihood strategies and population mobility—contributed to the natural recovery process of forested areas. This mirrors regeneration trends observed elsewhere in Central Africa [35]. Second, the Yabassi Forest Area partially overlaps with Key Biodiversity Areas (KBAs), where targeted community-based conservation initiatives have played a critical role. A notable example is the suspension of a proposed logging concession in the Ebo Forest (141,700 ha) in August 2020 by the government of Cameroon. This decision came in response to stiff opposition from local communities, environmental NGOs, scientists, and international partners, who highlighted the forest's global ecological significance and its role in supporting endemic and endangered species, such as the Nigeria–Cameroon chimpanzee and forest elephants. The government issued a public statement revoking the decree to allocate the concession. This helped to avert large-scale forest clearance and reaffirmed the value of community and civil society engagement in forest governance [36]. The intervention has since enabled continued forest recovery and strengthened the foundation for biodiversity conservation and local stewardship in the region. Third, certain blocks, particularly portions of the Makombé Forest, have remained relatively inaccessible due to topographic and infrastructural constraints, limiting commercial exploitation and preserving forest integrity. Last, the apparent forest gains may be partially attributable to improved classification methods in 2024, including higher-quality satellite imagery and the elimination of the "unclassified" category, which enhanced the visibility and detection of secondary forests and regenerating woodlands previously masked by cloud cover or spectral confusion.

It is evident that there has been a net gain in forest cover within this landscape. However, the reported +151% increase in forest cover between 2004 and 2024 should be interpreted with caution, as it may partially reflect classification differences rather than the true ecological change. Classification accuracy was notably lower in the earlier years (overall accuracy: 73.02% in 2004; 60.44% in 2014) compared to 2024 (73.85%), with high proportions of unclassified pixels in 2004 (41.87%) and 2014 (32.16%), and none in 2024. These discrepancies indicate that improved image quality and classification techniques in 2024 likely contributed to the forest gain estimate, because it reduced omission errors and expanded the detectable area. While a formal error-adjusted area estimation [37] was not applied, the study now incorporates this limitation in the interpretation and recommends such methods for future research to derive more robust change estimates.

The observed mutations in forest landscapes underscore the volatility of agricultural land use, which declined sharply by 50.72% between 2004 and 2014 before witnessing a partial rebound by 2024. Agriculture has thus acted both as a driver and a recipient of land use change, confirming its role as a core feedback variable within the SES framework. This finding aligns with [28], who emphasized the bidirectional nature of agricultural pressure and forest transformation in Cameroon. It also reflects broader African trends, where shifting cultivation, market-driven farming, and tenure uncertainty destabilize landscapes [9]. These dynamics challenge [38], which projected a linear decline in forest cover under expanding agricultural fronts, underestimating the potential for forest regeneration under hybrid land use regimes.

The drivers of forest landscape mutations in Yabassi, mainly population growth (57%), agricultural expansion (56%), logging (48%), and urban development (48%), further illuminate the complex interplay of ecological and social subsystems. These pressures mirror patterns found elsewhere in the Congo Basin, where demographic trends and infrastructural development amplify land conversion. Interestingly, the perceived effects of climate change (36%) were also identified as a key driver, particularly through its effects on rainfall variability and soil productivity, which redefine local land use decisions. These findings support [39], which demonstrated that vulnerability to climate variability accelerates land transitions in rural forest communities. However, they differ from [40], which rather emphasized the dynamics of global commodity markets. In the Yabassi Forest Area, shifts in rainfall patterns, rising temperatures, and increased frequency of extreme events have altered species distribution, promoted pest outbreaks, and increased the risk of fire—ultimately degrading biodiversity and disrupting key ecosystem services such as water regulation and soil retention. Studies elsewhere support these concerns; for example, Ref. [41] observed that in Southwest China, climate change contributed to water yield reduction (84%) and to variations in soil conservation (91%), thus surpassing the impacts of land use change [42]. These changes in ecosystem service provision highlight the scale-dependent uncertainties that climate variability introduces, particularly for water-related functions. These local observations are consistent with broader regional and global patterns of climate-induced forest change. Recent studies further highlight how climate change reshapes forest landscapes and ecosystem services through linked drivers such as fires, drought, and biodiversity loss. For example, climate-induced shifts in species composition and forest structure are becoming increasingly common, as warmer and drier conditions promote more frequent and intense fires while reducing the resilience of late-successional forest ecosystems [43,44]. Drought-induced mortality alters species composition and reduces carbon storage in forest biomass; this creates potential feedback loops within the climate system [45,46]. In tropical forests like the Amazon, increased drought and fire risks may shift ecosystems toward more fire-prone and biodiversity-poor savanna states [47,48]. These findings underscore the importance of integrating climate resilience into forest management and conservation planning in Yabassi and similar forest systems worldwide. In the Yabassi context, where livelihoods depend on forest-derived ecosystem services, promoting ecosystem-based adaptation strategies, improving forest monitoring systems, and integrating climate resilience into conservation planning are essential.

The socio-ecological outcomes of forest transformations have been both enabling and exclusionary. On the ecological front, gains in forest cover were associated with forest regeneration (30%), perceived biodiversity conservation (25%), and increased opportunities for ecotourism (8%). These benefits demonstrate how landscape-level interventions can enhance ecosystem integrity and unlock new economic opportunities, particularly when combined with community engagement. Yet the legacy of earlier forest loss is still deeply felt. Wildlife decline was reported by 75% of respondents, while 76% reported a decline in biodiversity. This dissonance between quantitative forest gains and qualitative ecological degradation challenges simplistic metrics of conservation success, supporting [26], which argues that forest integrity, not just extent, is the true determinant of ecological resilience in the broader Congo Basin.

Socially, the positive outcomes of increased employment (66%), improvement in infrastructure (66%), and improved land accessibility (32%) were widely reported. These align with the SES emphasis on livelihood diversification as a component of resilience. Yet, these benefits were accompanied by deepening inequality and dispossession. Loss of traditional access (69%), rising land conflicts (67%), and migration due to deteriorating conditions (13%) highlight the social costs of forest mutations. This supports [49], which documented how conservation gains in Central Africa often coincide with social marginalization when tenure rights are weak or undefined. It also contradicts [50], which contended that forest transitions in community-managed landscapes in Cameroon are socially beneficial. In Yabassi, it is evident that without equitable governance, forest recovery can coincide with socio-spatial exclusion.

The implications of these findings for policy are profound. First, adaptive forest governance must move beyond ecological indicators to encompass social equity, livelihood security, and cultural access. Recognizing customary tenure, supporting agro-ecological transitions, and investing in inclusive monitoring systems remain crucial for success. Second, landscape management must be context-specific and flexible, integrating local knowledge and feedback into decision-making processes. Third, regional planning should anticipate and mitigate the unintended consequences of infrastructure and demographic growth factors that can undermine forest resilience.

In summary, the Yabassi case provides both caution and promise. It shows that forest recovery is possible but not inevitable, that ecological gain can coexist with social fragmentation, and that policy success lies not in technocratic fixes but in participatory, system-aware governance. As a microcosm of broader Congo Basin dynamics, Yabassi reveals the importance of aligning conservation goals with socio-ecological realities to ensure sustainable and just forest futures.

5. Conclusions

This study provides novel evidence that, contrary to prevailing regional and global trends of net forest loss, the Yabassi Forest Area experienced a significant increase in forest cover between 2004 and 2024. This gain reflects localized dynamics, driven by passive regeneration, community-based conservation, and improved classification accuracy rather than broader national or continental patterns. The findings reveal that ecological recovery can occur in socially contested forest landscapes when governance structures, local engagement, and restoration opportunities align. However, the uneven distribution of socio-ecological benefits highlights that forest gains alone do not guarantee social equity, underscoring the need for integrated governance that couples ecological objectives with livelihood security and tenure rights. These insights refine the application of the SES framework by demonstrating its utility in capturing both the drivers and trade-offs of forest landscape mutation in the Congo Basin.

Author Contributions: Conceptualization, P.K.N. and J.N.K.; methodology, P.K.N. and J.N.K.; writing—original draft, P.K.N. and J.N.K.; writing—review and editing, P.K.N. and J.N.K.; supervision, J.N.K. All authors have read and agreed to the published version of the manuscript.

Funding: This research received no external funding and was entirely self-funded by the authors.

Institutional Review Board Statement: Ethical review and approval were waived for this study because it involved non-invasive, perception-based data collection from adult community members regarding forest use, land cover change, and local governance. The research did not involve the collection of biological specimens or personal health data. All procedures were conducted in accordance with ethical research principles, and informed consent was obtained from all participants. Participation was voluntary, and respondents were assured of anonymity, confidentiality, and their right to withdraw at any time.

Data Availability Statement: The data presented in this study are available on request from the corresponding authors. The data are not publicly available due to ethical considerations and the protection of respondent confidentiality. Spatial datasets used for land use/land cover classification (Landsat imagery) are publicly available through the United States Geological Survey (USGS) Earth Explorer platform (https://earthexplorer.usgs.gov/).

Acknowledgments: We acknowledge the respondents who took time to participate in the data collection process. This paper was developed within the framework of the CIPSEM program, Dresden, Germany.

Conflicts of Interest: The authors declare no conflicts of interest.

References

1. Ostrom, E. *Governing the Commons: The Evolution of Institutions for Collective Action*; Cambridge University Press: Cambridge, UK, 1990.
2. Ameyaw, J.; Arts, B.; Wals, A. Challenges to responsible forest governance in Ghana and its implications for professional education. *For. Policy Econ.* **2016**, *62*, 78–87. [CrossRef]
3. Kimengsi, J.N.; Abam, C.E.; Forje, G.W. Spatio-temporal analysis of the 'last vestiges' of endogenous cultural institutions: Implications for Cameroon's protected areas. *GeoJournal* **2002**, *87*, 4617–4634. [CrossRef]
4. Kimengsi, J.N.; Owusu, R.; Charmakar, S.; Manu, G.; Giessen, L. A global systematic review of forest management institutions: Towards a new research agenda. *Landsc. Ecol.* **2023**, *38*, 307–326. [CrossRef]
5. Geist, H.J.; Lambin, E.F. Proximate Causes and Underlying Driving Forces of Tropical Deforestation. *BioScience* **2002**, *52*, 143. [CrossRef]
6. Hansen, M.C.; Potapov, P.V.; Moore, R.; Hancher, M.; Turubanova, S.A.; Tyukavina, A.; Thau, D.; Stehman, S.V.; Goetz, S.J.; Loveland, T.R.; et al. High-Resolution Global Maps of 21st-Century Forest Cover Change. *Science* **2013**, *342*, 850–853. [CrossRef]
7. *The State of the World's Forests 2024*; FAO: Rome, Italy, 2024. [CrossRef]
8. López-Carr, D.; Ryan, S.J.; Clark, M.L. Global Economic and Diet Transitions Drive Latin American and Caribbean Forest Change during the First Decade of the Century: A Multi-Scale Analysis of Socioeconomic, Demographic, and Environmental Drivers of Local Forest Cover Change. *Land* **2022**, *11*, 326. [CrossRef]
9. *Global Forest Resources Assessment 2020*; FAO: Rome, Italy, 2020. [CrossRef]
10. Masolele, R.N.; Marcos, D.; De Sy, V.; Abu, I.O.; Verbesselt, J.; Reiche, J.; Herold, M. Mapping the diversity of land uses following deforestation across Africa. *Sci. Rep.* **2024**, *14*, 1681. [CrossRef]
11. Pacheco, P.; Mo, K.; Dudley, N. *Deforestation Fronts Drivers and Responses in a Changing World*; WWF: Gland, Switzerland, 2021.
12. Chia, E.L.; Nsubuga, F.W.; Chirwa, P.W. Assessing the Enabling Conditions for Translating Restoration Commitments to Restoration Actions: Case of Cameroon. *J. Sustain. Dev.* **2022**, *16*, 77. [CrossRef]
13. Piabuo, S.M. Community forest enterprises in Cameroon: Tensions, paradoxes and governance challenges. *Environ. Dev.* **2022**, *44*, 100762. [CrossRef]
14. Mahmoud, M.I.; Campbell, M.J.; Sloan, S.; Alamgir, M.; Laurance, W.F. Land-cover change threatens tropical forests and biodiversity in the Littoral Region, Cameroon. *Oryx* **2020**, *54*, 882–891. [CrossRef]
15. Adamson, D. *The Golden Gift of Groundwater in Australia's MDB*; The University of Adelaide: Adelaide, Australia, 2021.
16. Ewane, E.B. Forest Governance Effectiveness of Community-and Government-managed Forests in Cameroon. *Int. J. Environ. Clim. Chang.* **2022**, *12*, 83–102. [CrossRef]
17. AJESH. *AJESH Annual Report*; UNO: Delhi, India, 2020.
18. Ostrom, E. A General Framework for Analyzing Sustainability of Social-Ecological Systems. *Science* **2009**, *325*, 419–422. [CrossRef]
19. Verhegghen, A.; Eva, H.; Desclée, B.; Achard, F. Review and Combination of Recent Remote Sensing Based Products for Forest Cover Change Assessments in Cameroon. *Int. For. Rev.* **2016**, *18*, 14–25. [CrossRef]
20. Ojong, E.J. Local Inhabitants' Opinion of Timber Logging on Livelihoods: The Case of Yabassi Sub-Division in Nkam Division of Cameroon. *Int. J. Innov. Sci. Res. Technol. IJISRT* **2024**, *9*, 2135–2141. [CrossRef]
21. Stone, R.D.; Tchiengué, B.; Cheek, M. The endemic plant species of Ebo Forest, Littoral Region, Cameroon, with a new Critically Endangered cloud forest shrub, *Memecylon ebo* (Melastomataceae-Olisbeoideae). *Kew Bull.* **2024**, *79*, 867–879. [CrossRef]
22. Ndongo, P.A.M.; Eyango, M.T.-T.; Tamesse, J.L.; Ewoukem, E.; Rabone, M.; Albrecht, C.; Missoup, A.D.; von Rintelen, K.; Clark, P.F.; Schubart, C.D.; et al. Discovery of two new populations of the rare endemic freshwater crab Louisea yabassi Mvogo Ndongo, von Rintelen & Cumberlidge, 2019 (Brachyura: Potamonautidae) from the Ebo Forest near Yabassi in Cameroon, Central Africa, with recommendations for conservation action. *J. Threat. Taxa* **2021**, *13*, 18551–18558. [CrossRef]

23. *Global Forest Watch*; WRI: Washington, DC, USA, 2023.
24. Owusu, R.; Kimengsi, J.N.; Giessen, L. Institutional Change and Compliance in Forest Landscape Restoration Governance: Insights from the Western Highlands of Cameroon. *J. Land Use Sci.* **2024**, *19*, 36–58. [CrossRef]
25. Alvarez, M. *Kupeantha yabassi* (Coffeeae-Rubiaceae), a new Critically Endangered shrub species of the Ebo Forest area, Littoral Region, Cameroon. *Kew Bull.* **2021**, *76*, 735–743. [CrossRef]
26. Shapiro, A.; Grantham, H.; Aguilar-Amuchastegui, N.; Murray, N.; Gond, V.; Bonfils, D.; Rickenbach, O. Forest condition in the Congo Basin for the assessment of ecosystem conservation status. *Ecol. Indic.* **2020**, *122*, 107268. [CrossRef]
27. MINFOF. *Joint Annual Report 2015*; MINFOF: Limbe, Cameroon, 2015.
28. Kimengsi, J.N.; Mukong, A.K.; Forje, G.W.; Giessen, L. Institutional change pathways and implications for forest resource use in the Bakossi landscape of Cameroon. *J. Nat. Conserv.* **2024**, *78*, 126567. [CrossRef]
29. Foody, G.M. Status of land cover classification accuracy assessment. *Remote Sens. Environ.* **2002**, *80*, 185–201. [CrossRef]
30. Harris, D.R.; Anthony, N.; Mir, M.; Delcher, C. geoPIPE: Geospatial Pipeline for Enhancing Open Data for Substance Use Disorders Research. *AMIA Annu. Symp. Proc.* **2022**, *2022*, 522–531. [PubMed]
31. Lambin, E.F.; Geist, H.J.; Lepers, E. Dynamics of Land-Use and Land-Cover Change in Tropical Regions. *Annu. Rev. Environ. Resour.* **2003**, *28*, 205–241. [CrossRef]
32. Ewane, E.B.; Deh-Nji, A.; Mfonkwet, N.Y.; Nkembi, L. Agricultural expansion and land use land cover changes in the Mount Bamboutos landscape, Western Cameroon: Implications for local land use planning and sustainable development. *Int. J. Environ. Stud.* **2023**, *80*, 186–206. [CrossRef]
33. Ramachandra, T.V.; Negi, P.; Mondal, T.; Ahmed, S.A. Insights into the linkages of forest structure dynamics with ecosystem services. *Sci. Rep.* **2025**, *15*, 15606. [CrossRef]
34. Nana, E.D.; Njabo, K.Y.; Tarla, F.N.; Tah, E.K.; Mavakala, K.; Iponga, D.M.; Demetrio, B.M.; Kinzonzi, L.; Embolo, L.E.; Mpouam, S. Putting conservation efforts in Central Africa on the right track for interventions that last. *Conserv. Lett.* **2022**, *15*, e12913. [CrossRef]
35. Lambin, E.F.; Meyfroidt, P. Land use transitions: Socio-ecological feedback versus socio-economic change. *Land Use Policy* **2010**, *27*, 108–118. [CrossRef]
36. Whytock, R.C.; Abwe, E.E.; Mfossa, D.M.; Ketchen, M.E.; Abwe, A.E.; Nguimdo, V.R.V.; Maisels, F.; Strindberg, S.; Morgan, B.J. Mammal distribution and trends in the threatened Ebo 'intact forest landscape', Cameroon. *Glob. Ecol. Conserv.* **2021**, *31*, e01833. [CrossRef]
37. Olofsson, P.; Foody, G.M.; Herold, M.; Stehman, S.V.; Woodcock, C.E.; Wulder, M.A. Good practices for estimating area and assessing accuracy of land change. *Remote Sens. Environ.* **2014**, *148*, 42–57. [CrossRef]
38. Ndoye, O.; Kaimowitz, D. Macro-economics, markets and the humid forests of Cameroon, 1967–1997. *J. Mod. Afr. Stud.* **2000**, *38*, 225–253. [CrossRef]
39. Vermeulen, S.J.; Campbell, B.M.; Ingram, J.S.I. Climate Change and Food Systems. *Annu. Rev. Environ. Resour.* **2012**, *37*, 195–222. [CrossRef]
40. Cerutti, E.; Hale, G.; Minoiu, C. Financial crises and the composition of cross-border lending. *J. Int. Money Finance* **2015**, *52*, 60–81. [CrossRef]
41. Xie, X.; Peng, M.; Zhang, L.; Chen, M.; Li, J.; Tuo, Y. Assessing the Impacts of Climate and Land Use Change on Water Conservation in the Three-River Headstreams Region of China Based on the Integration of the InVEST Model and Machine Learning. *Land* **2024**, *13*, 352. [CrossRef]
42. Cheng, S.; Zhao, Y.H.; Zhu, Y.T.; Ma, E. Optimizing the strength and ductility of fine structured 2024 Al alloy by nano-precipitation. *Acta Mater.* **2007**, *55*, 5822–5832. [CrossRef]
43. Nitschke, C.R.; Innes, J.L. Interactions between fire, climate change and forest biodiversity. *CABI Rev.* **2007**, *2006*, 9. [CrossRef]
44. Deb, J.C.; Phinn, S.; Butt, N.; McAlpine, C.A. Climate change impacts on tropical forests: Identifying risks for tropical Asia. *J. Trop. For. Sci.* **2018**, *30*, 182–194. [CrossRef]
45. Gustafson, E.J.; Sturtevant, B.R. Modeling Forest Mortality Caused by Drought Stress: Implications for Climate Change. *Ecosystems* **2013**, *16*, 60–74. [CrossRef]
46. Zhang, T.; Niinemets, Ü.; Sheffield, J.; Lichstein, J.W. Shifts in tree functional composition amplify the response of forest biomass to climate. *Nature* **2018**, *556*, 99–102. [CrossRef]
47. Fearnside, P.M. Climate Change as a Threat to Brazil's Amazon Forest. *Int. J. Soc. Ecol. Sustain. Dev.* **2013**, *4*, 1–12. [CrossRef]
48. Cochrane, M.A.; Barber, C.P. Climate change, human land use and future fires in the Amazon. *Glob. Change Biol.* **2009**, *15*, 601–612. [CrossRef]

49. Bele, M.Y.; Sonwa, D.J.; Tiani, A.-M. Adapting the Congo Basin forests management to climate change: Linkages among biodiversity, forest loss, and human well-being. *For. Policy Econ.* **2015**, *50*, 1–10. [CrossRef]
50. Schure, J.; Ingram, V.; Sakho-Jimbira, M.S.; Levang, P.; Wiersum, K.F. Formalisation of charcoal value chains and livelihood outcomes in Central-and West Africa. *Energy Sustain. Dev.* **2013**, *17*, 95–105. [CrossRef]

MDPI AG
Grosspeteranlage 5
4052 Basel
Switzerland
Tel.: +41 61 683 77 34

Land Editorial Office
E-mail: land@mdpi.com
www.mdpi.com/journal/land

MDPI

Academic Open
Access Publishing

mdpi.com

ISBN 978-3-7258-5578-0